

**ISOLATION AND  
CHARACTERISATION OF A NOVEL  
GLYCOSAMINOGLYCAN  
WITH ANTICANCER ACTIVITY**

**Olanrewaju D Ogundipe**

**School of Environmental and Life Sciences**

**University of Salford, Salford, UK**

**Submitted in Partial Fulfilment of the**

**Requirements of the Degree of Doctor of Philosophy,**

**May, 2015**

<b>Contents</b>	ii
<b>List of figures</b>	xi
<b>List of tables</b>	xvi
Abbreviations	xxiii
Acknowledgements	xxiv
Abstract	xxvi
<b>Section 1: Introduction and overall aim of this study</b>	1
1.0    General introduction	2
1.1    Glycosaminoglycans	7
1.2    GAG's structure and functions	10
1.3    Heparin /HS structures and functions	11
1.4    CS/DS structures and functions	13
1.5    Glycosaminoglycans isolated from shellfish	17
1.6    Biosynthesis of GAGs	17
1.7    Biosynthetic modification of HS- GAGs chain	21
1.8    Biosynthetic modifications CS/DS- GAGs chain	23
1.9    Analysis of GAGs and their oligosaccharides fragments	25
1.10   Traditional methods for extraction and purification of GAGs from Tissue Samples and Cultured Cells	25
1.11   Chemical and enzymatic depolymerisation of GAGs used in structural analysis	26

1.12	Use of separations techniques for structural analysis	28
1.13	Strong anion-exchange chromatography (SAX-HPLC)	29
1.14	Polyacrylamide gel Electrophoresis (PAGE)	30
1.15	GAG's degrading enzymes	30
1.16	Heparinases	31
1.17	Heparinase I from <i>F. heparinum</i> (EC 4.2.2.7)	33
1.18	Heparinase II from <i>F. heparinum</i>	34
1.19	Heparinase III from <i>f. Heparinum</i> (E.C 4.2.2.8)	35
1.20	Chondroitinases	36
1.21	Glycosaminoglycans and cancer	39
1.22	Tumour angiogenesis	42
1.23	Fibroblast growth factors receptors (FGFRs) in human breast cancer	47
1.24	The cell cycle	49
1.25	Cell Cycle regulation	52
1.26	Role of cell cycle regulatory molecules in Breast Cancer Development and Progression	53
1.27	Cyclin D1	54
1.28	Cyclin E1	56
1.29	p27 and p21	56
1.30	Therapeutic target in breast cancer	57

1.31	Modulation of the cell cycle	58
1.32	Direct inactivation of checkpoint controls	60
1.33	Cell death	63
1.34	Necrosis	63
1.35	Pathophysiology and physiological factors leading to necrosis	64
1.36	Apoptosis	65
1.37	Morphology of Apoptosis	70
1.38	Biochemical features of apoptosis	73
1.39	Activation of caspases	73
1.40	DNA fragmentation	76
1.41	Phosphatidylserine (PS) Translocation	76
1.42	Mechanism of apoptosis	77
1.43	Extrinsic Pathway (caspase -8 apoptosis)	80
1.44	Intrinsic Pathway (mitochondria apoptosis)	81
1.45	Perforin/granzyme Pathway	82
1.46	Execution Pathway	84
1.47	Importance of Apoptosis	86
1.48	Apoptosis and necrosis: compare and contrast	87
1.49	Apoptosis and cancer	90
1.50	GAG's and apoptosis	91
1.51	Overall aims of this study	92

<b>Section 2: Experimental Materials and Methods</b>	<b>95</b>
2.0 Experimental Materials	96
2.1 Methods	98
2.2 Preparation of GAGs	98
2.3 Desalting of Crude GAGs	99
2.4 Purification of crude GAGs by anion-exchange chromatography	99
2.5 Desalting of purified GAGs fractions	99
2.6 Enzyme digestion of GAGs	100
2.7 Chemical treatment (nitrous acid treatment)	100
2.8 Polyacrylamide gel electrophoresis (PAGE) analysis)	100
2.9 Superose-12 size exclusion chromatography	101
2.10 Cellulose acetate dot blotting of GAGs	102
2.11 Gel Filtration (TSK G2000 SW Column)	102
2.12 Disaccharide analysis of GAG chain by strong anion-exchange high` Performance liquid chromatography (SAX-HPLC)	102
2.13 Determination of cells viability (MTT assay).	103
2.14 Flow Cytometry Analyses of DNA Content (Cell cycle analysis)	104
2.15 Annexin V-FITC apoptosis detection	105
2.16 DAPI fluorescent microscopy for apoptosis detection	105
2.17 Statistical Analysis	106

<b>Section 3: Results</b>	107
3.0 Biological evaluation of cockle derived GAG mixtures	108
3.1 Effects of cockle derived GAG mixtures on MDA468 breast cancer cell growth (MTT assay results)	108
3.2 Effects of Cockle derived GAG mixtures on the MDANQ01 breast cancer cell	110
3.3 Effect of crude cockle GAG mixture on human lymphoblastic leukaemia (MOLT-4) cell proliferation <i>in vitro</i>	112
3.4 Effects of crude cockle GAG mixtures on the growth of K562 erythroleukaemia cells <i>in vitro</i> .	114
3.5 Effect of cockle GAG mixtures on 3T3 normal fibroblast cell line	116
3.6 Cell cycle analysis of the MOLT-4 cell line after treatment with cockle GAG extracts	118
3.7 Annexin V-FITC Apoptosis Assay of the MOLT-4 Lymphoblastic leukaemia cell line following treatment with crude cockle GAG	124
<b>Section 3B: Biological assay results for whelk GAG mixture</b>	128
3.8 Effect of crude whelk GAG extracts on growth of the MDANQ01 breast cancer cell line	129
3.9 Effect of crude whelk GAG extracts on the growth of MDA468 breast cancer cells	131

3.10	Effect of crude whelk GAG extracts on the growth of K562 and MOLT-4 leukaemia cells lines (K562 and MOLT-4)	133
3.11	Effect of crude whelk GAG extracts on growth of HeLa Cervical cells	135
3.12	Effect of crude whelk GAG mixtures on the growth of normal fibroblast cells (3T3)	137
3.13	Effect of Heparinase I, II, & III enzymes on anti-proliferative activity of whelk GAG mixtures using MDA468 and MDANQ01 breast cancer cell lines.	139
3.14	Cell cycle analysis of MDANQ01 cells after treatment with crude whelk GAG extracts	141
3.15	Cell cycle analysis of MDA468 breast cancer cell lines after treatment with crude whelk GAG extracts	144
3.16	Effects of crude whelk GAG mixtures on the induction of apoptosis in MDA468 breast cancer cells	147
3.17	Flow cytometry and Annexin V-FITC detection of MDANQ01 cells following incubation with whelk GAG extracts	151
3.18	Assessment of apoptosis using DAPI fluorescent microscopy following treatment of MDA468 breast cancer cell with Crude whelk GAG extracts	154
3.19	Assessment of apoptosis using DAPI fluorescent microscopy following treatment of MDANQ01 breast cancer cell with Crude whelk GAG	156

3.20	Assessment of apoptosis using annexin V-FITC apoptosis detection following treatment of HELA cells with crude whelk GAG extracts	159
3.21	Assessment of apoptosis using DAPI microscopy treatment of HELA cells with whelk GAGs	161
3.22	Fractionation of whelk GAG extracts by ion-exchange chromatography	164
<b>Section 3C: Biological activities of purified whelk fraction E</b>		168
3.23	Effect of purified whelk fraction E on the growth of MDANQ01 breast cancer cells	169
3.24	Effect of purified whelk fraction E on MDA468 breast cancer cell proliferation	171
3.25	Cell cycle analysis of the MDANQ1 breast cancer cell line after treatment with purified whelk fraction E	173
3.26	Cell cycle analysis of the MDA468 cell line after treatment with Purified whelk fraction E	175
3.27	Purified whelk fraction E induces mild apoptosis and necrosis on MDANQ01 breast cancer cells (revised Annexin V-FITC apoptosis detection assay results).	178
3.28	Annexin V-FITC apoptosis assay of the MDA468 breast cancer cell line following treatment with purified whelk fraction E	180
<b>Section 3D: Characterisation and purification assay results for cockle GAGs</b>		184
3.29	Assignment of unsaturated CS disaccharides from cockle GAG extracts.	185
3.30	Assignment of unsaturated HS disaccharides from cockle GAG extracts	188



3.31	Gel Filtration analysis (TSK 2000PW) of heparinase degraded cockle GAG extracts	191
3.32	Superose 12 size exclusion chromatography analysis of intact cockle extracted GAG chains	193
3.33	PAGE analysis of crude cockle GAG extracts and commercial GAGs after enzymatic depolymerisation.	195
<b>Section 3E: Characterisation of crude whelk GAG mixtures</b>		197
3.34	Assignment of unsaturated CS disaccharides for whelk GAG extracts	198
3.35	PAGE analysis of crude whelk GAG extracts and commercial GAGs after enzymatic depolymerisation	202
3.36	Superose-12 size exclusion chromatography of crude whelk GAG extracts.	204
<b>Section 3F: Characterisation of purified whelk GAG fractions</b>		206
3.37	Assignment of unsaturated CS disaccharides from purified whelk GAG fractions	207
3.38	Heparinase I-III enzymatic treatments and disaccharide analysis by SAX-HPLC of the active whelk fraction E	210
3.39	HPLC Gel Filtration analysis of whelk fraction E after heparinase degradation	214

3.40	PAGE analysis of purified whelk fractions and commercial GAGs after enzymatic depolymerisation	216
3.41	Superose-12 size exclusion chromatography of purified whelk fraction E	218
<b>Section 4: Discussion</b>		220
4.1	Outline of the major findings	221
4.2	Selective anti-cancer activity of cockle GAGs against leukemia cell lines	223
4.3	Evidence of broader and stronger anti-cancer activity of whelk GAGs extracts	224
4.4	Selective anti-cancer activity of whelk bioactive fraction E against breast cancer cell	227
4.5	Molecular mechanism of action of cockle GAG extracts on leukaemia cell lines	228
4.6	Molecular mechanism of action of whelk GAG extracts on breast cancer cell	231
4.7	Cockle GAG mixture inhibit proliferation of MOLT-4 leukaemia cell partly by apoptosis	233
4.8	Crude and purified whelk GAG extracts inhibit cancer cell growth by apoptosis, analysis by annexin V staining	235
4.9	PAGE and size exclusion analysis of cockle GAG mixture	236

4.10	SAX-HPLC and gel-filtration of cockle GAG extracts	238
4.11	Ion- exchange fractionation of crude whelk GAG mixture	243
4.12	PAGE and size exclusion analysis of both crude and ion-exchange purified whelk GAG extracts	244
4.13	SAX-HPLC and gel-filtration of whelk GAGs	246
4.14	SAX-HPLC and gel-filtration of whelk bioactive fraction E	248
4.15	Overall summary	254
4.16	Limitation of this study	255
4.16	Future direction	256
	References	257

### List of Figures

Figure 1.1	Schematic structures of GAGs.	9
Figure 1.2	Structure of different types of CS	16
Figure 1.3	Schema of the biosynthetic assembly of the GAG backbones by various glycosyltransferases.	20
Figure 1.4	HS chain elongation	22
Figure 1.5	Pathways of CS/DS chain elongation	24
Figure 1.6	Primary glycosidic linkages cleaved by Heparin lyases	32
Figure 1.7	Unsaturated disaccharides derived from HS by	34

	enzyme catalysed elimination	
Figure 1.8	Glycosidic linkages cleaved by chondroitin lyases	37
Figure 1.9	Unsaturated disaccharides derived from chondroitin sulfate by enzyme catalysed elimination	38
Figure 1.10	Stages involves in tumour angiogenesis	46
Figure 1.11	The cell cycle showing the two major events that takes place within the cell	49
Figure 1.12	The four stages of mitosis	51
Figure 1.13	The cell cycle and its regulation by cyclins, CDKs, and CDKIs	52
Figure 1.14	The processes involved in apoptosis	66
Figure 1.15	Stages of apoptosis	69
Figure 1.16	Morphology of apoptosis	71
Figure 1.17	Activation of apoptosis signaling pathway	75
Figure 1.18	Intrinsic and extrinsic pathway	79
Figure 1.19	Differences between apoptosis and necrosis	89
Figure 3.1	MTT cell viability assay for MDA468 cells after treatment with cockle derived and commercially sourced GAG chains	109
Figure 3.2	MTT cell viability assay for MDANQ01 cells after treatment with cockle derived and commercially sourced GAG chains	111
Figure 3.3	MTT cell viability assay for MOLT-4 lymphoblastic leukaemia cells after treatment with cockle derived and commercially sourced	113

## GAG chains

Figure 3.4	Concentration-dependent effect of Cockle GAG mixtures on K562 erythroleukaemia cell viability	115
Figure 3.5	MTT cell viability assay for normal fibroblast (3T3) cells after treatment with cockle GAGs	117
Figure 3.6 (i)	Cell cycle analysis of MOLT-4 lymphoblastic leukaemia cell line following treatment with 50µg/ml of cockle GAG extracts	119
Figure 3.6 (ii)	Cell cycle analysis of MOLT-4 lymphoblastic leukaemia cell line following treatment with low concentration (20µg/ml) of cockle GAG extract.	123
Figure 3.7	Detection of Apoptotic MOLT-4 cells treated with cockle GAG by Annexin V Staining.	126
Figure 3.8	MTT cell viability assay for MDANQ01 cells after treatment with Whelk extract and commercial GAGs	130
Figure 3.9	Concentration-dependent effect of whelk GAG extracts on MDA468 breast cancer cell viability	132
Figure 3.10	MTT cell viability assay for MOLT-4 and K562 leukaemia cells after treatment with whelk GAG extracts	134
Figure 3.11	MTT cell viability assay for HELA cervical cell after treatment whelk GAG extracts	136
Figure 3.12	MTT cell viability assay of normal fibroblast 3T3 cells after treatment with whelk GAGs extracts	138
Figure 3.13	MTT cell viability assay for MDANQ01 and MDA468 breast cancer cells after treatment with	140

heparinase depolymerised whelk GAG extracts

Figure 3.14	Cell cycle analysis of MDANQ01 breast cancer cell line following treatment with crude whelk GAG extract	142
Figure 3.15	Cell cycle analysis of MDA468 breast cancer cell line following treatment with crude whelk GAG extract	145
Figure 3.16	Detection of Apoptotic MDA468 breast cancer cells treated with crude whelk GAG extracts by Annexin V Staining	149
Figure 3.17	Detection of Apoptotic MDANQ01 breast cancer cells treated with crude whelk GAG extracts by Annexin V Staining	152
Figure 3.18	Detection of apoptotic MDA468 cells by DAPI fluorescent microscopy following treatment with crude whelk GAG extracts	155
Figure 3.19	Detection of apoptotic MDANQ01 cells treated with crude whelk GAG mixtures by DAPI fluorescent microscopy	157
Figure 3.20	Detection of Apoptosis in HELA cells by Annexin V Staining following treatment with whelk GAG extracts	160
Figure 3.21	Detection of apoptotic HELA cells by DAPI fluorescent microscopy following treatment with whelk GAG	162
Figure 3.22	Ion-exchange chromatography elution profile for whelk GAG extracts	165
Figure 3.23	MTT cell viability assay for MDANQ01 breast cancer cells after treatment with GAG mixtures	170

	and purified fraction E	
Figure 3.24	Concentration-dependent effect of purified whelk GAG fraction E on MDA468 breast cancer cell viability	172
Figure 3.25	Cell cycle analysis of MDA468 breast cancer cell line following treatment with purified whelk fraction E	174
Figure 3.26	Detection of Apoptotic MDANQ01 breast cancer cells treated with purified whelk fraction E by Annexin V Staining	176
Figure 3.27	Detection of Apoptotic MDANQ01 breast cancer cells treated with purified whelk fraction E by Annexin V Staining	179
Figure 3.28	Detection of time-dependent Apoptotic MDA468 breast cancer cells treated with purified whelk fraction E by Annexin V Staining	181
Figure 3.29	Kinetic of chondroitinase ABC enzyme degradation of commercial CS	187
Figure 3.30	Analytical TSK2000PW gel-filtration profiles of HS/Heparin and crude cockle GAGs after complete digestion with Heparinase I, II and III enzymes	193
Figure 3.31	Superose 12 size exclusion chromatography and cellulose acetate dot blotting result for crude cockle GAG mixture	194
Figure 3.32	PAGE analysis of enzymatic depolymerised GAGs.	196
Figure 3.33	Kinetic of chondroitinase ABC enzyme degradation of GAGs	199
Figure 3.34	PAGE analysis of enzymatic depolymerised GAGs	203
Figure 3.35	Superose 12 size exclusion chromatography and cellulose acetate dot blotting assay of crude whelk GAG extract	205

Figure 3.36	Analytical TSK2000PW gel-filtration profiles of HS/heparin and purified whelk fraction E after complete digestion with Heparinase I, II and III enzymes	215
Figure 3.37	PAGE analyses of enzymatic depolymerised whelk derived and commercial GAGs.	217
Figure 3.38	Superose-12 size exclusion chromatography and cellulose acetate dot blotting assay for purified fraction E GAG mixtures	219
 <b>List of tables</b>		
<b>Table 1</b>	Summary of biological effect of cockle GAGs	127
<b>Table 2</b>	Ion-exchange chromatographic separation of whelk GAG mixtures	158
<b>Table 3</b>	Summary of biological effect of whelk GAG	167
<b>Table 4</b>	Summary of biological effect of fraction E	183
<b>Table 5</b>	Disaccharides compositions of CS/DS-like glycans found in cockle GAG mixtures	186
<b>Table 6</b>	HS Disaccharides compositions from heparinase digest of cockle GAG extracts	190
<b>Table 7</b>	Disaccharides compositions of CS/DS-like glycans found in whelk GAG mixtures	201
<b>Table 8</b>	Disaccharides compositions of CS/DS-like GAGs present in ion-exchange purified whelk peaks B and C	209



<b>Table 9</b>	Disaccharides compositions of HS-like GAGs found in purified whelk fraction E	212
<b>Table 10</b>	Disaccharides compositions of HS-like GAGs found in purified 204 whelk fraction E depolymerised by heparinase III lyase	213

## Abbreviations

$\Delta$	delta
$\mu\text{g}$	microgram
$\mu\text{l}$	Microlitre
2-OST	2-O sulfotransferase
3-OST	3-O sulfotransferase
6-OST	6-O sulfotransferase
aFGF	acidic fibroblast growth factor
AIF	Apoptosis Inducing Factor
AKT	Protein kinase B
Ala	Alanine
ANOVA	Analysis of variance
Apo2L/DR	Apo2 ligand/ Death receptor
Apo3L	Apo3 ligand
APS	Ammonium Per Sulfate
AS	Acharan sulfate
ATIII	Antithrombin III
ATP	Adenosine triphosphate
Bax	BCL2 associated X protein
Bcl-2	B-cell lymphoma protein 2
bFGF	basic fibroblast growth factor
C4ST	Chondroitin 4- O –sulfotransferase
C6ST	Chondroitin 6- O –sulfotransferase
$\text{Ca}^{2+}$	Calcium ion
$\text{CaCl}_2$	Calcium Chloride
CAD	Caspase-Activated DNase
Caspase	Cysteinyl aspartic acid-protease
CD36	Cluster of differentiation 36
CD8+	Cluster of differentiation8+
CDK	cyclin dependent kinase
CDKI	cyclin dependent inhibitors
CE	capillary electrophoresis

ChPF	Chondroitin polymerizing factor.
ChSy	Chondroitin synthase
COO <sup>-</sup>	Carbonic acid
CPD	cetylpyridinium chloride
CS	Chondroitin sulfate
CS GlcAT-II	Chondroitin sulfate GlcA transferase-II
CS/DS2ST	uronyl 2- O –sulfotransferase
CTLs	Cytotoxic T lymphocytes
CZE	Capillary zone electrophoresis
D4ST	Dermatan 4- O –sulfotransferase
DAPI	4',6-diamidino-2-phenylindole
DEAE	Diethylaminoethyl
DIABLO	Direct IAP binding protein with low PI
DISC	Death-inducing signalling complex
DMSO	Dimethyl sulfoxide
DNA	Deoxyribonucleic acid
dp	Degree of polymerization
dp10	decasaccharides
dp2	disaccharides
dp4	tetrasaccharides
dp6	hexasaccharides
dp8	octasaccharides
DR	Death receptor
DS	Dermatan sulfate
ECM	Extracellular matrix
EDAC	1-ethyl-3-(3-dimethylaminopropyl) carbodiimide
EDTA	Ethylenediaminetetraacetic acid.
ER	Eostrogen receptor
ER <sup>-ve</sup>	Eostrogen receptor negative
ER <sup>+ve</sup>	Eostrogen receptor positive
EXT	Exostosin glycosyltransferase
FADD	Fas-associated death domain
Fas	Fatty acid synthetase

FasL	Fatty acid synthetase ligand
FasL/ FasR	Fatty acid synthetase ligand /Fatty acid synthetase receptor
FasR	Fatty acid synthetase receptor
FCS	fetal calf serum
FGF	Fibroblast growth factors
FGFR's	Fibroblast growth factors receptors
FITC	Flourescein isothiocyanate
FPLC	Fast Protein Liquid Chromatography
G1	Gap 1
G2	Gap 2
GAG-PG	Glycosaminoglycans proteoglycans
GAGs	Glycosaminoglycans/Galactosaminoglycans
Gal	Galactose
GalNAc	N-acetyl galactosamine
Gal-NAc4S-	
6ST	GalNAc 4-sulfate 6- O –sulfotransferase
GalNAcT,	GalNAc transferase
GalT	$\beta$ 4-galactosyl transferase
G-CSF	Follistatin Granulocyte colony-stimulating factors
GlcA	Glucuronic acid
GlcAT	$\beta$ 3-GlcA transferase
GlcNAc	N-acetyl glucosamine
GlcNAc(6S)	6-O-sulfated N-acetylglucosamine
GlcNS	N-sulfoglucosamine
GlcNS(6S)	6-O-sulfated N-sulphoglucosamine
GlcUA	$\beta$ -D-glucuronic acid
Gly	Glycine
HA	Hyaluronic acid
HCG	Human chorionic gonadotropin
HCl	Hydrochloride acid
HEPES	2-[4-(2-hydroxyethyl)piperazin-1-yl]ethanesulfonic acid
HGF	Hepatocyte growth factor
HS	Heparan sulfate

HS-GAGs	Heparan sulfate glycosaminoglycans
HSPG	Heparan sulfate proteoglycans
IAP	inhibitors of apoptosis proteins
IC <sub>50</sub>	half maximal inhibitory concentration
ICAD	Inhibitor of Caspase Activated DNase
IdoA	Iduronic acid
IdoA (2S)	2-O-sulfated IdoA
IdoUA	$\alpha$ -L-iduronic acid
Ig	immunoglobulin-like
Kb	kilo bytes
kDa	Kilodalton
KS	Keratan sulfate
LDL	low density lipoprotein
L-IdoA	L- iduronic acid
M	Mitosis
Mg <sup>2+</sup>	Magnesium Ion
ML	Millilitre
mM	millimolar
MOPS	3-(n-Morpholino) Propanesulfonic acid
MPT	mitochondrial permeability transition
MTT	3-(4,5-Dimethylthiazol-2-yl)-2,5-Diphenyltetrazolium Bromide
NDST	N-deacetylase, N-sulfotransferase
nm	nanometre
NO	Nitric oxide
NuMA	Nuclear mitotic apparatus protein
O-Ser	O Serine
PAGE	polyacrylamide gel electrophoresis
PAP	3' Phosphoadenosine 5' phosphosulfate
PARP	Poly (ADP-ribose) polymerase
PBS	Phosphate Buffer Saline
PI	propidium iodide

pRB	retinoblastoma gene products
Procaspase-8	Pro cysteinyl aspartic acid-protease 8
Rb	Retinoblastoma
RIP	Receptor-interacting protein
ROS	Reactive oxygen species
Rpm	Rotation Per Minute
RPMI	Roswell Park Memorial Institute
Rt	retention time
RTKs	receptor tyrosine kinases
S	Synthesis
SDS-PAGE	sodium dodecyl sulfate-polacrylamide gel electrophoresis
SEM	Standard Error of Mean
Ser	Serine
SGBS	Simpson–Golabi–Behmel syndrome
SMAC	Second mitochondrial activator of caspase
SNPs	Single nucleotide polymorphisms
SO <sub>3</sub>	Sulfur trioxide
SRC	Steroid receptor coactivator
TEMED	N,N,N',N'-Tetramethylethylenediamine
TGF-β	tumour growth factor beta
Th2	Type 2 helper
TK	Tyrosine kinase
TKR's	Tyrosine kinase receptors
TNF	tumour necrosis factor
TNFR1	Tumour necrosis factor receptor
TNF-α	tumour necrosis factor alpha
TRADD	TNF receptor-associated death domain
Tris	Trizma base
UCN-01	7-hydroxystaurosporine
UDP	Uridine diphosphate
UV	Ultraviolet
V <sub>0</sub>	Void volume
VEGF	Vascular endothelial growth factor

$V_t$	Final volume
Xyl	Xylose

## **Acknowledgement**

I dedicate this thesis to God almighty and the three special people in my life: my husband and our twins, David and Esther. Thank you for your support and understanding. I would like to thank my parents and my in-laws for their prayers and support over the past four years.

My sincere appreciation is also extended to Dr Jeremy Allen, Dr Lucy Smith, Helen and Ross for their support and training in fluorescent microscopy. Jeremy spent many hours with me in the laboratory to ensure I achieved the best results. I also appreciate the immense contribution of Ray (a former cell culture laboratory technician) during my cell culture assay in his laboratory. I would also like to thank Eyad for providing all the necessary support and help for my apoptosis detection assay. I am also grateful to the laboratory technicians in the Cockcroft Building for their unflicking technical and moral support throughout my laboratory work.

I appreciate all the contributions of my colleagues, the masters and the placement students in Dave's laboratory. I would also like to thank Drs James Wilkinson, Elder Rhoderik and Natalie Ferry for their help and support over the past four years. Jon Deakon is also highly appreciated for his professional support and help each time I became stuck with GAGs palava. ELS staff (Catriona and others) have been wonderful and supportive throughout my study. I also appreciate my mum for coming all the way from Nigeria to help care for my babies while I was busy writing this thesis. All my friends and family have been very supportive over the past four years. My sincere thanks also goes to my able boss and mentors back home, Professors E.O Agbedana, J.I Anetor, J.O Moody, J. Omotade, A. Sowumi, F.A.A Adeniyi, G.O Arinola and C.O Falade.



Finally, my sincere appreciation goes to my supervisor, Dr David Pye, for giving me unrestricted access to his office and providing invaluable advice and support. Without him, this work could not have been achieved.

## **Abstract**

Glycosaminoglycans (GAGs) are a family of complex mixture of linear polysaccharides that are present in both vertebrates and invertebrates. This polysaccharide plays important roles in physiological and pathological conditions, including cancer. In this study, GAGs were isolated from two different fish (whelks and cockles) belonging to mollusc invertebrates. The crude GAGs isolated from each shellfish demonstrated variable selective anti-cancer activities against many cancer cell lines including breast (MDANQ01 and MDA468), leukemia (MOLT-4 and K562) and ovarian (HeLa) cancer. None of the commercial GAGs exhibited any anti-cancer activities against all the cancer cells studied. Previous studies conducted on the isolation of GAGs from molluscs reported mainly its anti-coagulant and anti-inflammatory activities; thus neglecting its record of anti-cancer activity.

All purified whelk fractions (A – D & F) obtained failed to show any anti-cancer activity; with the exception of fraction E, which showed equal levels of selective anti-cancer activity against breast cancer cells. Mechanism of cell death caused by the three novel GAGs on cancers cells were investigated via cell cycle analysis and apoptosis detection assay. Cell cycle analysis revealed significant perturbations in the cancer cell cycle showing cell cycle arrests at different stages. Similarly, there were significant apoptosis inductions induced by the three novel GAGs on each of the cell lines investigated.

Structural elucidations of the two fish GAGs, using chemical, enzymatic, Polyacrylamide, Superose 12 size exclusion chromatography , gel filtration and SAX-HPLC methods of analysis, revealed the presence of both chondroitin sulfate (CS)/dermatan sulfate (DS)-like and HS-like GAGs. Discrepancies in the structural elucidations of the novel GAG mixtures and the commercial GAGs may be partly responsible for the anti-cancer activity of the novel polysaccharides, as changes in exogenous GAGs structural composition, especially sulfation levels or patterns, can alter its binding to growth factors, which is essential for cell proliferation.

# **Section 1**

## **Introduction and overall aim of this study**

## 1.0 General introduction

Glycosaminoglycans (GAGs) are a family of linear, complex, polydisperse polysaccharides extracted and purified from different animal tissues (Cassaró and Dietrich, 1977; Heinegård and Sommarin, 1987; Pejler *et al*, 1987a). They are very heterogeneous polysaccharides in terms of relative molecular mass, charge density, physico-chemical properties, biological and pharmacological activities (Jackson *et al*, 1991). GAGs are ubiquitous in nature, occurring in a wide variety of organisms, including both vertebrates and invertebrates. They are linked typically to a protein core in order to form proteoglycans. These anionic polysaccharides elicit many biological functions, largely through their interaction with proteins (Cesaretti *et al*, 2004). Major GAGs in vertebrates and invertebrates include heparin, heparan sulfate (HS), chondroitin sulfate/dermatan sulfate (CS/DS), chondroitin sulfate (AS), and hyaluronic acid (HA) and keratan sulfate (KS).

All GAGs chains except KS comprise alternating units of an amino sugar, either *N*-acetyl-D-glucosamine (GlcNAc) or *N*-acetyl-D-galactosamine (GalNAc) and a hexuronic acid (HexA), either glucuronic acid (GlcA) or iduronic acid (IdoA). Keratan sulfate contains GAGs chains comprising of galactose attached to acetyl-D-glucosamine (Afratis *et al.*, 2012; Yamada *et al*, 2011). HS and heparin are the most widely studied of these polysaccharides due to their involvement in many important biological processes. They have been shown to play important roles in the control of stem cell growth and differentiation (Patel *et al*, 2014 and Desai 2013). Moreover, they are involved in a number of important biological activities, such as developmental processes, angiogenesis, blood coagulation, cell adhesion and tumour metastasis (Sasisekharan *et al*, 2006; Wei *et al*, 2005; Vives *et al*, 1999; Lindahl *et al*, 1998; Salmivirta *et al*, 1996).

HS is also vital in regulation of embryonic development, as well as in pathophysiological conditions, such as inflammation, wound healing, angiogenesis and cancer (Tamm et al 2012: Lo et al, 2011: Sasisekharan et al, 2006). These activities are facilitated by the ability of HS proteoglycans (HSPG) to interact and regulate proteins, such as enzymes, cytokines, growth factors, and extracellular matrix (ECM) biomolecules (Wei et al, 2005: Vives et al, 1999). The divergent structure of HS allows it to bind to and regulate the activity of various growth factors, like fibroblast growth factors 1, 2, 4 etc (FGF-1, FGF-2, FGF-4 etc), chemokines, morphogens and enzymes at the cell surface and in the ECM: hence influencing cell adhesion, motility, growth and differentiation (Lo et al, 2011: Sasisekharan et al, 2006: Vives et al, 1999). The ability of HS to modulate the activities of many so-called heparin-binding growth factors, serve to co-ordinate the interaction of FGF with their tyrosine kinase receptors (FGFRs); moreover, this appears to play a critical role in receptor dimerization and activation (Iozzo and San Antonio 2001: Dickson et al 2000: Vives et al, 1999: Ernst et al, 1995). The modulatory effect of HS is critical to angiogenesis that occurs in pathological conditions, including tumour growth and progression; this has been implicated in the vascularisation of all solid tumours (Iozzo and San Antonio, 2001).

Biological activities of HS depend broadly on the interaction between polysaccharides and proteins, which appears to be mediated by distinct saccharides sequences within HS chains. Moreover, the expression of different sequences within the HS chains demonstrates various levels of specificity, selectivity and molecular organisation. Modulation of tumour growth occurs through the interaction with angiogenic growth factors, like FGF-10, or with negative regulators of angiogenesis like anti-angiogenic antithrombin III (Iozzo and San Antonio, 2001: Ernst et al, 1995).

The modulatory effects of HS on the growth factors and chemokines involved in tumour angiogenesis have been suggested to be mediated through one of the following mechanisms:

The voluntary binding of the growth factors to soluble ECM associated or cell-surface HS results in the fine control of the bioavailability of growth factors; for example, binding of tumour growth-factor beta (TGF- $\beta$ ) to betaglycan, a cell-associated PG, and decorin, which is present in the ECM, and also for fibroblast growth-factor-2 (FGF-2) that binds basement membrane perlecan in addition to cell-membrane syndecans (Mellor et al, 2007 and Massague 1992).

The binding of HS to growth factors protects them from proteolytic degradation and acid inactivation (Samuel et al, 2000: Szabo 1991 and Saksela et al, 1988).

HS modulates the access of FGF growth factors to specific signaling receptors by different mechanisms that may involve independent interaction of HS with an aspect of the transmembrane tyrosine kinase glycoprotein component of the FGFR complex (Kan et al, 1993).

HS may also trigger an intracellular transduction signal by interacting directly with growth-factor receptors with no growth factors being present (Rusnati et al, 1993).

Indeed, Rusnati and others have reported that heparin/HS can activate FGFRs in the absence of the growth-factor. This observation goes against the traditionally accepted proposal of a ternary complex involving GAGs, growth factors, and tyrosine kinase (TK) receptors (Rusnati et al, 1993). The introduction of this model led to an extensive study involving many research groups and there is still much debate on actual mechanisms by which GAGs mediate the activation of the FGF's. Regardless of this debate some general properties of the signalling complex can be surmised and these are outlined below:

Heparin/HS-related molecules can be useful tools to modulate the biological activity of heparin-binding angiogenic growth factors and cognate TK receptors (Mellor et al, 2007).

Heparin/HS-related molecules can be designed with various structures that are able to affect differently the biological activities of angiogenic growth (Mellor et al, 2007).

The ideas expressed above show some promise, therefore, there is need for the development of inhibitors of the activation of growth factors by GAGs and the subsequent development of new anti-cancer treatments aimed at the inhibition of tumour-cell proliferation.

The ability of low molecular weight heparin fragments administered systemically to reduce the angiogenic activity of FGF2 and vascular endothelial growth-factor (VEGF) validate this hypothesis (Ghandi and Mancera, 2010; Norrby 2000: Norrby and Ostergaard 1997 and 1996). Consequently, many HS/heparin fragments and mimics have been shown to have potential as inhibitors of tumour angiogenesis. In addition to the role played by HS in regulation of tumour angiogenesis, we shouldn't forget the potential roles for HS in directly regulating the growth of cancers through interactions at the tumour cell surface. The structural complexity of tumour-cell HS (both at the cell surface and extruded into the ECM) has been shown to play vital roles in tumour development. It enables them to modulate directly several aspects of tumour-cell phenotype, including growth kinetics, invasiveness and metastatic potential (Sasisekharan et al, 2002). Hence, a given tumour-derived HS-GAG or HSPG can be protumorigenic or antitumorigenic, depending on whether it is anchored at the cell surface or present in the ECM as soluble-free GAGs or/and depending on the HS-GAG sequence ( Gomes et al., 2013: Liu et al, 2002 and Sasisekharan et al, 2002).

Targeting tumour angiogenesis by interfering with the interaction of HS with angiogenic growth factors is a well-established model for the development of HS mimetic therapeutics. However, we shouldn't forget the ability of HS to modulate the growth and development of tumours via other mechanisms. This could certainly lead to the determination of, as yet unknown, HS structures and interactions that could pave way toward the development of novel cancer therapeutics.

The study describe in this thesis employs GAGs derived from shellfish in a novel approach that targets directly the growth of cancer cells, rather than the vasculature and angiogenic processes within the tumour. The anti-cancer activity of these shellfish-derived GAGs is a unique finding, with none of the commercially derived GAGs from mammalian sources demonstrating any anticancer activity.

The GAGs derived from these shellfish have not been characterised in terms of their structure, and their therapeutic effect on cancer cells is not reported in the literature.



## 1.1 Glycosaminoglycans

GAG's are natural heteropolysaccharides, belonging to the family of polyanionic polysaccharides. These highly negatively-charged polysaccharides are ubiquitous in nature, occurring in a wide variety of organisms and tissues attached typically to a protein core to form molecules known as proteoglycans (PGs). They are composed of repeating disaccharides units comprising either sulfated or non-sulfated disaccharides. Their properties have been shown to vary considerably depending on the tissue or cell type from which they are extracted. (Andrade et al, 2013; Vijayabaskar and Somasundaram 2012; Afratis et al, 2011; Heinegard and Sommarin 1987; Pejler et al, 1987; Cassaro and Dietrich 1977).

GAGs elicit numerous biological functions, largely through their interaction with proteins, including growth factors.

GAGs are found located within the cell membrane and in the extra-cellular matrix (ECM). They act by binding selectively to a variety of proteins and pathogens and are crucial to many disease processes, such as inflammation, neurodegeneration, angiogenesis, cardiovascular disorders, cancer and infectious diseases (Ghandi and Mancera et al, 2010; Mark et al 2002).

The GAG family has several archetypal members including heparan sulfate (HS), heparin, chondroitin sulfate/ dermatan sulfate CS/DS, keratan sulfate (KS) and chondroitin sulfate (AS). There is also the non-sulfated GAGs consists of hyaluronic acid HA (Figure 1.1). HA lack a covalently protein core and are generally synthesised at the intracellular surface of the plasma membrane. HA GAGs has been reported to be a key player in tissue homeostasis, cancer progression, inflammatory conditions, myocardial infarction and angiogenesis (Afratis et al., 2012; Slevin et al., 2002). HS and heparin are the most widely studied members of the GAG's family, because of their involvement in many biological activities including

angiogenesis, cell proliferation, wound healing, inflammation etc (Afratis et al., 2012; Vives et al, 1999; Gallagher et al, 1986).

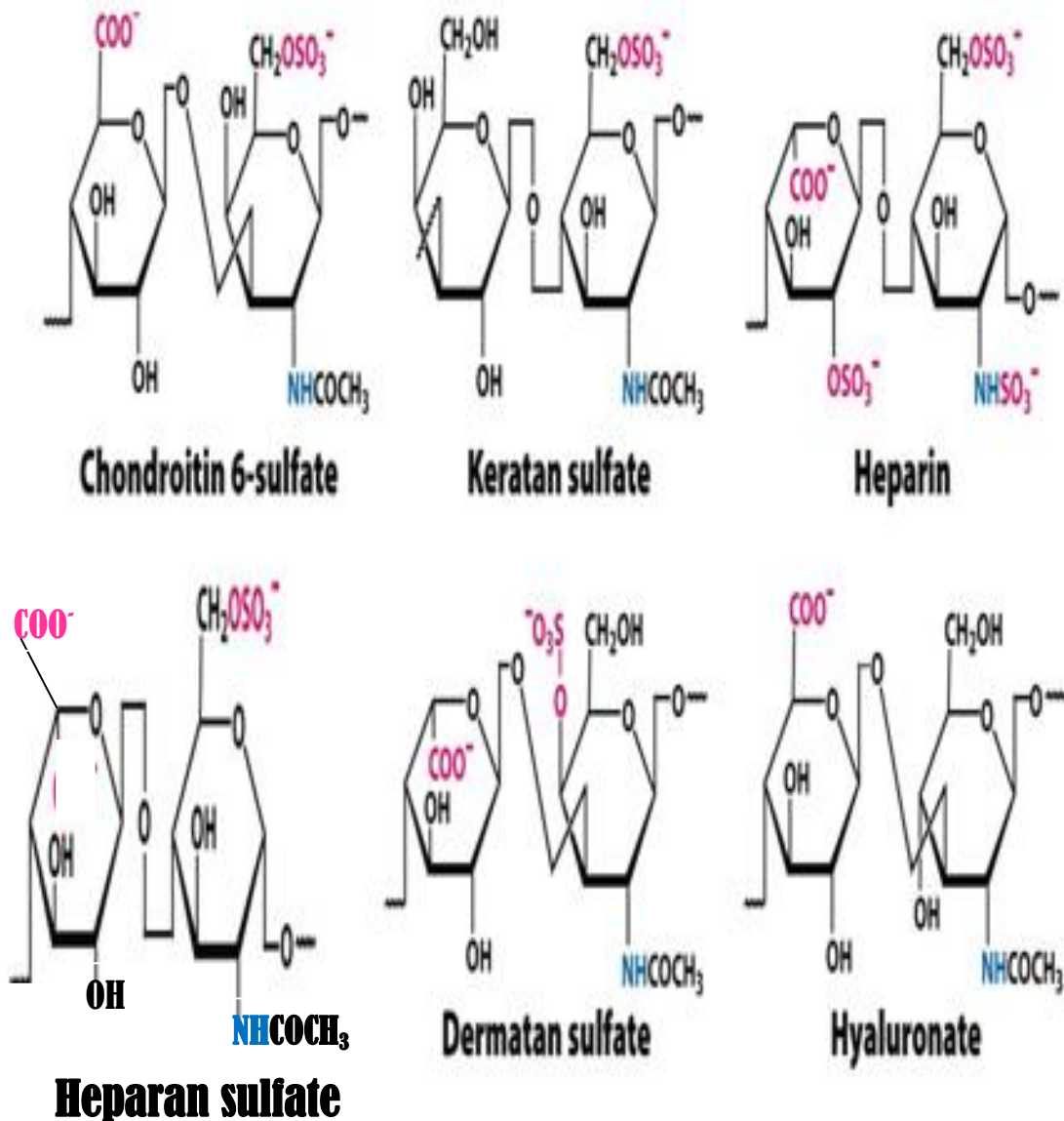


**Fig. 1.1: Schematic structures of GAGs.**

Heparin/HS and HA are glycosaminoglycans; chondroitin sulfate (CS) and dermatan sulfate (DS) are galactosaminoglycans; KS is a sulfated polyglucosamine. Abbreviation: R= H or SO<sub>3</sub>; R'= SO<sub>3</sub> or COCH<sub>3</sub>

## 1.2 GAG's structure and functions

GAGs comprise a linear chain of 10–200 disaccharide units of repeating *N*-acetyl-D-glucosamine/galactosamine, which is linked to uronic acid (iduronic or glucuronic acid) (Tumova et al, 2000: Lindahl et al, 1998). The disaccharide repeat unit can be modified to include *N*- and *O*-sulfation and also epimerisation of  $\beta$ -D-glucuronic acid to  $\alpha$ -L-iduronic acid (Conrad, 1998). In addition, the five different modifications for disaccharides give rise to  $2^5 = 32$  combinations. Thus, this modification makes the complexity of the GAG much greater than that of proteins, which are made up of 20 amino acids. With these 32 building blocks, a GAG octasaccharide could have in excess of a million possible sequences; thereby making HS-GAGs not only the most acidic, but also the most information-dense biopolymers found in nature (Conrad, 1998).

The physical form of GAGs and the specific interactions between them and other ECM components are controlled frequently by the sequence of disaccharide residues that they are comprised of. Usually, GAGs interact with transient components of the ECM, either at the cell surface, in solution or sequestered in the matrix. For instance, FGF-2 induced endothelial-cell proliferation requires trimolecular interactions between FGF-2, FGF -TK receptors (FGFR) and HS (Jaye et al., 1992: Kiefer et al, 1991: Klagsbrun and Baird, 1991: Yayon et al, 1991). This interaction activates TK activity of the intracellular domain of the FGF receptor, which, in turn, leads to secondary messenger activation (Dickson et al., 2000).

### 1.3 Heparin/HS structures and functions

Heparin/HS, usually isolated from animal tissue including vertebrates and invertebrates, is an important and chemically-distinct polysaccharide of considerable biological relevance. As explained above they are polydisperse, highly sulfated, linear polysaccharides, consisting of a repeat unit of uronic acid in either of its glucuronic or iduronic form attached to D-glucosamine residues (Figure 1.1) ( Koo et al., 2008; Volpi et al, 2005; Islam and Linhardt, 2003). This group of GAGs have a very complex structure yet they are the most widely studied members of the GAG family. The structural complexity of Heparin/HS can be considered at both PG and GAG levels;

At the PG level, different numbers of polysaccharide chain (possibly with different disaccharide sequences) can be attached to the various serine residues present in the protein core (Koo et al, 2008).

At the GAG level, some of HS/Heparin structural complexity results from their polydispersity.

GAG especially heparin has a molecular weight ranging from 5-40kDa (degree of polymerisation (dp) 10-80) with an average molecular weight of 13 kDa. Heparin/ HS structure has been partially characterised by studying their biosynthesis (Kjellen et al, 1992). Twelve sulfation profiles for HS/heparin disaccharides have been reported and these have equally been resolved and characterised by various separation techniques including chemical, enzymatic, and spectroscopic techniques (Malavaki et al., 2011; Sasisekharan et al., 2006; Linhardt, 1991).

Problems arise in the structural analysis of HS/Heparin GAGs since they are extensively modified by *O*- and *N*-sulfation in addition to isomerisation of the iduronic acid making them

the most structurally diverse members of the glycosaminoglycan family. The amino group may be either sulfated or acetylated and each disaccharide unit may have up to three of the hydroxyl groups sulfated (2-*O*-S, 3-*O*-S and 6-*O*-S). Glucuronic acid rich polymers are sometimes classed as HS while the iduronic acid rich polymers are also sometimes refers to as heparin. Heparin contain a pentasaccharide region (GlcNAc/NS(6S)-GlcA-GlcNS(3S,6S)-IdoA(2S)-GlcNS(6S) that bind to antithrombin III and this makes it the most widely used carbohydrate based therapeutic because the binding allows it to inhibit blood coagulation (Loganathan et al,1990: Marcum and Rosenberg,1989a: Linhardt et al,1988b: Atha et al,1985: Lindahl et al, 1984). Relating structure to biological activities, such as that described for heparin, is critical in our understanding of the role sulfation patterns and epimerisation play in the natural function of heparin/HS chains.

Sulfation patterns of HS/heparin play a very crucial role in their interactions with growth factors, proteins and cytokines, and therefore may affect their biological roles. HS/heparin have been implicated in numerous biological processes at the cell–tissue–organ interface ( Malavaki et al., 2011: Conrad 1998), which are triggered mainly by their interactions with a wide range of proteins, such as cofactors of the coagulation cascade, extracellular-matrix components and a variety of cytokines and growth factors (Vives et al 1999: Permimom and Belfield, 2000), angiogenesis (Sasisekharan and Venkataraman, 2000), viral invasion (Shukla et al, 1999 and Chen et al, 1997), and anticoagulation (Petitou et al, 1999).

The HS/heparin also exerts its modulatory effects on key biological processes by binding to growth factors, cytokines, morphogens, enzymes and other signaling molecules (Taipale and Keski-Oja, 1997). They can regulate the activity of signaling molecules by modulating their diffusion, receptor on and off rates, and effective concentration at the cell surface and

the ECM, However, these processes become especially important at the cell–tissue–organ interface.

Previous studies have added an extra dimension to this cell-surface event by indicating that HS mediates dimerization, either of FGF-2 or FGF receptor or of both, which may be a requirement for signal transduction (Ornitz et al, 1996; Pantoliano et al, 1994; Springer et al, 1994; Mascarelli et al, 1993; Ornitz et al, 1992). The binding of HS chains to FGF-2 and FGFR occurs through *N*-sulfated glucosamine (GlcNS) and 2-*O*-sulfated iduronic acid (Ido2S) units or 6-*O*-sulfated glucosamine (Glc6S). Once the FGFs bind to their receptors, FGFR complexes dimerise, in conjunction with HS/heparin moiety, leading to the activation of tyrosine kinase through autophosphorylation. Ultimately, these events facilitate the binding of second messenger proteins which in turn trigger many other intracellular signalling (Gallagher 2001; Dickson et al 2000).

The various roles played by these polysaccharides are becoming clearer as researchers continue studying them.

#### **1.4 CS structure and functions**

Chondroitin and dermatan sulfate make up a second GAG family, also known as galactosaminoglycans. These polysaccharide chains are, again as in HSPG's, normally found covalently bound to a protein core forming high molecular weight units, with a large number of GAG chains attached (Ernst et al, 1995). The basic structural unit of this class of GAG is a disaccharide in which a uronic acid (D-glucuronic and L-iduronic acid) is attached ( $\beta 1 \rightarrow 3$ ) to *N*-acetyl galactosamine (Figure 1.1). CS is the most abundant GAG in the body skeletal muscle and soft tissue.

There are various sulfation patterns of CS and among the most studied sulfated CS GAGs are the two common isomers CS-A (*O*-sulfo group attached at position 4 of galactosyl residue) and CS-C (*O*-sulfo group attached at position 6 of galactosyl residue) see Figure 1.2. Similarly, disulfated CS are also classified as CS-D (*O*- sulfo group attached at position 2 of glucuronic acid and position 6 of galactosyl residue) or CS-E (*O*- sulfo group attached at position 4 and 6 of galactosyl residue). The other CS isoform formerly designated as CS-B is called DS which is characterised by the presence of IdoA moiety in his disaccharide chains. Similar to HS/heparin, the various sulfation patterns of CS GAGs enable specific interaction with many molecules, including growth factors, cytokines, chemokines, adhesion molecules and lipoproteins (Asimakopoulou et al., 2008).

The size of CS chains varies greatly, with an average of about 40 repeating disaccharides units for the cartilage proteoglycans, corresponding to a molecular weight of approximately 20,000 (Iozzo, 1985). Their sulfo group content also varies depending on the number(s) attached to both or either of the galactosyl and uronic acid residues (Iozzo, 1985). Once again they all show a considerable degree of microheterogeneity within the polymer chain in a manner very similar to HS. The disaccharide unit present in CS/DS may be non-sulfated, mono-sulfated or disulfated and both iduronic and glucuronic acids may be present in a given polymer chain.

DS (CS-B) is a polydisperse; microheterogenous sulfated copolymer of D-Gal-NAc and primarily L- iduronic acid (L-IdoA), with *O*-Sulfate groups most commonly attached to position 4 of the galactosyl residue and position 2 of the L- Iduronic acid residues (Linhardt and Hileman, 1995). Many DS core proteins such as decorin and biglycan have been identified (Kresse et al, 1993: Coster, 1991). Decorin and biglycans have been reported to play vital roles in many biological activities including organisation of collagen fibrils,



regulation of the extravascular activities of thrombin, act as anticoagulants by inhibiting thrombin and lipid metabolism (Pangrazzi and Gianese, 1987). ). CS-B or DS is abundant in skin and is also found in heart valves, tendons and arterial walls. It is made up of linear repeating units containing D-galactosamine and either L-iduronic acid. Its molecular weight ranges from 15,000 to 40,000 daltons.

Moreover, CS-A is commonly found in humans in cartilage, bone, cornea, skin and the arterial wall. The molecular weight of CS-A ranges from 5,000 to 50,000 daltons and contains about 15 to 150 basic units of D-galactosamine and D-glucuronic acid (Wastenson, 197). CS-C, is primarily found in fish and shark cartilage, but also in humans, is also made up of linear repeating units of D-galactosamine and D-glucuronic acid.

## Chondroitin A B C GAGs

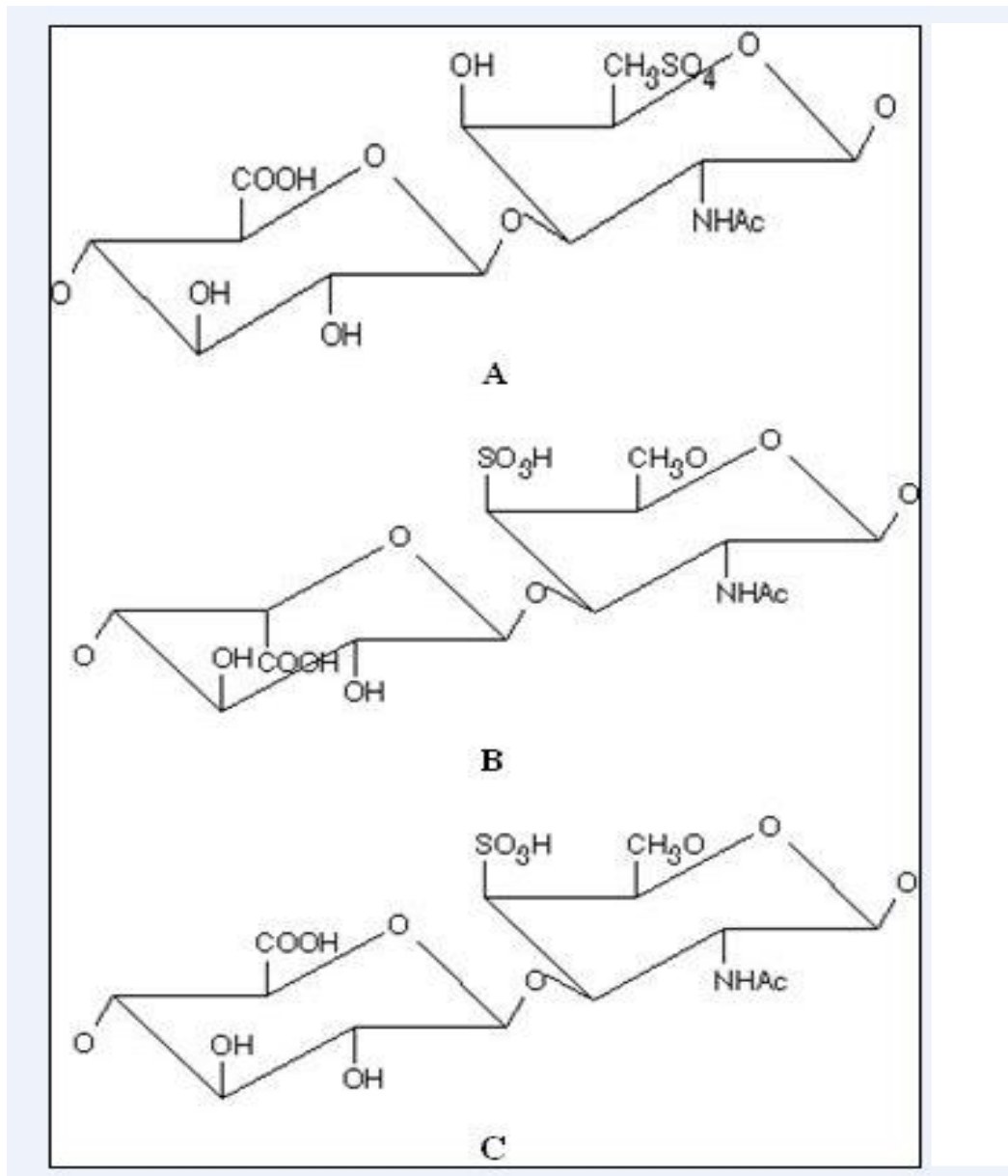


**Figure 1.2: Structure of different types of CS**

(A) Chondroitin-6-Sulfate; (B) DS; (C) Chondroitin-4-Sulfate

## 1.5 Glycosaminoglycans isolated from shellfish

Many researchers, including Dietrich and co-workers, reported the isolation of GAGs similar to heparin with comparable anti-thrombin activities from mollusc's invertebrates. Similarly, heparin-like substance with relative ability to bind antithrombin III (ATIII) has been isolated from the marine clams, *anomalocardia brasiliiana* (Pejler et al, 1987; Dietrich et al, 1985). Another GAG similar to heparin GAG, with an AT-binding region comparable to that of mammalian heparin has also been purified from another clam species, *Mercenaria mercenaria* (Jordan and Marcum, 1986). Additionally, heparin, (a highly sulfated polysaccharide, commonly isolated from mast cell or mucosa and also used as an anticoagulant in the clinic) (Bjork and Lindahl, 1982) has been reported to have some other biological activities, such as; anti-viral activity, bind to a variety of growth factors, inhibit complement activation, and regulate angiogenic activity (Weiler et al, 1992; Jackson et al, 1991; Casu 1985; Folkman et al, 1983).

## 1.6 Biosynthesis of GAGs

HS and CS are synthesised in the Golgi, whereby the individual GAG chains are O-linked to a core protein, forming a large polysaccharide-protein conjugate known as proteoglycan (PG) (Sasisekharan et al, 2006; Silbert and Sugumaran, 2002; Sugahara and Kitagawa, 2002). However, KS can be either N-linked or O-linked to the core protein of the PG (Funderburgh 2002). HA is not synthesised in the Golgi from the core protein but rather by an integral plasma membrane synthase, which secretes the nascent chain immediately (Itano and Kimata, 2002). All GAGs, with the exception of HA, are biosynthesised as proteoglycans and the linkage region is the same in all, except for keratan sulfate. This

linkage region consists of the tetrasaccharide; glucuronic acid (GlcA), galactose (Gal), Gal, and xylose (Xyl)-linked to the hydroxyl group of serine in the polypeptide core (Sugahara and Kitagawa, 2000). Biosynthesis of all GAGs, except HA is initiated from a core protein, rich in serine-glycine repeats, which create the platform for the attachment of one or more GAG chains via the linkage region (Kimura et al, 1984). Contrarily, HA GAGs lack a covalently bound protein core and is synthesised at the intracellular surface of the plasma membrane (Afratis et al., 2012)

Biosynthesis of GAG is a complex non-template-driven process that involves many enzymes that assemble the GAG polymer and then sulfate them at specific positions. GAGs are synthesised as homopolymers, which are modified subsequently by N-deacetylation and N-sulfation. This is followed by numerous modifications, including sulfation, epimerisation and desulfation; all of which are performed in a spatiotemporal manner, producing mature and functional GAG chains that exert biological functions dependent on their specific structure. This is common to both types of GAG chain and is formed through the stepwise addition of each monosaccharide residue by the respective specific glycosyltransferase (Grimshaw,1997).

After the attachment of the linker, the first modification to the chain determines whether the chain matures into a CS or HS. This modification involves the transfer of a GlcNAc (HS) or a GalNAc (CS) monosaccharide. The enzyme GlcNAcT-I transfers GlcNAc to the tetrasaccharide linker, initiating HS biosynthesis (Rohrmann et al, 1985). This enzyme is different from the glycosyltransferase GlcNAcT-II that is involved in the elongation of the HS GAG chains. In the case of CS, the initiating GalNAc residue is transferred to the linker region by the enzyme GalNAcT. It is not very clear whether the activity of this enzyme differs from the GalNAc transferase activity of chondroitin synthase, which is involved in the

chain-elongation process. In all cases real chain-building ensues after the transfer of GlcNAc (HS) or GalNAc (CS) to the linker.

In the case of HS chains, a multidomain glycosyl-transferase successively adds GlcNAc and GlcA; thus, initiating the chain-elongation process. This multidomain enzyme is encoded by EXT1 and EXT2 of the EXT family of genes. Although EXT1 and EXT2 possess the ability to transfer both GlcNAc and GlcA, it has been established that these enzymes form a single oligomeric unit, which is required for complete *in vivo* chain-elongation activity. Similarly, in the case of CS, chondroitin synthase, also a known multidomain enzyme, transfers GalNAc and GlcA successively for chain elongation (Sashisekhare et al, 2006). Molecular cloning has been achieved for four of the glycosyl transferases responsible for the biosynthesis of the linkage region tetrasaccharide (Uyama et al, 2007; Kitagawa et al, 1998).

Firstly, xylosyl transferase (XylT) transfers a Xyl residue from UDP-Xyl to specific serine residues in core proteins in the endoplasmic reticulum and the *cis*-Golgi compartments (Figure 1. 3) (Uyama et al, 2007). Secondly, Two XylTs, XylT-1 and XylT-2, were cloned, and their amino acid sequences found to be significantly homologous. In contrast enzymatic activities were only shown by XylT-1, not by XylT-2. Following the transfer of a Xyl residue, two Gal residues are transferred to the Xyl residue by two kinds of galactosyl transferases (GalTs), GalT-I and GalT-II, in the *cis*- 1-*O*-Ser, in the medial- and trans-Golgi compartments (Figure 1.3) (Uyama et al, 2007).

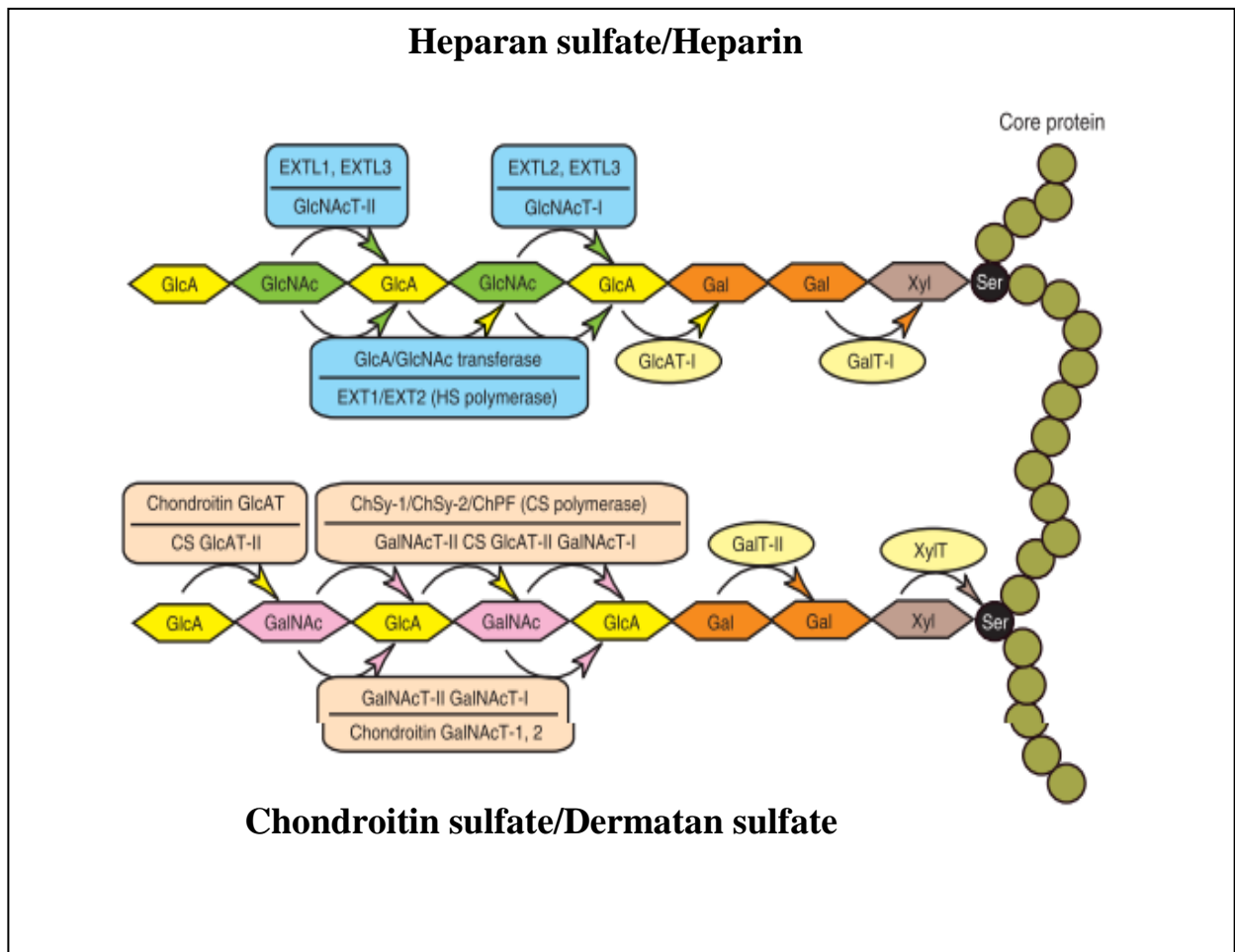


**Figure 1.3; Schema of the biosynthetic assembly of the GAG backbones by various glycosyltransferases.**

A number of glycosyltransferases are required for the synthesis of the backbones of GAG's.e.g XylIT, Xyl transferase; GalT-I, Gal transferase-I; GalT-II, Gal transferase-II, GlcAT-I, GlcA transferase-I; GalNAcT-I, GalNAc transferase-I; CS GlcAT-II, CS GlcA transferase-II;GalNAcT-II, GalNAc transferase-II; CS polymerase, GlcA/GalNAc transferase; GlcNAcT-I, GlcNAc transferase-I; GlcNAcT-II,GlcNAc transferase-II; HS polymerase, GlcA/GlcNAc transferase; ChSy-1, chondroitin synthase-1; ChSy-2, chondroitin synthase-2; and ChPF, chondroitin polymerising factor.

The biosynthesis of the linkage region is completed by the actions of GlcAT-I; transferring a GlcA residue to the linkage trisaccharide, Gal $\beta$ 1 $\rightarrow$ 3Gal $\beta$ 1 $\rightarrow$ 4Xyl $\beta$ . Moreover, one study highlights that the expression level of GlcAT-I correlates well with the amount of

GAGs; thereby suggesting that GlcAT-I regulates the overall expression of GAGs (Uyama et al, 2007). The resulting GAG chain backbone undergoes extensive sulfation modifications, during chain elongation, thus making GAG chains some of the most negatively-charged families of biopolymers in mammalian cells.

### **1.7 Biosynthetic modification of HS-GAG chain (HS chain elongation)**

The nascent HS chain is first modified by N-deacetylase, N-sulfotransferase (NDST), which is a multidomain enzyme that cleaves the N-acetyl group from the GlcNAc monosaccharides and transfers a sulfate group to the N-position. This is followed by the action of the C-5 uronyl epimerase, which converts GlcA to IdoA (Figure 1.4) in selected positions. 2-O-sulfation of the uronic acid by the 2-O sulfotransferase (2-OST) can follow the epimerisation process. The 2-OST acts on IdoA- as well as GlcA-containing HS chains; however, the IdoA containing chains are the catalytically preferred substrates (Pinhal et al, 2001; Rong et al, 2001). The final set of modification enzymes are the 6-O (6-OST) and 3-O (3-OST) sulfotransferases, which sulfate the 6-O and 3-O positions of the GlcNAc moiety, respectively. Many of the above biosynthetic enzymes have distinct isoforms that are selectively expressed in different tissues (Kusche-Gullberg and Kjellen 2003). Four different isoforms of NDST, three different 6-OSTs, and six different 3-OSTs have been characterised in humans and mice (Kusche-Gullberg and Kjellen 2003), they all have different specificities and as a result the wide diversity of HS chains produced by animal cells.

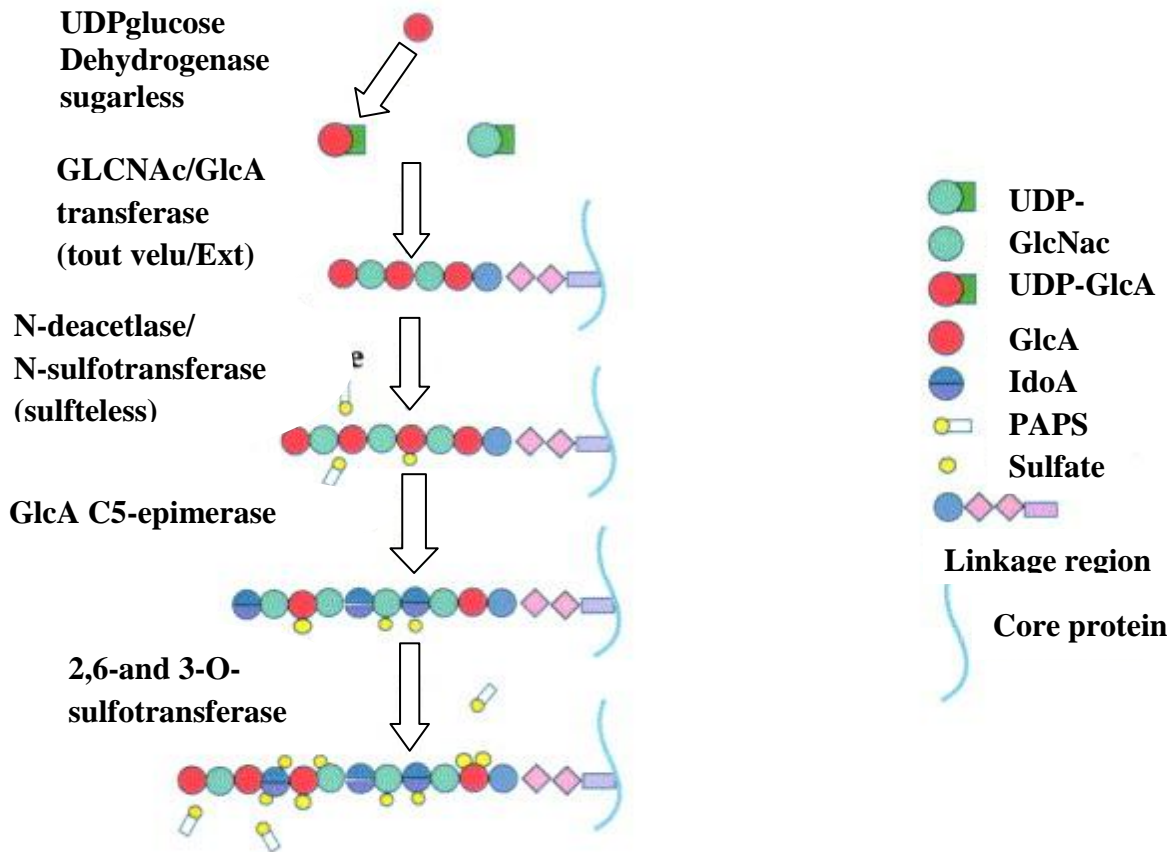


**Figure 1.4 HS chain elongation**

The chains are synthesised on the core protein by the sequential action of individual glycosyl transferases. A common tetrasaccharide linkage region is formed, followed by the addition of alternating GlcA and GlcNAc residues, producing in turn the precursor chain. This chain is then enzymatically modified by deacetylation and *N*-sulfation, epimerisation and *O*-sulfation, yielding individual chains whose sequence is distinct from all the other chains.



## 1.8 Biosynthetic modifications of CS/DS GAG chains (CS/DS chain elongation)

CS/DS sulfated GAGs [(CS)] are covalently attached to their respective core proteins through the GAG–protein linkage region,  $\text{GlcA}\beta 1 \rightarrow 3\text{Gal}\beta 1 \rightarrow 3\text{Gal}\beta 1 \rightarrow 4\text{Xyl}\beta 1 \rightarrow \text{O-Ser}$  (Figure 1.3). The biosynthesis of CS can be broadly divided into that of chondroitin and DS. CS is comprised of predominantly the GlcA epimer, whereas dermatan is predominantly comprised of IdoA. Thus, the CS C-5 uronyl epimerase is more prominent in the biosynthesis of DS. The first GalNAc transfer to the linkage region by the alleged GalNAc transferase-I leads to the synthesis of the repeating disaccharide region  $[(-\rightarrow 4\text{GlcA}\beta 1 \rightarrow 3\text{GalNAc}\beta 1 -)_n]$  of CS/DS through alternate additions of  $\beta$ -GalNAc and  $\beta$ -GlcA by the concerted actions of the putative GalNAc transferase-II and GlcA transferase-II enzymes, which are specific to CS backbone synthesis (Figure 1.5).

The three main sulfation events of the CS chains are *4-O* and/or *6-O*-sulfation of GalNAc and *2-O*-sulfation of uronic acid. There are four different isoforms of the CS GalNAc 4-OST (C4ST-1, C4ST-2, C4ST-3, and D4ST-1) and three different isoforms of the CS GalNAc 6-OST (C6ST, C6ST-2, and GalNAc4S-6ST) (Kusche-Gullberg and Kjellen 2003).

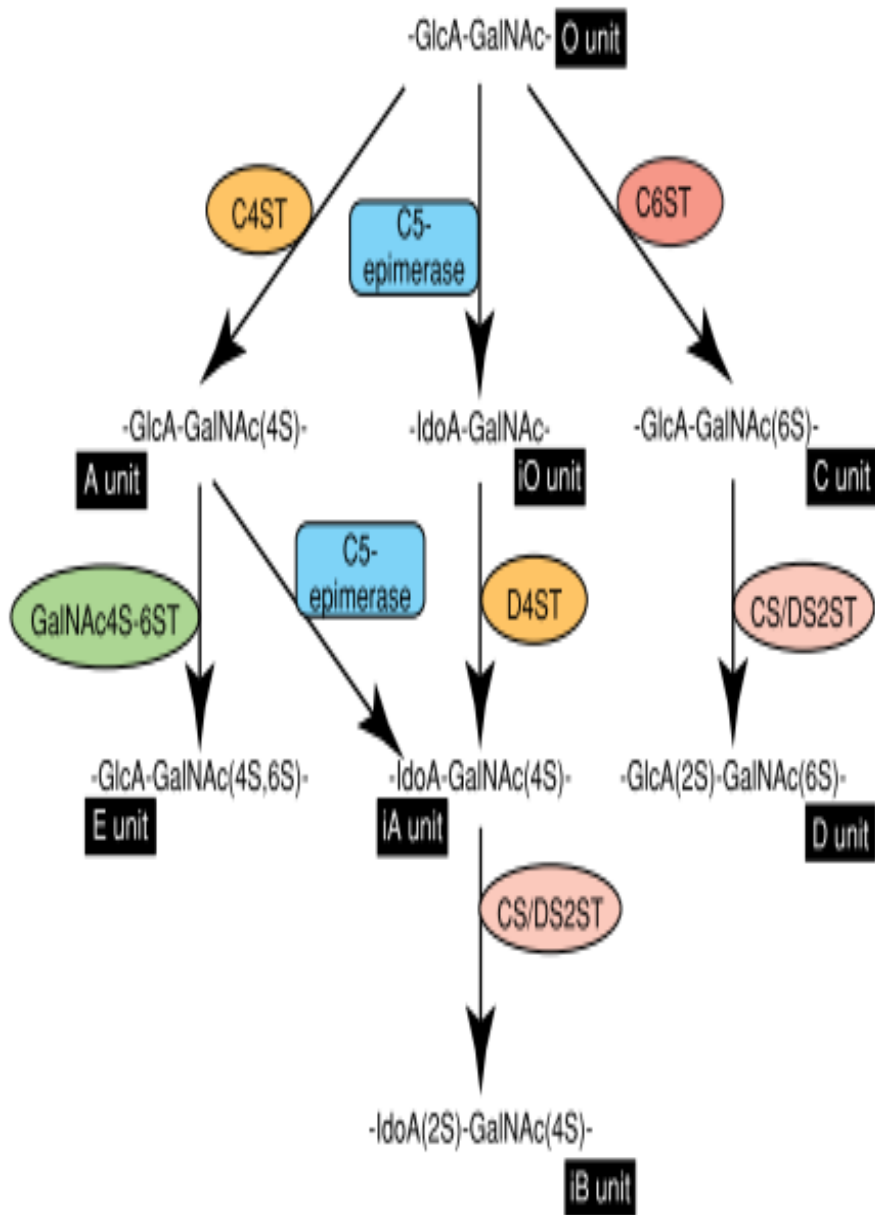


**Figure 1.5; Pathways of CS/DS chain elongation.**

C4ST, chondroitin 4- O -sulfotransferase; C6ST, chondroitin 6- O -sulfotransferase; D4ST, dermatan 4- O -sulfotransferase; CS/DS2ST, uronyl 2- O -sulfotransferase; Gal-Nac4S-6ST, GalNAc 4-sulphate 6- O -sulfotransferase; O unit, GlcA b 1-3GalNAc; iO unit, IdoA a 1-3GalNAc; A unit, GlcA b 1-3GalNAc(4S); iA unit, IdoA a 1-3GalNAc(4S); iB unit, IdoA(2S) a 1-3GalNAc(4S); C unit, GlcA b 1-3GalNAc(6S); D unit, GlcA(2S) b 1-3GalNAc(6S); and E unit, GlcA b 1-3GalNAc(4S,6S).

## **1.9 Analysis of GAGs and their oligosaccharide fragments**

There are various ways to study the biological function of GAGs structures in order to understand the structure-activity relationships (SAR). Traditionally, the determinations of GAG's structures are usually derived from the following steps:

Direct extraction and purification of HS populations from tissues or culture cells arising from different organs.

Partial chemical and enzymatic modifications of GAGs to produce oligosaccharides of defined modifications and size (Yates et al, 2004). The structure of these fragments can be confirmed using disaccharide compositional analysis as well as sequencing methods.

Chemically synthesised GAGs oligosaccharides (Grootenhuis et al, 1995) may shed light on specific HS structure activity relationships. Synthesis of GAGs structures is a very long and specialized process. However, solid-phase synthesis and combinatorial chemistry has greatly advanced this field in recent years (Vohra et al, 2008; Seeberger and Werz, 2005; Seeberger and Haaze, 2000)

## **1.10 Traditional methods for extraction and purification of GAGs from Tissue Samples and Cultured Cells**

In general, extraction of GAGs is initiated by the action of proteolytic enzyme (e.g. Alcalase) on the core protein of PGs. This enzyme degrades the core protein into short peptides, thereby releasing the corresponding GAGs chain. Dialysis with high concentrations of harsh organic solvents such as 8 M urea and addition of trichloroacetic acid (Lyon and Gallagher, 1991) or guanidinium chloride are also employed (Yanagishita et al, 1987). These chemicals are chaotropic agents that are capable of disrupting the three-dimensional (3D)

structures of proteins, DNA and RNA. Urea and other chaotropic agents usually disrupt the 3D structure of proteins by interfering with the stabilizing inter-molecular interactions which mediate non-covalent forces such as hydrogen bonds, van der Waals forces and hydrophobic effects (Puvirajesinghe and Turnbull, 2012). The disadvantages of these methods include: they are lengthy; they can involve multiple sample transfers; they can contain harsh chemicals; and they may alter pH and cause de-*N*-sulfation (Inoue and Nagasawa, 1976). Other methods include  $\beta$ -elimination, which involves alkaline borohydride treatment, which also acts to disrupt the serine-xyloside linkage that attaches GAG chains to the core protein backbone; all these methods result in the release of intact GAGs from protein cores (Stenstad et al, 1993).

Another method that can be used for GAGs purification, from cultured cells, involves the use of a non-ionic detergent solution, such as 1% Triton X-100 0.5 M KCl, which can then be subjected to density centrifugation using caesium chloride gradients. This separates the molecules according to their density (Jalkanen et al, 1988). Electrophoretic techniques can be used for separation of proteoglycans. This technique can be used either separately or in combination with SAX-chromatography, depending on the degree of purification required or type of HSPG to be purified.

### **1.11 Chemical and enzymatic depolymerisation of GAGs used in structural analysis**

The polydisperse nature and large size of GAG chains means that it is impossible to determine the structure of individual GAG chains. Structure activity relationships between GAG chains and proteins must therefore be determined by reducing the size of the chains into more manageable oligosaccharides. The most common method of determining differences in

GAGs derived from a variety of sources is the analysis of disaccharides composition, which is commonly achieved by depolymerisation of the GAGs chain by chemical or enzymatic treatment. Site-specific enzymes are used to degrade the polysaccharides for structural and analytical purposes (Murata and Yokoyama, 1987; Linhardt 1986). Depolymerisation of the polysaccharides can result in the creation of smaller saccharides chains, known as oligosaccharides by partial degradation enzymatic or chemical treatment.

They can also be degraded further by a combination of site-specific enzymes in order to yield disaccharides, subsequent analysis by SAX-HPLC can give the total disaccharide composition of the GAG chains. While similar disaccharides may be present in different tissues, the proportion of each varies considerably thereby allowing the identification of structural differences between tissues. Furthermore, the domain structures of GAGs can be analysed to understand the relative distributions of nonsulfated and sulfated domains from different cells and tissues (Esko and Lindhart, 2001). The structures found in different domains can be analysed further using oligosaccharide mapping, which provides a 'fingerprint' of the domain structures (Turnbull and Gallagher, 1991; Turnbull 1990; Turnbull and Gallagher, 1988). The development of GAG sequencing technology has been used to provide more detailed information on the structure of individual oligosaccharides involved in important biological interactions (Turnbull et al, 1999). GAG oligosaccharides structures have been studied extensively by using one or more of the following methods and have provided a wealth of information on the relationships between the fine structures of GAG chains.

Originally, depolymerisation of HS/heparin was achieved using nitrous acid hydrolysis. Nitrous acid cleaves in between the hexosamine residues and the hexuronate residues, where the amino group is either *N*-sulfated or unsubstituted. This result in the

conversion of the D-glucosamine at the reducing end of the structure into a 2, 5- anhydro-D-mannose residue and the hexuronate residues remain intact (Burdon and Van Knippenberg, 1985). This reaction has been studied extensively and is proven to be pH-dependent. Direct deamination of *N*-sulfated glucosamine residues is possible at a low pH condition (< 2.5). However, *N*-unsubstituted residues are deaminated more rapidly at an optimum pH 4 (Shively and Conrad, 1976).

This method cannot be used to fully characterise the GAG oligosaccharides directly as the depolymerisation process does not generate a suitable specific chromophore, in other words, chemical digestion and separation of such fragments can be followed only at low sensitivity by spectroscopic detection (Powell et al, 2004). Increased detection sensitivity is achieved by combining nitrous acid degradation with reducing end labelling methods, such as radiolabelling, or fluorescent tags. The labelling reaction of the reducing end of nitrous acid treated fragments is aided by the fact that the 2, 5- anhydro-D-mannose residue produced at the reducing end is highly reactive (Puvirajesinghe and Turnbull, 2012). Furthermore, this method is limited by its ability to cause reduced yield due to ring contraction of uronic acid residues or *p*-elimination of the glucuronic acid (Guo and Conrad, 1989).

## **1.12 Use of separations techniques for structural analysis**

GAGs can be analysed in many different ways, the choice of techniques depending on factors such as the source and quantity of materials, the type of data required and the preparation and/or treatment of GAGs prior to the analysis process. NMR spectroscopy and mass spectrometry are useful techniques for such analysis and have been able to provide direct sequence information (Kitagawa et al, 1995). However, both techniques require

specialized instruments, which are not routinely available and NMR in particular requires relatively large quantities of materials (millimolar to micromolar quantities). These drawbacks leave chromatographic techniques as the most common and easiest methods used to examine GAGs structure (Puvirajasinghe and Turnbull, 2012).

### **1.13 Strong anion-exchange chromatography (SAX-HPLC)**

To date, chromatography remains the most reliable technique for the routine separation of GAGs and the common ones generally in use are gel chromatography and high-performance liquid chromatography (HPLC). Oligosaccharide products can be purified and separated according to their molecular weight and other properties such as charge and hydrodynamic volume (Puvirajasinghe and Turnbull, 2012). Several methods, such as radioactivity measurement, UV detection at 232 nm, fluorescence detection, can be used for detection. Radioactivity measurement can be used to detect  $^{35}\text{S}$  and  $^3\text{H}$  in samples prepared by biosynthetic radiolabelling (e.g., cultured cells) or where oligosaccharides (digested using nitrous acid) are labelled at their reducing-ends with  $^3\text{H}$ -borohydride and UV detection at 232 nm can also be used to detect the disaccharide products. Another UV wavelength commonly used is 215 nm, which detects acetyl bonds, although this is less sensitive than detection at 232 nm. Fluorescence detection is another reliable and extremely sensitive method that can be used to detect fluorescently-tagged oligosaccharides. Strong anion-exchange chromatography (SAX-HPLC) techniques are used for the separation of structures according to their negative charge content. A common column is the Pro-Pac PA1, which is made of quaternary ammonium functional groups attached to nonporous core particles by agglomerated MicroBead™ resin. SAX-chromatography can be used in combination with PAGE separation, for the purification of GAGs oligosaccharides (Vives et al, 2001).

### **1.14 Polyacrylamide Gel Electrophoresis (PAGE)**

Electrophoresis is primarily an analytical technique for charged molecules. It is a technique that separates GAG oligosaccharides based on their mass to charge ratio ( $m/z$ ). Although, PAGE analysis is one of the common biochemical techniques used for the separation of protein and DNA, it has also been used to separate GAG samples in a similar manner for its use in the analysis of DNA and protein (Wong et al 2006). However, PAGE analysis of GAG oligosaccharides was initially complicated because of the demand for high resolution due to the polydispersity and structural heterogeneity of GAG samples: this drawback has now been resolved by the introduction of discontinuous gel electrophoresis, together with the development of specialised stacking gels and buffer (Rice et al 1989).

The use of fluorescent tags to label digestion products at their free reducing-ends via reductive amination reaction has also been determined and this has led to a technique known as fluorescence-assisted carbohydrate electrophoresis (FACE). The enzymes-digested products can be stoichiometrically coupled to a fluorescent tag and separated using high percentage gels. Picomolar concentrations can be viewed using a transilluminator (Puvirajesinghe and Turnbull, 2012).

### **1.15 GAG's degrading enzymes**

Overall GAG's degrading enzymes are an extremely important tool in relating GAG structure/sulfation pattern to biological activities therefore an understanding of the specificities of these enzymes is crucial to interpreting the data generated by the action of these enzymes on GAG chains. The most widely used enzymes are a family of structurally related heparin/HS lyase and their properties and specificities are described below.



## 1.16 Heparinases

Heparinases are enzymes lyases that can eliminatively cleave heparin or HS into disaccharide and oligosaccharide products: they are also involved in the release of heparin-bound growth factors from the ECM (Kim et al, 2000). Six different heparinase enzymes have been isolated from four different bacteria namely: *Flavobacterium heparinum*, *Bacillus sp.*, *Bacteroides heparinolyticus*, and an unclassified soil bacterium (Yoshida et al, 2002). At least 29 other bacteria expressing heparinase activity as determined by a qualitative plate assay has been isolated. (Yoshida et al, 2002: Steyn et al,1992: Salyers et al, 1977). Fractionation of crude heparinase afforded three different heparinases usually called lyases I, II and III, each of which have a different substrate specificities (Figure 1.6) (Desai, 1993). The individual heparinase enzymes cleave unique glycosidic linkages, allowing Heparin and HS to be degraded to specific types of oligosaccharide fragments which vary in length and sulfation pattern (Linhardt et al, 1990).

Isoelectric focusing (PI) showed that *Bacillus* species heparinase (PI = 6.6) has an overall negative charge at its optimal pH of 7.5 while all three *F. heparinum* heparinases (PI = 8.5- 10.1) are positively charged at their pH optima of 7-7.5. For enzymes that degrade a polyanionic substrate, this appears to be an important difference that may imply different mechanisms for heparinases from *Bacillus* sp. and from *F. Heparinum* (Lohse and Linhardt, 1992). However, the temperature optimum for *Bacillus* sp. heparinase is 50°C but 90% of the activity is lost after 3h at 45°C (Bellamy and Horikoshi, 1992). Moreover, for short digest sodium phosphate buffer has been reported to give higher activity than sulfonate-based buffers (MOPS, TES, and HEPES), but the latter seem to increase stability of heparinase's I, II, and III (Lohse and Linhardt, 1992). It appears in general that the optimal conditions for heparinases are different depending on the durations of the assay but there is some

controversy about this finding which could be critical in determining the completeness of GAG digestions.

There is very important substrate specificity associated with heparin lyases, which has been defined as a disaccharide containing a cleavable linkage. Heparinase I cleaves the linkages  $H_{NS(6X)-I-2S}$  [GlcNS (6S) (1 → 4) IdoA2S], heparinase II the linkages  $H_{NY,6X}-G/I_{2X}$  [GlcNS (6S) (1 → 4) IdoA (GIA) 2S], and heparinase III the linkages  $H_{NAC-I}$  and  $H_{NY,6X}-G$  [GlcNAc(1 → 4) IdoA] and [GlcNS (6S) 1 → 4) GlcA], in which H is glucosamine, I is iduronic acid, G is glucuronic acid, Y is sulfated or acetylated ( $CH_3CO$  or  $SO_3$ ) and X is sulfated or unsubstituted (H or  $SO_3$ ).

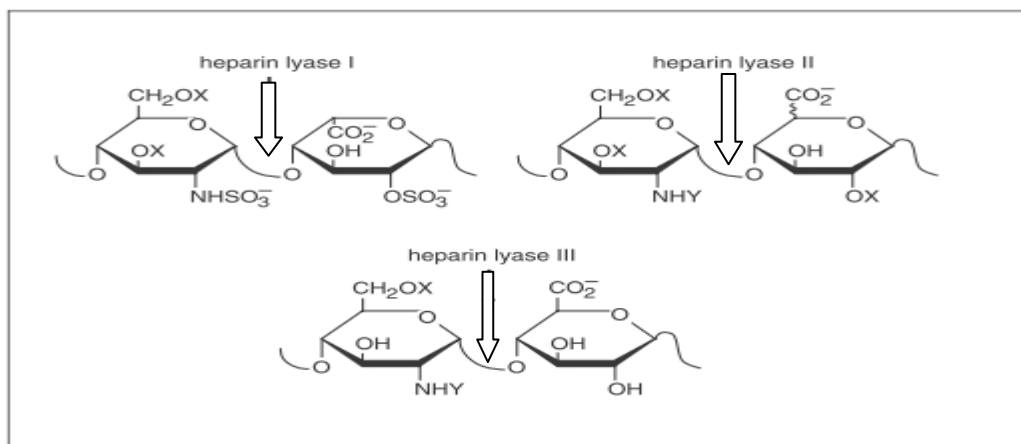


**Figure 1.6: Primary glycosidic linkages cleaved by Heparin lyases.**

Abbreviations: X, H or  $SO_3^-$ ; Y,  $CH_3CO$  or  $SO_3^-$ . Heparin lyase II cleaves at either glucuronic or iduronic acid residues.

The enzymatic action of individual heparinases leads to the generation of oligosaccharides with specific structural features. Degradation of HS with all the three heparinases reduces HS chains to their disaccharide components, an essential property in structural characterisation. These disaccharide units comprises of  $\Delta^{4,5}$ -uronic acid attached to N-acetylglucosamine at the reducing terminus and with varying degrees of sulfation (Lohse

and Linhardt, 1992). Both D-glucuronic acid and L-iduronic acid give the same  $\Delta^{4,5}$ -uronic acid after enzyme treatment (Lohse and Linhardt, 1992). The main disaccharides found in HS/heparin and their traditional abbreviations are;  $\Delta$ -UA-GlcNAc (IVA);  $\Delta$ -UA-GlcNS (IVS);  $\Delta$ -UA-GlcNAc (6S) (IIA);  $\Delta$ -UA(2S)-GlcNAc (IIIA);  $\Delta$ -UA-GlcNS (6S) (IIS);  $\Delta$ -UA (2S)-GlcNS (IIIS);  $\Delta$ -UA(2S)-GlcNAc (6S) (IA);  $\Delta$ -UA (2S)-GlcNS (6S) (IS).

### **1.17 Heparinase I from *F. heparinum* (EC 4.2.2.7)**

Heparinase I has also been shown to cleaves heparin at both the GlcNS (6S) (1  $\rightarrow$  4) IdoA (2S) and GlcNS (3S,6S) (1  $\rightarrow$  4) IdoA (2S) linkages (Xiao et al 2011). The GlcNS(3S6S) (1  $\rightarrow$  4) IdoA(2S) linkage, found primarily within the antithrombin III binding site, is more susceptible to heparinase I than the major heparin disaccharide repeating unit GlcNS(6S) (1  $\rightarrow$  4) IdoA(2S). The complete depolymerisation of heparin by heparinase I has been reported to mainly produce eight different disaccharides (Linhardt et al., 1992).

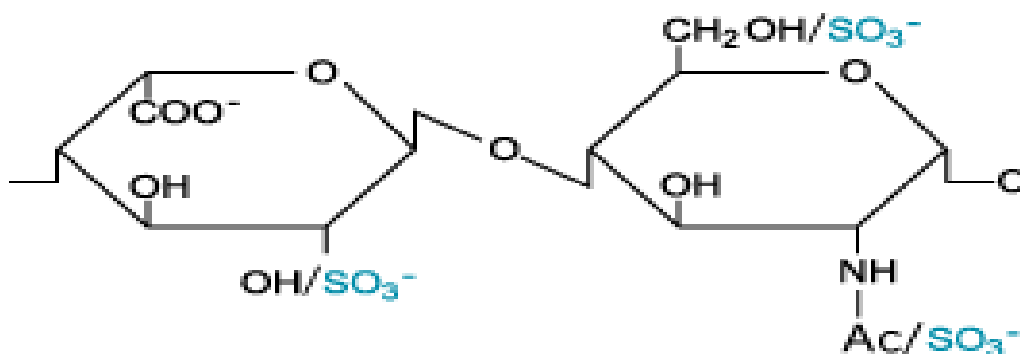


**Figure 1.7: Unsaturated disaccharide derived from HS by enzyme catalysed elimination.**

### 1.18 Heparinase II from *f. heparinum*

Heparinase II is also active on both heparin and HS, with the HS activity being approximately twice as high as the heparin activity (Lohse and Linhardt 1992; Linhardt et al, 1990; Nader et al, 1990). The distribution of products for heparinase II degradation of heparin is not as well characterised as for heparinase I and appears to reflect the composition of the substrate. Heparinase II degradation of heparin yields predominantly the trisulfated disaccharide structure with other minor detectable disaccharides being produced; this fits with the highly sulfated nature of the heparin polymers. Moffat and others have reported a broad substrate specificity of this enzyme. A characteristic that is contrary to the general property of enzyme reported previously (Desai et al., 1993a; Moffat et al, 1991a).

Furthermore, this enzyme has been demonstrated as capable of cleaving both of the isomeric forms of uronic acids (IdoA and GlcA) even though the epimerised C5 hydrogen is being abstracted in the reaction (Desai et al, 1993). This is unusual for enzymatic reactions which are normally stereospecific due to the defined structure of the enzyme catalytic site.

The susceptible linkages are  $H_{NY,6X}-U_{2X}$  where the uronic acid can be IdoUA or GlcUA, the X group can be sulfated or unsubstituted, and Y can be either sulfated or acetylated but not free.

### **1.19 Heparinase III from *f. Heparinurn* (E.C 4.2.2.8)**

Heparinase III is less active on standard heparin or heparin-like segments of HS, i.e. highly sulfated polymers and specifically degrades mono- or non-sulfated sequences within HS chains. None of the standard methods of oligosaccharides analysis of GAGs such as, SAX-HPLC (Linhardt et al., 1990), capillary zone electrophoresis (CZE) electropherograms (Ampofo et al., 1991), gradient PAGE (Desai et al., 1993a) yielded any appreciable disaccharide degradation products when heparin was incubated with heparinase III. The degradation products from heparinase III degradation of HS are poorly non- and mono-sulfated disaccharides, indicating a preference for the enzyme to degrade less modified regions of the polymer.

Previous studies conducted by Rice and colleagues have also highlighted that heparinase III is more active towards larger oligosaccharides than the smaller ones. It has also been shown to be active towards oligosaccharides with *N*, 6-disulfated (NS6S) or *N*-acetylated hexosamine (Linhardt et al, 1990; Rice and Linhardt, 1989). These findings have resulted in speculation that *N*-sulfation and 6-*O*-sulfation do not inhibit cleavage by this enzyme. This was confirmed by the existence of 6-*O*-sulfated and *N*-sulfated products following cleavage of polymeric HS with heparinase III (Moffat et al, 1991).

## 1.20 Chondroitinases

Chondroitinase enzymes are once again extremely important tools for the structural characterisation of GAGs and have been isolated and characterised from bacteria of the genera *Arthrobacter*, *Flavobacterium*, *Aeromonas*, *Bacillus*, *Bacteroides*, *Proteus* and an unclassified strain possibly *Aurebacterium* (Earnst et al, 1995: Yamagata et al, 1968). Chondroitinase-ABC (EC 4. 2. 2. 4) is a general purpose enzyme that cleaves all glycosidic linkages in the three members of the CS group and also with hyaluronan. It is been classified as a remarkable enzyme because of its ability to cleave linkages with iduronic acid as well as linkages with its isomer, glucuronic acid (Linhardt et al 2006).

In addition, chondroitinase activity has been detected in several other microorganisms (Linhardt et al., 1986: Salyers et al., 1977). It is an extremely important tool used to completely degrade CS/DS to their disaccharide components, which can be quantified by SAX-HPLC, CE, FACE, PAGE, etc. It acts on chondroitin 4-sulfate, chondroitin 6 sulfate, and DS, and acts slowly on hyaluronate (Figure 1.8). Inability of the chondroitinases to show any activity towards heparin or HS, which are entirely 1 →4 linked indicates, that the 1 →3 linkage of CS is a requirement for its enzymatic activity (Linhardt et al, 1986: Salyers et al, 1977).

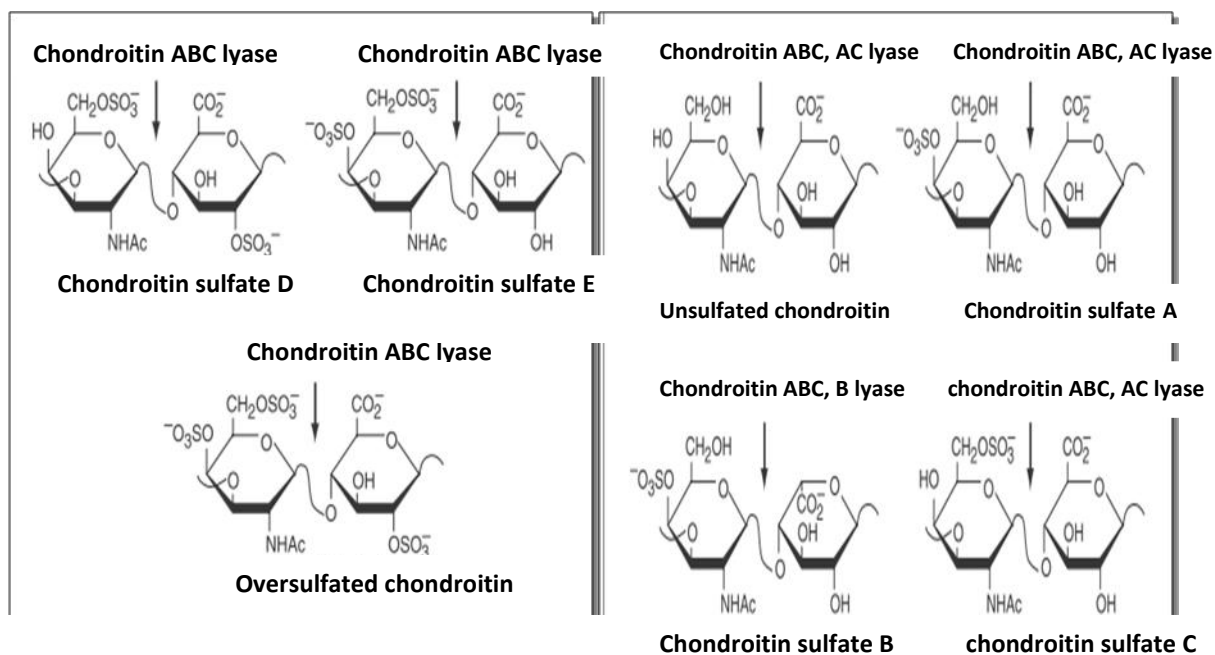


**Figure 1.8: Glycosidic linkages cleaved by chondroitin lyases.**

Abbreviation: Ac, CH<sub>3</sub>CO.

Chondroitinase-B lyase (EC 4.2.2.19) is specific for DS degradation and the resulting oligosaccharides as resolved by SAX-HPLC has been reported by Linhardt and others to yield  $\Delta$ UA-GalNAc (0S);  $\Delta$ UA-GalNAc6S (6S);  $\Delta$ UA-GalNAc4S (4S);  $\Delta$ UA2S-GalNAc4S disaccharides accounted for 50 to 65% of the 232 nm absorbance while the remaining 35 to 50% absorbance most likely originated from unidentified oligosaccharides (Linhardt et al, 1991). However, degradation of oversulfated DS GAG chains isomers additionally yielded the trisulfated disaccharide,  $\Delta$ UA (2S)-GalNAc (4S, 6S) (Figure 1.9) (Murata and Yokoyama, 1987). Purification of the crude enzyme by column chromatography over hydroxyl apatite led to discovery of chondroitinase-AC lyase (4.2.2.5) which only eliminates the amino sugar attached to glucuronic acid and to chondroitinase-B lyase which eliminates amino sugars attached to iduronic acid (Gu 1995). Separation of the hydrolysis products by SAX-HPLC

after treatment of GAGs with AC/ B lyases provides useful analytical information on their structure. They are also powerful tools used to generate CS/DS oligosaccharides and for internal evaluation of sulfation patterns within them for subsequent structure-activity studies.

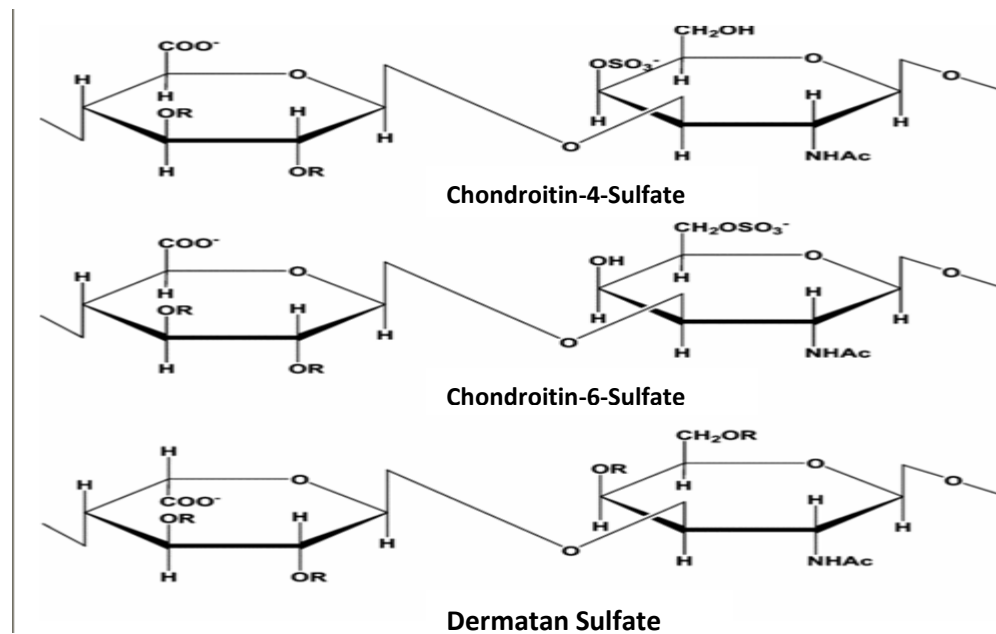


**Figure 1.9: Unsaturated disaccharides derived from CS by enzyme catalysed elimination.**

Abbreviation: R = SO<sub>3</sub><sup>-</sup> or H .



## 1.21 Glycosaminoglycans and cancer

Recent studies have demonstrated the significant roles played by GAGs and proteoglycans in tumourigenesis and tumour progression (Yip et al, 2008 and Conte et al, 2007). For example, in breast cancer, changes in GAG and PG expression on the cell surface and in the ECM allow tumour cells to proliferate, gain the ability to invade surrounding tissues, metastasize to distant organs and induce angiogenesis (Guo et al, 2007 and Polyak, 2007).

HS are present on the surface of every eukaryotic cell, inclusive of both tumour cells and the surrounding cells. This polymer has also been shown to be vital for tumour survival (Liu et al., 2002). This includes the endothelial-cell compartment that is very close to a growing tumour; indeed HS has been linked with the ability to modulate the process of tumour angiogenesis (Gandhi and Mancera, 2010 and Ram et al, 2002). HS chains on the tumour-cell surface have been proven to be important in many aspects of tumour phenotype and development, including cellular transformation, tumour growth, invasion and metastasis (Liu et al, 2002 and Sanderson et al, 2001). *In vivo* studies in mice highlight that changes in the fine structure of tumour cell surface HS have marked effects on tumour cell growth kinetics and metastasis formation (Liu et al, 2002). Some HS sequences expressed on the tumour cell surface appear pro-tumourogenic, whereas others are anti-tumourogenic (Gandhi and Mancera, 2010). Recent advances in structural elucidations of HS have led to the discovery of its anti-tumourogenic capability both *in vivo* and *in vitro* (Gandhi and Mancera, 2008). HS structure-activity relationship studies, such as this have opened up many new exciting avenues for the generation of polysaccharide-based anti-cancer therapeutics ( Linhardt 2013;Ram et al, 2002).

Changes in HS structure on the tumour cell surface seem to mediate their effects by regulating differential growth-factor signaling, cell adhesion, proliferation and migration (Liu

et al, 2002 a). Moreover, alterations in the level of expression of the protein core of HSPGs as well as HS structural differences and/or density on HSPGs, can potentially make cancer cells highly versatile in the modulation of their behaviour (Esko and Lindhal, 2001; Tumbull et al, 2001).

The structural complexity of HS arises from the differential modification of individual disaccharide units within an oligosaccharide chain (Esko and Lindhal, 2001; Tumbull et al 2001) which result ultimately in great structural diversity. One of the consequences of the great structural diversity of HS structure is that these molecules are able to bind and interact with a wide variety of proteins, such as growth factors, chemokines, morphogens, enzymes and other signaling molecules, that are important for tumour development, such as FGFs.

Cells can perform subtle changes to the biosynthesis of HS chains and hence have the ability to change how the cells interact with these molecular effectors that bind HS. This allows the tumour cell HS-GAGs (both at the cell surface and extruded into the ECM) to modulate directly several aspects of tumour-cell phenotype, including growth kinetics, invasiveness and metastatic potential (Varki and Varki, 2002). One of the consequences of tumour-derived HS or HSPG is that, it can be pro-tumourogenic or anti-tumourogenic depending on whether it is anchored at the cell surface or present in the ECM as soluble-free GAGs (Liu et al 2002), as well as depending on the HS-GAG sequence.

Recently, it has been demonstrated that cancer cells alter their cell-surface HS profile during the process of transformation, including differential expression of particular proteoglycan protein core sequences, in addition to changing the HS fine structure of given proteoglycans (Blackhall et al 2001). Other studies have revealed that HS chains are involved in the initial oncogenic transformation of a normal cell to a tumour-cell (Xiang et al, 2001; Filmus 2001). Changes in both the expression level and the oligosaccharide sequence characteristics of cell-surface HSPGs have been shown to correlate with transformation in

several malignancies (Ram et al, 2002). For example, the HSPG syndecans is required to maintain the differentiated morphology and localisation of epithelial cells. Syndecan-1 expression is down regulated in various malignant tumours, including uterine carcinoma and multiple myeloma (Ram et al, 2002). Its expression decreases as in situ carcinoma progresses to invasive carcinoma (Sanderson 2001). This decrease in expression may be linked to phenotype changes in these cancers. Specific HS structural changes have been noted during malignant transformation of colon cancer cells from adenoma to carcinoma (Jayson 1998).

Likewise, glypican-1, another cell-surface HSPG that closely control cell growth and division, has been shown to act as a negative regulator of cell proliferation for certain tumour types ((Ram et al, 2002). Glypicans have also been shown to modify cellular responses to bone morphogenetic proteins and insulin-like growth-factor-2 -factors that are important in cellular division and differentiation (Ram et al, 2002). An association has also been made between specific mutations in HS-related biosynthetic genes and inherited syndromes that increase cancer risk, implicating these molecules in tumourigenesis (DeBaun et al, 2001). *Simpson–Golabi–Behmel syndrome* (SGBS) is a complex congenital overgrowth syndrome with features that include macroglossia, macrosomia, and renal and skeletal abnormalities, as well as an increased risk of certain malignancies. Most cases of SGBS seem to arise as a result of either deletions or point mutations within the gene that encodes glypican-3 (GPC3) at Xq (Mundhenke 2002). GPC3 expression is also down regulated in a number of cancers, including breast and ovarian carcinomas, and mesotheliomas (Mundhenke 2002).

Tumour cell surface HS also binds growth factors, cytokines and structural proteins that are involved in modulating autocrine and paracrine signaling loops that are important for tumour growth and progression (Mundhenke 2002) .The diverse structural characteristics of HS enable them to act either as inhibitors or potentiators of these signalling loops, depending

on their sequence context (Liu et al, 2002). Recent studies have highlighted that, *in vitro*, tumour cell surface HS can promote growth-factor signaling and tumour-cell proliferation.

Tumour cells are reported to influence actively the affinity of their HSPGs for FGF-2, as well as for other growth factors, by modulating the overall density and sulfation pattern of their HSPGs. Modified HS and CS, have been studied as potential cancer therapeutics. In an attempt to generate a potentially therapeutic mimetic of syndecan-1, Pumphrey and colleagues discovered that carbodiimide-modified glycosaminoglycans reduced breast cancer and myeloma cell viability by inducing apoptosis (Pumphrey et al, 2002). Moreover, modified CS abolished breast tumour growth in nude mice. HS mimetics with anti-cancer properties such as KI-111 [2-(4-fluoro-3-nitro-benzoyl) benzoic acetic anhydride] inhibited tumour-cell adhesion, migration, growth, and invasion *in vitro* (Ishida et al., 2004).

In contrast, other KI related compounds inhibited cancer invasion and migration but promoted tumour cell adhesion (Ishida et al, 2004; Simizu et al, 2004).

HS has also been shown to be involved in the promotion and inhibition of tumour angiogenesis with many approaches aimed at blocking the interactions between HS and angiogenic growth factors (Sanderson. 2001).

## **1.22 Tumour angiogenesis**

Angiogenesis is a natural process that involves both the growth of new blood vessels from pre-existing vessels and also closely regulated sequence of events starting with the degradation of the basement membrane by activated endothelial cells (Hussain et al 2009).

Tumours cannot grow as a mass above few mm in size unless a new blood supply is induced.

The various stages involved in tumour angiogenesis are illustrated in Figure 1. 10.

Angiogenesis is controlled by a balance between proangiogenic factor [including FGFs: acidic (FGF-1) and basic (FGF-2), Vascular endothelial growth (VEGF), Tumour necrosis factor-alpha (TNF-alpha), Follistatin Granulocyte colony-stimulating factors (G-CSF), Hepatocyte growth-factor (HGF)] and anti-angiogenic factors [including anti-angiogenic antithrombin III, CD 59 complement fragment, heparin hexasaccharide fragment, human chorionic gonadotropin (hCG)]. The angiogenic switch represents the overall activities of the angiogenic stimulators and inhibitors which may either shift the balance towards inhibition or stimulation (Presta et al, 2003). Tumour neovascularization and angioproliferative diseases result in uncontrolled endothelial-cell proliferation.

HSPG's participates in the modulation of the neovascularization that happens in different physiological and pathological conditions. This modulation occurs through interaction with angiogenic growth factors (Presta et al, 2003), which is due, in part, to their capacity to bind to and modulate the activity of angiogenic growth factors. However contrasting effects can be obtained depending on the types of HSPGs and/or on the experimental conditions adopted e.g, purified perlecan enhances angiogenesis induced by FGF-2 while other purified HSPGs are ineffective (Azieuer et al, 1994). Glypicans support the binding of FGF-1 and FGF-2 to human tyrosine kinase FGF receptor-1 (FGFR-1) in a cell free system and replaces heparin in supporting FGF-2 induced cellular proliferation of HS-negative cells expressing FGFR-1 (Bonneh-Barkay et al, 1997). Soluble heparin/HS inhibit the binding of FGF-2 to FGFRs and HSPGs present on the surface of endothelial cells (Coltrini et al, 1994). Thus, this observation suggest that negative effects on angiogenesis may be exerted by the binding of angiogenic growth factors to soluble HSPGs or GAGs rather than to cell-associated HSPGs.

HSPGs may also modulate angiogenesis also by protecting angiogenic growth factors from heat (Gospodarowicz and Cheng, 1986) and proteolytic degradation (Coltrini et al, 1994) and by affecting their radius of diffusion (Flaumenhaft et al, 1989). Finally, HSPGs present in the ECM may act as a reservoir for angiogenic growth factors that will reach higher local concentrations and will sustain the long-term stimulation of endothelial cells (Presta et al, 1989). A common theme among growth factors interacting with TK receptors is the involvement of ligand-induced receptor dimerization in receptor activation (Ullrich and Schlessinger, 1990).

Crystal structures of HS/FGF/FGFR ternary complexes revealed markedly different geometrics (Pellegrini et al, 2000). A single molecule of heparin/HS may bind several molecules of FGF-2 (Coltrini et al, 1993) suggesting that GAGs induce oligomerization of angiogenic growth factors. Heparin has been reported to induce dimerization of FGF-2 in cell free system (Coltrini et al, 1993). It has also been demonstrated that the dimerization and activation of FGFR catalysed by heparin-dependent oligomerization of FGF is required to induce a mitogenic response (Spivak-Kroizman et al, 1994). FGF-2 molecules has been recently demonstrated to self-associate through specific interactions in a sequential pattern, resulting to the formation of bioactive FGF-2 dimmers, and that Heparin can serve as a platform to stabilize the inter-molecular FGF-2 interactions, thus favouring receptor dimerization (Kwan et al, 2001). The capacity of various angiogenic factors to bind heparin/HS indicates that molecules that are able to interfere with this interaction may act as angiogenesis inhibitors; for example, the ability of low molecular weight heparin fragments to be administered systemically in order to reduce the angiogenic activity of FGF-2 and VEGF (Norrby 2000; Norrby and Ostergaard, 1997).

The biological activity of angiogenic growth factors on endothelial cells is controlled by a complex interplay among free and cell-associated heparin/HS GAG chains. In this scenario, natural and synthetic heparin related angiostatic compounds play their pharmacological action (Presta et al, 2003). This observation indicates that distinct structural requirements are necessary for the interaction of heparin/HS with different growth factors. Even though these specific binding sequences may be masked in heparin due to its high degree of sulfation, the high heterogeneity in HS structure allows a more refined tailoring of selective binding regions that may influence the biological activity and bioavailability of heparin/HS-binding growth factors (Presta et al, 2003).

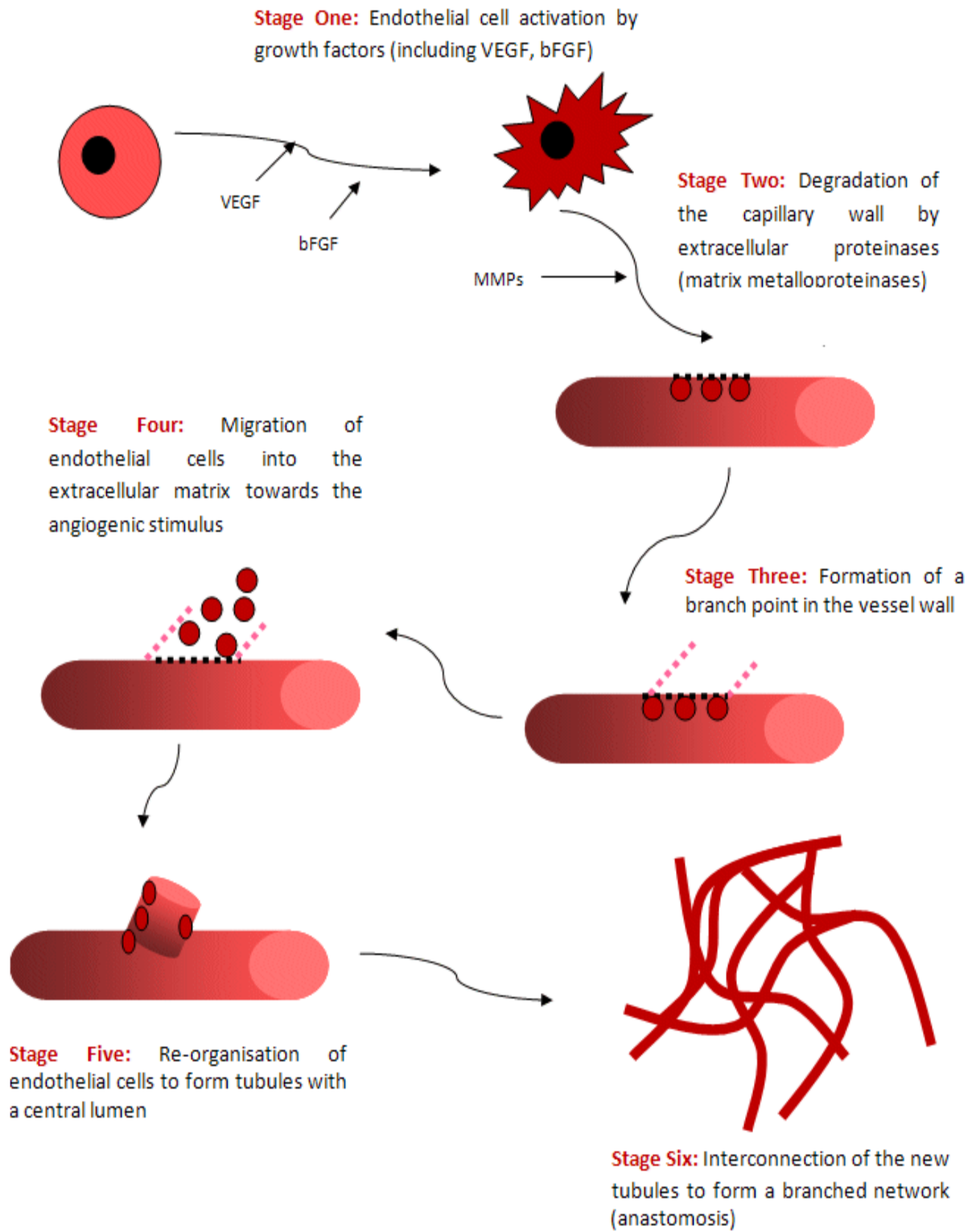


**Figure 1.10: Stages involved in tumour angiogenesis**



### **1.23 Fibroblast growth factors (FGFs) and their receptors (FGFRs) in human breast cancer**

The pleiotropic effects of FGFs are mediated through four highly conserved receptor tyrosine kinases (RTKs), known as FGF receptor 1-4 (FGFR1-4). The extracellular domain of these receptors contains three immunoglobulin-like (Ig) domains (D1, D2 and D3) (Turner and Gross 2010), which bind to specific members of the FGF family of growth factors.

The second and third Ig domains are the most important for FGF ligand binding and specificity; whereas the first Ig domain, absent in certain isoforms, is presumed to have an auto inhibitory function (Turner and Gross, 2010). Alternative splicing of the carboxyl half of the third Ig domain yields either the IIIb or the IIIc isoforms of FGFR1-3 (Turner and Gross, 2010; Eswarakumar et al, 2005). These various isoforms of FGFRs exhibit tissue-specific expression and respond to different spectrum of the 18 mammalian FGFs known to date (Beenken and Mohammadi, 2009).

Many researchers have linked overexpression of FGFs to human breast cancer and this finding has been substantiated by other in vitro studies which equally revealed multitudes of properties that suggest their involvement in breast cancer induction, progression and metastasis (Dickson et al 2000).

FGFR2-IIIb, expressed usually in epithelial cells, can be activated by FGFs of mesenchymal origin e.g. FGF-7 and FGF-10, whereas FGFR2-IIIc e.g FGF-1 and

FGFR 2IIIc expressed on mesenchymal tissues responds to ligands secreted by epithelial cells (Rusnati et al, 1994).

Studies have highlighted the critical role of aberrant FGFR2 signaling in cancer, including overexpression of FGFR2 and its ligands, mutations and amplifications of the receptor, and receptor isoforms switching (Turner and Gross, 2010; Eswarakumar et al, 2005). Single nucleotide polymorphisms (SNPs) of FGFR2 correlate with increased risk of breast cancer

development, presumably due to elevated FGFR2 expression. Missense, potentially activating, mutations of FGFR2 have been reported in multiple cancer types, including endometrial, ovarian, breast, lung, and gastric cancer (Turner and Gross, 2010).

Furthermore, the FGFR2 gene is amplified in a subset of gastric and breast cancers (Turner and Gross, 2010). The co-expression of FGFR-2IIIb and FGF7, in pancreatic and gastric cancers, as well as lung adenocarcinomas, is associated with poor prognosis (Turner and Gross, 2010), which may likely due to aberrant receptor activation through the formation of autocrine activation loop. However, decreased expression of FGFR-2IIIb has been reported in several cancer types during tumour progression and phenotypic change. (Turner and Gross, 2010), possibly reflecting the physiological role of FGFR2 in regulating tissue homeostasis.

A number of FGF family members and their receptors have been detected in both normal and malignant breast tissue through the application of reverse transcription polymerase chain reaction procedures (Matsuike et al, 2001). Increased expression of FGFR2-IIIb has been described in breast, colorectal, cervical, pancreatic and prostate cancers; however, it may also act as a tumour suppressor (Turner and Gross, 2010). Hence, interactions between GAG mediated growth-factor binding to these TK receptors has the potential to modify the growth and metastatic potential of tumours, which may enable new treatments for the growth and progression of solid tumours in the future.

## 1.24 The cell cycle

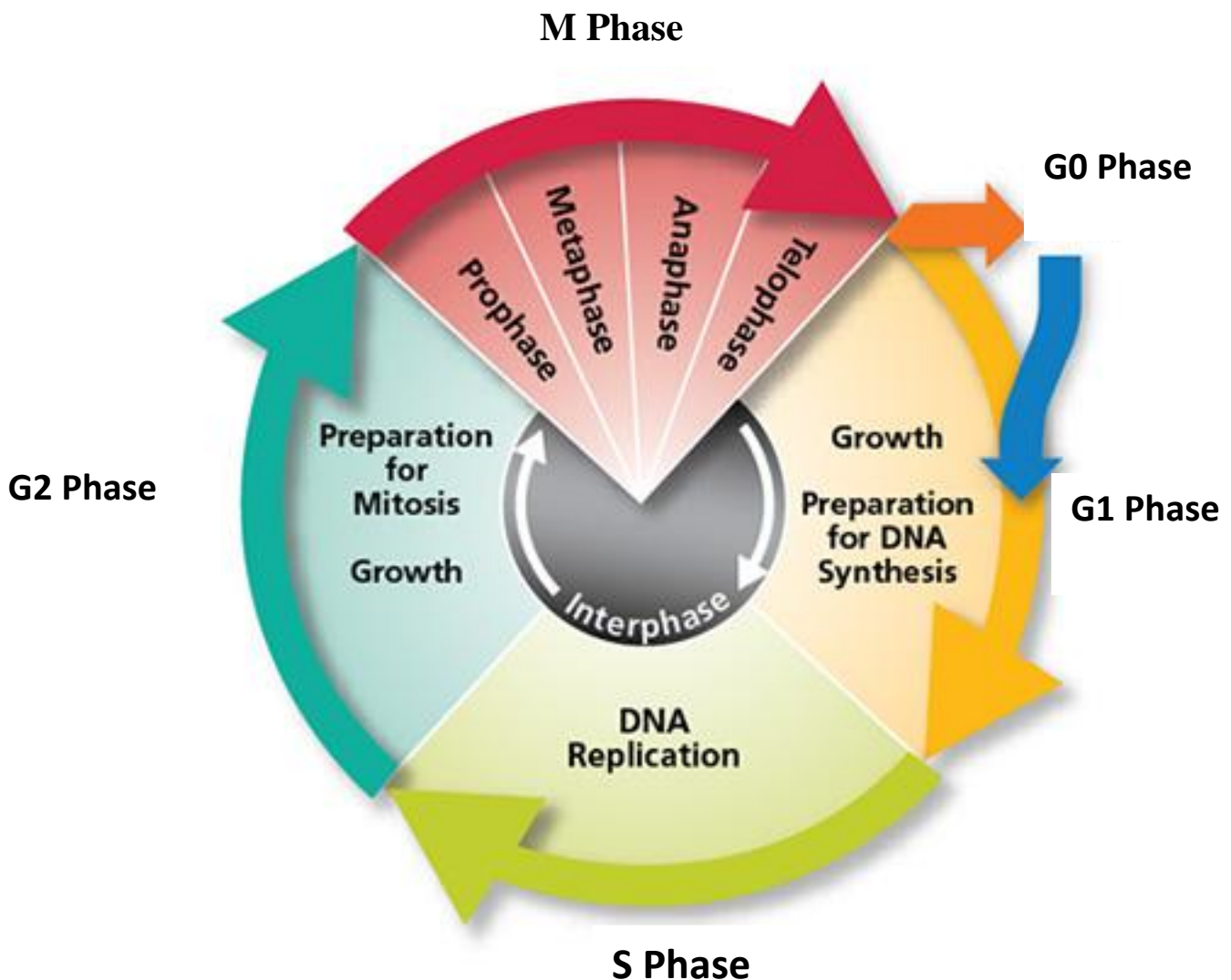


**Figure 1.11: The cell cycle showing the two major events that takes place within the cell.**

Control of the cell cycle is an extremely complex process that networks with numerous regulatory proteins, which control the events leading ultimately to proliferation, cell growth, organism development, regulation of DNA damage repair and diseases, such as cancer. The cell cycle can be divided into two major sections as illustrated in the diagram above (Figure 1.11). These are: Interphase, the non-dividing but metabolically active period of the cell cycle including Gap I (G1), DNA Synthesis (S), Gap (G2) and the Mitosis phase,

comprising prophase, metaphase, anaphase, and telophase. (Peng 1998: Rickert 1996 and Roy 1994). G<sub>1</sub> and G<sub>2</sub> phases of the cycle represent the gaps between the two major events that occur in the cell i.e. synthesis and mitosis.

The G<sub>1</sub> phase is the first gap in the cycle in which the cell is preparing for synthesis of DNA (replication) and is also a growing stage for the cell. S-phase is the first major events in the cell cycle in which the cell starts synthesising new DNA. During the S-phase the new daughter strands of DNA for each chromosome is synthesised and as a result of this DNA replication, each chromosome gains a second chromatid, hence, duplication of genomic information takes place (Johnson and Walker, 1999).

The G<sub>2</sub> phase is the second gap in the cell cycle that occurs before the cell progress to mitosis and follows the DNA synthesis phase. During the G<sub>2</sub> period of growth, materials are prepared for the next mitotic division. At this stage, the cell regulatory proteins check the entire cascade involved at the S-phase before the cell cross to this phase and if everything is incorrect, then the cell can progress to the next phase which is mitosis. The mitotic phase is where the actual cell division takes place through a cascade of events, as presented in the diagram below (Figure 1.12). Successful completion of mitosis leads to an onset of interphase and the cell begins a period of growth which spans through the first phase, called G<sub>1</sub> and continues through the S and G<sub>2</sub> phase. However, new cells generated from this series of events could either start a new cycle or remain in a state of quiescence known as G<sub>0</sub>. G<sub>0</sub> is a gap between mitosis and interphase. At this stage, the cell is inactive and no physiological growth is occurring; however, the cell has the potential to grow if the checkpoints adequately allow it.

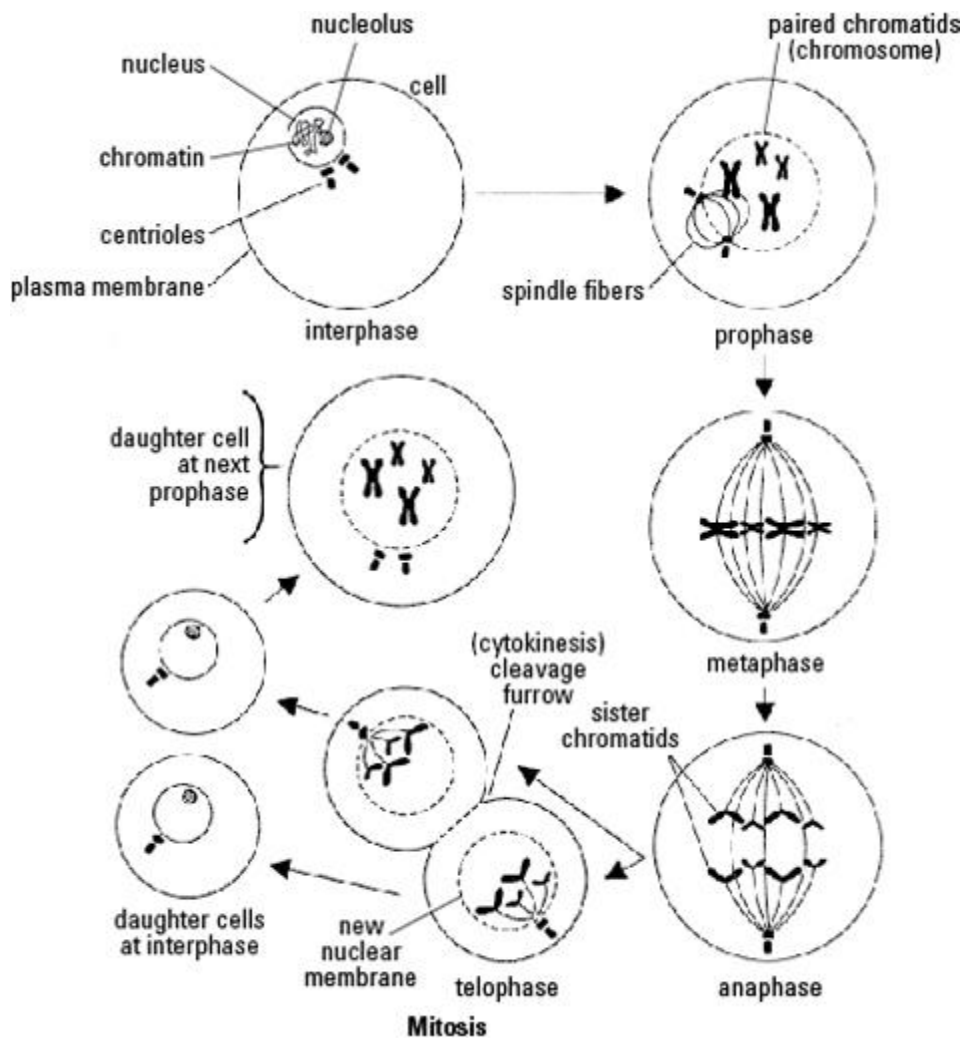


**Figure 1.12: The four stages of mitosis**

The cell cycle is a continuous event in both normal and cancer cells, including breast cancer. All the cell cycle events are strictly controlled by the regulatory proteins in order to control growth and development. However, there is uncontrolled and increased proliferation in cancer cells, especially breast cancer cells. This is probably a result of the impairments of some of the regulatory proteins that control or check abnormal proliferation. Some of these proteins are given in Figure 1.13

## 1.25 Cell Cycle regulation

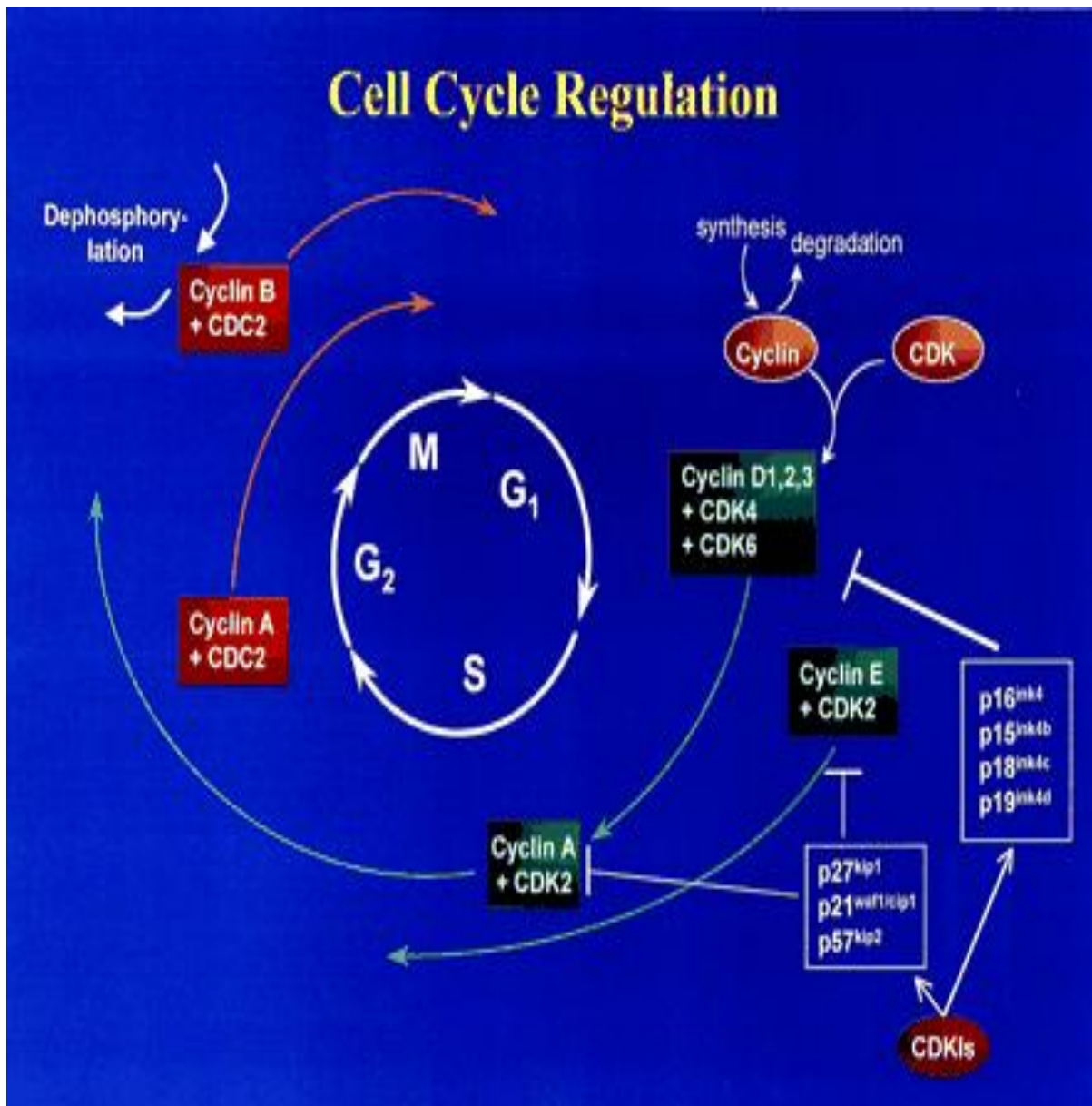


**Figure 1.13: The cell cycle and its regulation by cyclins, CDKs, and CDKIs.**

The cell cycle is divided into four distinct phases (G<sub>1</sub>, S, G<sub>2</sub>, and M). The progression of a cell through the cell cycle is promoted by CDKs, which are positively and negatively regulated by cyclins and CDKIs, respectively. As shown, cyclin D isoforms (cyclin D1–D3) interact with CDK4 and CDK6 to drive the progression of a cell through G<sub>1</sub>. The association of cyclin E with CDK2 is active at the G<sub>1</sub>-S transition and directs entry into S-phase. S-phase progression is directed by the cyclin A/CDK2 complex, and the complex of cyclin A with Cdc2 (also known as cdk1) is important in G<sub>2</sub>. Cdc2/cyclin B is necessary for the entry into mitosis. The INK4 (for inhibitor of cdk4) class of CDKIs, notably p16<sup>ink4a</sup>, p15<sup>ink4b</sup>, p18<sup>ink4c</sup>, and p19<sup>ink4d</sup>, bind and inhibit cyclin D-associated kinases (CDK4 and CDK6). The kinase inhibitor protein group of CDK inhibitors, p21<sup>waf1</sup>, p27<sup>kip1</sup>, and p57<sup>kip2</sup>, negatively regulate cyclin E/CDK2 and cyclin A/CDK2 complexes.

The cell cycle is regulated strictly at selected checkpoints that are controlled by group of modulators known as cyclin and cyclin-dependent kinases (CDKs), cyclin-dependent inhibitors (CDKI) and retinoblastoma gene products (pRB). These modulators are the key regulatory factors that dictate the orderly progression of the cell cycle through the activation and deactivation processes (Johnson and Walker, 1999). A number of CDKs have been identified including CDKs A, B1, B2, C, D1, D2, D3, E and many more (Figure 1.13). All cyclins contain a cyclin box, an important domain used to bind and activate CDKs. Cyclins and CDKs are also involved in the regulation of cell transcription, DNA repair, differentiation, and apoptosis (Peng 1998; Rickert 1996 and Roy 1994). Phosphorylation of CDK subunits can both positively and negatively regulate kinase activity (Arellano 1997) and ubiquitin-mediated proteolysis plays another crucial role in cell cycle control by targeting cyclins and other regulators for destruction at key times during the cell cycle (King 1996 and Pagano 1997). Some CDK's have been reported by LaBaer and co-workers to positively regulate the cell cycle by functioning as assembly factors for cyclin D/cdk complexes (LaBaer et al, 1997). CDK's are regulated by several methods, one of which includes phosphorylation of threonine and tyrosine residue. CDK's are very important to cell cycle control because its deactivation will prevent mitosis, which is the ultimate committal event in the cell cycle (Johnson and Walker, 1999).

### **1.26 Role of Cell-cycle Regulatory molecules in Breast Cancer Development and Progression**

The resulting DNA damage and the integrity of mitotic spindles caused by any intrinsic or extrinsic elements are assessed during transition between the four major phases of the cell cycle. Cell cycle progression is arranged by the relative activity of a family of serine

threonine kinases (Figure 1.14). The cyclins encode co-regulatory subunits of a holoenzyme that phosphorylates and inactivates a number of substrates including pRb (Hilakivi-Clarke et al, 2004). Cyclin D1 has been reported to be one of the commonly over expressed genes in breast cancer (Arnold and Papanikolaou, 2005; Sutherland and Musgrove, 2004). Oestrogen receptor (ER)-positive breast cancers has also been shown to produce cyclin D1 amplification and over expression more commonly than ER-negative cancers, and it is in the ER-positive subgroup that the most consistent association between cyclin D1 amplification and poor outcome has been found (Sutherland and Musgrove, 2004). Sutherland and others have suggested that the ability of cyclin D1 to modulate transcription may be important in mammary oncogenesis (reviewed in Arnold and Papanikolaou, 2005; Sutherland and Musgrove, 2004)

### **1.27 Cyclin D1**

Cyclin D1 encodes the labile regulatory subunit of the cyclin CDK4/6 holoenzyme. Phosphorylation of the pRb protein is thought to change the confirmation of pRb which, in turn, alters further upon phosphorylation by cyclin E/CDK2 complexes. It is considered that the phosphorylation of the pRb protein by the cyclin D1/CDK4/6 holoenzymes is required for transition through the G1 /S-phase of the cell cycle. The cyclin D1 gene has been reported by Zwijssen and his co-workers to physically associate with the ER and induce ER signaling in a CDK-independent manner (Zwijssen et al, 1997).

Immuno-neutralizing experiments performed by Lukas et al have revealed that cyclin D1 is required for oestrogen-induced cellular proliferation (Lukas et al, 1996). It has also been shown to enhance ER signaling through functioning as a coactivator-like protein,



analogous to the p160 steroid receptor coactivator (SRC) of the ER, in cultured cells. Research has revealed that up to 30- 50% overexpression of Cyclin D1 is present in primary breast cancers, partly due to amplification of the cyclin D1 gene, CCND1; hence, cyclin D1 is one of the most commonly overexpressed oncogenes in breast cancer (Arnold and Papanikolaou, 2005; Sutherland and Musgrove, 2004). This overexpression effect of Cyclin D1 is more pronounced in ER-positive breast cancers than ER-negative cancers, and it is in the ER-positive subgroup that the most consistent association between cyclin D1 amplification and poor outcome has been reported (Sutherland and Musgrove, 2004).

In addition, Cyclin D1 has been proven to be overexpressed in ductal hyperplasia and ductal carcinoma in situ as well as invasive cancers and these findings suggest that it may play a role in the evolution of breast cancer. In contrast to general opinion based on this finding that cyclin D1 overexpression might be expected to be associated with high proliferation rates, over expression of cyclin D1 in breast cancer is characteristic of slow-growing, more differentiated cancers (Sutherland and Musgrove, 2004).

Moreover, in a panel of breast cancer cell lines, CDK4 activity was not strictly related to cyclin D1 expression, suggesting that functions of cyclin D1 other than its ability to activate CDK4 and promote cell proliferation might contribute to its activity as a mammary oncogene ( Fu et al, 2004; Sutherland and Musgrove, 2004). Amplification of the cyclin D1 gene, CCND1, is observed in just a few of cyclin D1 overexpressing breast cancers. Furthermore, Cyclin D1 has been implicated in the oncogenic actions of Ras and Neu/erbB2. Murine mammary tumours induced by oncogene display increased expression of cyclin D1, while cyclin D1 expression is necessary for Ras or erbB2-mediated mammary tumourigenesis (Sutherland and Musgrove, 2004). However, the relationship between cyclin

D1overexpression and erbB2 amplification in human breast cancer is yet to be elucidated (Arnold and Papanikolaou, 2005).

### **1.28 Cyclin E1**

Cyclin E1 is reportedly overexpressed frequently in breast cancers, particularly ER-negative breast cancers. This observation is attributed to the presence of a number of low molecular weight isoforms, which appear to contribute to poor clinical outcomes (Sutherland and Musgrove, 2004). The low molecular weight isoforms display enhanced binding to CDK2 to produce a complex that is relatively resistant to inhibition by p21 and p27 (Wingate et al, 2005). Moreover, cyclin E1 overexpression is of greater prognostic significance when p27 expression is reduced and CDK2 activation increased (Caldon et al, 2010). The association between cyclin E1 overexpression and markers of proliferation together with the above mentioned role as suggested by Caldon and co-workers that the CDK dependent functions of cyclin E1 may be critical to its role in mammary oncogenesis (Caldon et al, 2010).

### **1.29 p27 and p21**

These two genes are tumour suppressor genes and many studies have confirmed this (Musgrove 2004). The role of p21 and its abundance as a modulator of outcome in primary breast cancer is still unclear. Expression is generally undetectable in normal breast epithelial cells and very variable in breast cancers, with conflicting data on the prognostic implications of p21 expression from a limited number of small patient groups (Tsihlias et al, 1999).

The use of p27 as a prognostic marker has been more widely investigated. Normal human mammary duct epithelial cells exhibit nuclear immunoreactivity for p27, while breast cancers often exhibit reduced p27 expression and/or mislocalisation of p27 to the cytosol (Alkarain et al, 2004). In general, reduced nuclear p27 expression is associated with high tumour grade and ER negativity, and in a small majority of studies, represents an independent prognostic indicator upon multivariate analysis (Alkarain et al, 2004). However, loss of heterozygosity at band 13 of chromosome 12, which harbours the p27 gene, has been reported in breast cancers, although, somatic mutations in this gene are rare (Alkarain et al, 2004), and the predominant mechanism for loss of protein expression appears to be linked to increased protein turnover. Newman and Spataro have reported that ErbB2 overexpression associates with low p27 levels in breast cancer patients overall (Newman et al, 2001) or in the lymphnode negative subset (Spataro et al, 2003). Hence, activation of signaling pathways downstream of this receptor may promote p27 degradation. However, RTK signaling can also lead to restriction of p27 to the cytosol. Additionally, in cancers with either low or high p27 expression, the presence of cytosolic p27 was associated with worse overall survival rate (Alkarain et al, 2004).

### **1.30 Therapeutic target in breast cancer**

There are two major therapeutic approaches that are useful in the treatment of breast cancer; namely: the modulation of the cell cycle and direct inactivation of checkpoint controls. The following section explores the recent evidence that validates this type of clinical intervention.

### **1.31 Modulation of the cell cycle**

Alteration to any of the major phases of the cell cycle may lead to carcinogenesis, which is a major concern in the field of cancer research. Subsequently, the cell cycle has become the bedrock of the major therapeutic interventions research, providing numerous opportunities to target checkpoint controls in order to develop new therapeutic strategies for combatting this disease.

These include induction of checkpoint arrest leading to cytostasis and, ultimately, apoptosis; arrest of proliferating cells in defined stages of the cell cycle, which may in turn sensitize them to treatment with other therapeutic agents, such as radiation; and targeting therapies towards specific regulatory components of the cell cycle (Caldon et al, 2010). Those drugs that have diverse mechanisms of action and ex-chromosome breakage can cause cell cycle arrest at both the G1/S and G2/M checkpoints (Lowe et al, 1993).

The most common and reliable chemotherapeutic approach is the induction of DNA damage, followed dogmatically by induction of apoptosis. Some chromosome breakers and DNA cross links agents such as cisplatin and Mustard have been reported to cause cell cycle arrest at both G1/S and G2/M checkpoints (Lowe et al 1993). G1 arrest caused by these agents is mediated by p53, which in turn induces an increase in p21, resulting in inhibition of cyclin/CDK2 and cyclin/CDK4 complexes and hypophosphorylation of Rb (Robert and Thompson, 1979). Up-regulation of p21 also results in sequestration of PCNA, which contributes to arrest at G1/S. The G2/M checkpoint induced by DNA damage can occur by either p53-dependent or independent mechanisms (Paules et al, 1995; Agawal et al, 1995). Both p21 and phosphorylation of CDK1 is required for passage of cell from G2 phase into M-phase and can participate in the DNA damage G2/M checkpoint. Tumour cells in which p53 are inactive can bypass the G1/S checkpoint and exhibit increased sensitivity to DNA-

damaging agents such as cisplatin (Fan et al, 1997) as a result of failure to arrest and repair their damaged DNA.

Another intervention is also made possible by the use of microtubular inhibitors such as taxol and vinca alkyloids. These act principally by disrupting the normal tubular polymerisation/depolymerisation and mitotic spindle formation (Gorbsky 1997). Hence, the cells are forced either to initiate a p53-dependent arrest at the mitotic spindle assembly checkpoint (Cross et al., 1995), a radiosensitive phase of the cell cycle, or continue to progress through M-phase and become aneuploid and arrest in G1 (Argawa, 1995).

Arrest in G2/M induced by these drugs (taxol and vinca alkaloids) is associated with stabilization of cyclin B complexes (Poon et al, 1997). Tumour cells treated with microtubule inhibitors can undergo apoptosis from both G1 and G2 arrest (Wood et al, 1995). Microtubule inhibitors have also proven effective in the clinic as radiosensitizers (Liebmann et al, 1994). Combined chemotherapy/radiotherapy with taxol, which blocks cells at the mitotic spindle assembly checkpoint, can enhance the sensitivity of radiation-resistant tumours to radiotherapy (Liebmann et al, 1994; Tischler et al, 1992).

G1 checkpoint arrest can also be triggered by depletion of ribonucleotide pools, caused by nucleoside analogs such as hydroxyurea and gemcitabine. G1 arrest at a point may be totally distinct from that associated with DNA damage (Linke et al, 1996). This latter G1 checkpoint is mediated by p53 and also requires up-regulation of p21 (Wharl et al, 1997). In checkpoint-defective cells, such as those with inactive p53, bypass of the G1/S checkpoint produces DNA strand breaks, resulting in cell death (Chang et al, 1998). Both gemcitabine and hydroxyurea have also been effectively used as radio sensitizers for a variety of tumour types (Shewach and Lawrence, 1996). Anti-metabolites such as methotrexate and 5-fluorouracil have been reported to inhibit thymidylate synthase and DNA synthesis and

induce a p53-dependent S-phase arrest (Matsui et al, 1996). However in tumour cells, in which p53 is inactive, DNA damage induced by these drugs goes undetected and cells progress to G2 and subsequently undergo apoptosis (Lowe et al, 1993).

These drugs are also used clinically as radiosensitizers as a result of their ability to arrest cells in the radiosensitive phase of the cell cycle (Robertson et al, 1996). Topoisomerase inhibitors have been reported to also cause DNA damage, resulting in increased levels of cyclin A and S-phase arrest or inactivation of cyclin B/CDK2 complexes and G2/M arrest (Kaufmann et al, 1999). Moreover, the prominent role of p53/p21-mediated activity for many of the above-named drugs in addition to the activity of topoisomerase inhibitors can also be mediated by the Rb/p16 pathway. In some cell types, drugs such as camptothecin and etoposide produce an increase in p16, which inhibits phosphorylation of Rb resulting in a G1 cell cycle arrest (Shapiro, 1998). Therefore, in addition to p53; their activity may also be dependent on the presence of a functional Rb protein. Tumour cells that lack functional Rb can bypass this checkpoint and progress through the cell cycle, becoming genetically unstable and acquiring additional genetic alterations including changes in ploidy.

### **1.32 Direct inactivation of checkpoint controls**

Some successful or potentially successful therapeutic strategies involve the use of agents that target cell cycle regulatory molecules. As mentioned previously, the activity of cyclin-kinase complexes is regulated by phosphorylation and several CDK inhibitors have been identified, which exhibit specificity for the ATP-binding pocket of these and block their phosphorylation CDKs (Walker et al, 1998). Chemical inhibitors of CDKs such as olomoucine and its analog

roscovitine exhibit specificity for CDK1 and CDK2 (Vesely, 1994). These inhibitors can induce both G1 and G2 arrest as well as apoptosis (Walker, 1998).

As mentioned above, in response to DNA-damaging agents, some tumour cells can arrest in G2 in a p53-independent manner. This G2/M checkpoint arrest occurs as a result of phosphorylation and inactivation of CDK1. Staurosporine and its second-generation analog 7-hydroxystaurosporine (UCN-01) inhibit the phosphorylation of CDK1, resulting in the activation of this M-phase regulator and abrogating the G2/M arrest (Wang et al,1996). Use of UCN-01 has been most successful in combination with DNA-damaging agents such as cisplatin (Bunch and Eastman, 1996) and camptothecin (Shao et al,1997) in p53- deficient cells that can bypass the G1 checkpoint and would otherwise arrest in G2. As a consequence of UCN-01 treatment, tumour cells that have sustained DNA damage progress through the cell cycle beyond the G2/M checkpoint and undergo apoptosis (Wang et al, 1995). Similar strategies with several agents (such as caffeine) that abrogate the G2 checkpoint by activating CDK1 have been shown to preferentially sensitize p53-deficient cells to other genotoxic agents such as radiation and etoposide (Yao et al, 1996).

Active cyclin D-kinase complexes, which serve to phosphorylate Rb and release E2F, can also be inhibited by small peptides derived from p16 (Fahraeus et al, 1998). A 20-amino-acid peptide of p16 can bind CDK4; inhibit activation of cyclin D-CDK4 activity, and block cell cycle progression through G1. As predicted, this cell cycle arrest requires a functional Rb protein (Fahraeus et al, 1998). Similarly, double-stranded DNA with high affinity for E2F can act as a molecular decoy, compete for E2F binding to DNA, and inhibit the ability of E2F to regulate target genes such as *cdc2* (CDK1) and cyclin E (Bandara et al, 1997; Morishita et al, 1995).

Targeting of breast cancer by anti-angiogenic drugs available to date have been shown to be a failure and regulators of the cell cycle in conjunction with radiotherapy and surgery are still the mainstay in the treatment of the disease. However, during the next 20 years more targeted therapy is likely to become the preferred method of treatment. It is hoped that the results shown in this study could lead to a new class of targeted cancer therapeutics aimed solely at the treatment of breast cancer.



### **1.33 Cell death**

Natural death is an integral part of cell development and this was also described by Cotter and Curtin as a natural event that can be related to an integral part of toad development (Cotter and Curtin, 2003). Natural death has been described newly in many ways after this observation. There are two major mechanisms by which cells undergo natural death: necrosis or apoptosis.

### **1.34 Necrosis**

Necrosis, otherwise known as cell murder, is described as the death of cells through external damage (extrinsic factors), usually caused by destruction of the plasma membrane or the biochemical pathways that support the cells integrity. The necrotic cell is characterised by swollen morphology and plasma membrane lyses, which releases cytoplasmic components (necrotic debris) into the surrounding tissue spaces, attracts inflammatory cells and ultimately leads to the tissue destruction characteristic of inflammation. The death of a single cell by this mechanism might be resolved in some tissues, but a large number of cells dying by necrosis usually results in inflammation, subsequent repair and scarring; leading to compromise and permanent alteration of tissue architecture.

Necrosis can occur in a matter of seconds (Collins et al, 1997) and also can cause loss of cell-membrane integrity followed by swelling of both cytoplasm and mitochondria; ultimately resulting to cell and many of its internal organelles lyses' (Leist and Jäättelä, 2001). The products of necrotic cells are usually phagocytosed by macrophages, and this process provokes an inflammatory response in vivo. Necrosis-like programmed cell death describes programmed cell death that does not involve chromatin condensation and has

varying degrees of other apoptotic features. In some cases caspase-1 and caspase-8 have been implicated in this type of programmed cell death (Leist and Jäättelä, 2001). Some of the factors that lead to necrosis are detailed in the following sections.

### **1.35 Pathophysiology and physiological factors leading to necrosis**

Cell and tissue death is a common phenomenon that usually arises suddenly as a result of some extreme conditions (high temperature, heat shock etc): a process that leads to unregulated process of both membranes and cytosol destruction. This finding led to the concept that when cell destruction is followed by rapid disruptions of the plasma membrane, cytoplasmic structures, and the nucleus, death is passive and unregulated. However, necrotic cell death could also be regulated by some specific physiological conditions such as bacterial infections, viral infection, bacterial toxins etc. (Warny et al, 2000: Dong et al, 1997).

Necrosis can also be triggered by components of the immune system, such as complement (Shimizu et al, 2000), activated natural killer cells (Blom et al, 1999), and peritoneal macrophages (Arantes et al, 2000).The pathogen-induced necrotic programs in cells of immunological barriers (e.g. intestine mucosa) may reduce invasion of pathogens through the surfaces affected by inflammation (Ehlers et al, 1999).

Necrotic cell death can also result from pathological conditions that are characterised by inadequate secretion of cytokines, nitric oxide (NO) and reactive oxygen species (ROS). A classic example of necrotic conditions is ischemia that leads to a drastic depletion of oxygen, glucose, and other trophic factors and evokes massive necrotic death of endothelial cells and non-proliferating cells of surrounding tissues (neurons, cardiomyocytes, renal cells, etc.) (Elmore, 2007).

### **1.36 Apoptosis**

Apoptosis is a form of cell death that usually occurs when cell is exposed to unfavourable conditions such as heat, hypoxia, and radiation, cytotoxic anti cancer drugs, toxicants or any physical damage (Elmore 2007). It is usually initiated in order to prevent inflammation associated with necrotic process by a careful removal of damaged cells from injury sites (Fin et al, 2005). Initiation of apoptosis triggers a series of events that culminate in the cell's destruction. This process is usually called "programmed cell death" as it is an innate response of the cell that protects the remainder of the organism from a potentially harmful agent (Wyllie et al, 1980). The process of apoptosis is illustrated in the diagram below.

# Apoptosis (Programmed Cell Death)

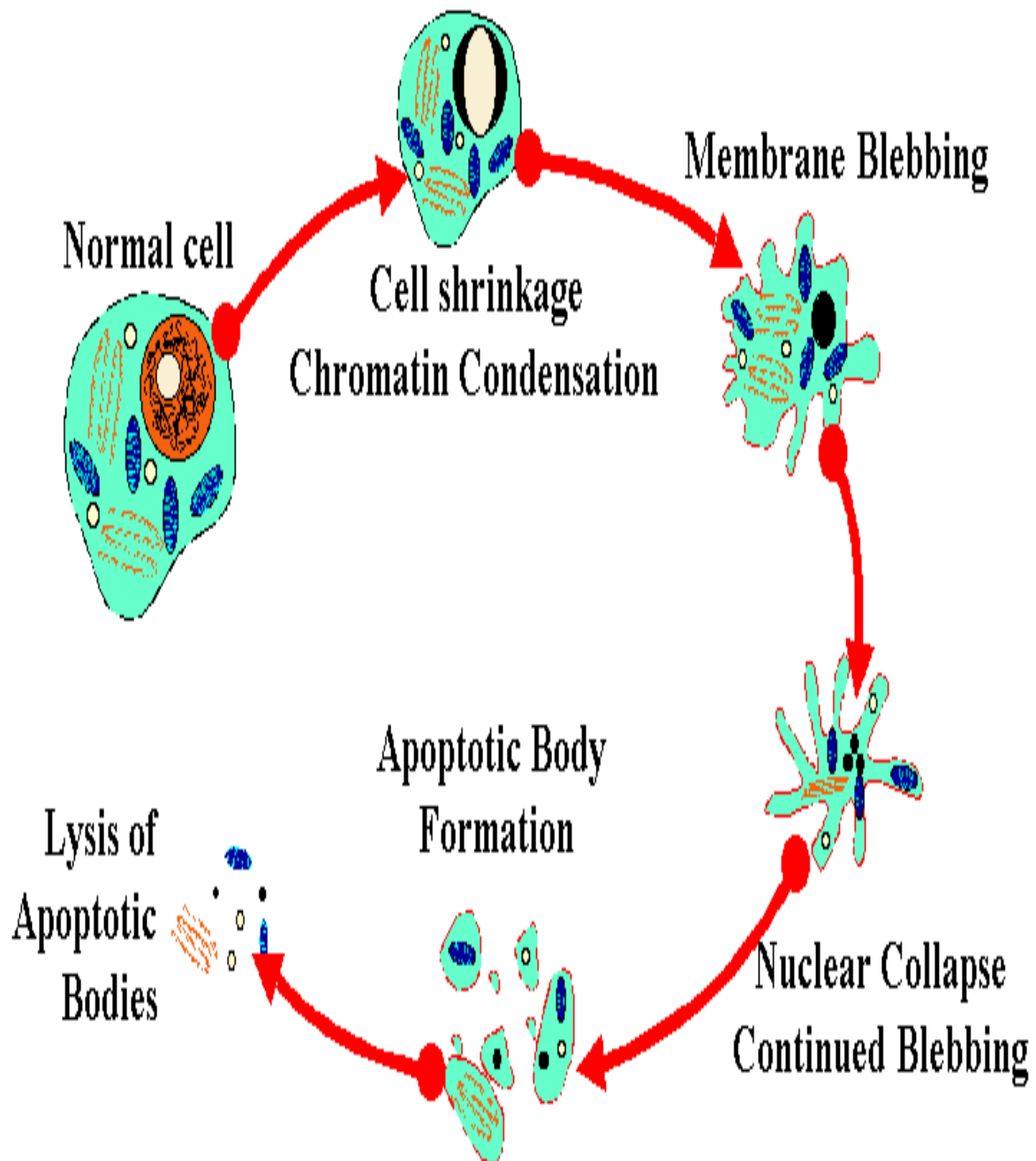


Figure 1.14: The processes involved in apoptosis

Apoptosis also describes a common mechanism by which cell undergoes natural death. It involves cascades of preprogrammed arranged events, including morphological and biochemical changes, which qualifies it as an example of programmed cell death (Wyllie et al, 1980). During the initial phases of apoptosis, cells shrink and their nuclei condense, after which they disintegrate into well-enclosed apoptotic bodies (Figure 1.14). The common features of apoptosis include cell shrinkage, plasma membrane blebbing, cell detachment, externalization of phosphatidylserine, nuclear condensation and ultimately DNA fragmentation (Brauchle et al., 2014; Majno and Joris, 1995).

Apoptosis is a normal occurrence during development and aging and as a homeostatic mechanism to maintain cell populations in tissues: it also occurs as a defence mechanism, such as in immune reactions or when cells are damaged by disease or noxious agents (Norbury and Hickson, 2001). However, many stimuli and conditions including physiological and pathological are among other factors that triggers apoptosis; yet not all cells will necessarily die in response to the same stimulus. At low doses, irradiation or some cytotoxic drugs used for cancer chemotherapy results in DNA damage in some cells, ultimately, leading to apoptotic death through a p53-dependent pathway (Elmore, 2007). Some cells express Fas (Fatty acid synthetase) or TNF (Tumour necrosis factor) receptors that can lead to apoptosis via ligand binding and protein cross-linking. Other cells have a default death pathway that must be blocked by a survival factor such as a hormone or growth-factor (Elmore, 2007).

Apoptosis and necrosis can occur independently, sequentially and simultaneously, but there is need to make a clear distinction between the two processes

(Zeiss 2003: Hirsch 1997 ); the type of stimuli and/or the degree of stimuli play a critical role in this process. Interestingly, low doses of some environmental perturbations such as heat, radiation, hypoxia and cytotoxic anti-cancer drugs can induce apoptosis but these same stimuli can result in necrosis at higher doses. In addition, apoptosis is a coordinated and often energy-dependent process that involves the activation of a group of cysteine proteases called “caspases” and a complex cascade of events that link the initiating stimuli to the final demise of the cell (Elmore, 2007: Fin et al 2005). Apoptosis can also be seen as a stage-dependent process from its induction to early, intermediate and late-stage apoptotic events (Figure 1.15 A-D)

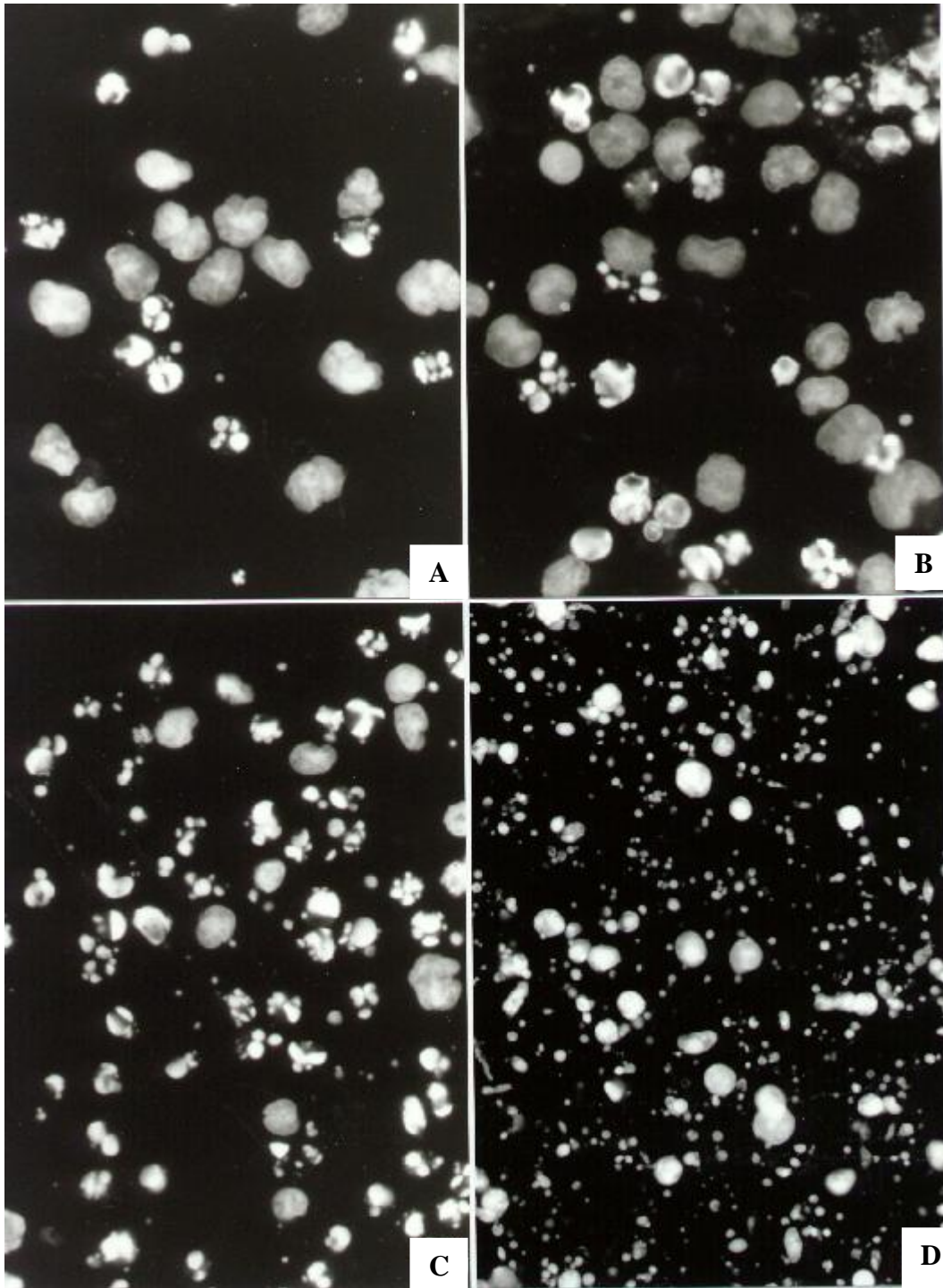


**Figure 1.15: Stages of apoptosis**

(A) Full blown apoptotic Figure (early apoptosis); (B) Different forms of chromatin aggregation (intermediate/mid apoptosis); (C) Late stage of apoptosis; (D) Very late apoptosis.

### **1.37 Morphology of Apoptosis**

There are various morphological changes that occur during apoptosis and some of these changes were characterised by nuclear and cytoplasmic condensation, and cellular fragmentation into membrane-bound fragments. Early apoptosis is usually characterised by cell dehydration followed by changes in cell size and shape, resulting into smaller, dense cytoplasmic and more tightly packed organelles cells (Fink and Cookson 2005). The membrane bound fragments or apoptotic bodies (Figure 1.16C) are consequently engulfed by microphages, parenchyma cells, or neoplastic cells and are desolved within the phagolysosomes (Figure 1.16D). This process allows cell deletion with little tissue disruption and no inflammation.

The process of apoptosis and removal of apoptotic cells are practically free of inflammatory reaction. Lockshin and William suggested this process of tissue deletion without inflammation allows reutilization of cellular components (Lockshin and William, 1965). The morphological characteristics of apoptosis were purported to result from a general mechanism of controlled cell deletion, which plays a complementary role to mitosis and cytokinesis in maintaining stable cell populations within tissues. The concept of apoptosis furthered the hypothesis that living cells are programmed genetically to contain components of a metabolic cascade that, when activated, can lead to cellular death (Lockshin and Zakeri, 2001).

Various morphological changes that occur during apoptosis can be measured by scatter light analysis (flow cytometry) and some of these changes are characterised by some of the features described above. In short, the cells traversing through the focus of a laser beam in a flow cytometer scatters the laser light. Analysis of the degree of scattered light



gives indepth information about the morphological changes that characterise the onset of apoptosis (Darzynkiewicz et al 1992).

Hacker also described the various morphological changes that occur in apoptosis by light and electron microscopy (Hacker, 2000). Cells view under the electron microscope shows cell shrinkage and pyknosis as the major morphological changes that characterised early stage of apoptosis (Kerr et al., 1972). On histologic examination with haematoxylin and eosin stain, apoptosis involves single cells or small clusters of cells. The apoptotic cell appears as a round or oval mass with dark eosinophilic cytoplasm and dense purple nuclear chromatin fragments (Figure 1.16 A). Electron microscopy also shows other subcellular changes that occur during early chromatin condensation and some of these changes involve aggregation of electron-dense nuclear material under the nuclear membrane although there can also be uniformly dense nuclei (Figures 1.16 B). This process leads to extensive plasma membrane blebbing followed by karyorrhexis and separation of cell fragments into apoptotic bodies during a process called “budding.” The organelle integrity is still maintained and all of this is enclosed within an intact plasma membrane. Macrophages that engulf and digest apoptotic cells are called “tingible body macrophages” and are found frequently within the reactive germinal centers of lymphoid follicles or occasionally within the thymic cortex. The tingible bodies are the bits of nuclear debris from the apoptotic cells. The anti inflammatory activity associated with both apoptosis process and removal of apoptotic bodies is due to the following reasons: (1) apoptotic cells do not release their cellular constituents into the surrounding interstitial tissue; (2) they are quickly phagocytosed by surrounding cells thus likely preventing secondary necrosis; and (3) the engulfing cells do not produce anti-inflammatory cytokines (Kurosaka et al, 2003; Savill and Fadok, 2000).

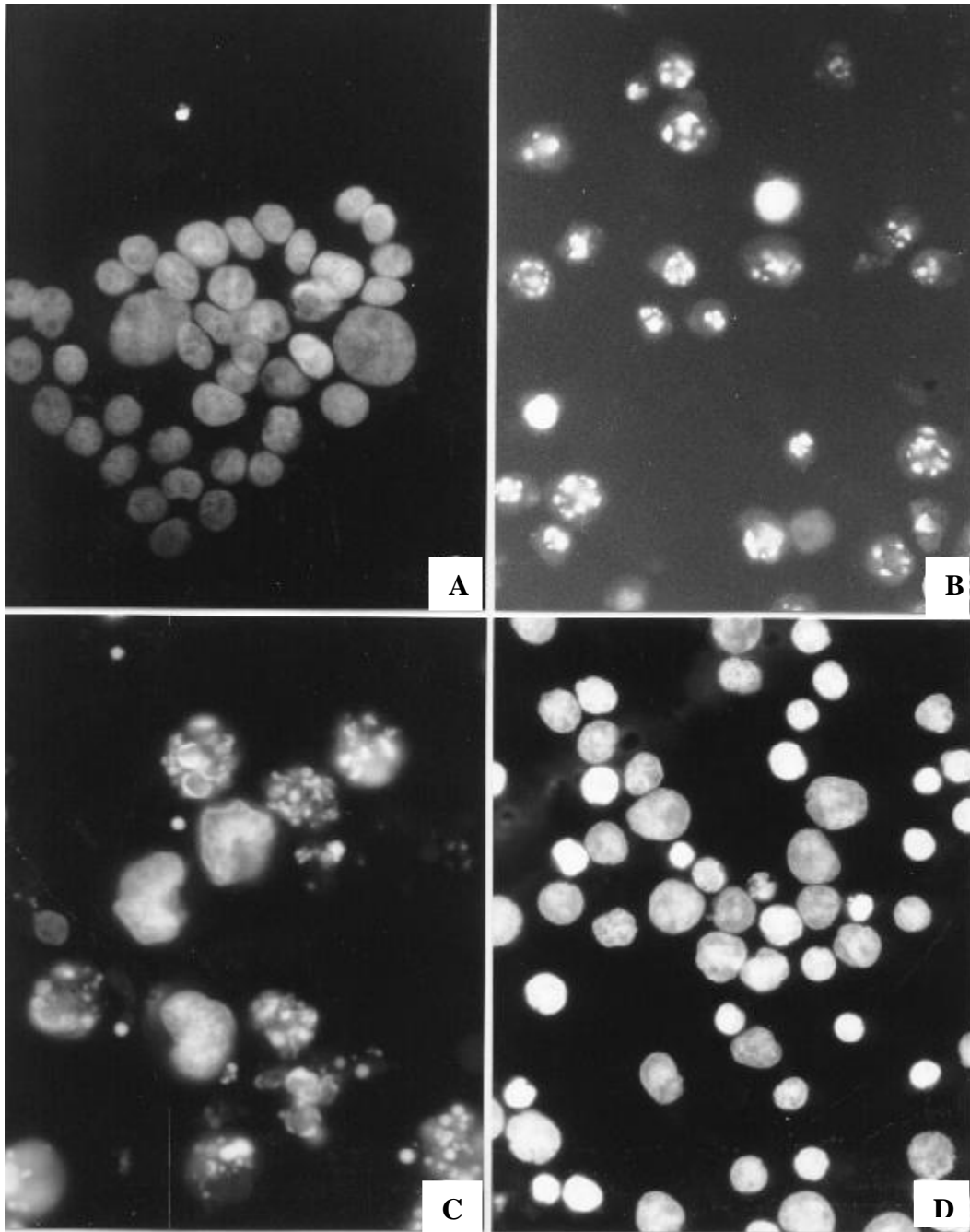


**Figure 1.16: Morphology of apoptosis.**

(A) Normally shaped nuclei (B) Chromatin clumping in apoptotic nuclei (C) Different features of chromatin clumps (D) Chromatin superaggregation.

### **1.38 Biochemical features of apoptosis**

Apoptotic cells have been described previously as exhibiting several biochemical modifications, such as protein cleavage, protein cross-linking, DNA breakdown, and phagocytic recognition that together result in the distinctive structural pathology (Hengartner 2000). There are various biochemical features that ensue once apoptosis programme has been initiated and some of these biochemical features are discussed below;

### **1.39 Activation of caspases**

Activation of caspases is one of the biochemical features of programme cell death. This process is triggered by some of the external stimuli that causes apoptosis. Caspases are usually expressed widely in an inactive proenzyme form in most cells: activation of this proenzymes lead to cascade of events including activation of other procaspases, initiation of a protease cascade, aggregation and autoactivation of other procaspases. This cascade of events amplifies the apoptotic signaling pathway; thus leading to rapid cell death (Figure 1.17). Caspases have proteolytic activity and are able to cleave proteins at aspartic acid residues, although different caspases have different specificities involving recognition of neighbouring amino acids. Once caspases are activated, there appears to be an irreversible commitment towards cell death (Elmore 2007).

Ten major caspases have been identified and categorised broadly into initiators (caspase-2,-8,-9,-10) (Cysteiny aspartic acid-protease-2-8-9-10), effectors or executioners (caspase-3,-6,-7) (Cysteiny aspartic acid-protease-3-6-7) and inflammatory caspases (caspase-1,-4,-5) (Cysteiny aspartic acid-protease-1-4-5) (Cohen, 1997; Rai et al, 2005). Other caspases such as caspase-11 (Cysteiny aspartic acid-protease-11), have been shown to

regulate apoptosis and cytokine maturation during septic shock and caspase-12 (Cysteinyln aspartic acid-protease). This mediates endoplasmic-specific apoptosis and cytotoxicity by amyloid- $\beta$  has been reported (Kang et al, 2002: Koenig et al, 2001: Nakagawa et al, 2000: Hu et al, 1998). Extensive protein cross-linking is another characteristic of apoptotic cells, which is achieved through the expression and activation of tissue transglutaminase (Nemes et al, 1996).

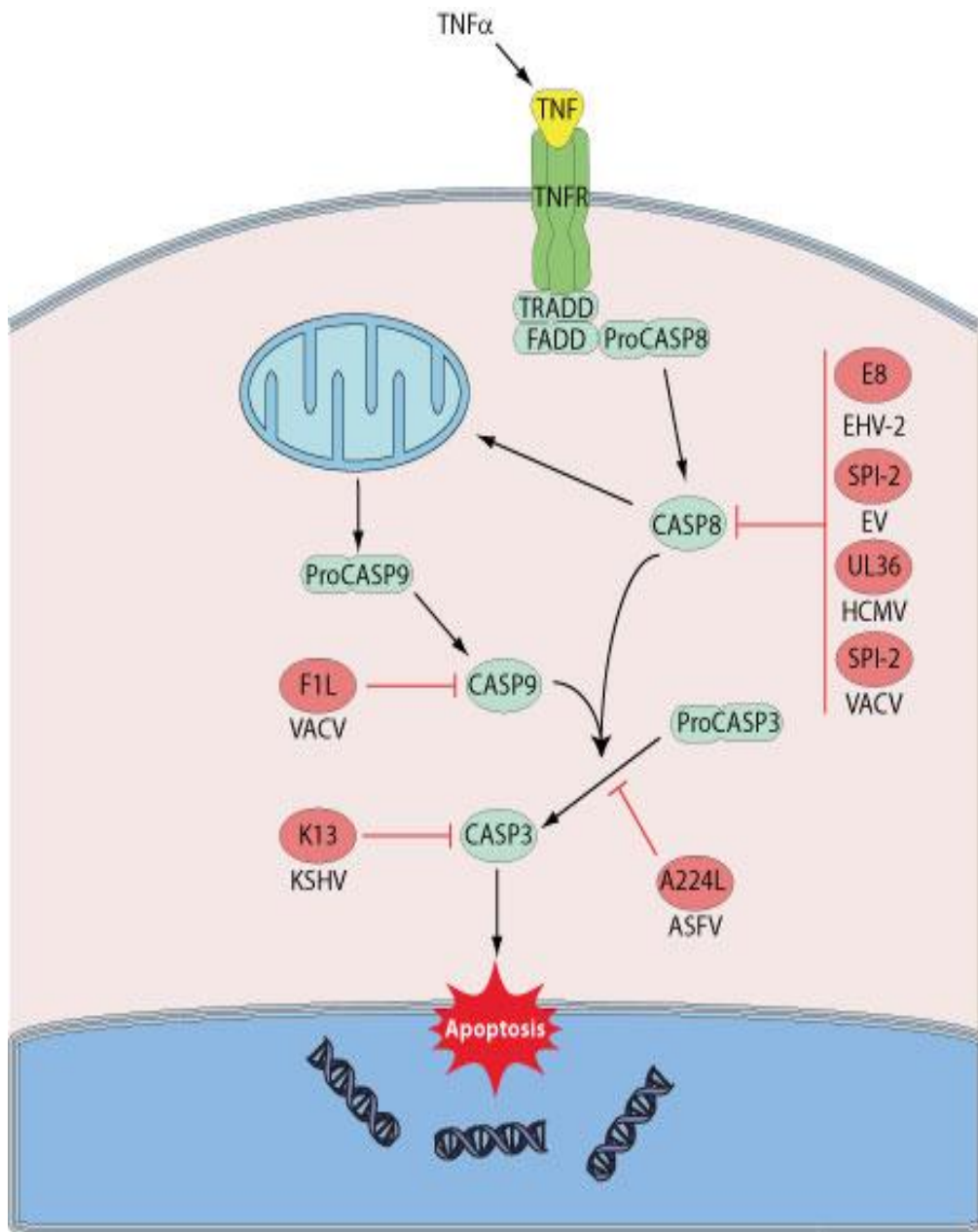


**Figure 1.17: Activation of apoptosis signalling pathway**

#### **1.40 DNA fragmentation**

DNA fragmentation is one of the earliest recognizable changes that characterised irreversible commitment to programmed cell death (Wyllie 1980). This process is initiated by breakdown effect caused by  $\text{Ca}^{2+}$ -and  $\text{Mg}^{2+}$ -dependent endonucleases, resulting in DNA fragments of 180 to 200 base pairs (Bortner et al, 1995). Oberhammer and co workers have reported that formation of the larger DNA fragments is unconnected to oligonucleosome formation (Oberhammer et al., 1993). Similarly, cleavage of DNA into these larger fragments is sufficient to allow chromatin condensation and subsequent apoptosis, without oligonucleosome formation. DNA fragmentation can be clearly seen when the sample are run on agarose gel electrophoresis and stained with ethidium bromide: a characteristic ladder pattern is evident when viewed under UV light (Allen et al 1997).

#### **1.41 Phosphatidylserine (PS) Translocation**

Translocation of PS is another biochemical changes that takes place during early apoptosis (Allen et al 1997). Bratton and co-workers described this biochemical feature of apoptosis as the expression of cell-surface markers that result in the early phagocytic recognition of apoptotic cells by adjacent cells, permitting quick phagocytosis with little compromise to the surrounding tissue. This is achieved by the movement of the normal inward-facing phosphatidylserine of the cell's lipid bilayer to expression on the outer layers of the plasma membrane (Bratton et al, 1997). Although externalization of phosphatidylserine is a popular identified ligand for phagocytes on the surface of the apoptotic cell, however, recent studies have shown that other proteins like annexin1 and calreticulin are also exposed on the cell surface during apoptotic cell clearance.

Annexin V, an anticoagulant with other biological effects, is a member of a family of proteins which exhibits  $\text{Ca}^{2+}$ -dependent binding to negatively charged phospholipids (Allen et al 1997). Annexin V binds strongly and specifically to phosphatidylserine residues and can be used for the detection of apoptosis (Allen et al 1997). Externalisation of PS occurs in early apoptosis when membrane integrity is still intact: this process make flow cytometric analysis using fluorescein isothiocyanate- (FITC) labeled annexin V a useful quantitative measure of early apoptosis; this method has also been used with the DNA intercalating dye PI. During apoptosis the cells become reactive with annexin V after the onset of chromatin condensation but prior to the loss of the plasma membrane (Arur et al, 2003). Annexin V binding has been shown to reveal a much higher level of cells committed to apoptosis than PI staining, However, PI staining enter necrotic cells while apoptotic cells are excluded (Allen et al 1997). Calreticulin is a protein that interacts with LDL (low density lipoprotein)- receptor-related protein on the engulfing cell and is suggested to cooperate with phosphatidylserine as a recognition signal (Gardai et al, 2005). The adhesive glycoprotein, thrombospondin-1, can be expressed on the outer surface of activated microvascular endothelial cells and, in conjunction with CD36 (Cluster of differentiation 36), caspase-3-like proteases and other proteins, induce receptor-mediated apoptosis (Jimenez et al, 2000).

#### **1.42 Mechanisms of apoptosis**

The mechanisms of apoptosis have been described as a complex and sophisticated processes involving energy-dependent cascade of molecular events (Figure 1.18). There are two major mechanisms by which cells commit suicide by apoptosis, namely the extrinsic or death-receptor pathway and the intrinsic or mitochondrial pathway (Figure 1.18). However, Igney

and Krammer have recently shown that the two pathways are linked and that molecules in one pathway can influence the other (Igney and Krammer, 2002). There is also an additional pathway known as perforin/granzyme which involves T-cell mediated cytotoxicity and perforin-granzyme-dependent killing of the cell. The perforin/granzyme pathway can induce apoptosis via either granzyme B or granzyme A (Elmore 2007).

The extrinsic, intrinsic, and granzyme B pathways converge on the same terminal otherwise known as execution pathway. This pathway is initiated by the cleavage of caspase-3 and results in DNA fragmentation, degradation of cytoskeletal and nuclear proteins, cross-linking of proteins, formation of apoptotic bodies, expression of ligands for phagocytic cell receptors and finally uptake by phagocytic cells (Elmore 2007). The granzyme A pathway activates a parallel, caspase-independent cell death pathway via single stranded DNA damage (Martinvalet et al, 2005).



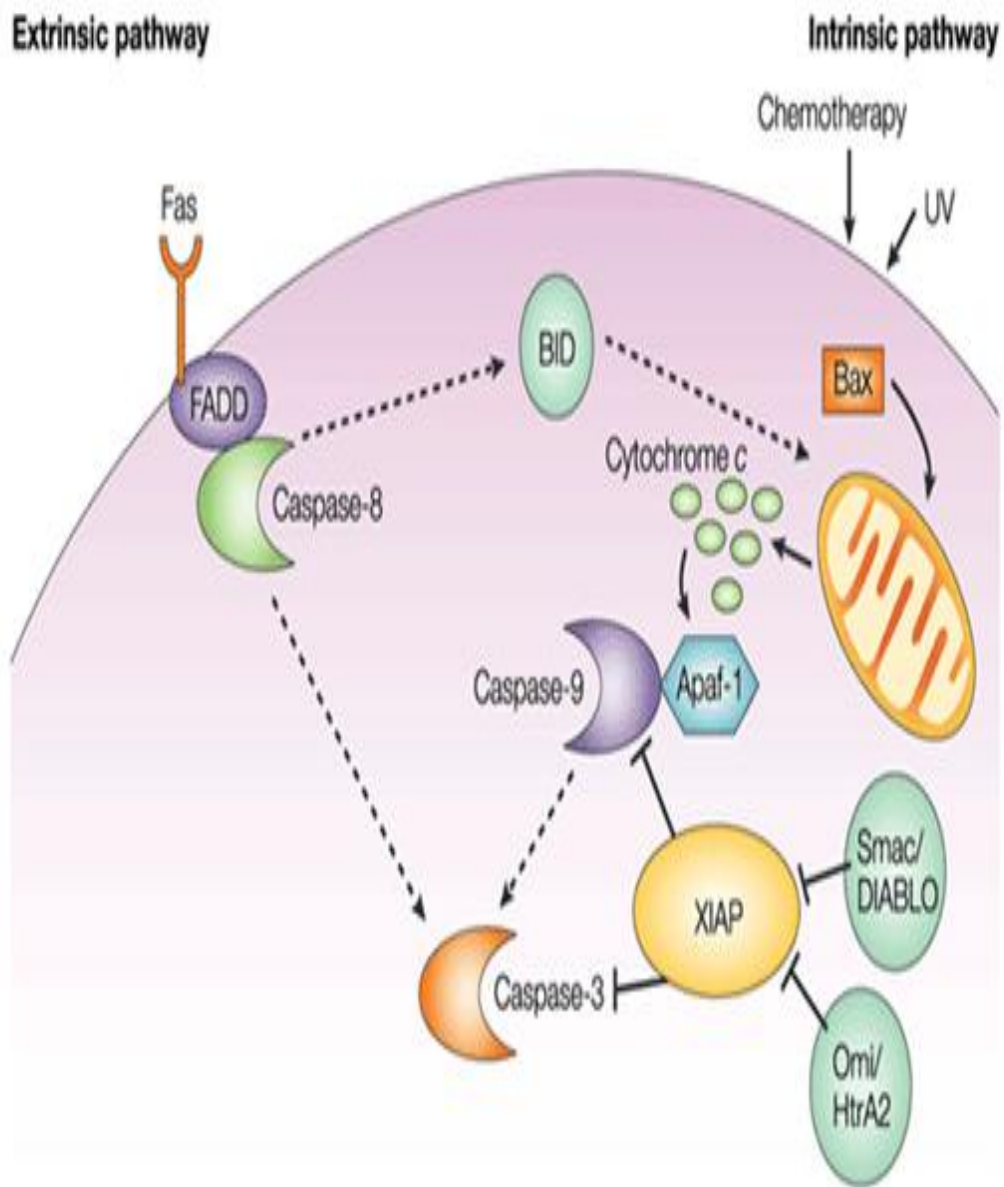


**Figure 1.18: Intrinsic and extrinsic pathway**

### 1.43 Extrinsic Pathway (caspase -8 apoptosis)

The extrinsic signaling pathways that initiate apoptosis involve activation of caspase 3- which is usually activated either by caspase -8 or -9. Activation of caspase -8 involves transmembrane receptor-mediated interactions which also include death receptors

(FasL/FasR, TNF- $\alpha$ /TNFR1, Apo3L/DR3 (Apo3 ligand/ Death-receptor 3), Apo2L/DR4 (Apo2 ligand/ Death-receptor 4) , and Apo2L/DR5 (Apo2 ligand/ Death-receptor 5) that are members of the TNF receptor gene super family ( Weber et al 2010; Rubio-Moscardo et al, 2005; Locksley et al, 2001; Suliman et al, 2001; Ashkenazi et al, 1998; Peter and Kramer, 1998; Chicheportiche et al, 1997).

Ashkenazi and Dixit also reported that members of the TNF receptor family share similar cysteine-rich extracellular domains and have a cytoplasmic domain of about 80 amino acids called the “death domain” (Ashkenazi and Dixit, 1998). This plays a critical role in transmitting the death signal from the cell surface to the intracellular signaling pathways. The sequence of events that define the extrinsic phase of apoptosis are best characterised with the FasL/ FasR (Fatty acid synthetase ligand /Fatty acid synthetase receptor) and TNF- $\alpha$  /TNFR1 (tumour necrosis factor-alpha /tumour necrosis factor receptor 1) models, which involve clustering of receptors and binding with the homologous trimeric ligand. Upon ligand binding, cytoplasmic adapter proteins are recruited which exhibit corresponding death domains that bind with the receptors.

The binding of Fas ligand to Fas receptor results in the binding of the adapter protein FADD (Fas-associated death domain) and the binding of TNF ligand to TNF receptor results in the binding of the adapter protein TRADD (TNF receptor-associated death domain) with recruitment of FADD and RIP (Receptor-interacting protein) (Wajant, 2002: Hsu et al,

1995). FADD then associates with procaspase-8 via dimerization of the death effector domain, leading to the formation of a mitochondrial permeability transition (MPT). Subsequently, this causes auto-catalytic activation of procaspase-8 (Pro cysteinyl aspartic acid-protease 8) (Kischkel et al, 1995). Activation of caspase-8 automatically triggers the execution phase of apoptosis (Figure 1.18).

#### **1.44 Intrinsic Pathway (mitochondria apoptosis)**

Mitochondria apoptosis appears to be much more common than caspase -8 dependent apoptosis *in vivo* and this apoptotic pathway is controlled by bcl-2 (B-cell lymphoma protein 2) family of proteins (Cory and Adams, 2002). BH3 protein belonging to bcl-2 protein family is the only protein that usually regulates the activation of the effectors Bax and Bak (Figure 1.18). Once Bax and Bak are activated, cytochrome c will be automatically released from the mitochondria intermembrane space into the cytosol, where it binds to Apaf-1 inducing its oligomerisation and thereby causing the activation of caspase-9 (Grepsi et al 2010). Some stimuli like, radiation, toxins, hypoxia, hyperthermia, viral infections, free radicals have been reported to cause such changes in the inner mitochondria leading to an opening of the MPT pore, loss of the mitochondrial transmembrane potential and release of two main groups of normally sequestered pro-apoptotic proteins from the intermembrane space into the cytosol (Saelens et al., 2004). The clustering of procaspase-9 in this manner leads to caspase-9 activation. Smac/DIABLO and HtrA2/Omi (second mitochondrial activator of caspases/direct IAP binding protein with low PI) has been reported to promote apoptosis by inhibiting IAP (inhibitors of apoptosis proteins) activity (Schimmer 2004: Van Loo et al, 2002).

The second group of pro-apoptotic proteins, AIF (Apoptosis Inducing Factor), endonuclease G and CAD (Caspase-Activated DNase), are released from the mitochondria during apoptosis, but this is a late event that occurs after the cell has committed to die. AIF translocates to the nucleus and causes DNA fragmentation into ~50,300 kb pieces and condensation of peripheral nuclear chromatin (Joza et al, 2001). This early form of nuclear condensation is referred to as “stage I” condensation (Susin et al, 2000). Endonuclease G also translocates to the nucleus where it cleaves nuclear chromatin to produce oligonucleosomal DNA fragments (Li et al, 2001). AIF and endonuclease G both function in a caspase-independent manner. CAD is subsequently released from the mitochondria and translocates to the nucleus where, after cleavage by caspase-3, it leads to oligonucleosomal DNA fragmentation and a more pronounced and advanced chromatin condensation (Enari et al, 1998). This later and more pronounced chromatin condensation is referred to as “stage II” condensation (Susin et al, 2000). The control and regulation of these apoptotic mitochondrial events occurs through members of the Bcl-2 family of proteins. The anti-apoptotic members of the Bcl-2-family appear to block apoptosis by binding either BH3-only proteins or Bax/Bak (Grepsi et al 2010).

#### **1.45 Perforin/granzyme Pathway**

T-cell mediated cytotoxicity is a variant of type IV hypersensitivity where sensitized CD8<sup>+</sup> (Cluster of differentiation 8<sup>+</sup>) cells kill antigen-bearing cells. These cytotoxic T lymphocytes (CTLs) are able to kill target cells via the extrinsic pathway and the FasL/FasR interaction is the predominant method of CTL-induced apoptosis (Brunner et al, 2003). Conversely, they can also exert their cytotoxic effects on tumour cells and virus-infected cells through a new pathway that involves secretion of the transmembrane pore-forming molecule called perforin

with a subsequent exophytic release of cytoplasmic granules through the pore and into the target cell (Trapani and Smyth, 2002).

The serine proteases granzyme A and granzyme B are the most important component within the granules. Granzyme B will cleave proteins at aspartate residues and this leads to activation of procaspase-10 and can cleave factors like ICAD (inhibitor of caspase-activated DNase) (Sakahira et al, 1998). Barry and Bleackley and others have also shown that granzyme B can utilise the mitochondrial pathway for amplification of the death signal by specific cleavage of BID and induction of cytochrome c release (Barry and Bleackley, 2002; Russell and Ley, 2002). However, granzyme B can also directly activate caspase-3 by passing the upstream signaling pathways resulting into direct induction of the execution phase of apoptosis (Elmor, 2007). Goping and co-researchers has suggested that both the mitochondrial pathway and direct activation of caspase-3 are critical for granzyme B-induced killing (Goping et al, 2003). Recent research has shown that this method of granzyme B cytotoxicity is critical as a control mechanism for T-cell expansion of type 2 helper T (Th2) cells (Devadas et al., 2006). In addition, findings indicate that neither death receptors nor caspases are involved with the T-cell receptor-induced apoptosis of activated Th2 cells because blocking their ligands has no effect on apoptosis. On the other hand, Fas-Fas ligand interaction, adapter proteins with death domains and caspases are all involved in the apoptosis and regulation of cytotoxic Type 1 helper cells whereas granzyme B has no effect (Elmore 2007).

Granzyme A is also important in cytotoxic T-cell induced apoptosis and activates caspase-independent pathways. Once in the cell, granzyme A activates DNA nicking via DNase NM23-H1, a tumour suppressor gene product (Fan et al, 2003). This DNase has an important role in immune surveillance to prevent cancer through the induction of tumour-cell

apoptosis. Granzyme A protease cleaves SET (the nucleosome assembly protein that normally inhibits the NM23-H1 gene) complex thereby releasing inhibition of NM23-H1, resulting in apoptotic DNA degradation. In addition to inhibiting NM23-H1, the SET complex has important functions in chromatin structure and DNA repair. The proteins that make up this complex (SET, Ape1, pp32, and HMG2) appear to work together to protect chromatin and DNA structure (Lieberman and Fan, 2003). Therefore, inactivation of this complex by granzyme A most likely also contributes to apoptosis by blocking the maintenance of DNA and chromatin structure integrity.

#### **1.46 Execution Pathway**

Execution pathway is the final pathway of apoptosis and both extrinsic and intrinsic pathways end at the point. This phase of apoptosis is initiated by the activation of the execution caspases. Execution caspases activate cytoplasmic endonuclease, which degrades nuclear material, and proteases that degrade the nuclear and cytoskeletal proteins. Caspase-3, caspase-6, and caspase-7 function as effector or “executioner” caspases, cleaving various substrates including cytokeratins, PARP (Poly (ADP-ribose) polymerase), the plasma membrane cytoskeletal protein alpha fodrin, the nuclear protein NuMA (Nuclear mitotic apparatus protein) etc., that ultimately cause the morphological and biochemical changes seen in apoptotic cells (Slee et al, 2001).

Caspase-3 is known to be the most important of the executioner caspases and is activated by any of the initiator caspases (caspase-8, caspase-9, or caspase-10). Caspase-3 specifically activates the endonuclease CAD. In proliferating cells CAD is complexed with its inhibitor, ICAD (Inhibitor of CAD). In apoptotic cells, activated caspase-3 cleaves ICAD

to release CAD (Sakahira et al, 1998). CAD then degrades chromosomal DNA within the nuclei resulting to chromatin condensation. Caspase-3 also triggers cytoskeletal reorganisation and disintegration of the cell into apoptotic bodies.

Gelsolin, an actin binding protein, has been identified as one of the key substrates of activated caspase-3. Gelsolin will typically act as a nucleus for actin polymerisation and will also bind phosphatidyl inositol biphosphate, linking actin organisation and signal transduction. Caspase-3 will cleave gelsolin and the cleaved fragments of gelsolin, in turn, cleave actin filaments in a calcium independent manner. These result in disruption of the cytoskeleton, intracellular transport, cell division, and signal transduction (Kothakota et al, 1997). Phagocytic uptake of apoptotic cells is the last component of apoptosis. Phospholipid asymmetry and externalization of phosphatidyl serine on the surface of apoptotic cells and their fragments is the hallmark of this phase. Although the mechanism of phosphatidyl serine translocation to the outer leaflet of the cell during apoptosis is not well understood, it has been associated with loss of aminophospholipid translocase activity and nonspecific flip-flop of phospholipids of various classes (Bratton et al, 1997). Ferraro-Peyret and others have shown that Fas, caspase-8, and caspase-3 are involved in the regulation of phosphatidyl serine externalization on oxidatively stressed erythrocytes, however caspase-independent phosphatidyl serine exposure occurs during apoptosis of primary T lymphocytes (Mandal et al., 2005; Ferraro-Peyret et al, 2002). The appearance of phosphatidyl serine on the outer leaflet of apoptotic cells then facilitates non-inflammatory phagocytic recognition, allowing for their early uptake and disposal (Fadok et al, 2001). This process of early and efficient uptake with no release of cellular constituents, results in essentially no inflammatory response.

### **1.47 Importance of Apoptosis**

Apoptosis plays significant roles in normal physiology relative to its counterpart, mitosis. Although it demonstrates a complementary but opposite role to mitosis and cell proliferation in the regulation of various cell populations. It is estimated that to maintain homeostasis in the adult human body, around 10 billion cells are made each day just to balance those dying by apoptosis (Renehan et al, 2001). This number can increase significantly when there is enhanced apoptosis during normal development and aging, or during disease. Apoptosis is also critically important during various developmental processes (Opferman and Korsmeyer, 2003; Nijhawan et al, 2000).

Furthermore, apoptosis is significant in getting rid of the body pathogen-invaded cells; moreover, it is an important component of wound healing due to its involvement in the removal of inflammatory cells and the evolution of granulation tissue into scar tissue (Greenhalgh, 1998). Dysregulation of apoptosis during wound healing can lead to pathologic forms of healing, such as excessive scarring and fibrosis. Apoptosis is also required to eliminate activated or auto-aggressive immune cells either during maturation in the central lymphoid organs (bone marrow and thymus) or in peripheral tissues (Osborne, 1996).

Moreover, apoptosis is central to remodelling in the adult, such as the follicular atresia of the postovulatory follicle and post-weaning mammary gland involution, just to mention a few (Lund et al, 1996; Tilly, 1991). Further, as organisms' age, some cells begin to deteriorate at a faster rate and are eliminated via apoptosis. One theory is that oxidative stress plays a primary role in the pathophysiology of age-induced apoptosis via accumulated free-radical damage to mitochondrial DNA (Ozawa, 1995; Harman, 1992). Apoptosis has to be tightly regulated since excessive or insufficient cell death may lead to pathology, including cancer.



#### **1.48 Apoptosis and Necrosis: compare and contrast**

Necrosis, a known toxic process whereby the cell is a passive victim and follows an energy-independent mode of death, has been considered an alternative cell death to apoptosis. Although necrosis, as a form of cell death, has been a subject of debate since it refers to the degradative processes that occur after cell death, it is considered by some to be an inappropriate term to describe the mechanism of cell death (Elmore, 2007). Oncosis is therefore used to describe a process that leads to necrosis with karyolysis and cell swelling whereas apoptosis leads to cell death with cell shrinkage, pyknosis, and karyorrhexis (Majno and Joris, 1995; Levin et al., 1999).

Necrosis is also considered an uncontrolled and passive process that usually affects large fields of cells whereas apoptosis is controlled and energy-dependent and can affect individual or clusters of cells. Necrotic cell injury is mediated by two major mechanisms: interference with the energy supply of the cell; and direct damage to cell membranes. Whereas, apoptosis is mediated by two major mechanisms: extrinsic or death-receptor pathway; and the intrinsic or mitochondrial pathway (Figure 1.18). There is also an additional pathway, known as perforin/granzyme (Elmore, 2007).

Some of the major morphological changes that occur with necrosis include cell swelling; formation of cytoplasmic vacuoles; distended endoplasmic reticulum; formation of cytoplasmic blebs; condensed, swollen or ruptured mitochondria; disaggregation and detachment of ribosomes; disrupted organelle membranes; swollen and ruptured lysosomes; and eventually disruption of the cell membrane (Trump et al, 1997; Majno and Joris, 1995; Kerr et al, 1972). This loss of cell-membrane integrity results in the release of the cytoplasmic contents into the surrounding tissue, sending chemotatic signals with eventual recruitment of inflammatory cells (Figure 1.19).

In contrast to necrotic cells, apoptotic cells do not release their cellular constituents into the surrounding interstitial tissue and are quickly phagocytosed by macrophages or adjacent normal cells, and there is ultimately no inflammatory reaction (Kurosaka et al, 2003: Savill and Fadok, 2000). Although the mechanisms and morphologies of apoptosis and necrosis differ, there is overlap between these two processes. Research has shown that necrosis and apoptosis represent morphologic expressions of a shared biochemical network described as the “apoptosis necrosis continuum” (Zeiss, 2003). For example, two factors that will convert an ongoing apoptotic process into a necrotic process include a decrease in the availability of caspases and intracellular ATP (Denecker et al, 2001: Leist et al, 1997). Whether a cell dies by necrosis or apoptosis depends in part on the nature of the cell death signal, the tissue type, the developmental stage of the tissue and the physiologic milieu (Zeiss, 2003: Fiers et al, 1999).

Therefore, distinguishing necrosis from apoptosis is regarded as a difficult task; especially with the use of conventional histology. This is because the two processes can occur simultaneously, depending on factors such as the intensity and duration of the stimulus, the extent of ATP depletion and the availability of caspases (Zeiss, 2003). It is also important to note that pyknosis and karyorrhexis are not exclusive to apoptosis and can be a part of the spectrum of cytomorphological changes that occurs with necrosis (Cotran et al, 1999).

## Apoptosis Vs Necrosis

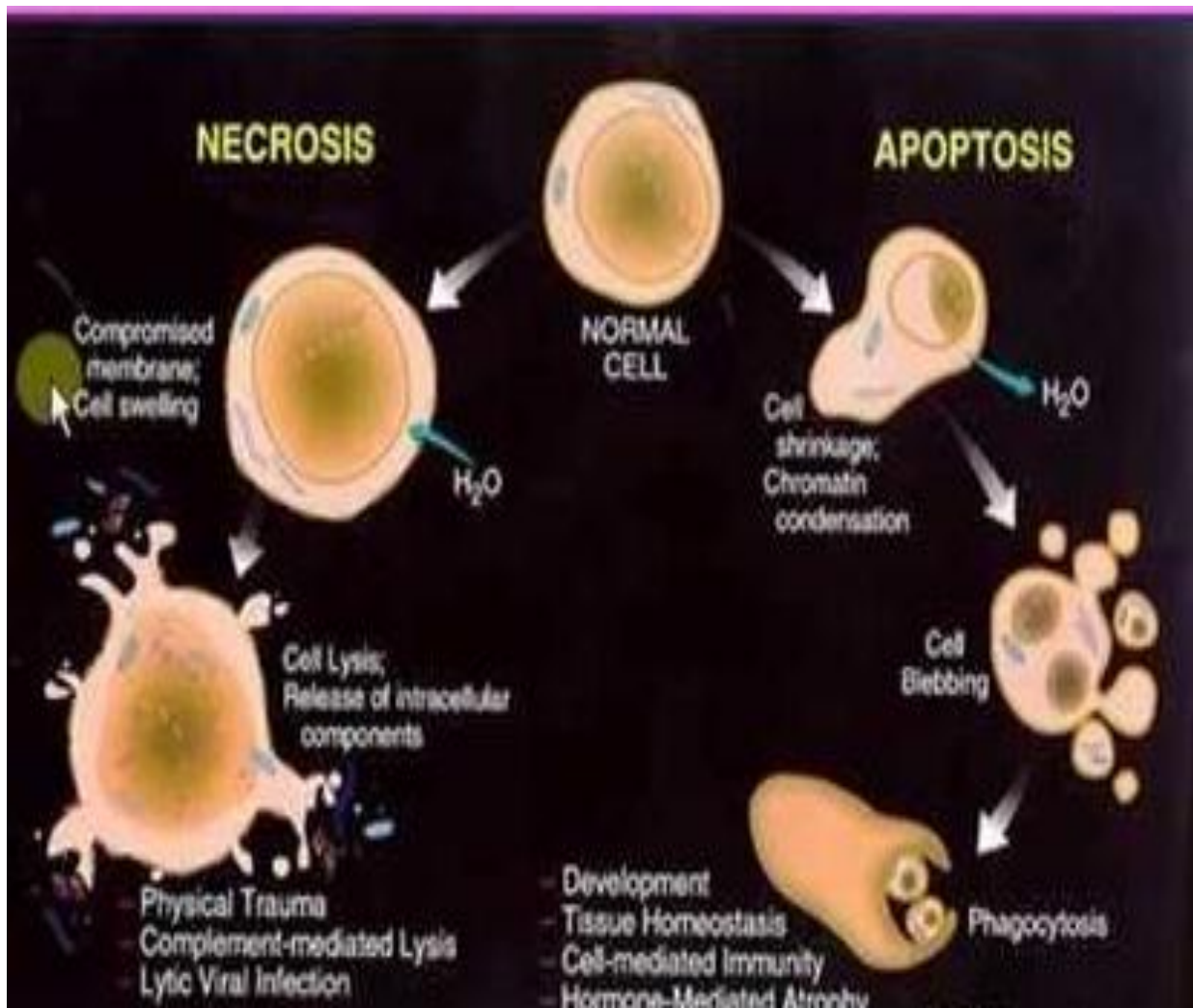


Figure 1.19: Differences between apoptosis and necrosis

## 1.49 Apoptosis and Cancer

Abnormalities in cell death regulation can be a significant component of diseases such as cancer. Cancer formation is a possibility when there is dysfunctional regulation of the normal mechanisms of cell cycle, with either an over proliferation of cells and/or decreased removal of cells (King and Cidlowski, 1998). In fact, suppression of apoptosis during carcinogenesis is thought to play a central role in the development and progression of some cancers (Wong 2011; Kerr et al, 1994). There are a variety of molecular mechanisms that tumour cells use to suppress apoptosis and some of these molecular mechanisms are briefly discussed below: Tumour cells can acquire resistance to apoptosis by the expression of anti-apoptotic proteins such as Bcl-2 (B-cell lymphoma protein 2) or by the down-regulation or mutation of pro-apoptotic proteins such as Bax (Bcl-2 associated X protein). The expression of both bcl-2 and bax is regulated by the p53 tumour suppressor gene (Miyashita, 1994). Vaux and co workers reported that certain forms of human B-cell lymphoma have overexpression of Bcl-2, and this is one of the first and strongest lines of evidence that failure of cell death contributes to cancer (Vaux et al, 1988).

Another method of apoptosis suppression in cancer involves evasion of immune surveillance (Smyth et al, 2001). Certain immune cells (T cells and natural killer cells) normally destroy tumour cells via the perforin/granzyme B pathway or the death-receptor pathway. In order to evade immune destruction, some tumour cells will diminish the response of the death-receptor pathway to FasL produced by T cells. This has been proven to occur in a variety of ways including down-regulation of the Fas receptor on tumour cells. Other mechanisms include expression of non-functioning Fas receptor, secretion of high levels of a soluble form of the Fas receptor that will sequester the Fas ligand or expression of Fas ligand on the surface of tumour cells (Elnemr et al, 2001; Cheng et al, 1994). In addition, some

tumour cells are capable of a Fas ligand-mediated “counter attack” that results in apoptotic depletion of activated tumour infiltrating lymphocytes (Koyama et al, 2001).

Alterations of various cell signaling pathways can result in dysregulation of apoptosis and lead to cancer; for example, the p53 tumour suppressor gene is a transcription factor that regulates the cell cycle. This is the most widely mutated gene in human tumourigenesis (Wang and Harris, 1997). The critical role of p53 is evident by the fact that it is mutated in over 50% of all human cancers. p53 can activate DNA repair proteins when DNA has sustained damage, can hold the cell cycle at the G1/S regulation point on DNA damage recognition, and can initiate apoptosis if the DNA damage proves to be irreparable (Pientenpol and Stewart, 2002) and dysregulation of this system can lead to tumourigenesis. For example, if the p53 gene is damaged (by chemical, radiation, viruses etc), tumour suppression is severely reduced or people who inherit only one functional copy of this gene will most likely develop Li–Fraumeni syndrome. This is characterised by the development of tumours in early adulthood (Gu et al, 2001: Varley et al, 1997).

Other cell signaling pathways that can also be involved in tumour development include, phosphatidyl inositol 3-kinase/AKT pathway. Up-regulation of the phosphatidyl inositol 3-kinase/AKT pathway in tumour cells renders them independent of survival signals. In addition to regulation of apoptosis, this pathway regulates other cellular processes, such as proliferation, growth, and cytoskeletal rearrangement (Vivanco and Sawyers, 2002).

### **1.50 GAG’s and apoptosis**

GAGs have been shown to play a modulatory role in the apoptotic processes. For example, heparin has been shown to inhibit glomerular cell apoptosis in cell culture and

attenuates trophoblast apoptosis (Bose et al 2005; Ishikawa and Kitamura 1999). The GAG hyaluronan attenuates apoptosis induced by dexamethasone in malignant multiple myeloma cells (Vincent et al 2003). Similarly, chondroitin CS and HS have also been reported to have attenuated apoptosis in fetal lung fibroblasts (Cartel and Post 2005).

However, numerous data indicate the ability of GAGs to induce apoptosis. Hence, they may contribute to the natural processes of the body for the removal of tumour cells. Heparin in particular has been shown to induce apoptosis in human hepatoma cells (Karti et al 2003), human nasopharyngeal carcinoma cells (Li et al 2001) and peripheral blood neutrophils (Manaster et al 1996), possibly by interfering with transcription factor function (Berry et al 2004). Likewise, derivatives of heparin and CS also induce apoptosis of myeloma and breast cancer cells in vitro (Pumphrey et al 2002).

### **1.51 Overall aims of this study**

Comprehensive surveys of previous research into different classes of invertebrates, including molluscs, have demonstrated that GAG-like compounds, such as HS and/or heparin-like compounds, and CS and or DS, are present in many species (Medeiros et al, 2000). However, commercial available preparations of GAGs compounds are mainly sourced from porcine and bovine intestinal or bovine lung tissue. A link between bovine spongiform encephalopathy and the similar prion-based Creutzfeldt-Jakob disease in humans (Schonberger, 1998), has limited the use of bovine GAGs in the clinic. Moreover, porcine GAGs also have problems associated with religious restrictions on its use (Volpi, 2005). Non-animal sources of GAGs with clinical useful activities are unavailable currently for pharmaceutical purposes. However, there is scant information on isolation/characterisation of GAGs from molluscs such as whelk and cockles. There is even less information on the

potential biological activities of these mollusc derived polysaccharides and their potential use as new therapeutics for the treatment of human disease such as cancer.

The primary aim of the work presented in this thesis is to isolate GAGs from whelks and cockles using a method similar to that described by Kim et al (1996), albeit with some slight modifications. Initial pilot studies revealed that novel GAG chains isolated from these two molluscs contain HS and CS/DS GAGs. The anticancer activities of these mollusc derived GAGs was assessed and commercial HS and CS/DS, from bovine sources, were used as comparative controls.

The second aim of this project was to investigate the relationship between the structure of these mollusc derived GAGs and the observed anticancer activities. Studies have previously shown that modulation of HS GAGs structure on the surface of tumour cells could inhibit or promote tumour growth and metastasis (Liu et al, 2002). Understanding the fine structure and specific biological roles of GAGs has resulted in novel therapeutic approaches, including the development of HS/heparin-like compounds, which may act as inhibitors of tumour metastasis (Afratis et al, 2012). The anticancer activities of these HS/heparin related compounds have been shown to result primarily from their interaction, and inhibitory effects, on hundreds of different proteins, including FGFs, VEGF etc. The direct inhibition of tumour cell growth seen with our mollusc derived GAGs indicates a totally new mechanism for GAG related anticancer activity and the structural difference seen in these polysaccharides must be determined as a priority.

The third aim of the presented work was to study the possible mechanism of action of the novel GAGs on cancer cells using cell cycle analysis and determination of apoptotic induction and to hopefully link with the GAG structural findings.

Overall the results obtained from this study will undoubtedly serve as the basis for the future development of these novel mollusc derived GAGs as potential anticancer agents.



## **Section 2**

# **Experimental Materials and Methods**

## 2.0 Experimental materials

PD-10 pre-packed columns were purchased from Amersham Pharmacia Biotech. The TSK3000PW gel-filtration column and Pro-Pac PA-1 SAX-HPLC column (4.6 x 25cm) was purchased from Phenomenex (Macclesfield, UK)

Cockles and whelks were purchased from Arndale fish market, Manchester, UK. Polcine HS and CS commercial GAGs were purchased from Celsus laboratories (Cincinnati, OH, USA). Heparin sodium salt was purchased from Sigma Aldrich, UK. ). Heparinase I (*Flavobacterium heparinum*; EC 4.2.2.7), heparinase II (*F. heparinum*; no EC number assigned) and heparinase III (*F. heparinum*; EC 4.2.2.8) were purchased from Grampian Enzymes (Orkney, UK).

TEMED, Acrylamide/bisacrylamide 19:1 ratio, 40% solution, Ammonium persulphate, Cetylpyridium chloride, Ethylene diaminetereacetic acid, chondroitinase-ABC from *Proteus Vulgaris* (0.83 units/mg), 99% Glycerol, Trizma base (Tris HCl), Cisplatinium (cis-Diammineplatinum(11)dichloride), 2-(4,5-Dimethylthiazol-2-yl)-2,5-diphenyltetrazolium bromide (MTT), Acrylamide/bisacrylamide 19 :1 ratio, 40% solution, Foetal calf serum (FCS) – Biosera, Streptomycin and Penicillin, L-Glutamine, RPMI 1640 (Roswell Park Memorial Institute) – Biosera, DEAE-Sepacel, Propiodide (PI), (4',6-diamidino-2-phenylindole (DAPI), Protease from *Streptomyces griseus* (Type XIV,  $\geq 3.5$  units/mg) and AZURE A dye were purchased from Sigma, UK. Acetone, Ethanol, ependof tubes,

Micropipettes (10-1000  $\mu$ l), Micropipettes (10-1000  $\mu$ l) and other cell culture laboratory consumables were purchased from Fischer Scientific, UK. Dialysis tubing 'Visking' was purchased from iBOTZ, USA. Sodium Chloride, Potassium acetate, Sodium bicarbonate, Trichloroacetic acid (TCA) and Sulphuric acid were purchased from Merck Millipore, UK. Bromophenol red and Glyceine (aminoacetic acid) were purchased from

Chemicals VWR BDH, UK. Annexin V-FITC stain was purchased from BIORAD, UK.

Phosphate buffer saline was purchased from Partec.

## 2.1 Methods

### 2.2 Preparation of GAGs

Whelk (*Buccinum undatum*) and cockle (*Cerastoderma edule*) from the Irish Sea were sourced from local fish markets in Fleetwood, UK and were defatted using three 24h extractions with acetone and dried. The fat-free dried cockles and whelks were crushed into a fine powder using an industrial blender. Approximately 40g of dried, defatted, pulverised powder was suspended in 400ml of 0.05 M sodium carbonate buffer (pH 9.2) and 20ml of the proteolytic enzyme Alcalase (Type XIV,  $\geq 3.5$  units/mg; 10 mg/ml) was added to the suspension in order to detach the carbohydrate chains from proteins. The suspension was shaken for 48 h at 200 rpm at 60 °C. The digestion mixture was cooled to 4 °C, and trichloroacetic acid added to a final concentration of 5% (to remove non degraded proteins/peptides and nucleic acids).

The sample was mixed, allowed to stand for 10 min, and then centrifuged for 20 min at 8000 rpm. The supernatant was recovered by decanting and the precipitate discarded. 3 volumes of 5% potassium acetate in ethanol were added to one volume of supernatant. After mixing, the suspension was stored overnight at 4 °C and then centrifuged for 30 min at 8,000 rpm. The supernatant was discarded, and the precipitate was washed with absolute alcohol. The precipitate was dissolved in 400 ml of 0.2 M NaCl, centrifuged for 30 min at 8,000 rpm and the insoluble material discarded. GAGs were recovered from the supernatant by addition of 5 ml of a 5 % solution of cetylpyridinium chloride and the precipitate collected by centrifugation.

The precipitate was dissolved in 100 ml of 2.5 M NaCl followed by the addition of 5 volumes of ethanol and the precipitate removed by centrifugation for 30 min at 10,000 rpm. The crude GAG precipitate was then dissolved in distilled water and dialysed as described below.

### **2.3 Desalting of crude GAGs**

Crude GAGs obtained from the extraction procedure were desalted using dialysis tubing pre-treated with 100mM EDTA. The dialysis tubes containing GAG extracts were dialysed against 100 volumes of distilled water for 72 hours under constant agitation with the distilled water changed at 24 hour intervals. After 72 hours, the desalted GAG extracts were freeze dried and stored at  $-20^{\circ}\text{C}$  for further use.

### **2.4 Purification of crude GAGs by anion-exchange chromatography**

GAG samples (10mg) derived from the shellfish samples were dissolved in 10ml distilled water and manually injected onto a column (1.5x 5cm) of DEAE-sephacel equilibrated with 50 mM sodium phosphate buffer, pH 7.0. The column was eluted using a linear gradient of 0-3 M NaCl in 50mM phosphate buffer, pH 7.0 over a hundred minutes at flow rate of 1ml/min. The elution was monitored spectrophotometrically at 210, 232 and 254nm and 1ml fractions collected. Peak were pooled, freeze dried and finally desalted using PD 10 column

### **2.5 Desalting of purified GAGs fractions**

The purified GAGs fractions were desalted on PD-10 column pre-calibrated with 1mg/ml dextran (blue colour) and potassium dichromate (yellow colour) solution (the blue eluents were equivalent to GAGs, while the yellow eluents were equivalent to salt). The calibrated column was equilibrated with distilled water; the void volume and salt fractions were discarded while the GAGs fractions were pooled and stored at  $-20^{\circ}\text{C}$  overnight before

being transferred to the freeze drier. The desalted GAGs samples were lyophilised and a dried and a pure white, fluffy GAG powder were obtained.

## **2.6 Enzyme digestion of GAGs**

Samples of GAGs (1mg/ml) were treated with either heparinases or chondroitinase ABC lyase (30mIU) and incubated for 24 hours at 37<sup>0</sup>C.

## **2.7 Chemical treatment (nitrous acid treatment)**

Samples of GAGs were treated with nitrous acid according to the method described by Zhang et al., 2009. Powdered GAGs (100µg) were dissolved in distilled water (30µl) and 0.5M sulphuric acid (10 µl) and sodium nitrite (600µg) added. The combined reagents released gaseous nitrogen and formed nitrous acid. The reaction was halted after 15 minutes by adding an equal amount of 0.1M NaOH to neutralize excess nitrous acid. Treated samples were used for PAGE analysis, as described below.

## **2.8 Polyacrylamide gel electrophoresis (PAGE analysis)**

PAGE was conducted on Bio-Rad MiniProtean II systems. A resolving gel (15 ml of 40% acrylamide, 5 ml of 1.5 M Tris/HCl pH 8.5, 100 µl of APS, 60 µl of TEMED) were poured vertically, using a gel-pouring stand (Hoffer), between glass plates (16 cm x 32 cm) separated by 1.5 mm spacers. Butanol saturated with water (0.5 ml) was layered across the top of the gel and polymerisation, which began at the top of the gel, was completed within 20 min. The polymerised gel top layer was rinsed thoroughly with water to remove any excess gel and saturated butanol. Excess water was removed by filter paper.

The stacking gel (3 ml of 40% acrylamide, 5 ml of 0.5 M Tris/HCl pH 8.5, 100  $\mu$ l of ammonium per sulphate (APS), 60  $\mu$ l of TEMED and 12 ml of distilled water) was layered on top of the polymerised gel and a well comb was inserted. Samples were mixed with equal volume of loading buffer (20% glycerol) and applied to the wells using a micro syringe; a marker (20% v/v bromophenol blue) was applied to one of the wells. The gel was run at a constant voltage (200V) in a running buffer (25 mM Tris, 0.192 M glycine pH 8.3) until the tracking dye in the marker lane, reached the bottom of the gel. Gels were stained with aqueous 0.5 % Azure A under constant agitation for about 2 minutes and were destained by successive washes with distilled water and gels were scanned to preserve gels images.

## **2.9 Superose-12 size exclusion chromatography**

Samples (at 10mg/ml) in a total volume of 20ul of water were applied to a Sepharose-12 column, eluted in 0.2M ammonium hydrogen carbonate at a flow rate of 0.5ml/minute and 0.5ml fractions collected. Column  $V_0$  and  $V_t$  values were established by application of Bromophenol blue and sodium dichromate (1mg/ml).

$V_0$  fraction 15/16

$V_t$  fraction 34/35

Fractions were assessed for GAG content by cellulose acetate dot blotting.

## **2.10 Cellulose acetate dot blotting of GAGs**

Cellulose acetate sheets were marked with a grid of 1cm<sup>2</sup> squares using a pencil. Multiple applications of each fraction were applied to the membrane using a pipette. The acetate sheet was dried thoroughly between applications in an oven at 75<sup>0</sup>C for 5 minutes each. Following the final drying the sheet was stained using a solution of 0.5% Azure A stain for 10-20 seconds, then de-stained in tap water until a good contrast between stained dots and background was achieved.

## **2.11 Gel-filtration (TSK G2000 SW column)**

The TSK column was equilibrated in normal saline overnight prior the experiment. 20 µl of the filtered oligosaccharides obtained from each heparinase enzyme samples (shell fish and commercial HS/ Heparin) were injected via 20µl sample loop into the equilibrated column at a flow rate 250 µl/ml for 180 minutes and the elutes were monitored at 232 nm.

## **2.12 Disaccharide analysis of GAG chain by strong anion-exchange high**

### **Performance liquid chromatography (SAX-HPLC)**

Samples from enzymes digestion assay were applied to a Pro-Pac PA-1 SAX-HPLC column (4.6 x 25cm) pre-equilibrated in water adjusted to pH 3.5 with HCl at a flow rate 1 ml/min. The disaccharides were resolved using a linear gradient of 0 -3M NaCl in deionised water, pH 3.5 for 70 min at flow rate of 1ml/min. Elutes were monitored for UV absorbance at 232nm and peaks were identified according to standard derived from commercial CS/DS and HS.



### **2.13 Determination of cells viability (MTT assay).**

The breast cancer cell MDA468 and MDANQ01, and human lymphoblastic and erythrocytic cell line (Molt-4 and K562) were grown in RPMI 1640 medium supplemented with 1 % L-glutamine, 1 % of 100 Units/ml penicillin and 0.1 mg/ml streptomycin and 10% inactivated FCS. While the ovarian cell line HeLa and fibroblast cell line 3T3 were grown in DMEM medium supplemented with 20 % inactivated FCS, 1 % L- glutamine, 1 % of 100 units/ml penicillin & 0.1 mg/ml streptomycin. All cell lines were maintained in a humidified incubator with an atmosphere of 95% air and 5% CO<sub>2</sub> at 37°C.

Cell viability was determined by the MTT

(3-(4,5dimethylthiazol2-yl)-2,5 diphenyltetrazolium bromide) test method. Cells were cultured overnight in 96-well plates ( $2.0 \times 10^4$  cells/ well) containing 100 µl medium prior to treatment with crude GAG extract, commercial GAGs and cisplatinum at 37°C. A pilot study was conducted to choose the dose range used for this experiment. This was followed by addition of 100 µl of fresh medium containing various concentrations of GAGs (10-100 µg/ml) or cisplatinum (0.35-25mM/ml) into each well, and incubated for another 96 hrs. The metabolic activity of each well was determined by the (MTT) assay and compared to those of untreated cells. At the end of the incubation period, 50µl of MTT solution (5 mg/ml in PBS) was added to each well and incubated for three hours at 37<sup>0</sup>C. After incubation the supernatants were carefully aspirated, then 200 µl of DMSO was added to each well and the plates agitated to dissolve the crystal product. Cell viability was determined based on mitochondrial conversion of 3[4,5-dimethylthiazol-2-yl] 2,5-diphenyltetrazolium bromide (MTT) to formazan. The amount of MTT converted to formazan is indicative of the number of viable cells.

The plates were gently agitated until the colour reaction was uniform and the absorbance was measured at 570 nm using a multi-well plate reader, Sigma Plot 2000 software was used for data analysis. The cell viability effects from exposure of cells to each concentration of crude whelk GAGs, commercial GAGs and cisplatinum were analysed as percentages of the control cell absorbance, which were obtained from control wells plated in RPMI,1% L- glutamate and 10% FCS media. The average cell survival obtained from triplicate determinations at each concentration was plotted as a dose response curve. The 50% inhibition concentration ( $IC_{50}$ ) of the active substances was determined as the lowest concentration which reduced cell growth by 50 % in treated compared to untreated cells.

#### **2.14 Flow Cytometry Analyses of DNA Content (Cell cycle analysis).**

Cells were seeded into 25-cm plastic sterile culture flasks, and incubated for 24 hours prior to treatment with different concentrations of crude and purified GAGs samples. Cells were harvested at different time intervals (8-48 hours), centrifuged at 1500 rpm for 5 minutes, washed three times with phosphate buffer saline (PBS) and fixed in ice cold 70% (v/v) ethanol for 30 minutes. Before analysis, cells were centrifuged to remove ethanol and washed with PBS three times. Cells were then incubated at room temperature with 50  $\mu$ l of Ribonuclease A (RNase) (50mg/ml) and finally stained with a solution containing 50 g/ml propidium iodide (PI) for 30 min in the dark. The stained samples were analysed with Partec flow cytometer. The cell cycle distribution was evaluated on DNA plots by Partec cyflow space version 2.4 software.

### **2.15 Annexin V-FITC apoptosis detection**

Cells were seeded into sterile 6 well plates at  $5 \times 10^5$  cells/ml, and incubated with or without GAG extracts at  $37^{\circ}\text{C}$ . Cells were harvested at different time intervals (8-48 hours), centrifuged at 1500 rpm for 5 minutes, washed twice with cold PBS and resuspended in 1x binding buffer (0.1M HEPES, 1.4 M NaCl and 25 mM  $\text{CaCl}_2$ ) at a concentration of  $1 \times 10^6$  cells/ml. Cells (100  $\mu\text{l}$ ) were transferred into 5 ml culture tubes and stained with Annexin V FITC (5  $\mu\text{l}$ ) and PI (10  $\mu\text{l}$ ). The stained cells were gently vortexed and then incubated in the dark for 15 minutes at room temperature. 400  $\mu\text{l}$  of 1 x binding buffer was added to each tube prior to analysis using a BD flow cytometer.

### **2.16 DAPI fluorescent microscopy for apoptosis detection**

Cells were seeded into sterile 8 well plates at  $5 \times 10^5$  cells/ml, and incubated with or without GAG samples at  $37^{\circ}\text{C}$ . Cells were harvested at different time intervals (8-48 hours). The harvested cells were washed twice with cold PBS followed by 1x binding buffer (0.1M HEPES, 1.4 M NaCl and 25 mM  $\text{CaCl}_2$ ). The cells were immediately stained with DAPI and incubated in the dark for 10 minutes before finally being rinsed with binding buffer. The stained cells were viewed under the highest lens objective and the images obtained were scanned by Hamatsu 1394 ORCA-285 camera.

## 2.17 Statistical analysis

All of the results represent the mean  $\pm$  SEM from triplicate experiments performed in a parallel manner unless otherwise indicated. Statistical comparisons between groups were made using one-way ANOVA followed by Student's *t*-test, and significant differences were indicated as  $p < 0.05$  and highly significant as  $p < 0.01$

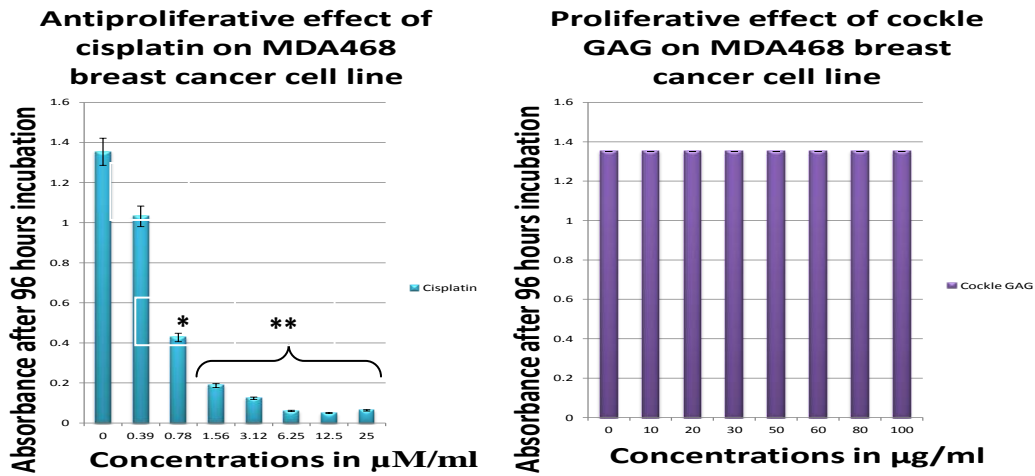
## **SECTION 3**

## **RESULTS**

### **3.0 Biological evaluation of cockle derived GAG mixtures**

#### **3.1 Effects of cockle derived GAG mixtures on MDA468 breast cancer cell growth (MTT assay results)**

The effects of crude cockle GAG mixtures on MDA468 breast cancer cell proliferation were measured using the MTT assay. Cells were exposed to different concentrations of crude cockle GAGs (10-100 µg/ml) for 96 hours. Crude cockle GAG treatment had no growth inhibitory effect on the cell proliferation of MDA468 cell line (Figure.3.1A). Other commercial sourced GAGs (HS and CS) derived from bovine sources were tested along with crude cockle GAG on this cell line and none demonstrated any growth inhibitory effect on MDA468 breast cancer cell, as illustrated in Figure 3.1B. However, cisplatin, a standard anticancer drug did show growth inhibitory effects on MDA468 cell proliferation and this serves as a positive growth inhibitory control for all subsequent MTT experiments (Figure 3.1B).



A

B

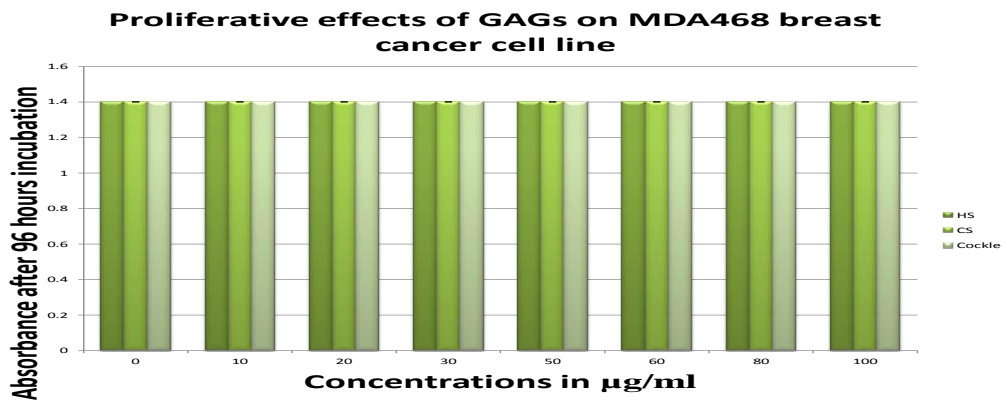


**Figure 3.1: MTT cell viability assay for MDA468 cells after treatment with cockle derived and commercially sourced GAG chains.**

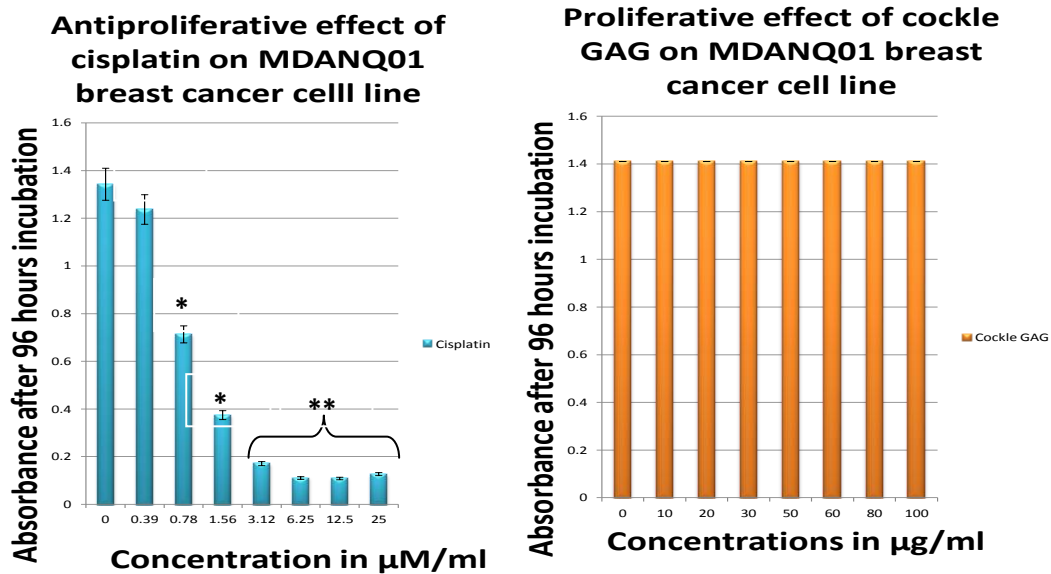
Cells were incubated with various concentrations of GAGs for 96 hours after which time cell viability was measured using an MTT assay (A) Cockle GAGs and cisplatin as a positive inhibitory control, (B) Commercial and cockle GAGs with cisplatin as a positive control. Each value is presented as the mean SEM of three independent determinations. The bars in each chart are presented as relative values in comparison to untreated cells.

Abbreviations: \*-Significant ( $p \leq 0.05$ ): \*\*-Highly significant ( $p \leq 0.01$ )

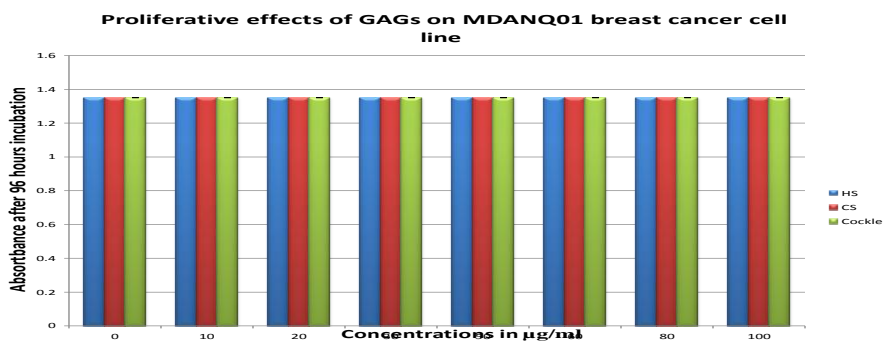
### **3.2 Effects of Cockle derived GAG mixtures on the MDANQ01 breast cancer cell**

In order to further examine any possible anti-cancer activity of cockle derived GAGs may have on breast cancer, the crude cockle GAG extracts was also exposed to another breast cancer cell (MDANQ01) using the MTT assay. Similarly, the crude cockle GAG did not show any growth inhibitory effect on MDANQ01 breast cancer cell proliferation (Figure 3.2A). Moreover, MDANQ01 cells treated with the commercial GAGs (HS and CS) also showed no growth inhibitory effect (Figure 3.2B). However, cisplatin standard anti-cancer drug did exhibits growth inhibitory effects on MDANQ01 cell after the same period of exposure to the crude extract (Figure 3.2A and B).





A



B

**Figure 3.2: MTT cell viability assay for MDANQ01 cells after treatment with cockle derived and commercially sourced GAG chains.**

Cells were incubated with various concentrations of GAGs for 96 hours after which time cell viability was measured using an MTT assay (A) Cockle GAGs and cisplatin as a positive inhibitory control, (B) Commercial and cockle GAGs with cisplatin as a positive control. Each value is presented as the mean SEM of three independent determinations. The bars in each chart are presented as relative values in comparison to untreated cells. Abbreviations: \*-Significant ( $p \leq 0.05$ ): \*\*-Highly significant ( $p \leq 0.01$ )

### **3.3 Effect of crude cockle GAG mixture on human lymphoblastic leukaemia**

#### **(MOLT-4) cell proliferation *in vitro***

Despite the lack of anticancer activity seen with the breast cancer cell lines, the crude cockle GAGs was also tested on other cancer cell lines. The effects of crude cockle GAGs on cancer cell proliferation using a lymphoblastic leukaemia cell line (MOLT-4) showed much more promise. This cell line was similarly exposed to different concentrations of crude cockle GAGs (10-100 µg/ml) for 96 hours using an MTT assay.

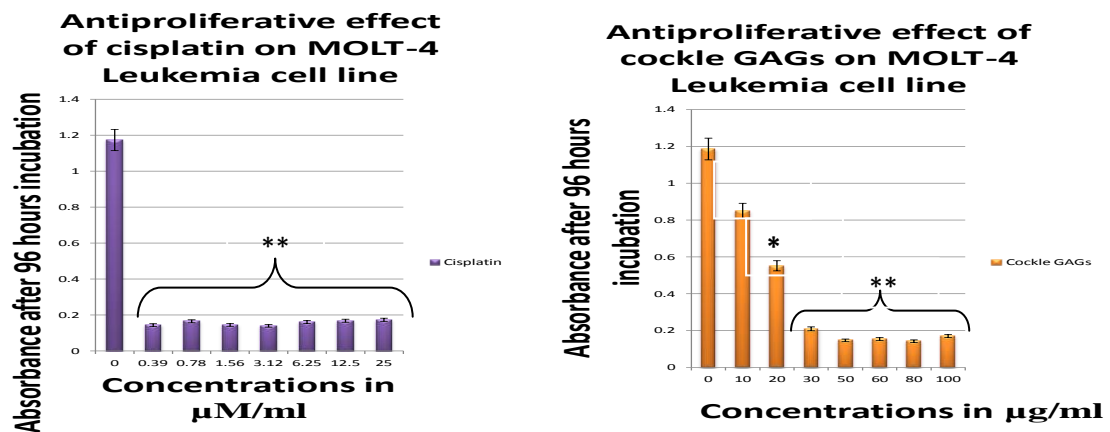
Crude cockle GAGs decreased significantly the proliferation of MOLT-4 cell ( $p < 0.001$ ) in a dose dependent manner with a recorded  $IC_{50}$  of 16µg/ml (Figure 3.3A). According to the standard criteria set by the National Cancer Institute (Chen et al, 1988; Geran et al, 1972), crude extracts having  $IC_{50}$  values of less than 20 µg/ml are considered active against the tested cancer cell lines and this recommendation categorised this crude extract as a potential anti-leukaemia drug.

The ability of the crude extract to inhibit cell proliferation of leukaemia cell lines was also compared favourably with the anti-proliferative effect of the DNA damaged anti-cancer drug (cisplatinum) (Figure 3.3A). These results show the potential of cockle derived GAGs as a future anti-leukaemia drug.

Almost as interesting as the anticancer activity of the cockle derived GAG was the complete lack of anticancer activity with the commercial GAGs (HS and CS) on the MOLT-4 cell line

(Figure 3.3B). These results suggest for the first time that GAGs chains may have selective anticancer activity against some cancer cell lines and that this based on their animal origin and ultimately their fine structure.

A



B

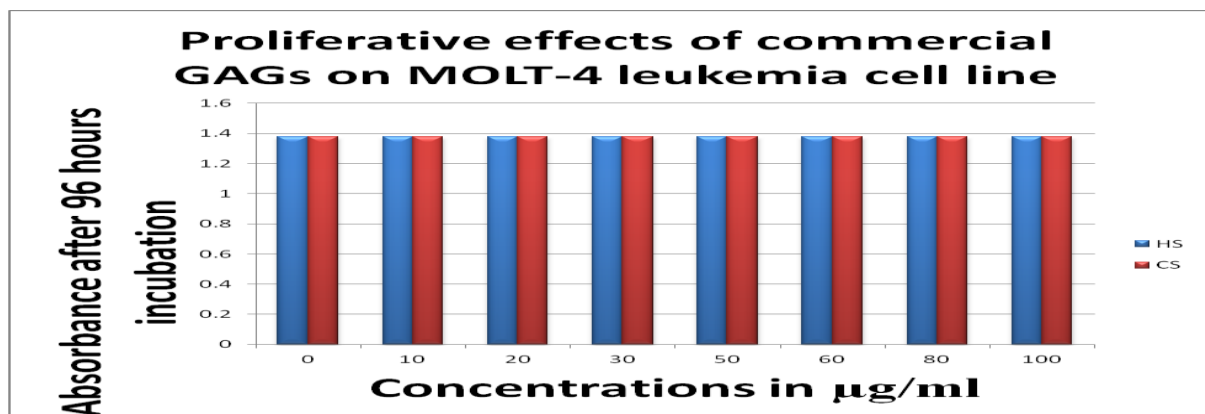


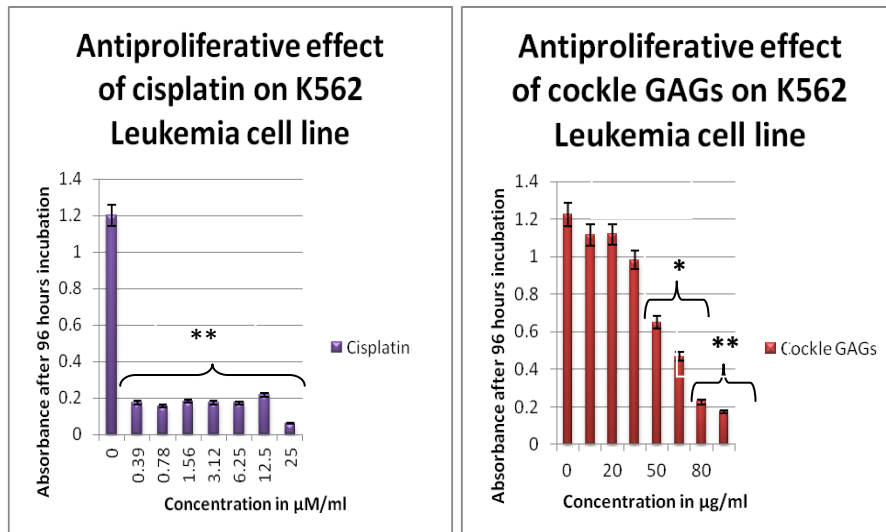
**Figure 3.3: MTT cell viability assay for MOLT-4 lymphoblastic leukaemia cells after treatment with cockle derived and commercially sourced GAG chains.**

Cells were incubated with various concentrations of GAGs for 96 hours after which time cell viability was measured using an MTT assay (A) Cockle GAGs and Cisplatin as a positive inhibitory control (B) Commercial GAGs and Cisplatin as a positive control. Each value is presented as the mean SEM of three independent determinations. The bars in each chart are presented as relative values in comparison to untreated cells.

Abbreviations: \*-Significant ( $p \leq 0.05$ ) \*\*-Highly significant ( $p \leq 0.01$ ).

### **3.4 Effects of crude cockle GAG extracts on the growth of K562 erythroleukaemia cells *in vitro*.**

In order to investigate fully the selective activity of crude cockle GAGs against some cancer cells, its effects on cell proliferation of erythroleukaemia cell line (K562) was also measured using MTT assay. Crude cockle GAGs were shown to decrease proliferation of K562 cells in a dose –dependent manner with a recorded IC<sub>50</sub> of 52 µg/ml [Figure 3.4 (A)]. Similarly, the growth inhibitory activity of the cockle GAG extract on K562 leukaemia cell line was also comparable to the growth inhibitory effect of the DNA damaged anti-cancer drug (cisplatin) (Figure3.4A). These results suggest that the cockle GAG extract has comparative activity with the standard anti-cancer drug (cisplatin) to treat this leukaemia cell line. Again all commercial GAGs (HS and CS) tested along with the crude extract showed no inhibitory effect on K562 cell proliferation (Figure 3.4B).



A

B

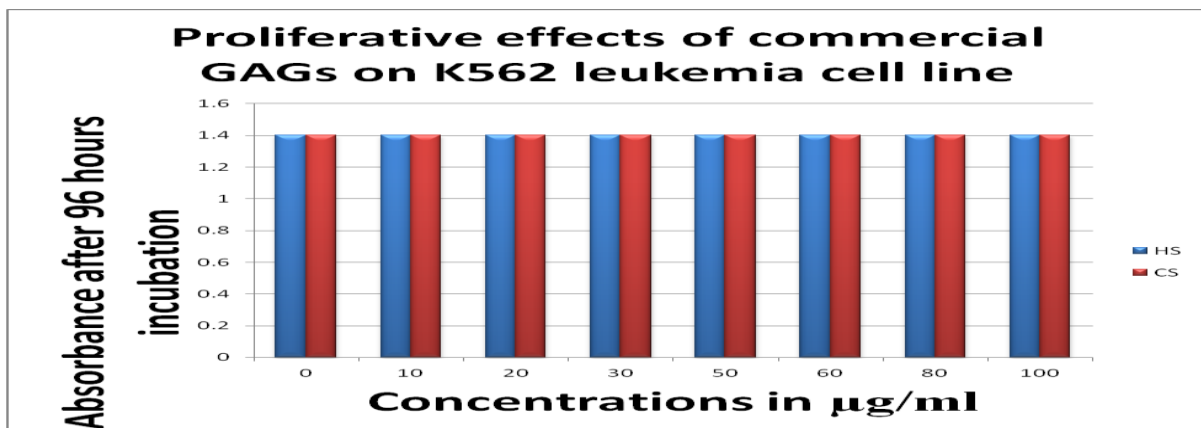


**Figure 3.4: Concentration-dependent effect of Cockle GAG extracts on K562 erythroleukaemia cell viability.**

Cells were incubated with various concentrations of cockle GAGs extracts for 96 hours after which time cell viability was measured using an MTT assay (A) cockle GAGs and Cisplatin as a positive inhibitory control, (B) commercial and cockle GAGs with cisplatin as a positive control. Each value is presented as the mean SEM of three independent determinations. The bars in each chart are presented as relative values in comparison to untreated cells.

Abbreviations: \*-Significant ( $p \leq 0.05$ ): \*\*-Highly significant ( $p \leq 0.01$ ).

### **3.5 Effect of cockle GAG mixtures on 3T3 normal fibroblast cell line**

The cockle derived GAGs have demonstrated a degree of selective activity against some cancer cells *in vitro*. Selectivity is one of the positive characteristics of any potent anti-cancer drug for future development. For this to be fully established, selective activity of crude cockle GAGs extracts was tested on the standard, non cancerous, 3T3-fibroblast cell line. Interestingly, the crude extract did not show any growth inhibitory effect on the 3T3 cells as shown in Figure 3.5. This result suggests that this extract may be highly selective against the leukemic cell lines; however this needs to be established with a much wider range of normal cell type e.g. MCF-12, C13589, MCF-12F and HUVEC.

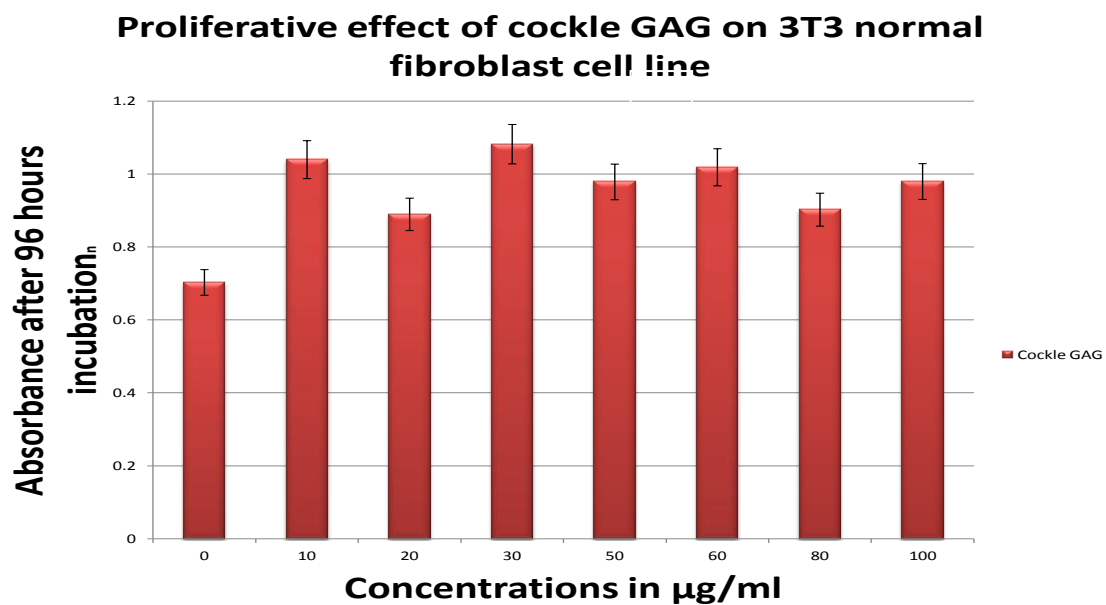


**Figure 3.5: MTT cell viability assay for normal fibroblast (3T3) cells after treatment with cockle GAGs.**

Cells were incubated with various concentrations of cockle GAGs for 96 hours after which time cell viability was measured using MTT assay and cisplatin was used as a positive inhibitory control. Each value is presented as the mean SEM of three independent determinations. The bars in each chart are presented as relative values in comparison to untreated cells.

### **3.6 Cell cycle analysis of the MOLT-4 cell line after treatment with cockle GAG extracts**

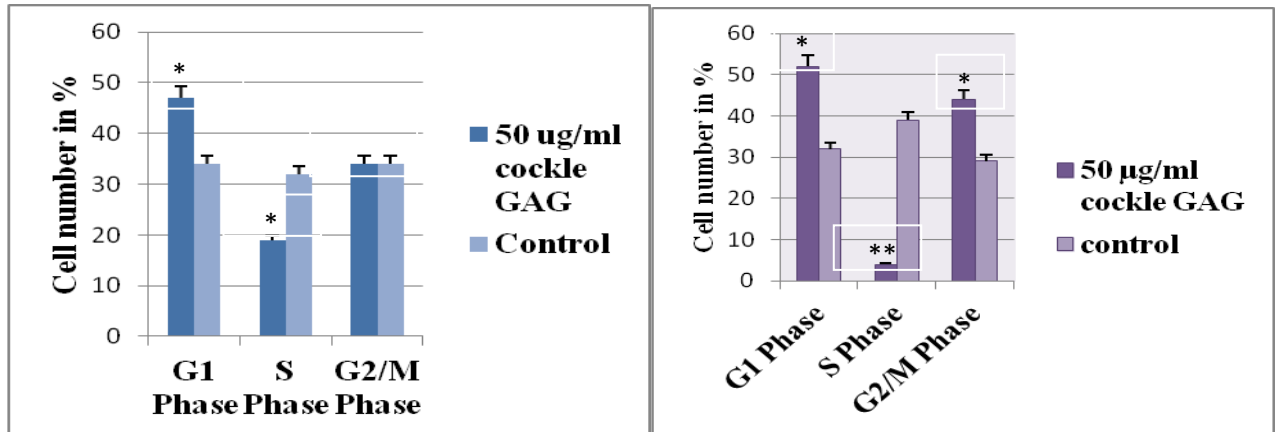
Our preliminary studies have highlighted that cockle derived GAGs induces cell death in leukaemia cell lines including MOLT-4 cell line; However, the mechanism of this anticancer activity was initially unknown. Therefore, the mechanism of cell death induced by crude cockle GAGs treatment on leukaemia cell using MOLT-4 cell line was examined by subjecting treated and untreated cells to cell cycle analysis by flow cytometry. A pilot study was conducted to choose the dose used for this experiment. Results obtained from this study demonstrated marked disruptive effects on MOLT-4 DNA composition following a brief (16-24 hours) treatment with the high concentration (50 µg/ml) of the crude extract [Figure 3.6 (i) A-C]. The dose was chosen based on the result obtained from pilot study.

Significant MOLT-4 cell cycle arrest at G1phase with crude cockle GAGs was observed after 16 hours incubations using 50µg/ml with concomitant cell arrest at both G1 and G2/M-phase at 24 hours incubations. 16 hours incubations of the cell with 50µg/ml crude cockle GAGs increased the G1 phase population by 13 % and 20 % at 24 hours. 24 hours incubations also increased the cell population at G2/M-phase by 15 %. Crude cockle GAGs decreased the S- phase population by 13 % at 16 hours and 35 % at 24 hours. The observed effect of the extract on the cell cycle of MOLT-4 cells were statistically significant ( $p < 0.05$ ) at 16 hours and highly significant ( $p < 0.01$ ) at 24 hours; when compared the corresponding values of the test samples with the control [Figure 3.6 (i) A-C].



**A**

**Cell cycle arrest caused by cockle GAGs treatment on MOLT-4 leukemia cell line**

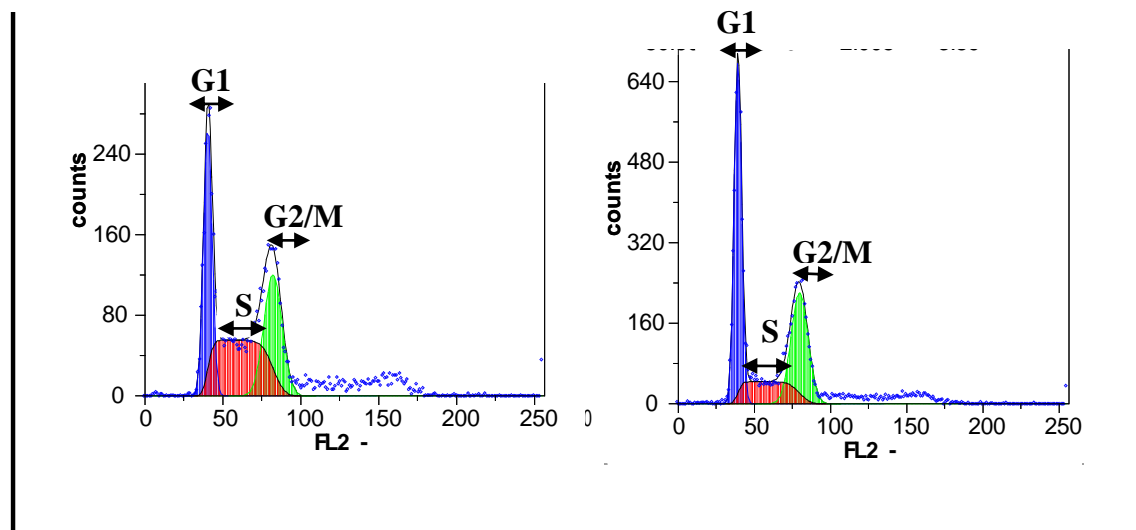


**B**

**16 hours**

**Untreated**

**Treated**



**C**

**24 hours**

**Untreated**

**Treated**

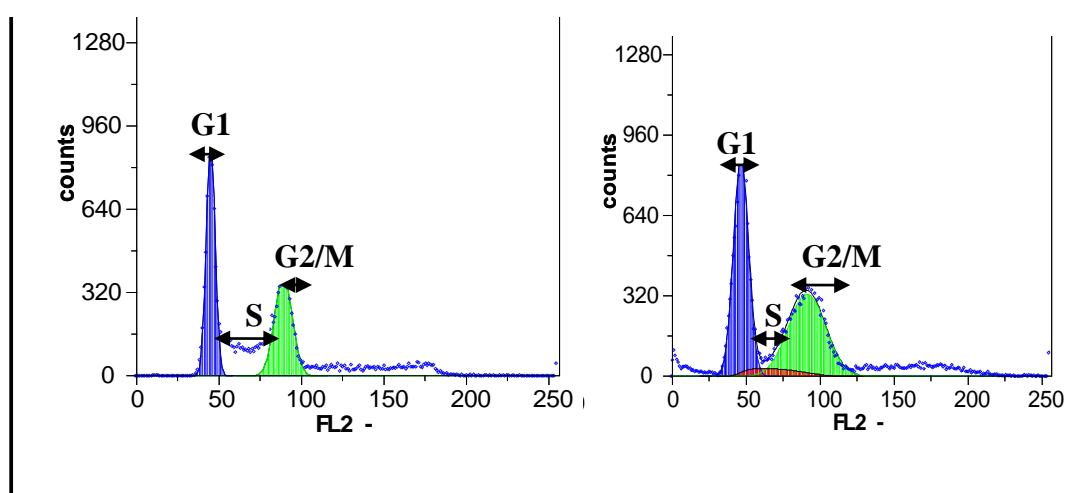


**Figure 3.6 (i): Cell cycle analysis of MOLT-4 lymphoblastic leukaemia cell line following treatment with 50µg/ml of cockle GAG extracts.**

MOLT-4 cell were stained with PI stain and subjected to cell cycle analysis by flow cytometry. (A) Charts showed averages of three independent experiments after treatment with or without crude cockle GAGs. (B) Flow cytometry of MOLT-4 cells after 16 and 24 hours incubation without GAGs. (C) Flow cytometry histogram of MOLT-4 cells after 16 and 24 hours incubation with 50 µg/ml crude cockle GAGs.

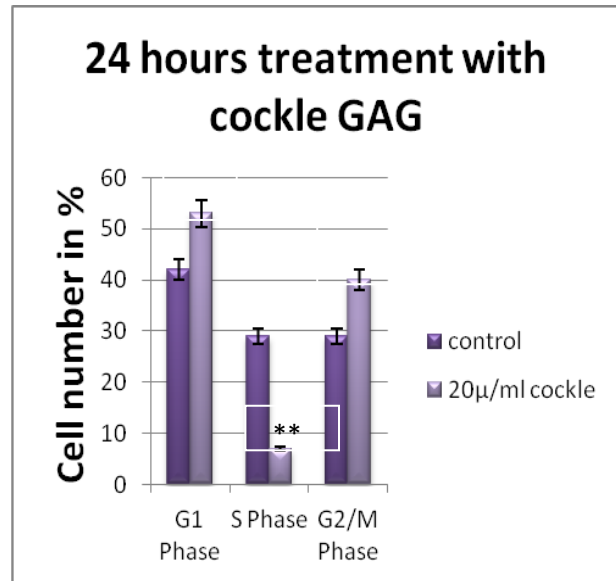
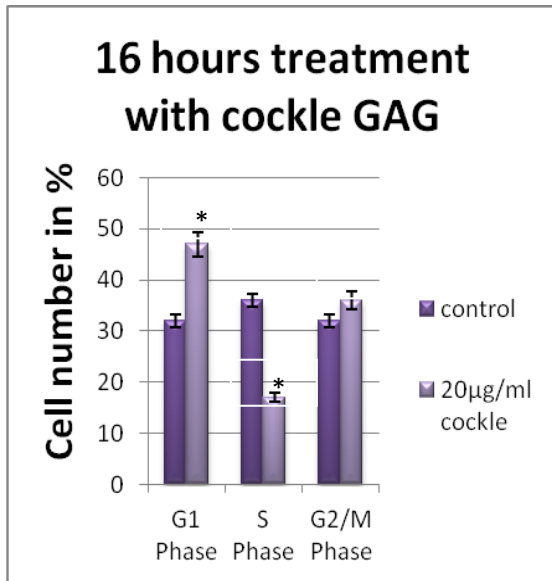
Abbreviations: \*-Significant ( $p \leq 0.05$ ); \*\*-Highly significant ( $p \leq 0.01$ ).

To investigate whether the deleterious effect of the crude extract on MOLT-4 cell was dose-dependent, we also examined its effect on DNA composition of MOLT-4 cell line following treatment with lower concentration (20 $\mu$ g/ml) of the crude extract, using cell cycle analysis by flow cytometry. Results obtained showed time-dependent marked disruptive effects similar to that obtained for the higher concentration (50 $\mu$ g/ml) of the crude extract on MOLT-4 cell cycle [Figure 3.7 (ii) A-C]. The DNA disruptive effect was assessed between 8 and 48 hours time intervals using lower concentrations (20 $\mu$ g/ml) of the crude extract. Significant MOLT-4 cell cycle arrest at G1 and G2/M-phase with concomitant cell reduction at S-phase was also observed at 16 and 24 hours following cockle GAG mixture treatment (20 $\mu$ g/ml).

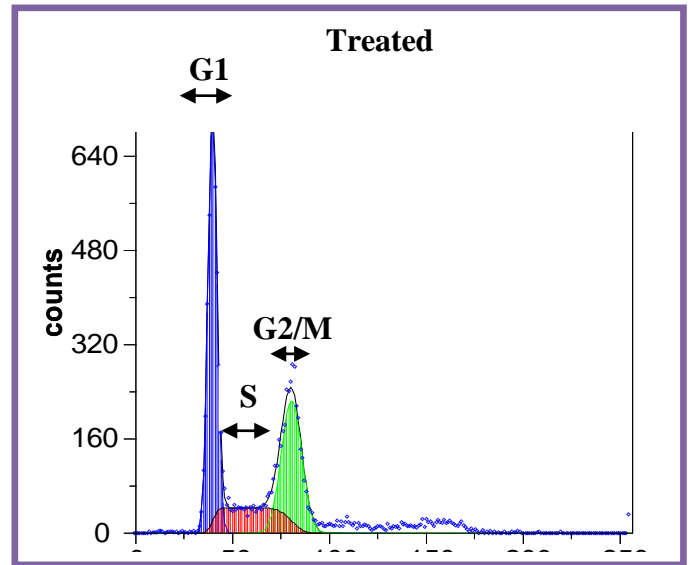
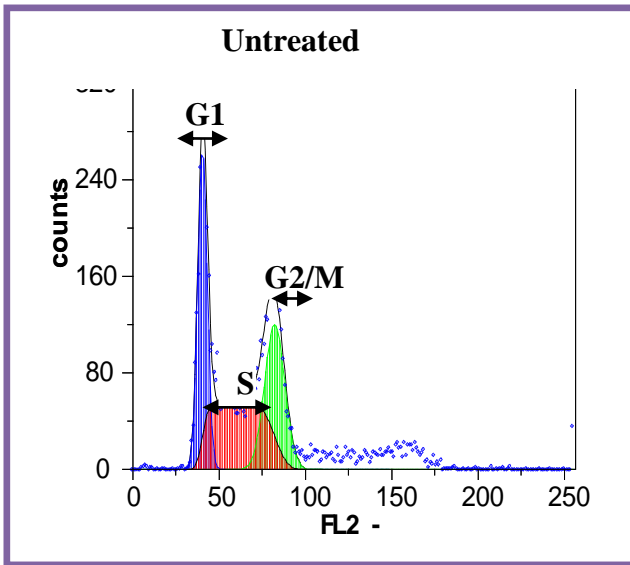
Additionally, 16 hours incubations of the cell with 20 $\mu$ g/ml crude cockle GAGs increased the G1 phase population by 4 % and 21 % at 24 hours. 24 hours incubations also increased the cell population at G2/M-phase by 6 and 11 % respectively [Figure 3.6 (ii) A-C]. Low concentration of crude cockle GAGs decreased the S- phase population by 10 % at 16 hours and 32 % at 24 hours. The observed effect of the extract on the MOLT-4 cell cycle were statistically significant ( $p < 0.05$ ) when comparing the corresponding values of the test samples with the control. There was no noticeable effect observed at 8 and 48 hours incubations on both concentrations tested (result not shown).

A

Cell cycle arrest caused by cockle treatment on MOLT-4 leukemia cell line



B 16 hours



C 24 hours

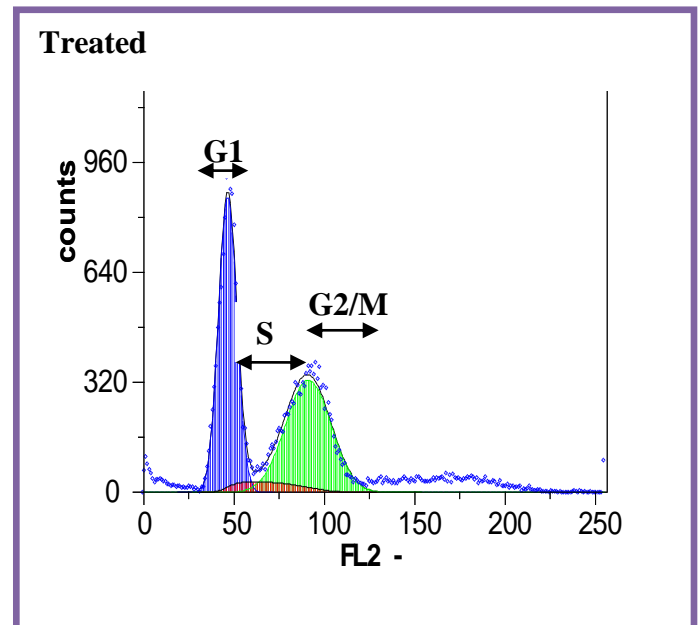
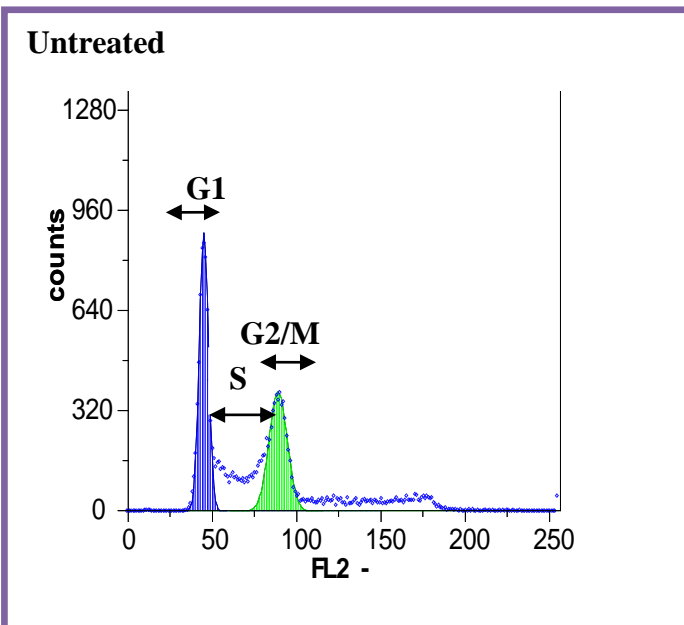


**Figure 3.6 (ii): Cell cycle analysis of MOLT-4 lymphoblastic leukemia cell line following treatment with low concentration (20µg/ml) of cockle GAG extract.**

MOLT-4 cell were stained with PI stain and subjected to cell cycle analysis by flow cytometry (A). Charts showed averages of three independent experiments after treatment with or without crude cockle GAGs. (B) Flow cytometry of MOLT-4 cells after 16 hours incubations with or without crude cockle GAGs. (C) Flow cytometry of MOLT-4 cells after 24 hours incubation with or without crude cockle GAGs.

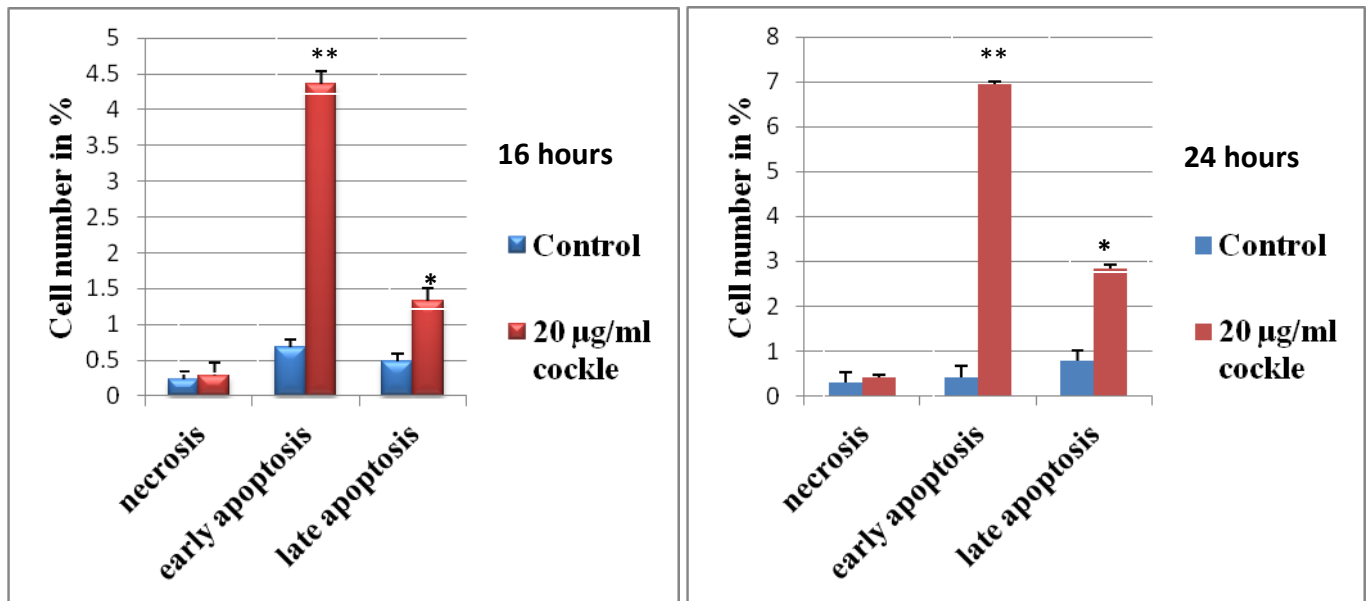
Abbreviations: \*-Significant ( $p \leq 0.05$ ): \*\*-Highly significant ( $p \leq 0.01$ )

### **3.7 Annexin V-FITC Apoptosis Assay of the MOLT-4 Lymphoblastic leukemia cell line following treatment with crude cockle GAG**

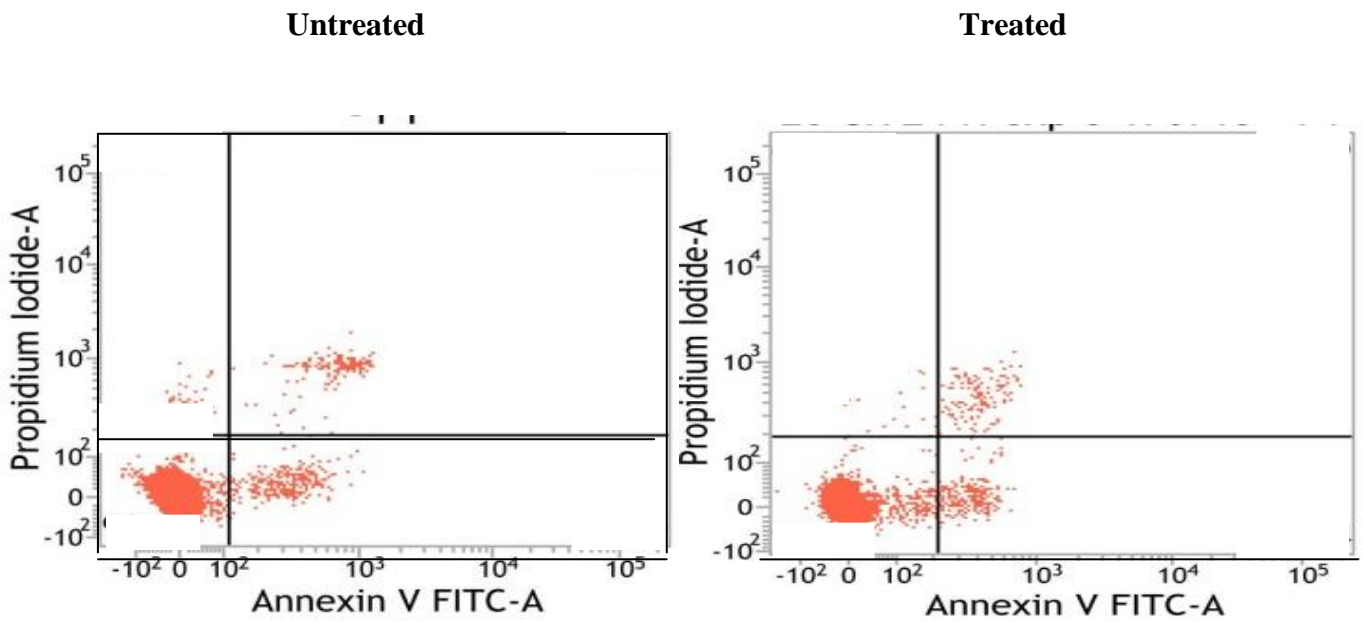
The role of apoptosis in the anticancer effects seen with the cockle GAG extracts was studied using the Annexin V apoptotic assay induced by crude cockle GAG on the MOLT-4 leukemia cell line. We incubated different concentrations obtained from a pilot study (20 & 50 µg/ml) of the crude cockle extract with the MOLT-4 cells at different time intervals (8-48 hours). Both treated and untreated cells were stained with both PI and annexin V-FITC stains and analysed by flow cytometry. The results obtained demonstrate that the numbers of early apoptotic cells increased significantly at both 16 ( $p \leq 0.01$ ) and 24 ( $p \leq 0.01$ ) hours time points following incubation with cockle GAGs when compared with the corresponding values of the control group. At 16 hours post-treatment, the proportion of early apoptotic cells in the cockle GAG treated cells reached 4.36%, which was significantly higher ( $p < 0.05$ ) than the control group (0.68%) [Figure 3.7(A-C)]. At 24 hours post treatment, the proportion of early apoptotic cells increased from 0.48% (control) to 6.95% (cockle GAG). This finding suggests that the anticancer effects seen with crude cockle GAGs on the leukaemia cell line is, in part, linked to time-dependent apoptosis.

However, there was no noticeable apoptotic effect observed at 8 and 48 hours for both concentrations treated (results not shown).

**A** Apoptosis induced by cockle GAG treatment on MOLT-4 leukemia cell line



**B** 16 hours



**C** 24 hours

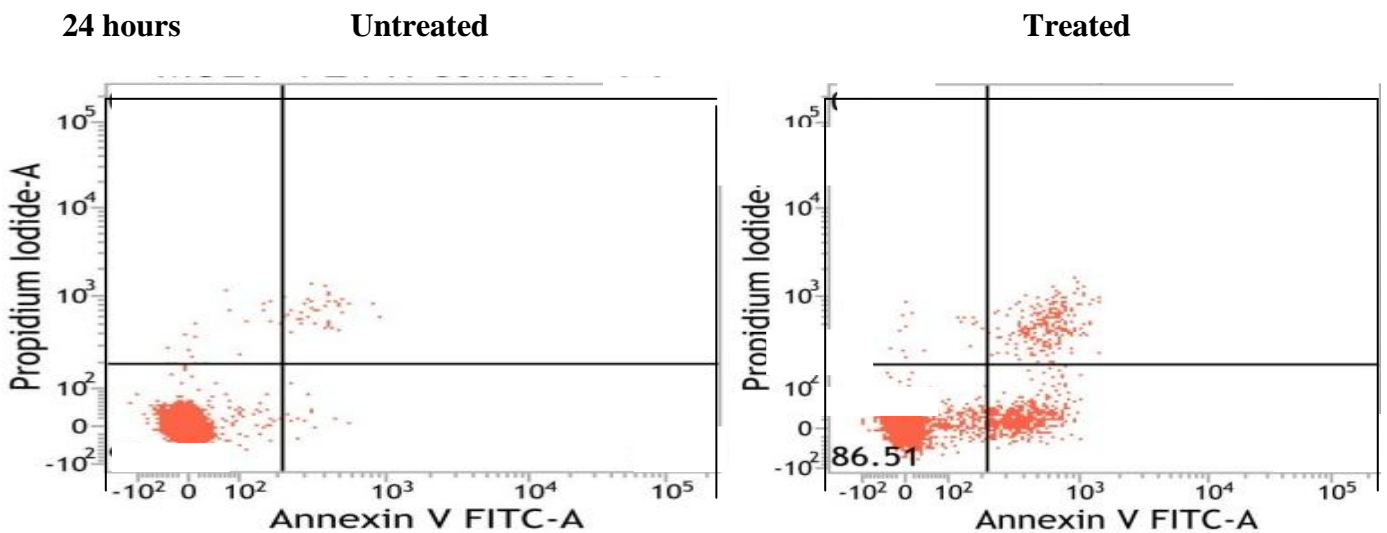


**Figure 3.7: Detection of Apoptotic MOLT-4 cells treated with cockle GAG's extracts by Annexin V Staining.**

MOLT-4 cells were treated with cockle crude GAGs for 16 and 24 hours and then stained using Annexin V-FITC and PI provided in the Annexin V-FITC Apoptosis Detection Kit (see materials and methods). The combination of Annexin V-FITC and PI allows for the distinction between early apoptotic cells (annexin V-FITC positive), late apoptotic and/or necrotic cells (Annexin V-FITC and PI positive), necrotic (PI stained positive) and viable cells (unstained). (A) MOLT-4 cell treated with or without cockle GAGs for 16 and 24 hours respectively. (B) MOLT-4 cell treated with or without cockle GAGs for 16 hours. (C) MOLT-4 cells treated with or without cockle GAGs for 24 hours.

Abbreviations: \*-Significant ( $p \leq 0.05$ ): \*\*-Highly significant ( $p \leq 0.01$ ).



**Table 1: Summary of biological effects of cockle GAGs**

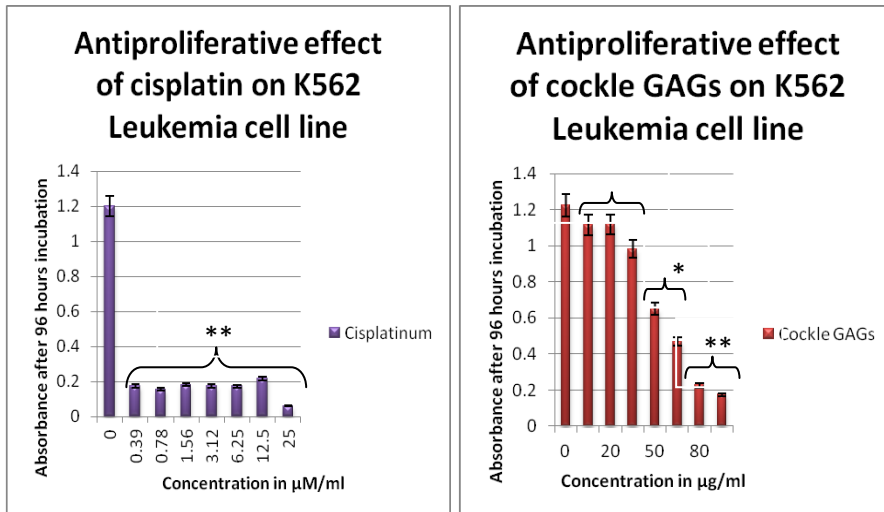
	<b>MDA468</b> breast cancer cell line	<b>MDANQ01</b> breast cancer cell line	<b>K562</b> erythrocytic leukemia cell line	<b>MOLT-4</b> lymphoblastic leukemia cell line	<b>3T3</b> normal fibroblast cell line
<b>Proliferative assay results</b>	Supported cell growth	Supported cell growth	Inhibited cell growth	Inhibited cell growth	Supported cell growth
<b>IC<sub>50</sub></b>	-	-	<b>52µg/ml</b>	<b>16µg/ml</b>	-
<b>Cell cycle arrest</b>	-	-	-	<b>Induced cell cycle arrest at both S and G2M phase</b>	-
<b>Apoptosis detection assay</b>	-	-	-	<b>Induced early apoptosis</b>	

## **SECTION 3B**

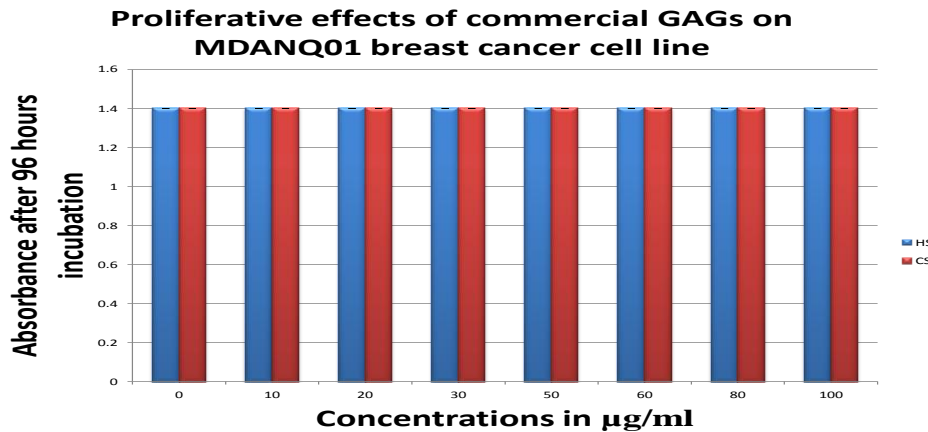
### **Biological assay results for whelk GAG Mixtures**

### **3.8 Effect of crude whelk GAG extracts on the growth of the MDANQ01 breast cancer cell line**

The proliferation of MDANQ01 breast cancer cells was found to be inhibited strongly by crude whelk GAG extracts with a recorded  $IC_{50}$  of 25.14  $\mu\text{g/ml}$  (Figure 3.8A). The observed inhibitory effect of whelk GAGs on this cell line compared favourably with cisplatin (a DNA-damaging agent) anticancer drug (Figure 3.8A-B). The results obtained are in stark contrast to the activities seen with cockle GAG extracts on this breast cancer cell line. This may indicate the presence of unique structural differences between the GAG chain present in the whelk and cockle samples. Again, the commercial GAG samples of HS and CS failed to show any appreciable anticancer effects (Figure 3.8B). These findings are unique and identify whelk derived GAG chains as potential treatments for breast cancer. The selective nature of this activity between whelk and cockle GAGs is also a fascinating new discovery with huge potential for specific targeted therapy in the treatment of different cancers.



**A**



**B**

**Figure 3.8: MTT cell viability assay for MDANQ01 cells after treatment with Whelk extract and commercial GAGs.**

Cells were incubated with various concentrations of GAGs for 96 hours after which time cell viability was measured using an MTT assay (A) whelk extract GAGs with Cisplatin as a positive inhibitory control, (B) commercial GAGs with cisplatin as a positive control. Each value is presented as the mean SEM of three independent determinations. The bars in each chart are presented as relative values in comparison to untreated cells.

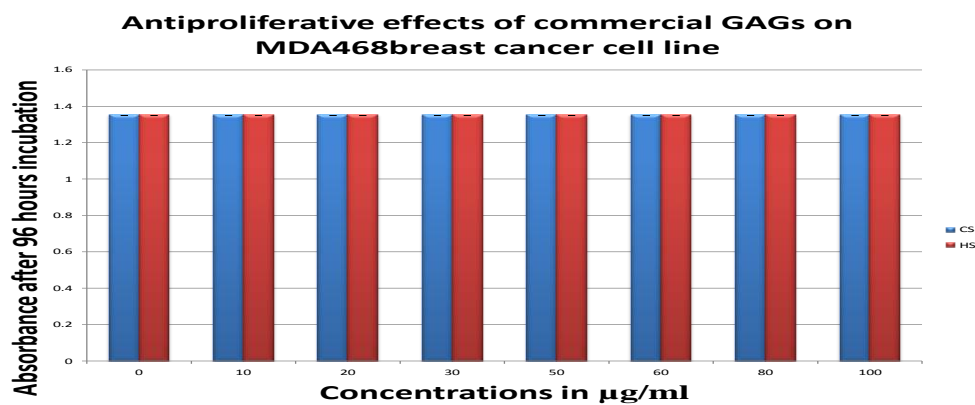
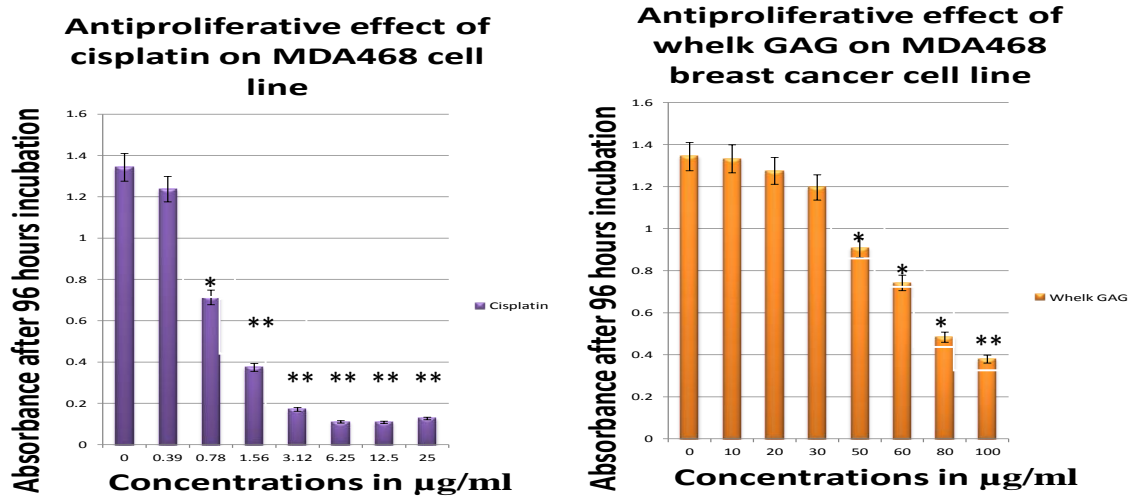
Abbreviations: \* Significant ( $p \leq 0.05$ ): \*\*-Highly significant ( $p \leq 0.01$ )

### **3.9 Effect of crude whelk GAG extracts on the growth of MDA468 breast cancer cells**

The proliferation of MDA468 breast cancer cell was similarly inhibited, in a dose dependent, by crude whelk GAGs with a recorded  $IC_{50}$  of 70.94  $\mu\text{g/ml}$  (Figure 3.9A). In contrast, the whelk GAGs had a more profound anticancer activity with the MDANQ01 cell line. Again the activity was dose-dependent with an  $IC_{50}$  of 25.14 $\mu\text{g/ml}$  (Figure 3.8A). These results suggest that the MDANQ01 cell line is more sensitive to whelk GAGs treatment than MDA468 cells. The observed inhibitory effect of whelk GAGs on this cell line also compared favourably with cisplatin (a DNA-damaging agent) anti-cancer agent at a concentration range between 1-25  $\mu\text{M}$  with a recorded  $IC_{50}$  of 0.88  $\mu\text{M}$  (Figure 3.9A-B). Once again, the commercial GAGs (HS and CS) (Figure 3.9B), did not have growth inhibitory effect on this cell line but rather serve as a growth catalyst for this cell line.

These results suggest that the whelk derived GAG's possesses a unique activity against the growth of breast cancer cells and shows great potential for the treatment of this disease. Indeed the differences in  $IC_{50}$  values for the two breast cancer cell lines suggests that the whelk derived GAG's could be selective to certain cell types and this selectivity may well be important in targeting the effects of these molecules towards tumour cells. Further studies to establish the effects of these GAG's on other tumour and normal cell lines have also been performed; the results of which are outlined in the following section.

A



B

**Figure 3.9: Concentration-dependent effect of whelk GAG extracts on MDA468 breast cancer cell viability.**

Cells were incubated with various concentrations of GAGs for 96 hours after which time cell viability was measured using an MTT assay (A) Whelk crude GAGs with Cisplatin as a positive inhibitory control, (B) Commercial and crude whelk GAGs with cisplatin as a positive control. Each value is presented as the mean SEM of three independent determinations. The bars in each chart are presented as relative values in comparison to untreated cells.

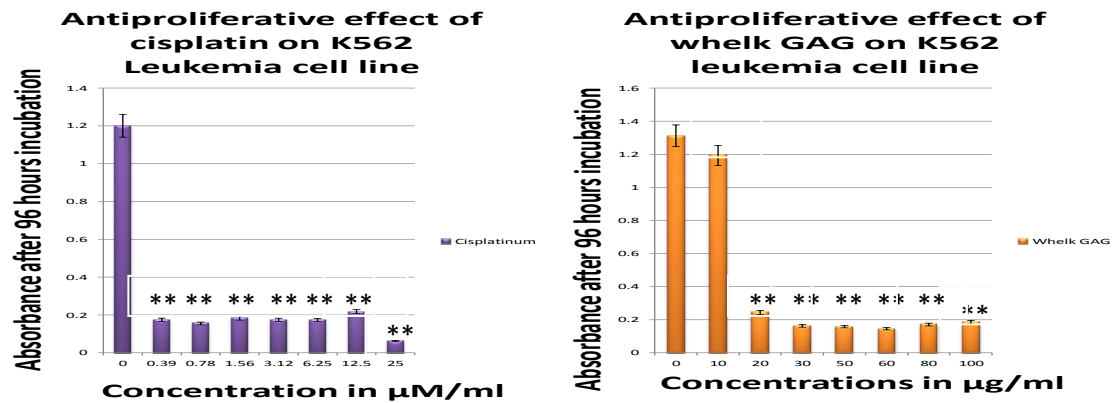
Abbreviation: \* Significant ( $p \leq 0.05$ ): \*\* Highly significant ( $p \leq 0.01$ )

### **3.10 Effect of crude whelk GAG extracts on the growth of K562 and MOLT-4 leukaemia cells lines (K562 and MOLT-4)**

Further investigation of anticancer effects of crude whelk GAG was performed using two different cancer cell lines (MOLT-4 and K562). The results obtained from this study confirm the whelk derived GAGs anticancer activities. The anti-proliferative activities of these polysaccharides are dose-dependent on both leukaemia cell lines with the best activity seen against K562 cell line (Figure 3.10B). Surprisingly, the growth inhibitory activities of the crude whelk was more pronounced on erythroleukaemia cell line (K562) than MDANQ01 breast cancer cell. The recorded IC<sub>50</sub> for crude whelk GAG extract on k562 leukemia cell was 14µg/ml. Contrarily, the crude whelk GAG extracts inhibited the growth of MOLT-4 leukaemia cell proliferation in a concentration-dependent manner with arecorded IC<sub>50</sub> of 41.11µg/ml and the lowest concentration (10µg/ml) of the extract did not show any growth inhibitory effect on lymphoblastic leukaemia cell (MOLT-4) Figure 3.10A).

The anti-proliferative activities of the crude whelk GAG extracts on the two leukaemia cell lines compare favourably with the cisplatin positive control and the low IC<sub>50</sub> observed for K562 suggests the crude whelk GAG extracts would show promise as the basis for an anti-leukemia drug, based on the recommendation of the standard National Cancer Institute criteria. More importantly, the different anticancer activities display by the crude whelk GAG extracts on these two cell lines also suggests that the whelk derived GAG's could be selective for certain cell types and this selectivity may well be important in targeting the effects of these molecules towards tumour cells.

A



B

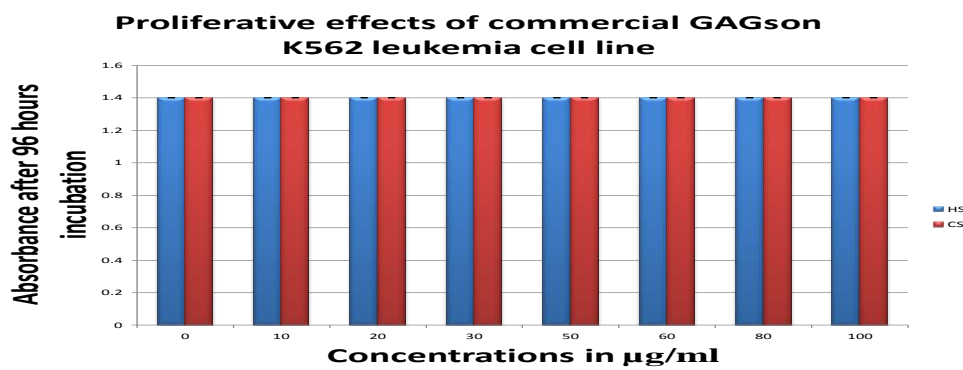


**Figure 3.10: MTT cell viability assay for MOLT-4 and K562 leukaemia cells after treatment with whelk GAG extracts**

Cells were incubated with various concentrations of GAGs for 96 hours after which time cell viability was measured using an MTT assay (A) MOLT-4 leukaemia cells treated with crude whelk GAGs with cisplatin as a positive inhibitory control, (B) K562 leukaemia cell line treated with crude whelk GAGs and cisplatin as a positive control. Each value is presented as the mean SEM of three independent determinations. The bars in each chart are presented as relative values in comparison to untreated cells.

Abbreviations- \*-Significant ( $p \leq 0.05$ ): \*\*-Highly significant ( $p \leq 0.01$ )



### **3.11 Effect of crude whelk GAG extracts on the growth of HeLa Cervical cells**

The anticancer activity of whelk GAG mixture was also tested on the standard HeLa cell line as this cell line is particularly susceptible to induction of apoptosis. The result shows that crude whelk GAG mixture strongly inhibited the growth of the HeLa ovarian cell line and its anticancer effects were more pronounced than on all other cancer cells investigated so far in this study, with a typically recorded  $IC_{50}$  of 12 $\mu$ g/ml. Moreover, it is clear that the anti-cancer activities of this whelk GAG mixture are greater than that observed for cisplatin anti-cancer drug (Figure 3.11A-B).

Once again all commercial GAGs tested along with whelk crude GAGs did not demonstrate any inhibitory effect on the HeLa cells proliferation: suggesting that the inhibitory effect may be a unique feature of the GAG's derived from whelks. This result also suggests that this polysaccharide's anti-cancer activity is stronger than cisplatin anti-cancer drug. In addition, the data suggests that the whelk derived GAG's could be more selective to this cell types than other cells tested and this selectivity may well be important in targeting the effects of these molecules towards tumour cells.

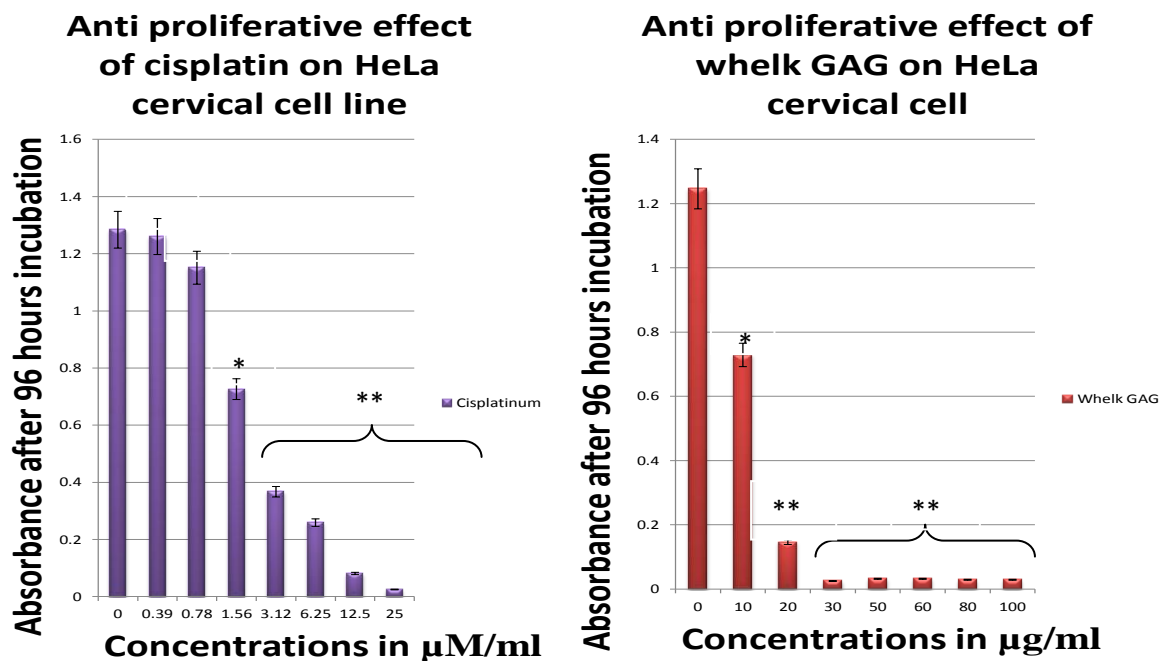


**Figure 3.11: MTT cell viability assay for HeLa cervical cell after treatment with whelk GAG extracts**

Cells were incubated with various concentrations of GAGs for 96 hours after which time cell viability was measured using an MTT assay with cisplatin as a positive inhibitory control. Each value is presented as the mean SEM of three independent determinations. The bars in each chart are presented as relative values in comparison to untreated cells.

Abbreviations: \*- Significant ( $p \leq$ ): \*\*-Highly significant ( $p \leq 0.01$ )

### **3.12 Effect of crude whelk GAG mixtures on the growth of normal fibroblast cells (3T3)**

The effects of crude whelk GAGs on growth of normal fibroblast cells (3T3) was measured using MTT colorimetric assay. Cells were exposed to different concentrations of the crude whelk GAGs for 96 hours. Crude whelk GAG extracts did not show any growth inhibitory effect on 3T3 cell proliferation (Figure 3.12). Moreover, the effects of crude whelk GAGs on 3T3 cells compare favourably with the results obtained for commercial GAGs. These results suggest that whelk derived GAG's is selective against cancer cell types and at least on a normal cell type and shows great potential in the treatment of this disease.

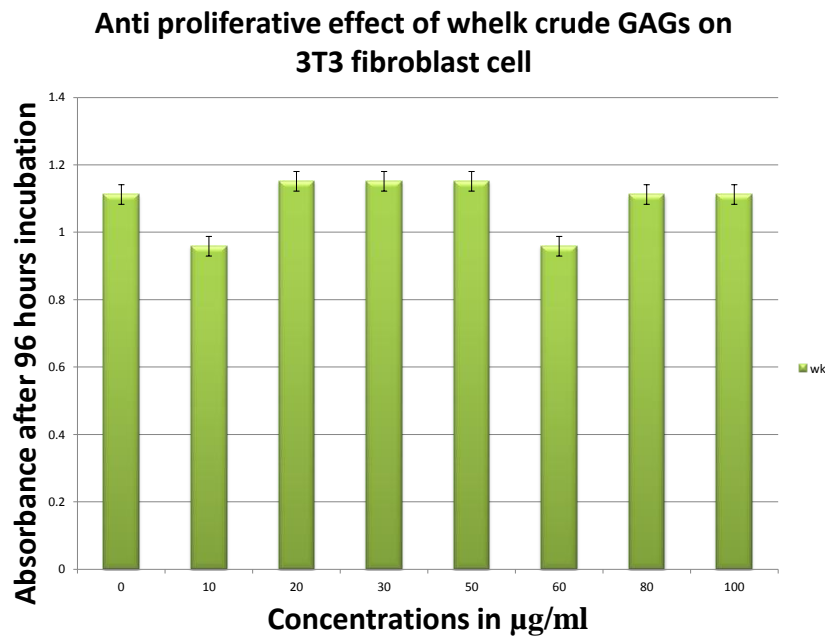


**Figure 3.12: MTT cell viability assay of normal fibroblast 3T3 cells after treatment with whelk GAGs extracts.**

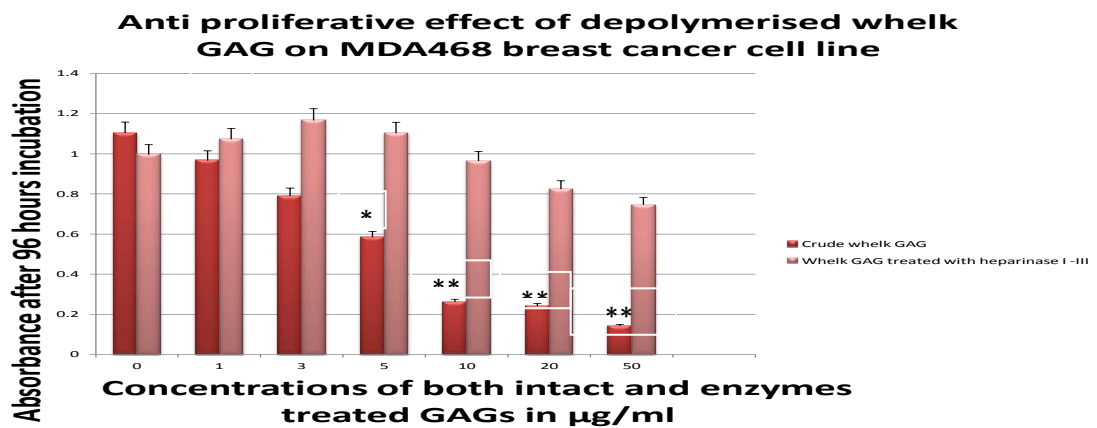
Cells were incubated with various concentrations of GAGs for 96 hours after which time cell viability was measured using an MTT assay. Each value is presented as the mean SEM of three independent determinations.

The bars in each chart are presented as relative values in comparison to untreated cells.

### **3.13 Effect of Heparinase I, II, & III enzymes on anti-proliferative activity of whelk GAG extracts using MDA468 and MDANQ01 breast cancer cell lines.**

The crude whelk GAG extract was depolymerised with Heparinase I, II&III enzymes to break the long linear chain polymer to smaller oligosaccharides chains, this has previously been shown to destroy any GAG related biological activities. The oligosaccharide product was then incubated with the two breast cancer cell lines (MDANQ01 and MDA 468) for 96 hours, as described under materials and methods. The results obtained showed a dramatic reduction in the growth inhibitory effects of whelk GAG extracts on both breast cancer cell lines (Figure 3.13A-B). These results suggest that the anticancer activities of these novel GAG extracts appears to be connected to the intact linear polysaccharide chains that were present in the crude GAG mixture.

A



B

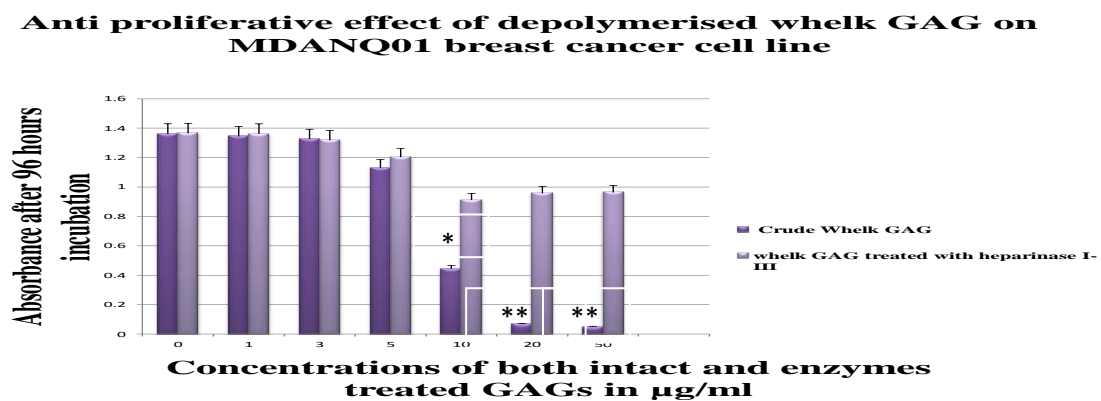


**Figure 3.13: MTT cell viability assay for MDANQ01 and MDA468 breast cancer cells after treatment with heparinase depolymerised whelk GAG extracts.**

Cells were incubated with various concentrations of GAGs for 96 hours after which time cell viability was measured using an MTT assay (A) MDA468 cells after treatment with whelk GAG Heparinase I-III enzyme digest with cisplatin as a positive inhibitory control, (B) MDANQ01 cells treated with whelk GAG Heparinase I-III enzyme digest with cisplatin as a positive inhibitory control. Each value is presented as the mean SEM of three independent determinations. The bars in each chart are presented as relative values in comparison to untreated cells.

Abbreviations: \*-Significant ( $p \leq 0.05$ ): \*\*-Highly significant ( $p \leq 0.01$ )

### **3.14 Cell cycle analysis of MDANQ01 cells after treatment with crude whelk GAG extracts**

Flow cytometry was used to investigate the effects of the whelk GAG extracts on the progression of the cell cycle. Cells exposed to either 20ug/ml or 50ug/ml whelks GAG's showed perturbation of MDANQ01 cell's cycle after 24-72 hours exposure to the crude extract.

Whelk GAGs induced cell cycle arrest of MDANQ01 cells at both S and G2M phases was observed as shown in Figure 3.14A-C. This brought about a significant accumulation of cells at S and G2/M phases leading to the subsequent reduction of number of cells in G1 phase. 24 hours treatment of MDANQ01 cells with 50µg/ml whelk GAGs caused a marginal increase in the number of cells at G2/M-phase from  $26.97\% \pm 6.28$  (control) to  $29.16\% \pm 0.1$  (50 µg/ml wk). At 48 h the cell population at S-phase (Figure 3.14A-C) increased from  $20.48\% \pm 8.19$  (control) to  $26.76\% \pm 2.26$  (50 µg/ml whelk). Similarly lower concentrations of whelk GAGs disrupted MDANQ01 cell cycle progression at both S and G2/M. The longest incubation time (72 hours) with low doses of the crude GAGs (Figure 3.14A-C) significantly altered the cell cycle by inducing a more than two fold increase in the percentage of cell population at the G2/M-phase ( $p < 0.02$ ). [Control cell ( $18.82\% \pm 1.70$ )] treated cell ( $37.39\% \pm 3.48$ ).

# Cell cycle arrest caused by whelk GAG treatment on MDANQ01 breast cancer cell line

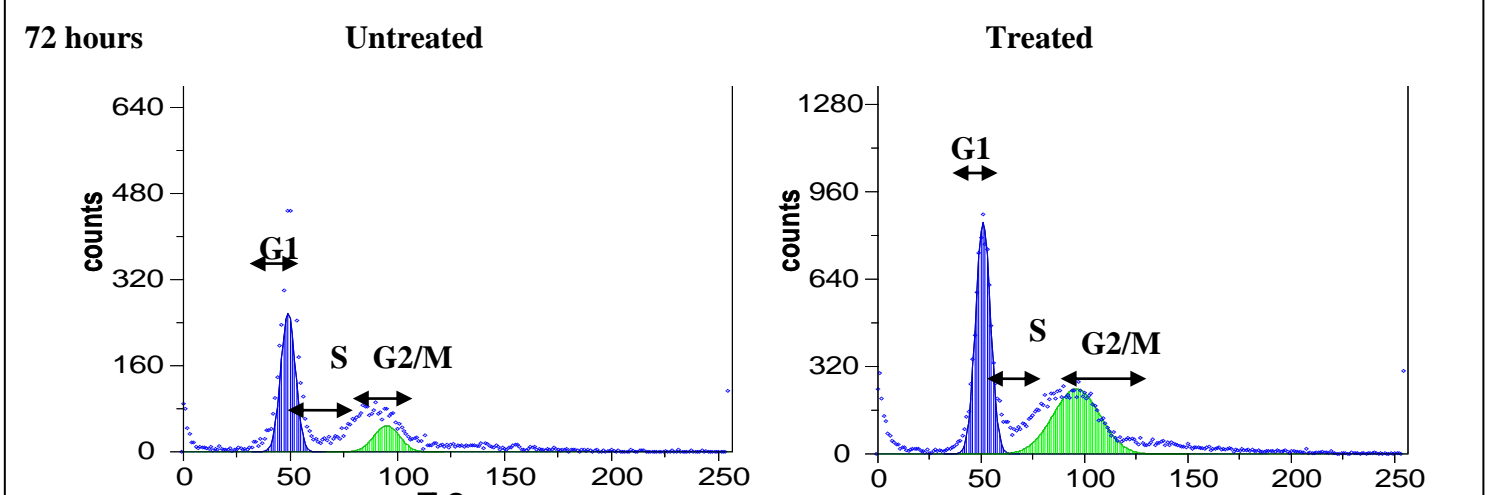
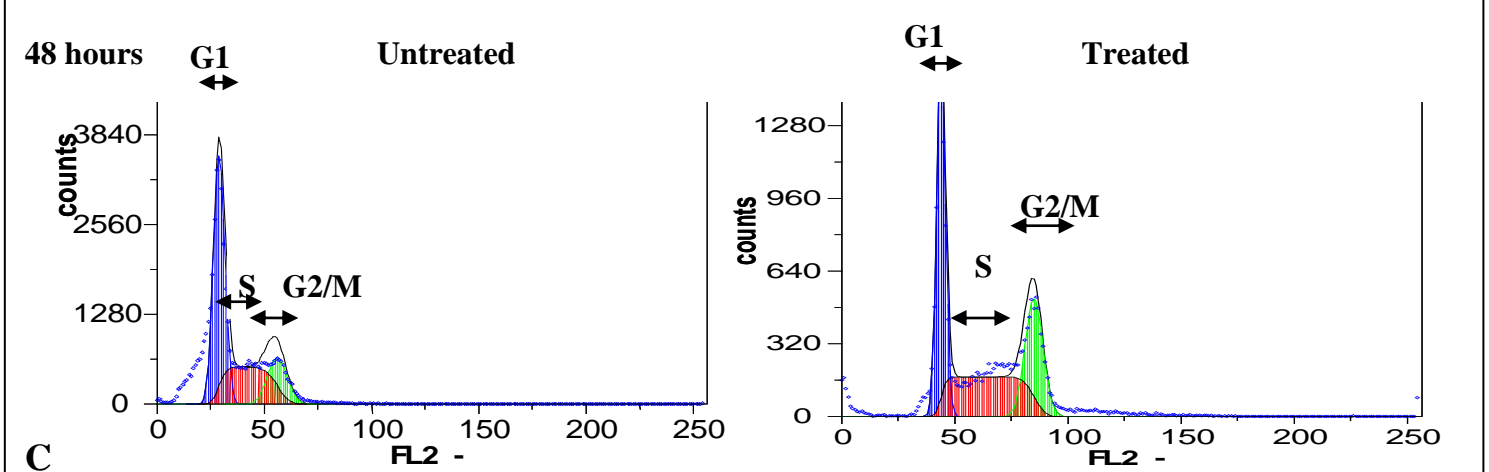
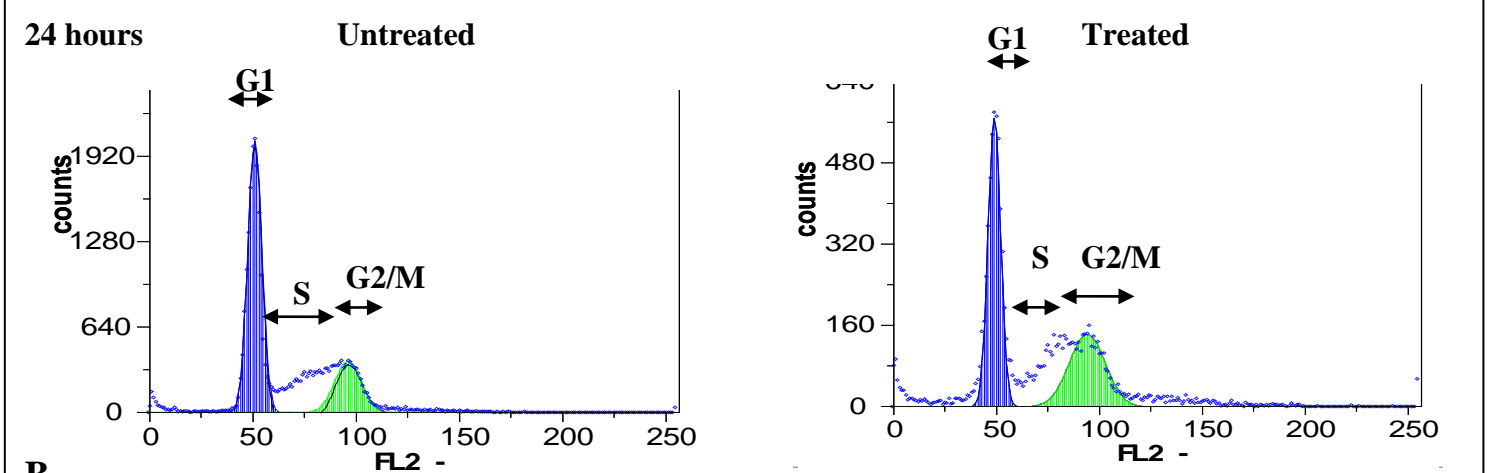
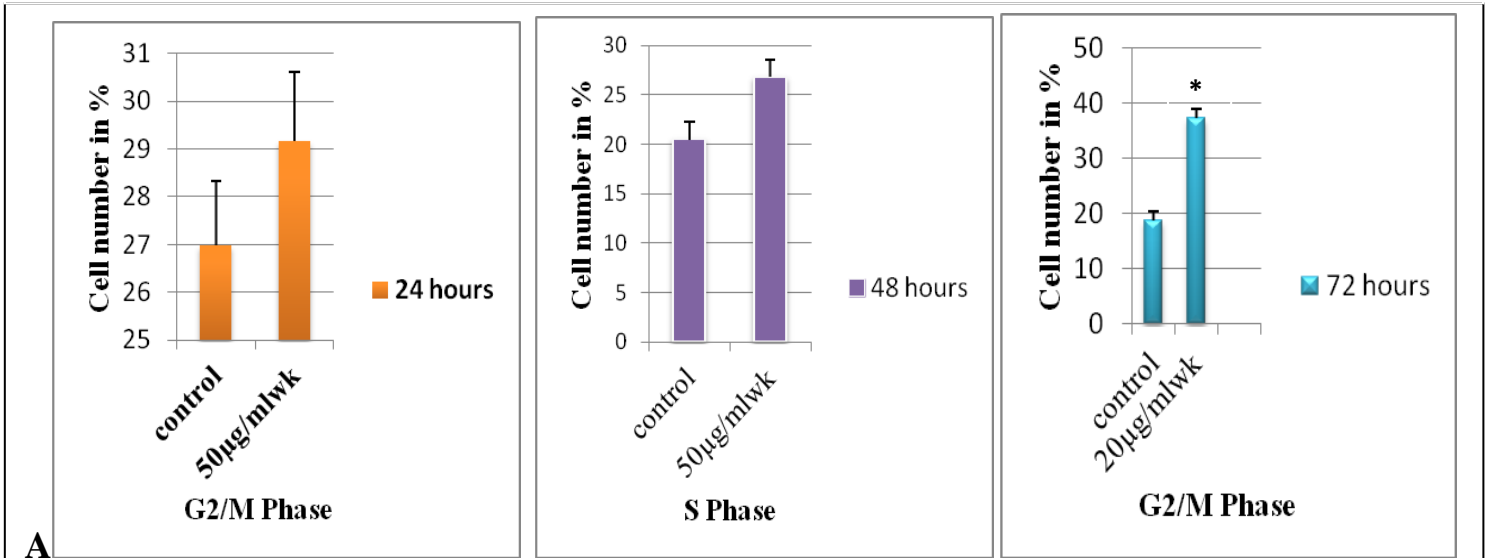




**Figure 3.14: Cell cycle analysis of MDANQ01 breast cancer cell line following treatment with crude whelk GAG extract.**

MDANQ01 breast cancer cells were treated with PI stain and subjected to cell cycle analysis by flow cytometry (A). Charts showed averages of three independent experiments after treatment with or without crude whelk GAGs. (B) Flow cytometry of MDANQ01 cells after 24 hours incubations with or without crude whelk GAGs. (C) Flow cytometry of MDANQ01 breast cancer cells after 48 hours incubation with or without crude whelk GAGs and (D) Flow cytometry of MDANQ01 breast cancer cells after 72 hours incubation with or without crude whelk GAGs.

Abbreviations: \*- Significant ( $p \leq 0.05$ )

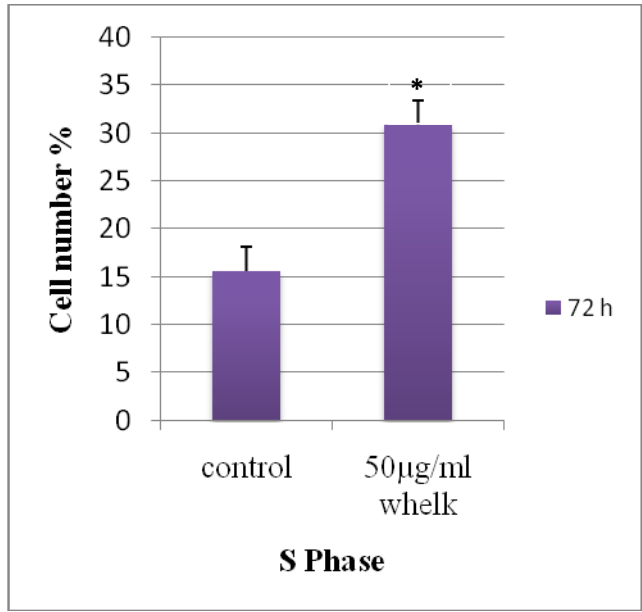
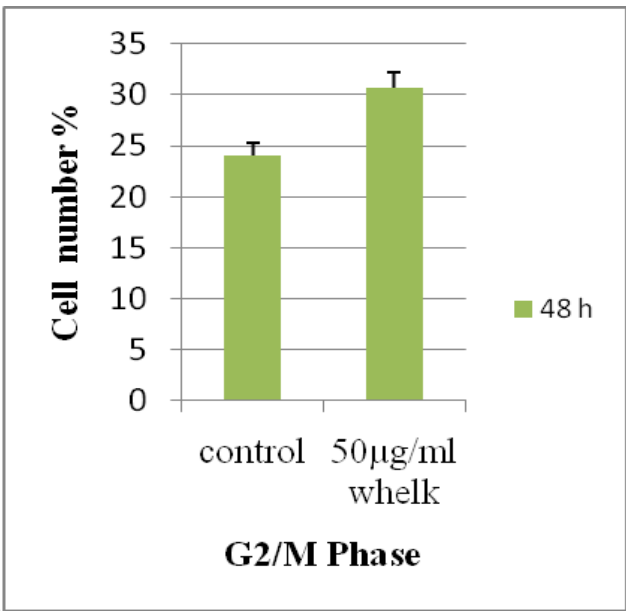
### **3.15 Cell cycle analysis of MDA468 breast cancer cell lines after treatment with crude whelk GAG extracts**

Whelk GAGs treatment also caused significant cell cycle disruptions in the MDA468 breast cancer cell line in a similar manner to that observed in the MDANQ01 cells. Cell cycle disruptions were observed at both S and G2/M phases (see Figure 3.15A-C). Higher concentrations of whelk GAGs (50µg/ml) also induced a time-dependent DNA disruptive effect on MDA468 cells as shown in Figure 3.15A-B. A short hour (48 hours) incubation of the crude whelk GAG extracts with MDA468 cells induced cell accumulation at G2/M; however, these differences were not statistically significant ( $p>0.05$ ) when compared with the corresponding values of the control.

The longer 72 hours incubations of the cells with high doses of crude GAGs significantly altered the cell cycle by inducing more than a two-fold increase in the percentage of cell population at the S-phase ( $p<0.02$ ). Crude whelk GAG extracts increased cell population at G2/M-phase from  $24 \pm 4.8$  % (control) to  $31 \pm 3.4$ % (50µg/ml whelk) after 48 hours incubation but this increase is not statistically significant ( $p<0.14$ ).

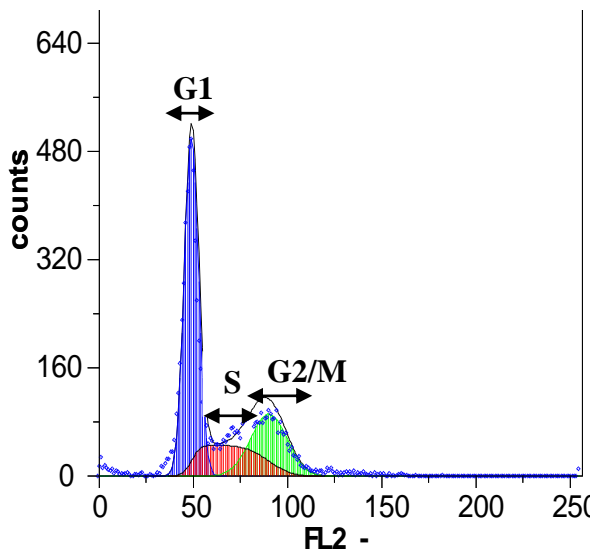
# Cell cycle arrest induced by whelk GAG treatment on MDA468 breast cancer

...

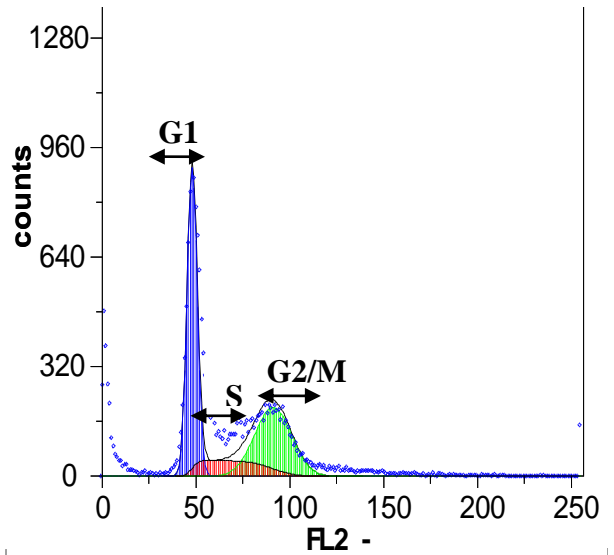


**A**

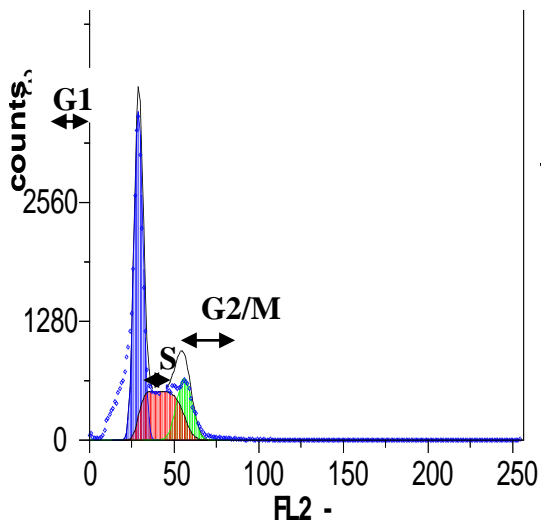
**B 48 hours**                      **Untreated**



**Treated**



**C 72 hours**                      **Untreated**



**Treated**

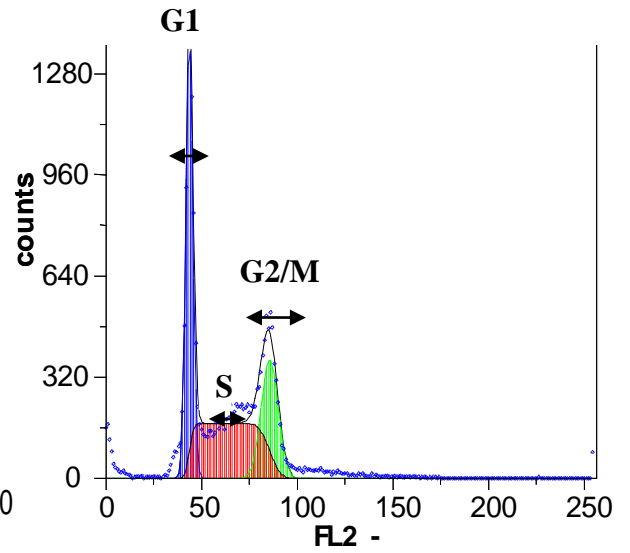


**Figure 3.15: Cell cycle analysis of MDA468 breast cancer cell line following treatment with crude whelk GAG extract.**

MDA468 breast cancer cells were stained with PI stain and subjected to cell cycle analysis by flow cytometry (A). Charts showed averages of three independent experiments after treatment with or without crude whelk GAGs (B) Flow cytometry of MDA468 breast cancer cells after 48 hours incubation with or without crude whelk GAGs and (C) Flow cytometry of MDA468 breast cancer cells after 72 hours incubation with or without crude whelk GAGs.

Abbreviations: \*- Significant ( $p \leq 0.05$ )

.

.

### **3.16 Effects of crude whelk GAG mixtures on the induction of apoptosis in MDA468 breast cancer cells**

Previous investigations revealed that whelk GAGs induced cell death in MDA468 breast cancer cells; however, the mechanism of cell death induced by this crude polysaccharide was not yet known. An Annexin V-FITC Apoptosis Detection Kit was used in order to elucidate the mechanism of cell death induced by whelk GAG extracts. The two cell lines were incubated with varying concentrations of the whelk GAGs at different time intervals and the apoptosis determination was carried out as described under the materials and methods section. The results reveal that high concentration (50 $\mu$ g/ml) of the whelk GAG extract appears to have caused the breast cancer cells death by inducing apoptosis (late apoptosis) in proportion to the rate of cell death caused by the crude extract on the cells Figure 3.16A-C).

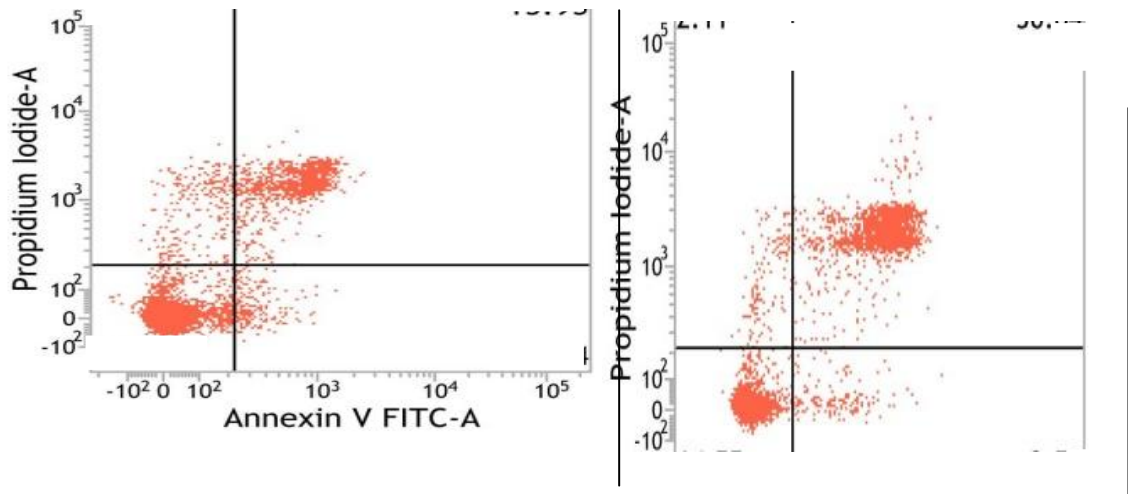
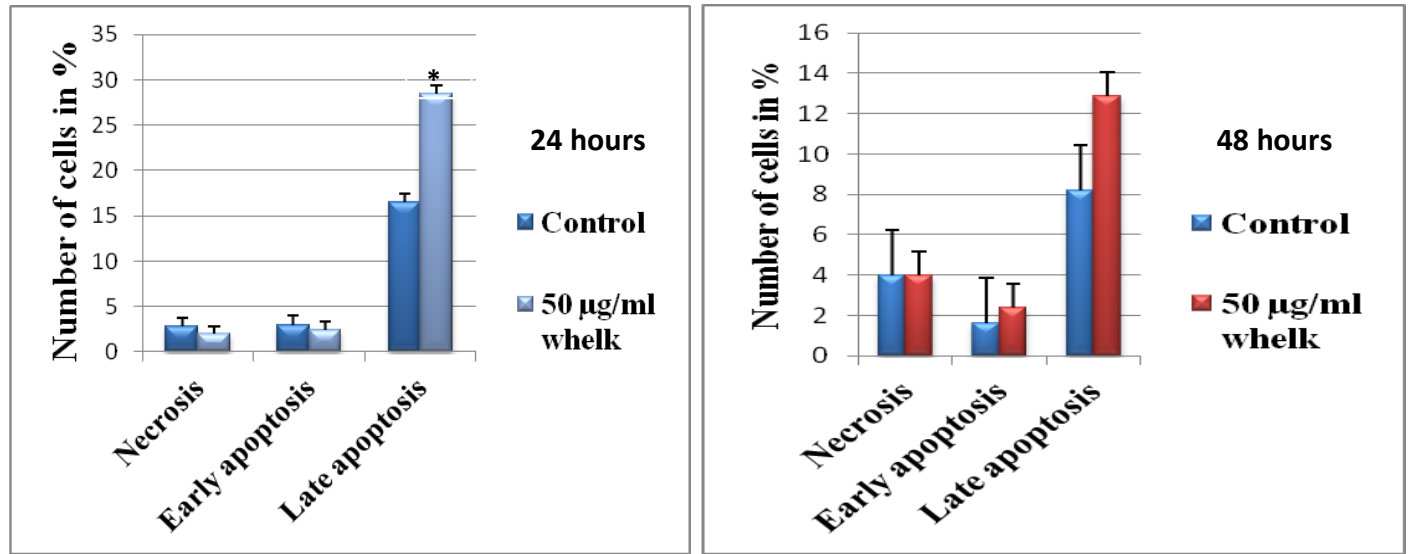
Whelk GAG extracts (50  $\mu$ g/ml) increased the percentage of cells stained positive for both Annexin V-FITC and PI after 24 hours treatment from 16.48 (control) to 28.40 (50 $\mu$ g/ml). 48-hour incubations with the whelk GAGs also slightly increased the number of cells stained with annexin V-FITC from 1.64 % (control) to 2.4 % (50 $\mu$ g/ml). However there were signs of substantial cell lysis at this time point. Moreover, the number of cells stained positive for both Annexin V-FITC and PI increased marginally from 8.2 % (control) to 12.89 % (50 $\mu$ g/ml). However, lower concentration (20 $\mu$ g/ml) of the whelk GAG extract did not show any apoptotic effect on MDA468 cell line: both 8 and 72 hours incubations of the cells with the crude extract did not show any noticeable apoptotic effect on the two cell lines (results not shown).

In addition to the late apoptotic effect of the extract on MDA468 breast cancer cell, there was a false apoptotic effect observed in the control cells 24 hours after incubation,

likely caused by trypsinisation of the cells after incubation. In order to eliminate this false apoptotic effect, both the treated and untreated cells were stained with DAPI and viewed under the fluorescent microscope as described under the materials and methods.

A

Apoptosis induced by whelk GAG treatment on MDA468 breast cancer cell line



C 48 hours Untreated Treated

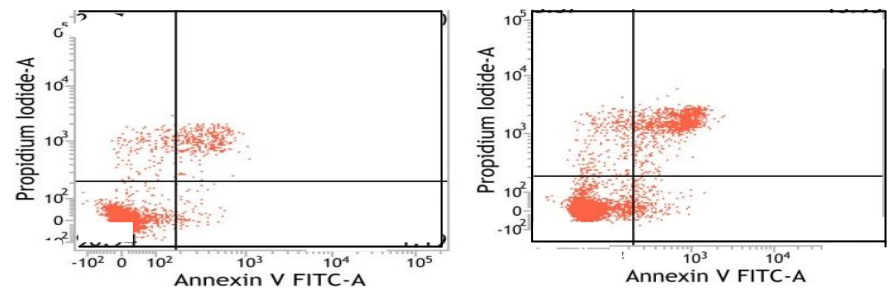


**Figure 3.16: Detection of Apoptotic MDA468 breast cancer cells treated with crude whelk GAG extracts by Annexin V Staining.**

MDA468 breast cancer cells were treated with crude whelk GAGs for 24 and 48 hours and then stained using Annexin V-FITC and PI provided in the Annexin V-FITC Apoptosis Detection Kit (see materials and methods). The combination of Annexin V-FITC and PI allows for the distinction between early apoptotic cells (annexin V-FITC positive), late apoptotic and/or necrotic cells (Annexin V-FITC and PI positive), necrotic (PI stained positive) and viable cells (unstained). (A) MDA468 cell treated with or without crude whelk GAGs for 24 and 48 hours respectively. (B) MDA468 cell treated with or without crude whelk GAGs for 24 hours. (C) MDA468 cell treated with or without crude whelk GAGs for 48 hours.

Abbreviations: \*- Significant ( $p \leq 0.05$ )



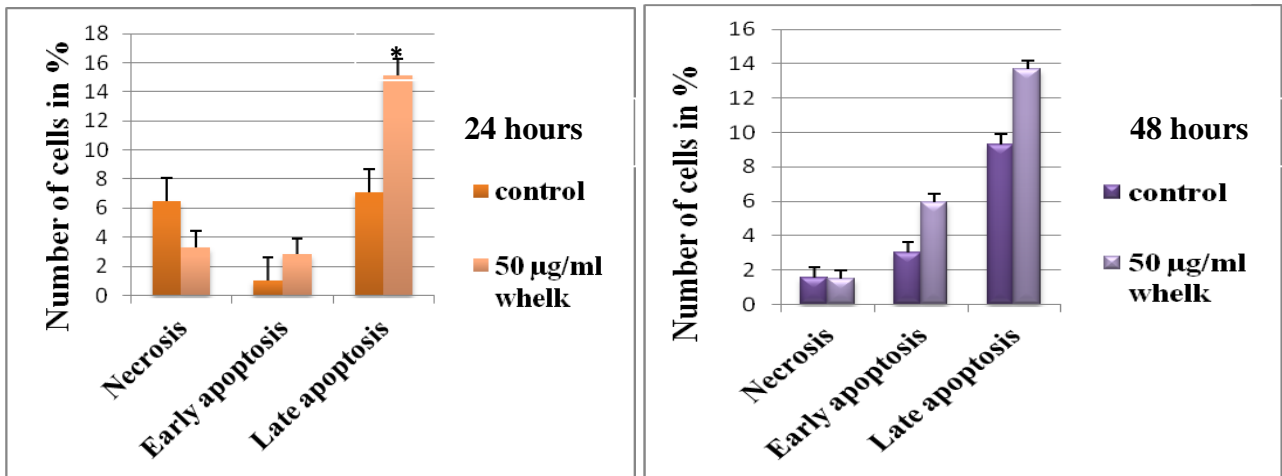
### **3.17 Flow cytometry and Annexin V-FITC apoptosis detection of MDANQ01 cells following incubation with whelk GAG extracts**

Whelk GAGs induced cell death in MDANQ01 breast cancer cells; however, the mechanism of cell death induced by this crude GAG required further study. In order to elucidate the mechanism of cell death induced by crude whelk GAGs, Annexin V-FITC Apoptosis Detection Kit was utilised (see materials and methods). High concentration (50µg/ml) of crude whelk GAGs induced time-dependent apoptosis on MDANQ01 cells (Figure 3.17A-C). 24-hour incubation of the crude whelk GAG extracts with the cells, increased the number of cells stained with annexin V-FITC from 1.02 % (control) to 2.84 % (50 µg/ml) and the number of cells stained with both Annexin V-FITC and PI was also increased from 7.07 % (control) to 15.16 % (50 µg/ml).

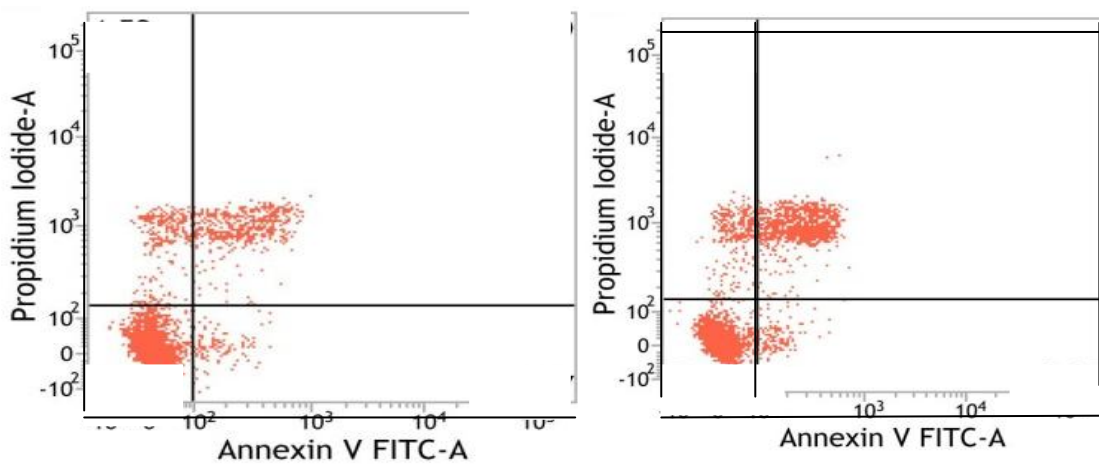
Similarly, 48-hour incubation of the whelk GAG extract also induces apoptosis on MDANQ01 cells but the apoptotic effect was slightly reduced than the observations made at 24 hours. At 48 hours, the number of cells stained with annexin V-FITC increased from 2.99% (control) to 5.92 (50µg/ml) and those cells stained with both Annexin V-FITC and PI also increased from 9.28 % (control) to 13.66 % (50µg/ml). However, lower concentration (20µg/ml) of the crude extract did not show any apoptotic effect on this cell line. Both 8 and 72 hours incubations of the cells with the crude extract did not show any noticeable apoptotic effect on MDANQ01 cell line (results not shown).

Similarly, a false apoptotic effect was observed in the control cells, which may be caused by the trypsinisation's step draw back of the cells after incubation. In order to rule out this false apoptotic effect, both the treated and untreated cells were also stained with DAPI and viewed under the fluorescent microscope, as described under the materials and methods. The results obtained are discussed later in this section.

**A** Apoptosis induced by whelk GAG treatment on MDANQ01 breast cancer



**B** 24 hours                      Untreated                      Treated



**C** 48 hours                      Untreated                      Treated

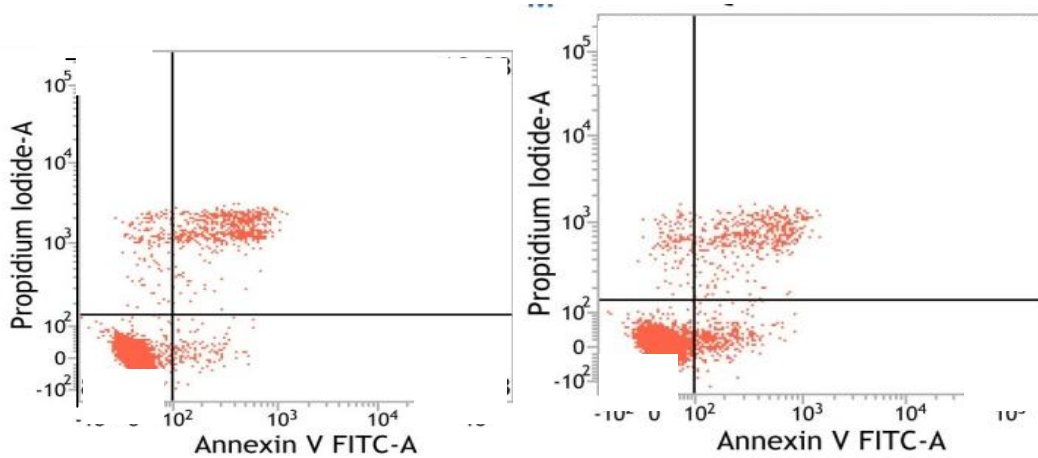


**Figure 3.17: Detection of Apoptotic MDANQ01 breast cancer cells treated with crude whelk GAG extracts by Annexin V Staining.**

MDANQ01 breast cancer cells were treated with crude whelk GAGs for 24 and 48 hours and then stained using Annexin V-FITC and PI provided in the Annexin V-FITC Apoptosis Detection Kit (see materials and methods). The combination of Annexin V-FITC and PI allows for the distinction between early apoptotic cells (annexin V-FITC positive), late apoptotic and/or necrotic cells (Annexin V-FITC and PI positive), necrotic (PI stained positive) and viable cells (unstained). (A) MDANQ01 cell treated with or without crude whelk GAGs for 24 and 48 hours respectively. (B) MDANQ01 cell treated with or without crude whelk GAGs for 24 hours. (C) MDANQ01 cell treated with or without crude whelk GAGs for 48 hours.

Abbreviations: \*- Significant ( $p \leq 0.05$ )

### **3.18 Assessment of apoptosis using DAPI fluorescent microscopy following treatment of MDA468 breast cancer cell with Crude whelk GAG extracts**

To confirm whether the anti-proliferative effect of whelk GAG extracts on MDA468 breast cancer cell line was due to apoptosis; cells were incubated with or without crude whelk GAGs, stained with DAPI stain and the cells morphology examined under a fluorescent microscope. MDA468 cells were treated with 50 µg/ml of crude whelk GAGs or negative control (FCS media) for 24 and 48 hours and subsequently analysed by DAPI staining. Control cells incubated with media and without crude whelk GAGs showed no signs of apoptosis or oncosis and exhibited brightly fluorescing round, blue-stained nuclei (Figure 3.18A-B). In contrast, those cells treated with crude whelk GAGs for 24 and 48 hours showed a number of cells with condensed and fragmented nuclei, an indication of apoptosis (Figure 3.18A-B).

Trypsinisation, which is known to cause membrane damage, is one of the major steps involved in annexin V-FITC apoptosis detection assay. It may be responsible for some false annexin V-FITC positive staining observed in the untreated group. The above result obtained from DAPI stain confirms this hypothesis and shows clearly that the control group showed no induction of any apoptosis. This result also confirms that crude whelk GAG extracts induces apoptosis on MDA468 breast cancer cell. Therefore, the combined results of apoptosis detections by annexin V-FITC and DAPI stains suggest that the breast cancer cell death caused by crude whelk GAGs treatment was caused in part by apoptosis.

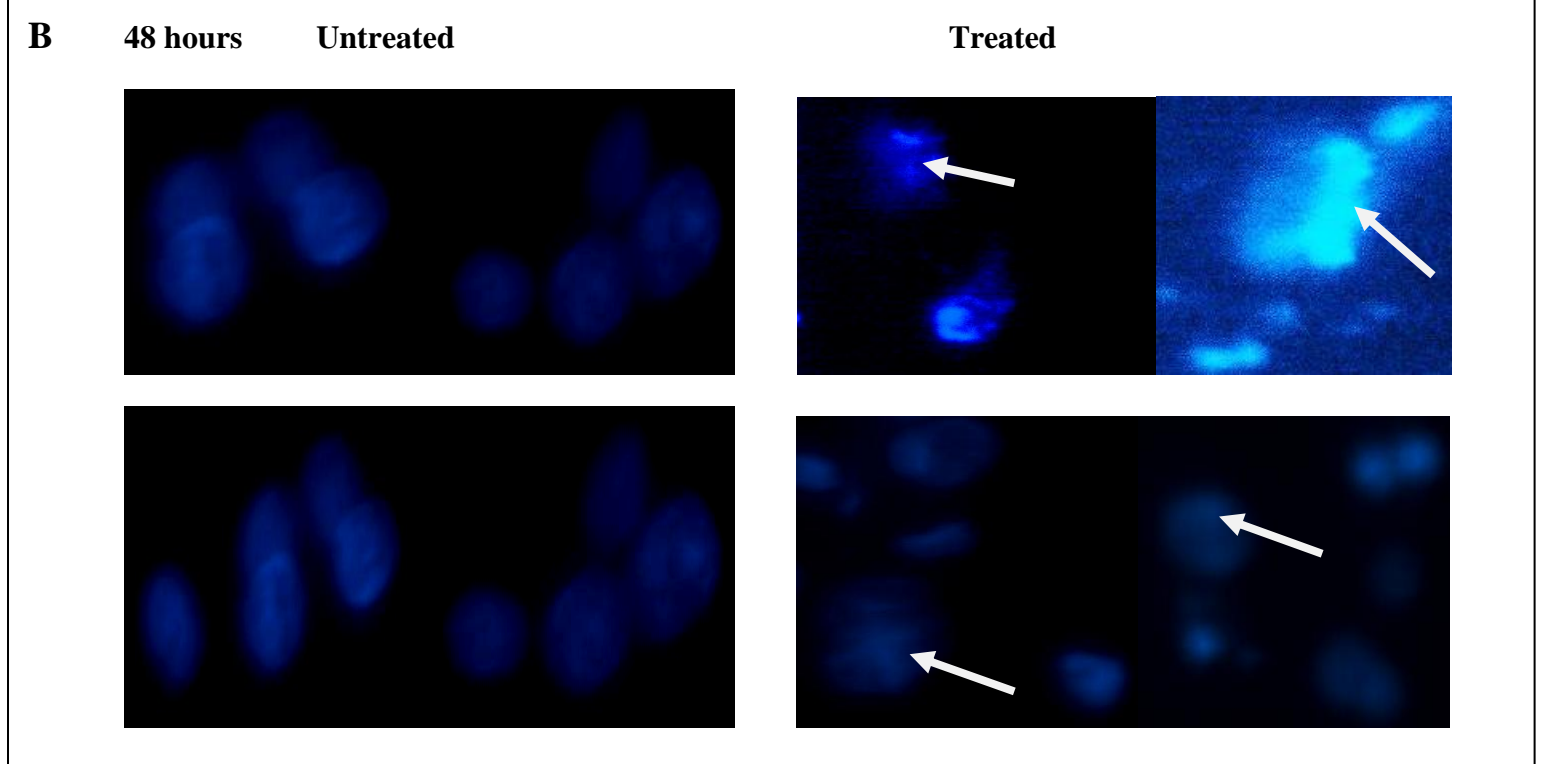
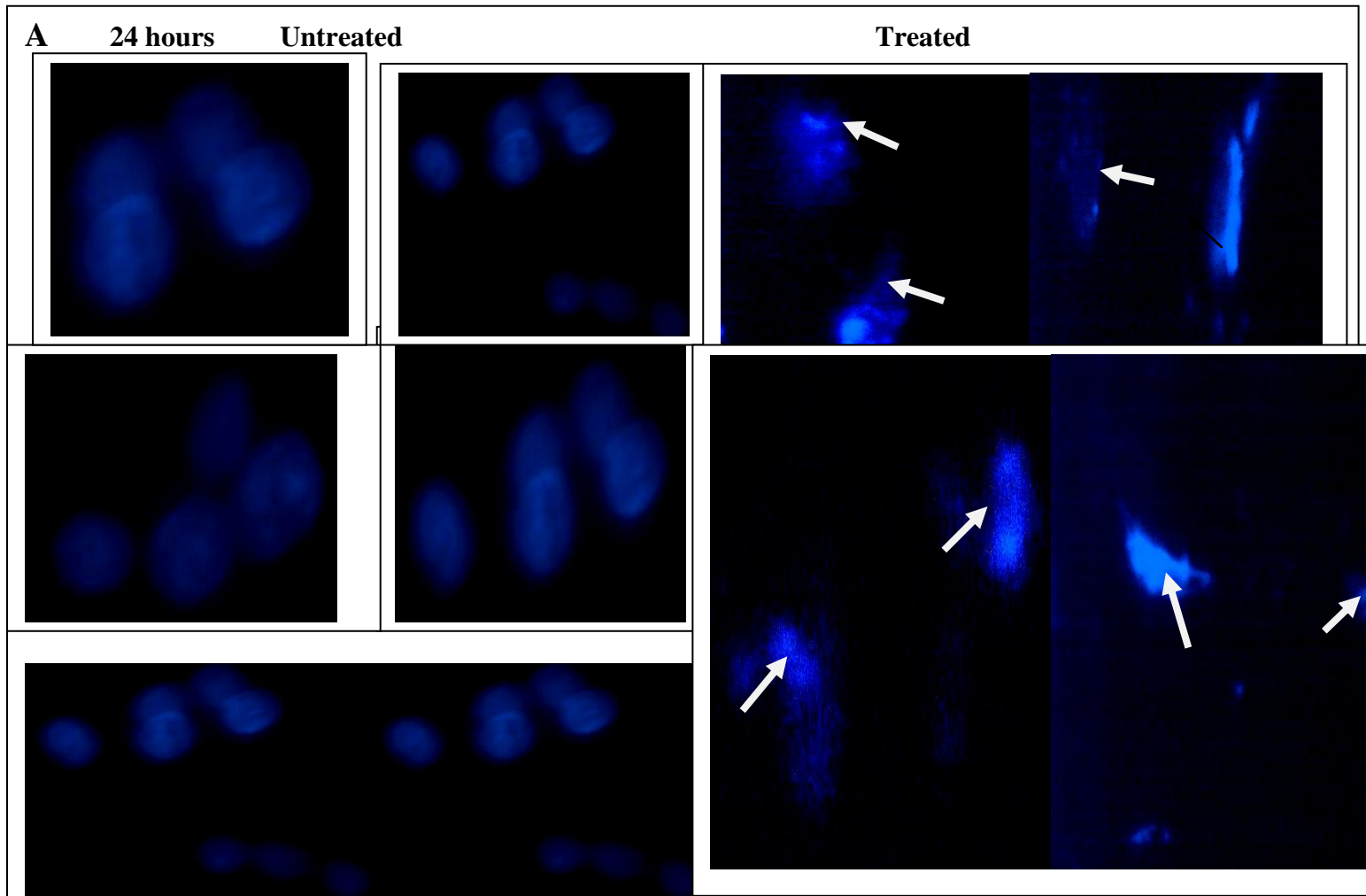


**Figure 3.18: Detection of apoptotic MDA468 cells by DAPI fluorescent microscopy following treatment with crude whelk GAG extracts.**

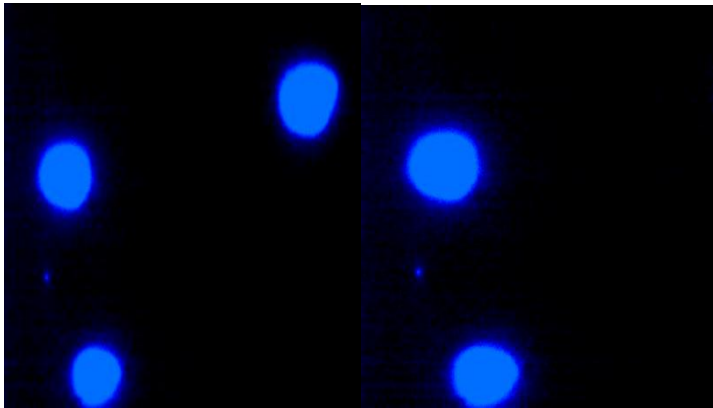
MDA468 cells treated with crude whelk GAGs were stained and morphology of apoptotic cell nuclei was observed by DAPI staining using a fluorescence microscope. Nuclei were stained with DAPI (blue). Images were photographed at the same exposure time under a x40 objective with Hamatsu 1394 ORCA-285 camera. (A) MDA468 cells treated with or without crude whelk for 24 hours. (B) MDA468 cells treated with or without crude whelk GAGs for 48 hours. Arrows represent the condensed or fragmented nuclei of cells.

**3.19 Assessment of apoptosis using DAPI fluorescent microscopy following treatment of MDANQ01 breast cancer cell with Crude whelk GAG**

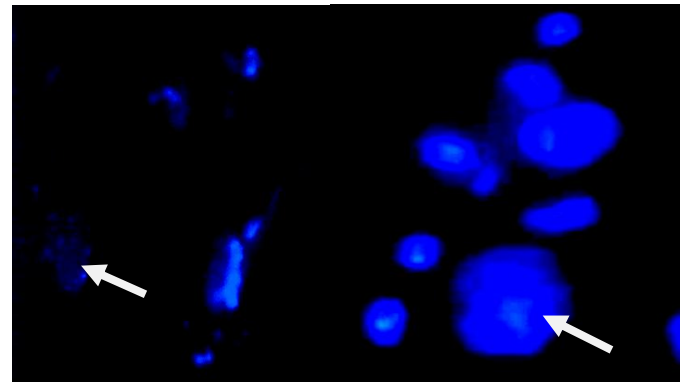
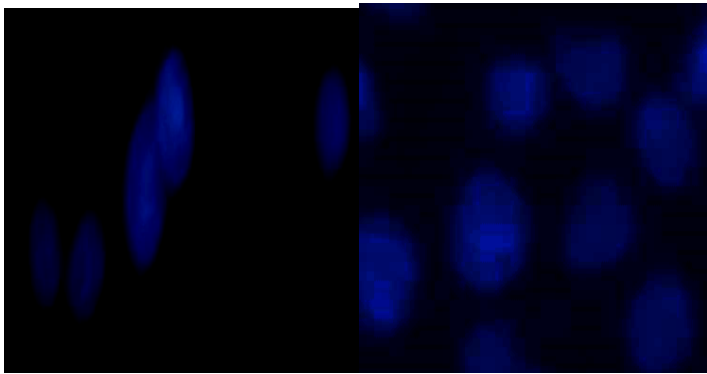
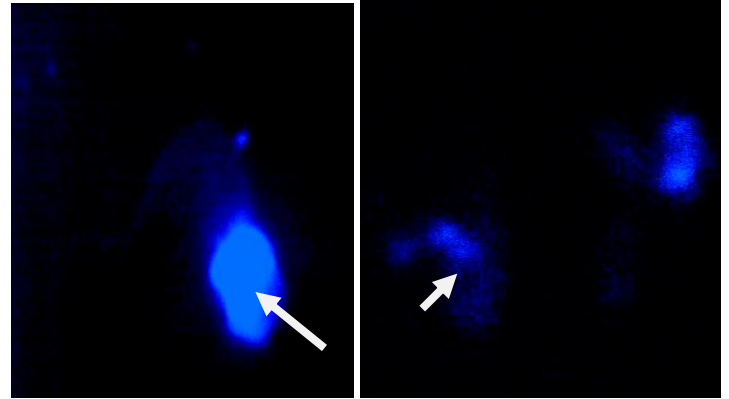
Similarly, to confirm whether the reduced cell growth observed in MDANQ01 cell line treated with crude whelk GAGs was due to apoptosis as revealed by annexin V-FITC apoptosis detection. MDANQ01 cells treated with or without 50µg/ml of crude whelk GAGs for 24 and 48 hours were stained with DAPI and cell morphology examined under fluorescent microscope. Control cells incubated with media without crude whelk GAGs showed no signs of apoptosis or oncosis and exhibited brightly fluorescing round, blue-stained nuclei (Figure 3.19A-B). However, the treated cells showed a numbers of cells with condensed and fragmented nuclei, an indicator of apoptosis (Figure 3.19A-B).

Furthermore, this result confirms that crude whelk GAG extracts induce apoptosis on MDANQ01 cells. Therefore, the combined results of apoptosis detections by annexin V-FITC and DAPI staining suggest that the anti-proliferative activity of the crude whelk GAGs on MDANQ01 breast cancer cells was partly due to apoptosis.

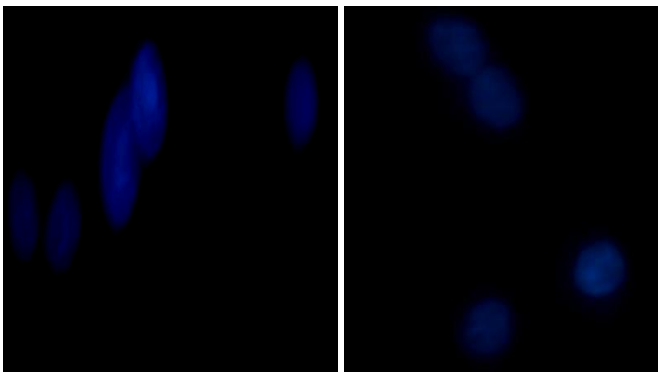
**A**    **24 hours**    **Untreated**



**Treated**



**48 hours**    **Untreated**



**Treated**

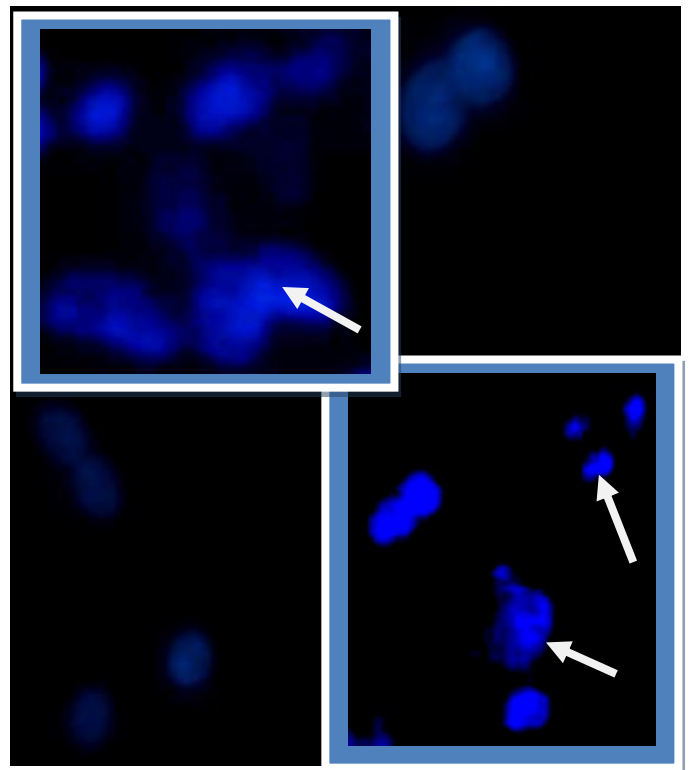


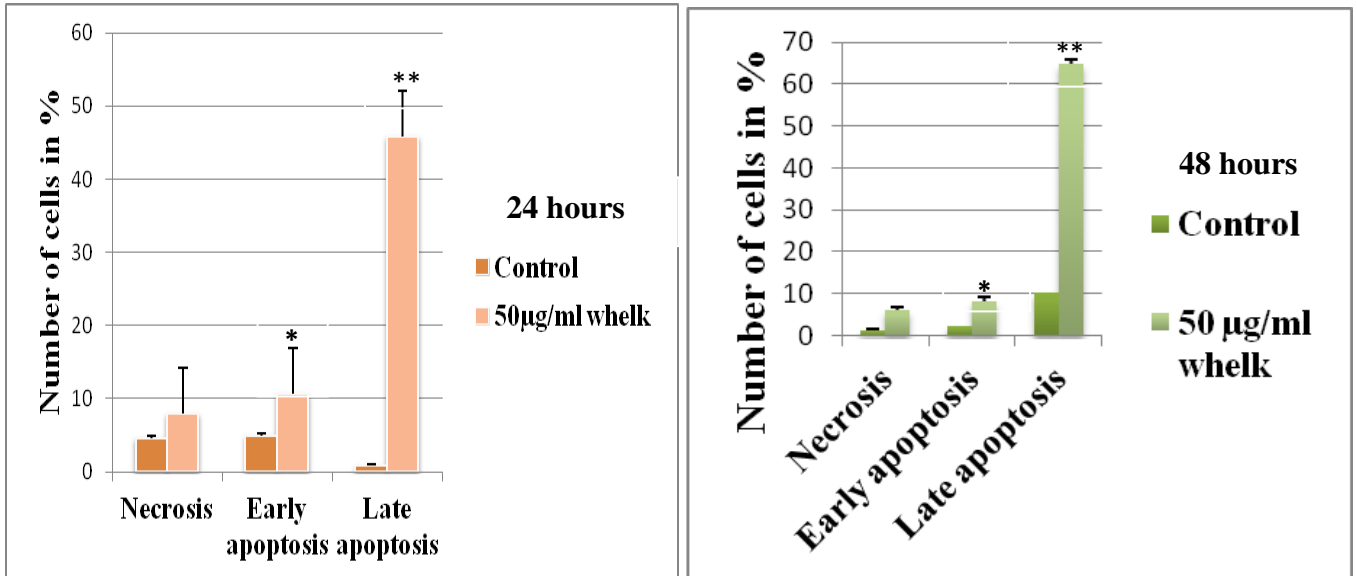
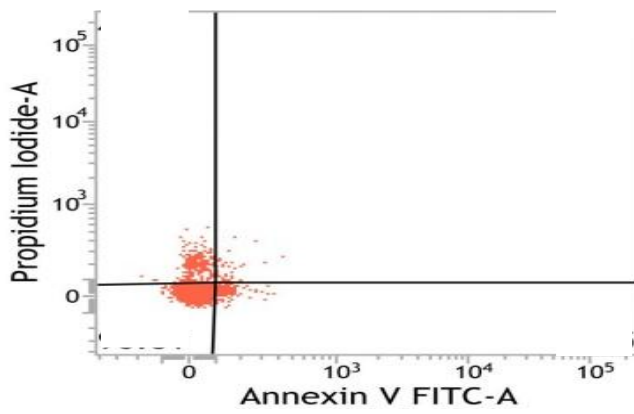
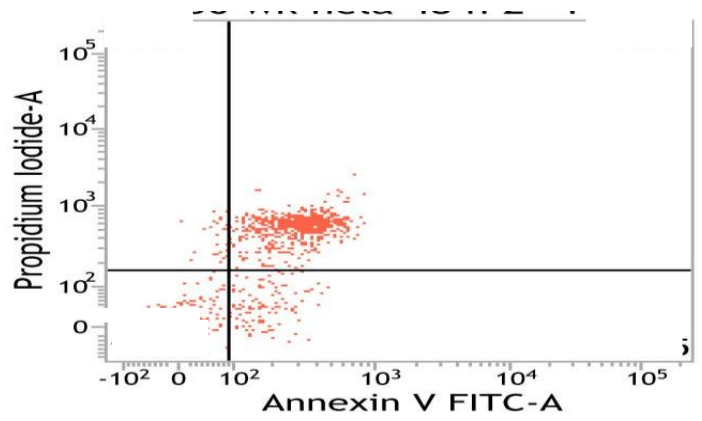
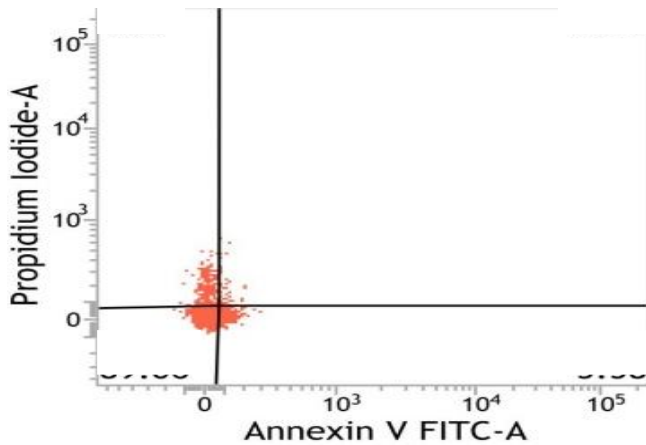
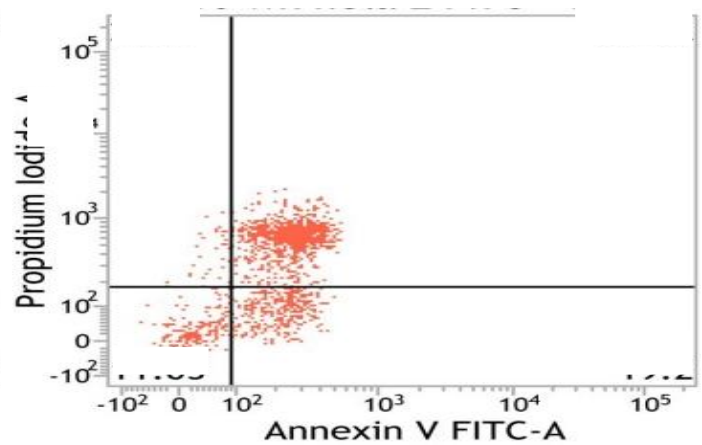
**Figure 3.19: Detection of apoptotic MDANQ01 cell treated with crude whelk GAG mixtures by DAPI fluorescent microscopy**

MDANQ01 cells treated with crude whelk GAGs were stained with DAPI and morphology of apoptotic cell nuclei was observed by DAPI staining using a fluorescence microscope. Nuclei were stained with DAPI (blue). Images were photographed at the same exposure time under a x40 objective with Hamatsu 1394 ORCA-285 camera. (A) MDANQ01 cells treated with or without crude whelk for 24 hours. (B) MDANQ01 cells treated with or without crude whelk GAGs for 48 hours. Arrows represent the condensed or fragmented nuclei of cells



### **3.20 Assessment of apoptosis using annexin V-FITC apoptosis detection following treatment of HeLa cells with crude whelk GAG extracts**

Preliminary studies reveal that crude whelk GAGs cause cell death in HeLa cells but the mechanism of this cell death is not yet known. This study was performed to elucidate the mechanism of cell death induced by crude whelk GAGs on HeLa ovarian cells using an Annexin V-FITC Apoptosis Detection Kit. HeLa cells are one of the most susceptible cells to apoptosis, as demonstrated and confirmed in this study. The apoptotic effects of whelk GAGs were more pronounced and better established with this cell line than that seen in either the leukaemia or breast cancer cell lines. 24-hour incubation of the crude whelk extracts with HeLa cells induce almost 50% apoptosis (late apoptosis) with an additional 10% early apoptosis detected and this difference was highly significant ( $p=0.000$ ) when compared with the corresponding values of the control. Moreover, a number of cell deaths were caused by necrosis, as illustrated in (Figure 3.20A-C). Additionally, 48-hour incubation of the crude whelk GAGs with HeLa cells also induced almost 70% late apoptosis and almost 10% early apoptosis, with a few cells ( $< 10\%$ ) affected by necrosis (Figure 3.20A-C). Small amounts of positive apoptosis and necrosis were observed in the untreated control cells. This was easily resolved by fluorescent microscopy and DAPI staining, which reveals no false positive for either necrosis or apoptosis detection in the untreated cells.

**A****Apoptosis induced by whelk GAG treatment on HeLa cervical cell line****B****24 hours****Untreated****Treated****C****48 hours****Untreated****Treated**

**Figure 3.20: Detection of Apoptosis in HeLa cells by Annexin V Staining following treatment with whelk GAG extracts.**

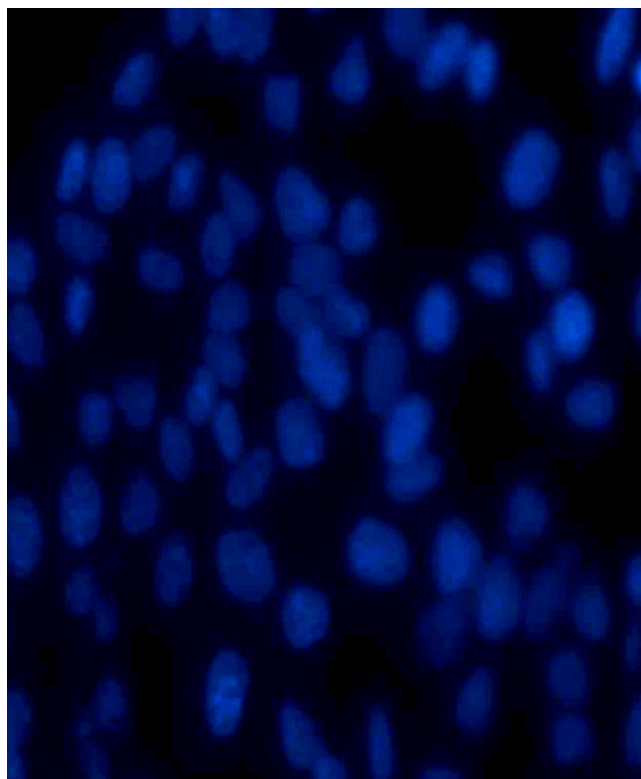
HeLa cells were treated with crude whelk GAGs for 24 and 48 hours and then stained using Annexin V-FITC and PI provided in the Annexin V-FITC Apoptosis Detection Kit. The combination of Annexin V-FITC and PI allows for the distinction between early apoptotic cells (annexin V-FITC positive), late apoptotic and/or necrotic cells (Annexin V-FITC and PI positive), necrotic (PI stained positive) and viable cells (unstained). (A) HeLa cell treated with or without crude whelk GAGs for 24 and 48 hours respectively. (B) HeLa cell treated with or without crude whelk GAGs for 24 hours. (C) HeLa cells treated with or without crude whelk GAGs for 48 hours

Abbreviations: \*-Significant ( $p \leq 0.05$ )

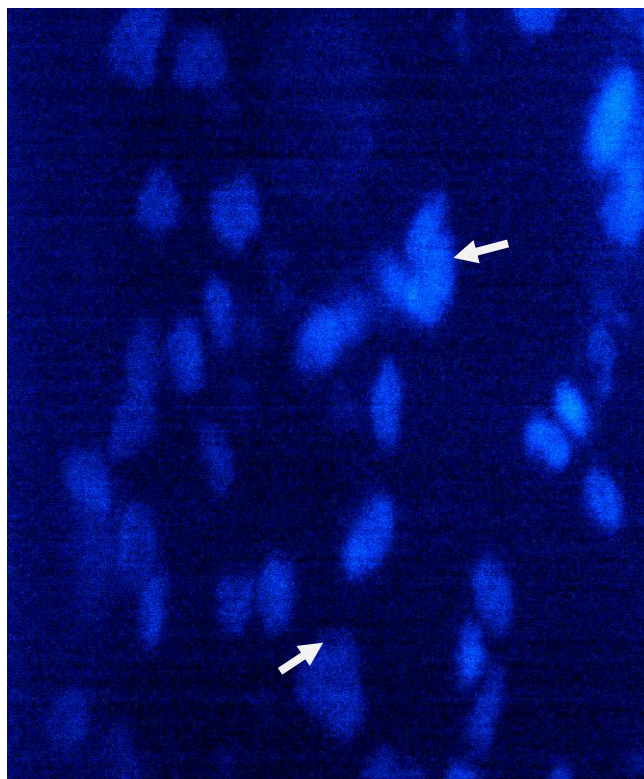
**3.21 Assessment of apoptosis using DAPI fluorescent microscopy following treatment of HeLa cells with whelk GAGs**

Apoptotic effects of crude whelk GAGs on HeLa cervical cells were confirmed as follows: Cells treated with 50 $\mu$ g/ml of crude whelk GAGs or negative control (FCS media) for 24 and 48 hours were stained with DAPI and viewed under fluorescent microscope. Control cells incubated in ordinary FCS media without crude whelk GAGs exhibited no signs of apoptosis and exhibited brightly fluorescing round, blue-stained nuclei (Figure 3.21A-B). In contrast, cells treated with whelk GAG extracts showed a number of cells with condensed and fragmented nuclei; a clear indication of apoptosis induction (Figure 3.21A-B). This result confirms that whelk GAG extracts induce apoptosis with the HeLa cells. Both the DAPI and annexin V-FITC results suggest that cell growth inhibitory activity of whelk GAGs on HeLa cells was due in part to apoptosis.

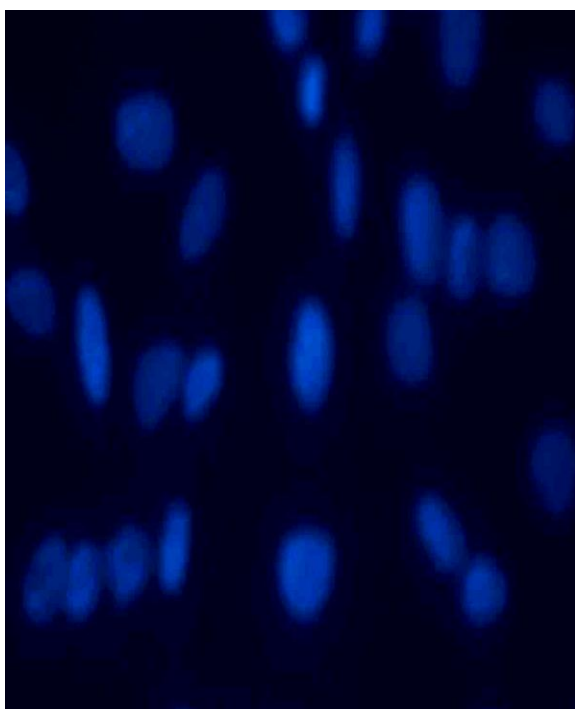
**A** 24 hours Untreated



**Treated**



**B** 48 hours Untreated



**Treated**

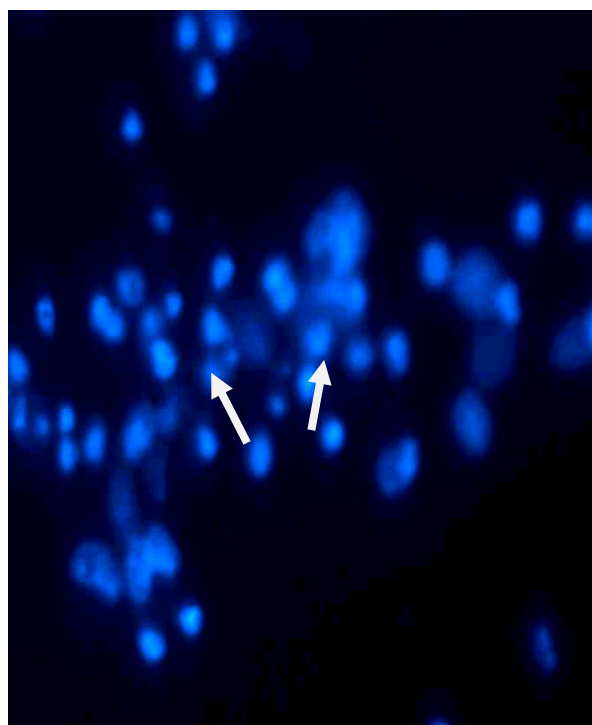


**Figure 3.21: Detection of apoptotic HeLa cells by DAPI fluorescent microscopy following treatment with whelk GAG**

HeLa cells, treated with crude whelk GAGs, were stained with DAPI and the morphology of apoptotic cell nuclei was observed by DAPI staining using a fluorescence microscope. Nuclei were stained with DAPI (blue). Images were photographed at the same exposure time under a x40 objective with Hamatsu 1394 ORCA-285 camera. (A) HeLa cells treated with or without crude whelk for 24 hours. (B) HeLa cells treated with or without crude whelk GAGs for 48 hours. Arrows represent the condensed or fragmented nuclei of cells.

### **3.22 Fractionation of whelk GAG extracts by ion-exchange chromatography**

Crude whelk GAG extracts were next subjected to ion-exchange chromatography in order to identify the biologically active component. Ion-exchange chromatography is used routinely to separate GAG mixtures into their respective GAG family members; for example, HS, CS and DS. Six major peaks were identified, when the whelk GAG extracts were subjected to ion-exchange separation; each peak was believed to contain different GAGs family members (Figure 3.22). Peaks were designated, A-F, in order of increased elution time (table 1). In some preparations fraction D was absent; however, the remainders of the fractions were consistently present. When assayed in the MTT assay against both breast cancer cell lines, only a single fraction (E) had any significant anti-proliferative effect (Figure 3.23)

### Fractionation of whelk GAG by anion exchange chromatography

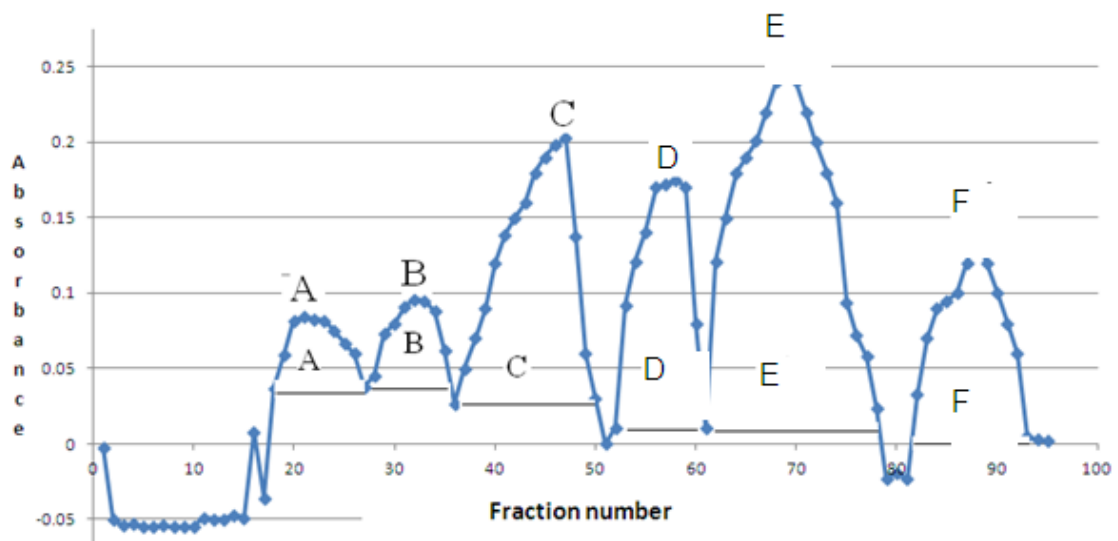


**Figure 3.22: Ion-exchange chromatography elution profile for whelk GAG extracts.**

Samples were applied to a DEAE-Sephadex ion-exchange column and resolved using a linear 0-3 M NaCl gradient in 50mM sodium phosphate buffer pH 7.0 at a flow rate of 1ml/min for 100 min. Fractions were collected and the absorbance monitored at a wavelength of 254nm. Fractions were pooled as indicated, desalted and lyophilised before further analysis.

**Table 2: Ion-exchange chromatographic separation of whelk GAG extracts**

<b>Fraction name</b>	<b>Fraction number</b>	<b>GAGs type</b>	<b>Percentage yield (%)</b>	<b>Elution time (minutes)</b>	<b>NaCl gradient (M)</b>
<b>A</b>	<b>27-37</b>	<b>HS-like</b>	<b>19.90</b>	<b>27-37</b>	<b>0.9-1.24</b>
<b>B</b>	<b>39-47</b>	<b>CS/DS-like</b>	<b>13.50</b>	<b>39-47</b>	<b>1.26-1.62</b>
<b>C</b>	<b>49-62</b>	<b>CS/DS-like</b>	<b>18.00</b>	<b>49-62</b>	<b>1.63-2.1</b>
<b>D</b>	<b>65-73</b>	<b>Unknown</b>	<b>16.00</b>	<b>65-73</b>	<b>2.14-2.5</b>
<b>E</b>	<b>75-88</b>	<b>HS-like</b>	<b>23.30</b>	<b>75-88</b>	<b>2.56-2.9</b>
<b>F</b>	<b>89-94</b>	<b>Unknown</b>	<b>9.30</b>	<b>89-94</b>	<b>2.91-3.0</b>

Samples were applied to a DEAE-Sephadex ion-exchange column and resolved by a linear 0-3 M NaCl gradient in 50mM sodium phosphate buffer pH 7.0 at a flow rate of 1ml/min for 100 min. Fractions were collected and the absorbance monitored at wavelengths of 254nm. Fractions were pooled as indicated, desalted and lyophilized before further analysis.



**Table 3: Summary of biological effects of whelk GAGs**

	<b>MDA468 breast cancer cell line</b>	<b>MDANQ0 1 breast cancer cell line</b>	<b>K562 erythrocyti c leukemia cell line</b>	<b>MOLT-4 leukemia cell line</b>	<b>HeLa cervical cell line</b>	<b>3T3 normal fibrobla st cell line</b>
<b>Proliferati ve assay</b>	<b>Inhibited cell growth</b>	<b>Inhibited cell growth</b>	<b>Inhibited cell growth</b>	<b>Inhibited cell growth</b>	<b>Inhibited cell growth</b>	<b>Suppor ted cell growth</b>
<b>IC<sub>50</sub></b>	<b>70.94µg/ml</b>	<b>25.14µg/ml</b>	<b>14µg/ml</b>	<b>41.11µg/ ml</b>	<b>12µg/ml</b>	<b>-</b>
<b>Cell cycle arrest</b>	<b>Induced cell cycle arrest at both S and G2/M phase</b>	<b>Induced cell cycle arrest at both S and G2/M phase</b>	<b>-</b>	<b>-</b>	<b>-</b>	<b>-</b>
<b>Apoptosis detection assay</b>	<b>Induced late apoptosis</b>	<b>Induced late apoptosis</b>	<b>-</b>	<b>-</b>	<b>Induced late apoptosis</b>	<b>-</b>

Note: Also included in this section was proliferative effect of depolymerised whelk GAG on both MDA468 and MDANQ01 breast cancer cell lines.

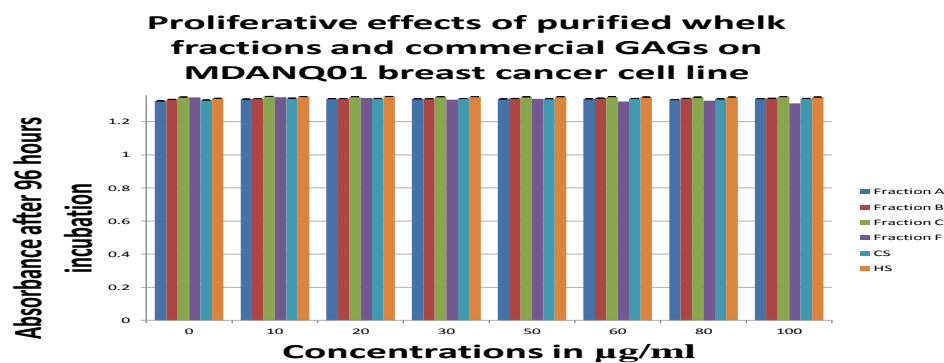
## **Section 3C**

# **Biological activities of purified whelk fraction E**

### **3.23 Effect of purified whelk fraction E on the growth of MDANQ01 breast cancer cells**

Fraction E samples showed significant ( $p < 0.05$ ) growth inhibitory effects on MDANQ01 breast cancer cells proliferation (Figure 3.23A) after 96 hours incubation as described under materials and methods section. The growth inhibitory effects of fraction E on MDANQ01 was similar to that observed for crude whelk GAGs extracts but the recorded  $IC_{50}$  (41.89  $\mu\text{g/ml}$ ) was higher than what was recorded for crude whelk GAGs (25.14  $\mu\text{g/ml}$ ). However, the growth inhibitory effect of fraction E was more pronounced with higher concentrations (50-100  $\mu\text{g/ml}$ ) than the lower concentrations (10-30  $\mu\text{g/ml}$ ).

In addition to the above result, other purified whelk fractions (A,B,C,& F) and commercial GAGs were also tested along with fraction E. Interestingly none of them showed any growth inhibitory effect on MDANQ01 breast cancer cells proliferation (Figure 3.23B)



**B**

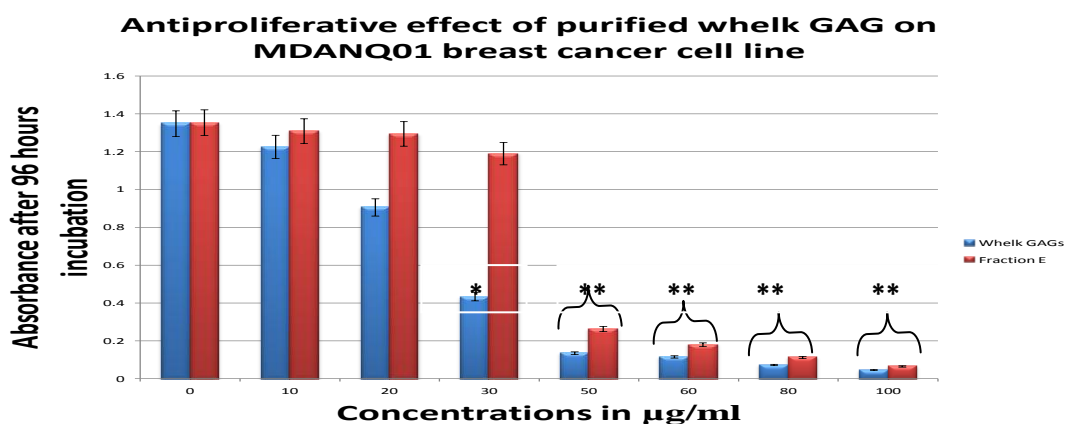


**Figure 3.23: MTT cell viability assay for MDANQ01 breast cancer cells after treatment with GAG mixtures and purified whelk fraction E.**

Cells were incubated with various concentrations of GAGs for 96 hours after which time cell viability was measured using an MTT assay (A) MDANQ01 breast cancer cell line treated with crude whelk's purified fractions and commercial GAGs (B) MDANQ01 breast cancer cells treated with fraction E and crude whelk GAGs. Each value is presented as the mean SEM of three independent determinations. The bars in each chart are presented as relative values in comparison to untreated cells.

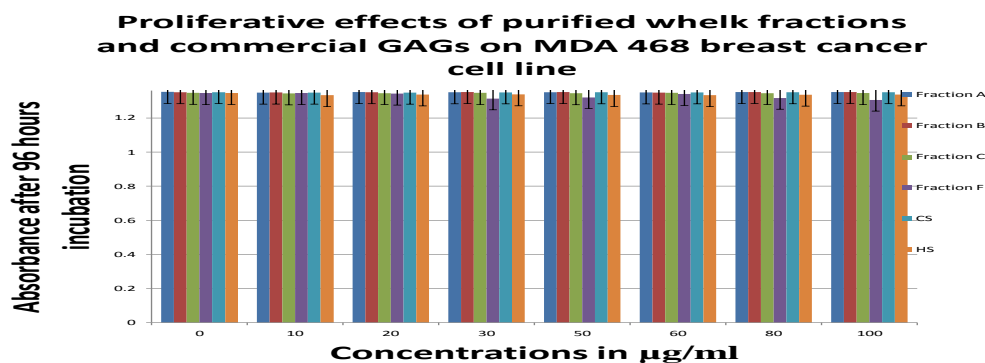
Abbreviations: \*-Significant ( $p \leq 0.05$ ): \*\*-Highly significant

### **3.24 Effect of purified whelk fraction E on MDA468 breast cancer cell proliferation**

Fractions E also showed dose-dependent growth inhibitory effects on MDA468 breast cancer cell line (Figure 3.24A) after 96 hours treatment (see materials and methods section). Its growth inhibitory effect on MDA468 compares favourably to the effect of the crude whelk GAG extracts with a lower recorded  $IC_{50}$  of 45.98 $\mu$ g/ml against an  $IC_{50}$  of 70.96  $\mu$ g/ml recorded for crude whelk GAGs. Similarly, higher concentrations (50-100  $\mu$ g/ml) of fraction E show more effective growth inhibitory activity against MDA468 than their lower concentrations (10-30  $\mu$ g/ml) counterpart (Figure 3.24A).

However, other purified whelk fractions (A, B, C & F) and commercial GAGs did not reveal any growth inhibitory activity against MDA468 cells (Figure 3.24B)

A



B

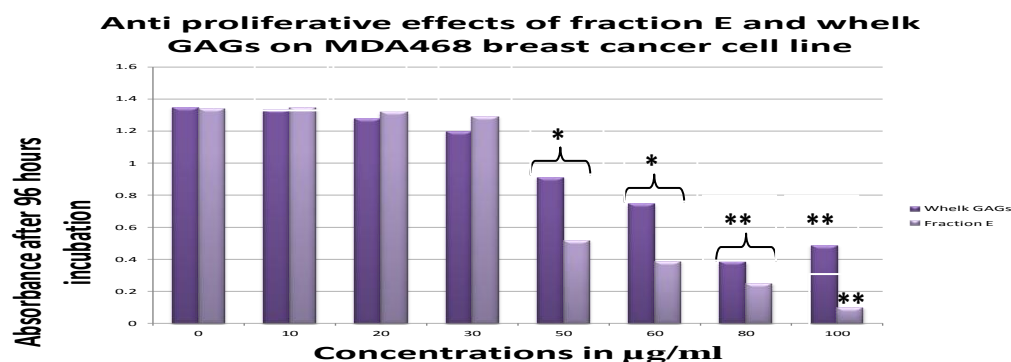


**Figure 3.24: Concentration-dependent effect of purified whelk GAG fraction E on MDA468 breast cancer cell viability.**

Cells were incubated with various concentrations of cockle GAGs for 96 hours after which time cell viability was measured using an MTT assay (A) Cells treated with commercial GAGs and whelk’s purified fractions (B) Cells treated with fraction E and crude whelk GAG extracts. Each value is presented as the mean SEM of three independent determinations. The bars in each chart are presented as relative values in comparison to untreated cells.

Abbreviations: \*\*- Highly significant ( $p \leq 0.01$ )

### **3.25 Cell cycle analysis of the MDANQ01 breast cancer cell line after treatment with purified whelk fraction E**

Whelk fraction E induced cell cycle arrest on MDANQ01 cells at both S and G2/M phases as shown in Figure 3.25A-C. It caused significant accumulations of cells at S and G2/M phases, leading to the subsequent reduction in the overall number of cells in G1 phase. After 48 hours treatment with 50µg/ml whelk fraction E, the percentage of cell population at S-phase increased from 20.48 % (control) to 25.06 % (50 µg/ml fraction E). At 72 hours, the cell population at G2/M-phase increased from 21.27 % (control) to 38.46 % (Figure 3.25A-C)

This result suggests that purified fraction E partly elicits its anti-proliferative activity on MDANQ01 breast cancer cells by inducing cell cycle arrest at S and G2/M-phase.

Cell cycle arrest caused by fraction E treatment on MDANQ01 breast cancer cell line

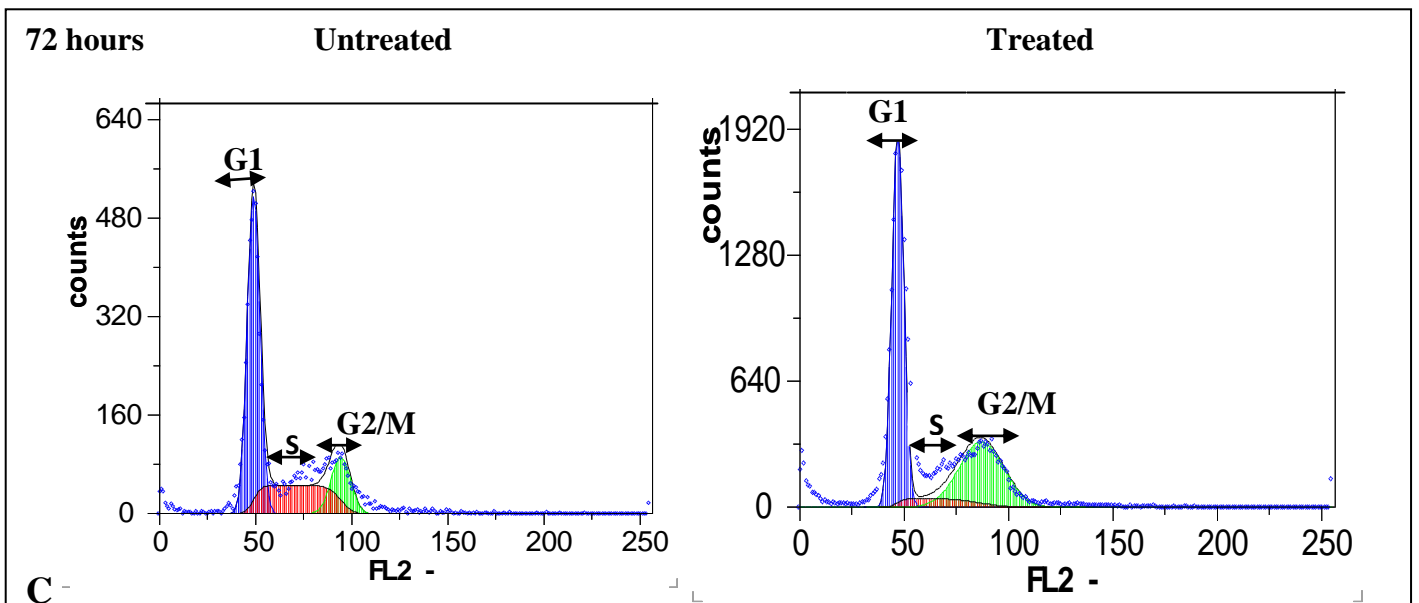
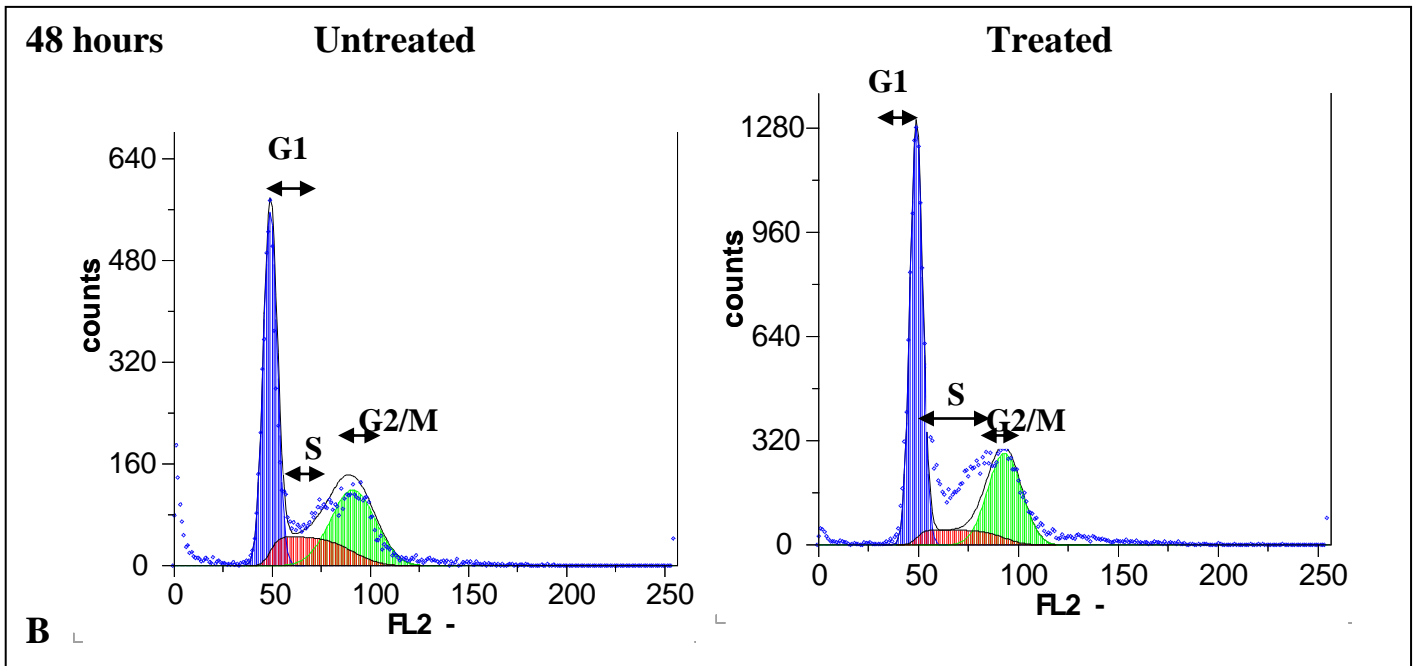
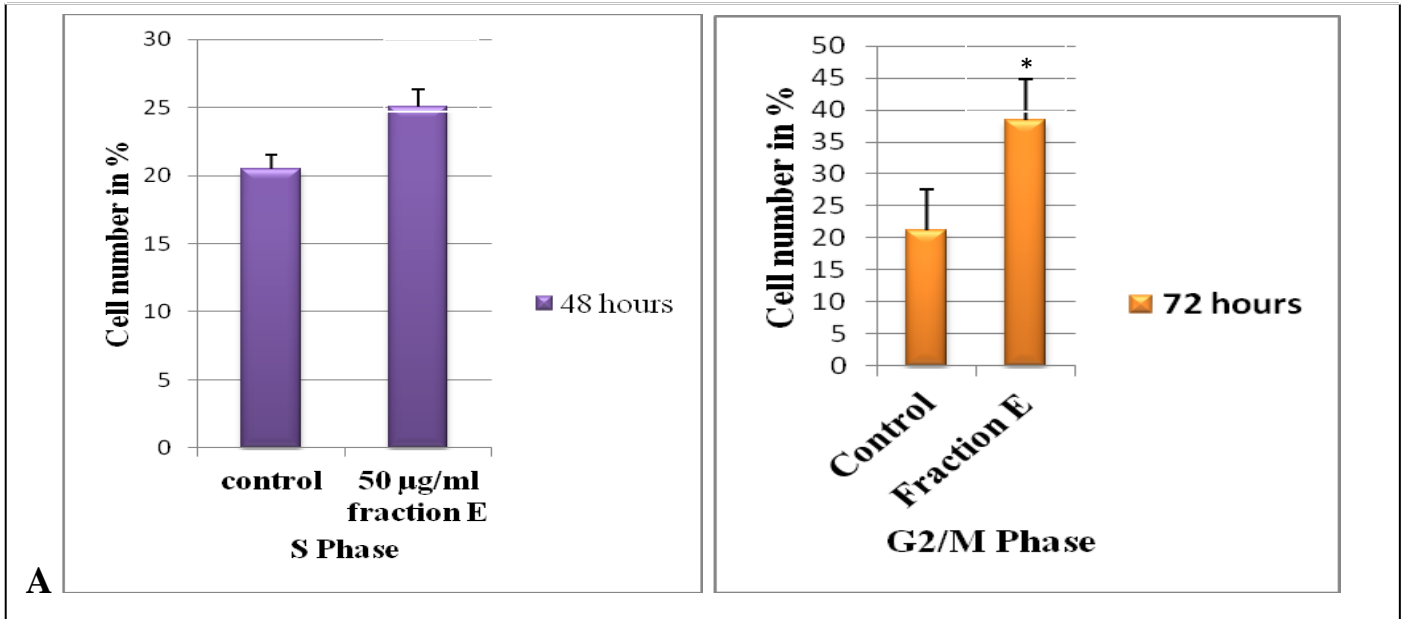




**Figure 3.25: Cell cycle analysis of MDANQ01 breast cancer cell line following treatment with purified whelk fraction E.**

MDANQ01 breast cancer cells were stained with PI stain and subjected to cell cycle analysis by flow cytometry (A). Charts showed averages of three independent experiments after treatment with or without purified whelk fraction E (B) Flow cytometry of MDANQ01 breast cancer cells after 48 hours incubation with or without purified whelk fraction E and (C) Flow cytometry of MDANQ01 breast cancer cells after 72 hours incubation with or without purified whelk fraction E.

Abbreviations: \*- Significant ( $p \leq 0.05$ )

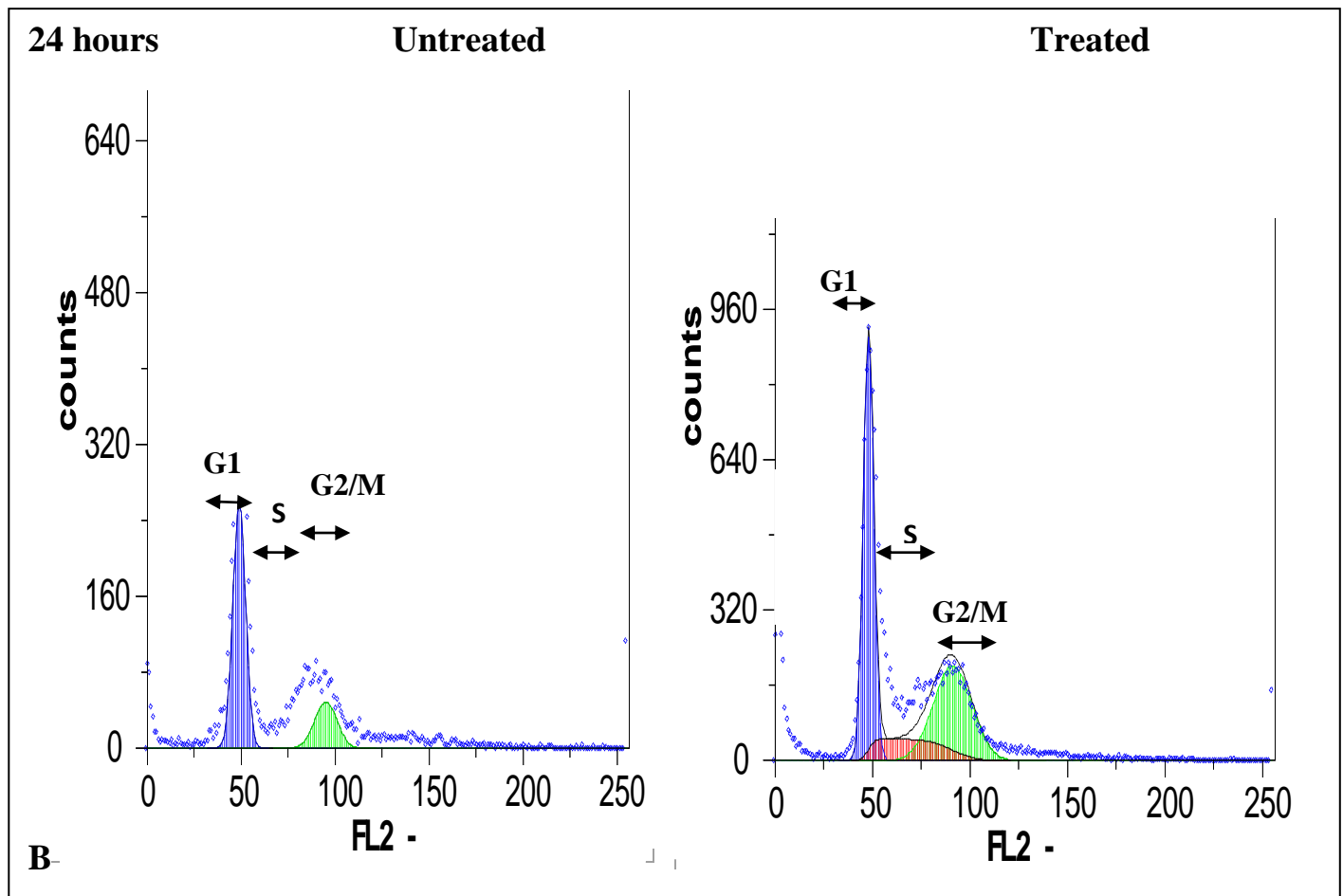
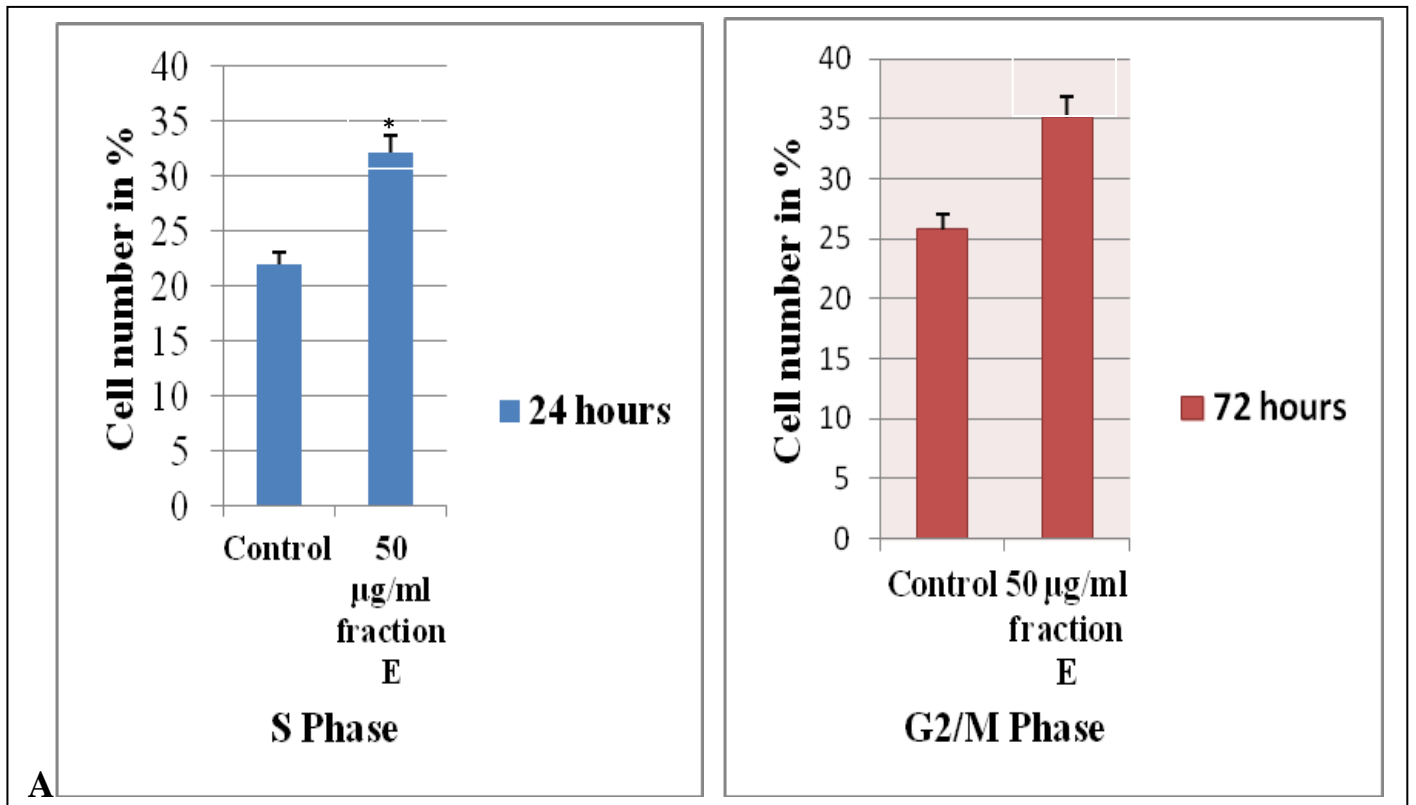
**3.26 Cell cycle analysis of the MDA468 cell line after treatment with Purified whelk fraction E**

Cells exposed to 50ug/ml whelks fraction E showed perturbation of MDA468 cell's cycle after 24-72 hours exposure to the purified extract.

Whelk fraction E induced mild cell cycle arrest of MDA468 cells at both S and G2/M phases as shown in Figure 3.26A-C. After 24 hours treatment with 50µg/ml whelk fraction E, MDA468 cells population at S-phase increased from 21.94% (control) to 29.19% (50 µg/ml fraction E). 72 hours incubation of the cell with purified fraction E also increased the cell population at G2/M from 25.75% (control) to 35.75% (50 µg/ml fraction E). However, 48-hour incubation of the purified fraction E with MDA468 cell did not have any effect on the cell cycle.

The purified fraction E showed consistent DNA disruptive effect on both breast cancer cell lines and these results suggest that the purified fraction E induces growth inhibitory effect on the MDA468 and MDANQ01 breast cancer cells via cells cycle arrest at S and G2/M-phase.

Cell cycle arrest caused by fraction E treatment on MDA468 breast cancer cell line



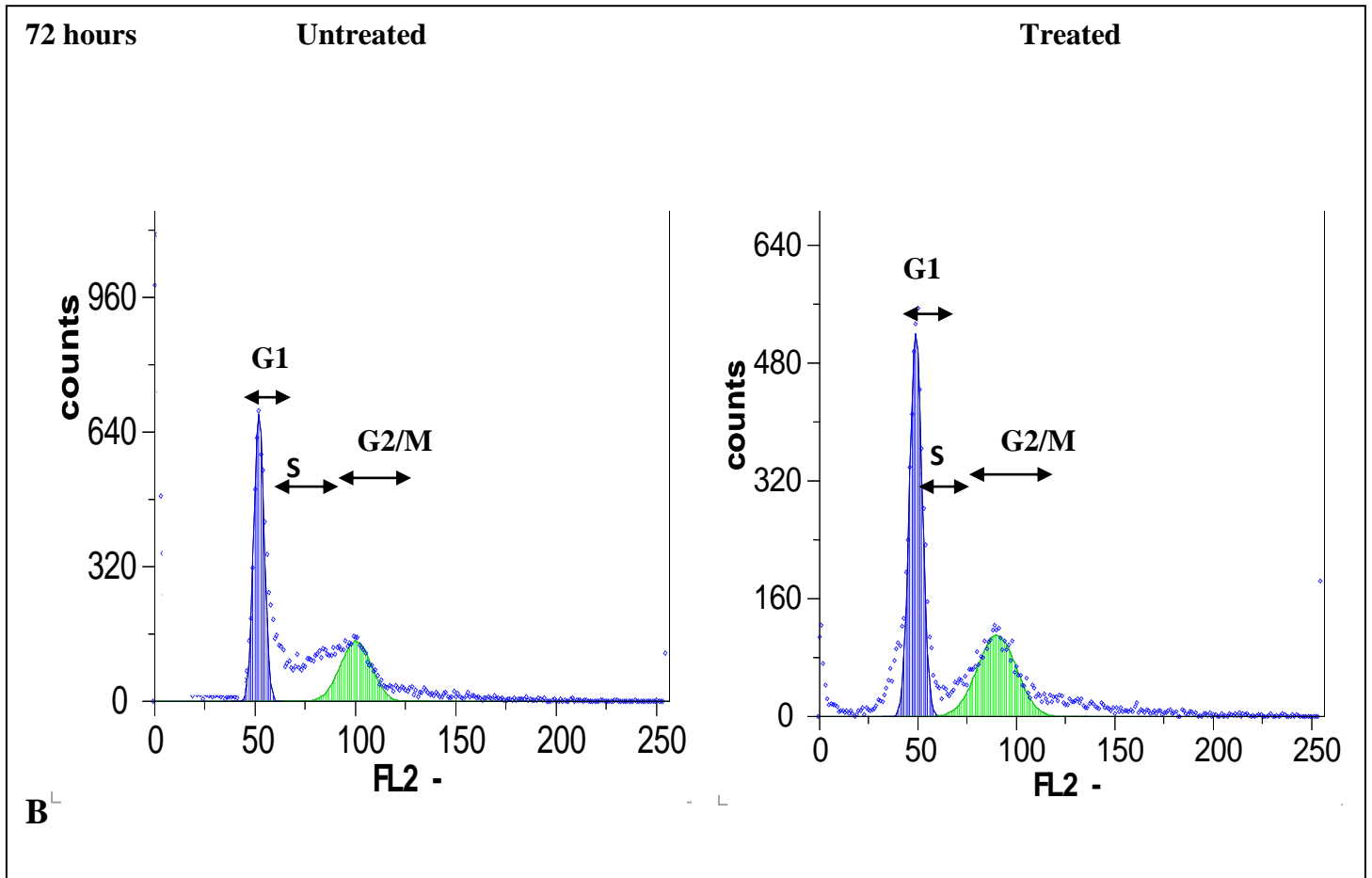


**Figure 3.26: Cell cycle analysis of MDA468 breast cancer cell line following treatment with purified whelk fraction E.**

MDA468 breast cancer cells were stained with PI stain and subjected to cell cycle analysis by flow cytometry (A). Charts showed averages of three independent experiments after treatment with or without purified whelk fraction E (B) Flow cytometry of MDANQ01 breast cancer cells after 24 hours incubation with or without purified whelk fraction E and (C) Flow cytometry of MDANQ01 breast cancer cells after 72 hours incubation with or without purified whelk fraction E.

Abbreviations: \*- Significant ( $p \leq 0.05$ )

### **3.27 Purified whelk fraction E induces mild apoptosis and necrosis on MDANQ01 breast cancer cells (revised Annexin V-FITC apoptosis detection assay results).**

High concentration (100 $\mu$ g/ml) of purified whelk fraction E induces mild apoptosis and necrosis on MDANQ01 cell (Figure 3.28 (A-B). 24-hour incubation of the purified fraction with the cells increased the number of cells stained with Annexin V-FITC from 1.02 % (control) to 2.01 % (100 $\mu$ g/ml). The number of cells stained with both Annexin V-FITC and PI also increased from 7.07 % (control) to 9.3 % (100 $\mu$ g/ml). In addition, this extract induces mild necrosis on MDANQ01 cells: the cell stained with PI increased from 6.47 % (control) to 7.56 % (100 $\mu$ g/ml).

However, lower concentration (20-50 $\mu$ g/ml) of the purified fraction did not yield any apoptotic effect on this cell line: both 8 and 72-hour incubations of the cells with the purified fraction did not exhibit any noticeable apoptotic effect on MDANQ01 cell line (results not shown).

**Apoptosis induced by fraction E treatment on MDANQ01 breast cancer cell line**

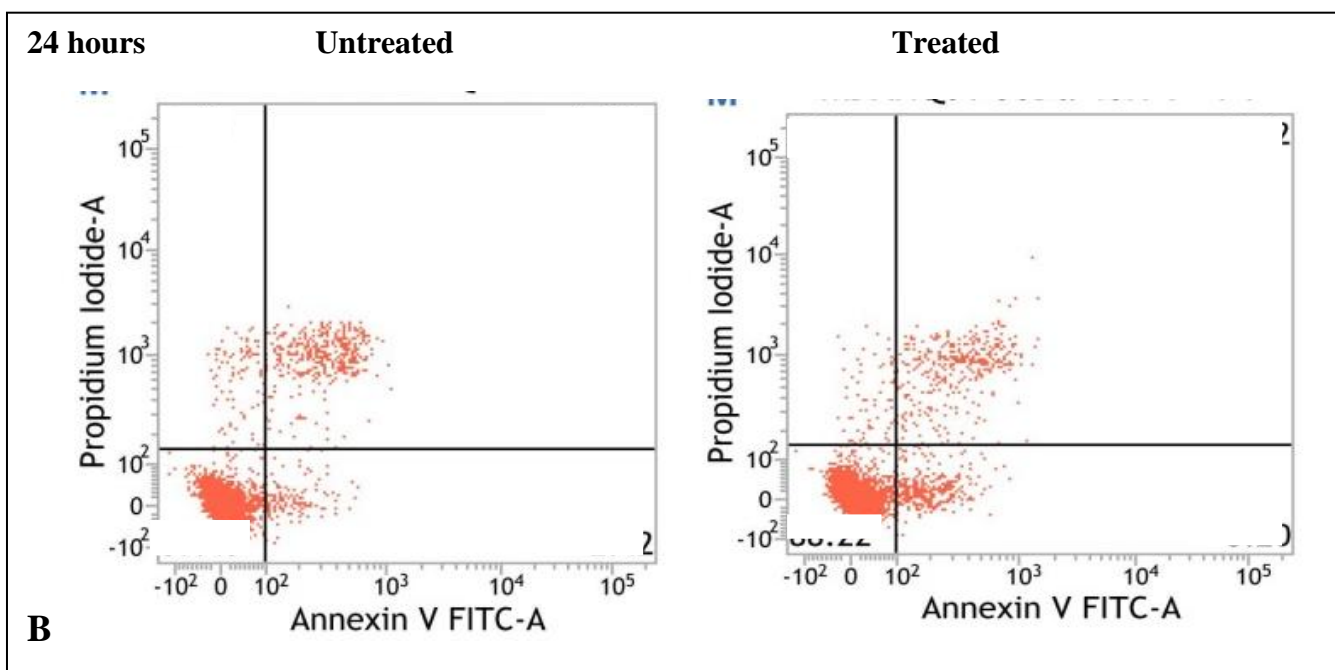
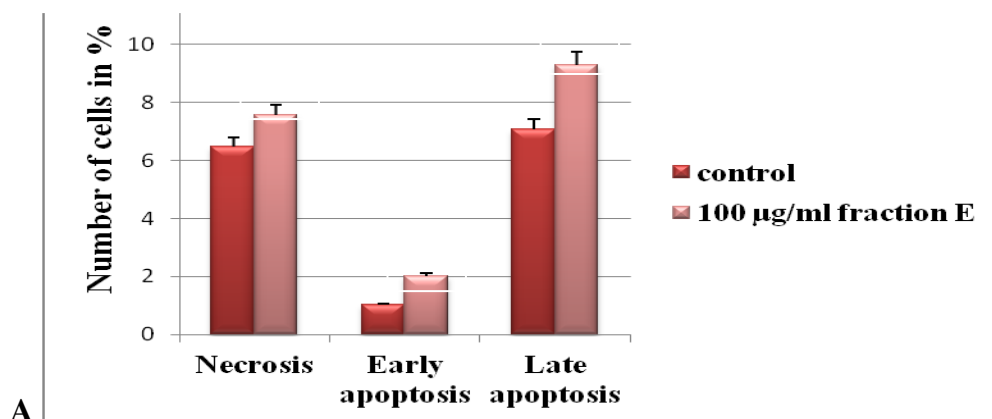


**Figure 3.27: Detection of Apoptotic MDANQ01 breast cancer cells treated with purified whelk fraction E by Annexin V Staining.**

MDANQ01 cells were treated with purified whelk fraction E for 24 hours and then stained using Annexin V-FITC and PI provided in the Annexin V-FITC Apoptosis Detection Kit (see materials and methods). The combination of Annexin V-FITC and PI allows for the distinction between early apoptotic cells (annexin V-FITC positive), late apoptotic and/or necrotic cells (Annexin V-FITC and PI positive), necrotic (PI stained positive) and viable cells (unstained). (A) MDANQ01 cell treated with or without purified whelk fraction E 24 hours. (B) Flow cytometry of MDANQ01 treated with or without purified whelk fraction E for 24 hours.

### **3.28 Annexin V-FITC apoptosis assay of the MDA468 breast cancer cell line following treatment with purified whelk fraction E**

Purified fraction E induces time-dependent apoptosis on MDA468 cells (Figure 3.28A-C). 24 hours incubations of purified fraction E with the cells increased the number of cells stained with both Annexin V-FITC and PI from 16.48 % (control) to 20.96 % (50 $\mu$ g/ml). Similarly, 48-hour incubations of the purified fraction E also induce late apoptosis on MDANQ01 cells but the apoptotic effect was more pronounced than that observed at 24 hours. At 48 hours, the number of cells stained with Annexin V-FITC and PI increased from 8.2 % (control) to 14.16 % (50 $\mu$ g/ml). In addition to the apoptotic effect of the purified fraction on MDA468 cells, there was also an increase in the number of cells stained with PI; an indication of necrosis. At 48 hours, the number of cells stained with PI increased from 4.0 % (control) to 7.4 % (50 $\mu$ g/ml).

However, other concentrations (20 and 100 $\mu$ g/ml) of the purified fraction did not show any apoptotic effect on this cell line: both 8 and 72-hour incubations of the cells with the crude extract did not show any noticeable apoptotic effect on the MDA468 cell line (results not shown) presumable due to the extent of cell death seen in the higher doses.

The observed apoptotic and necrotic effect of the purified fraction E on both breast cancer cells suggest the possible growth inhibition of these cells proliferation was caused by apoptosis and oncosis.

Apoptosis induced by fraction E treatment on MDA468 breast cancer cell line

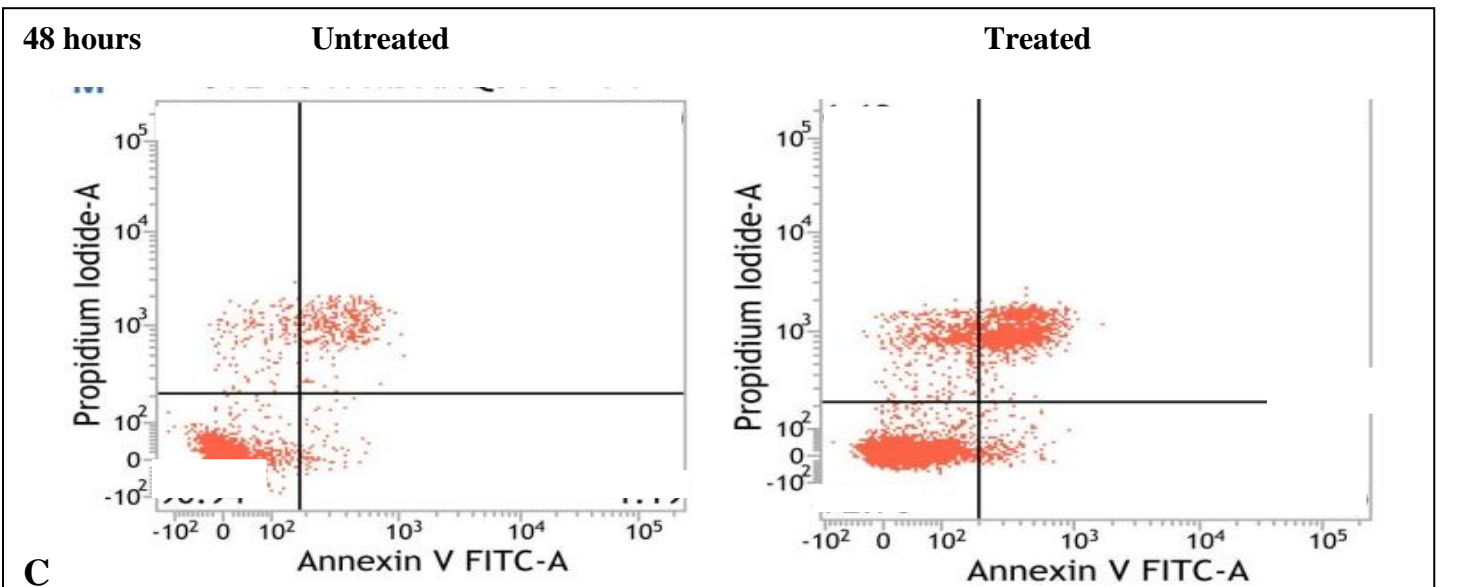
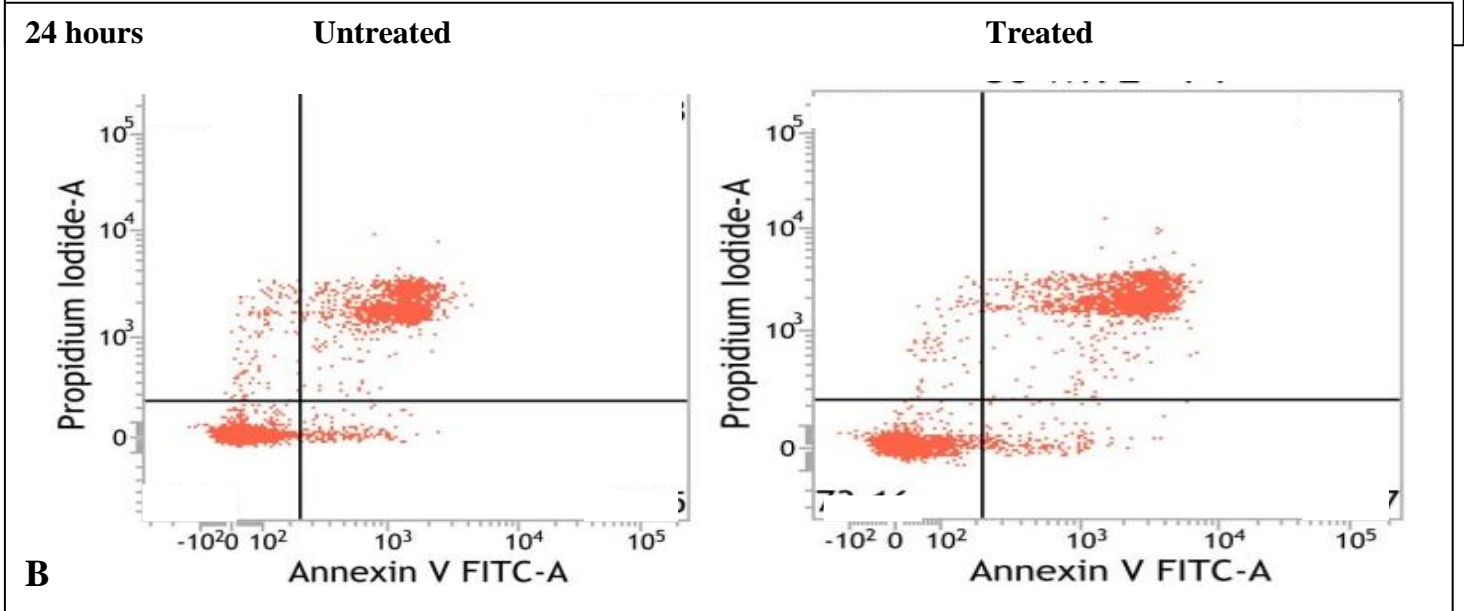
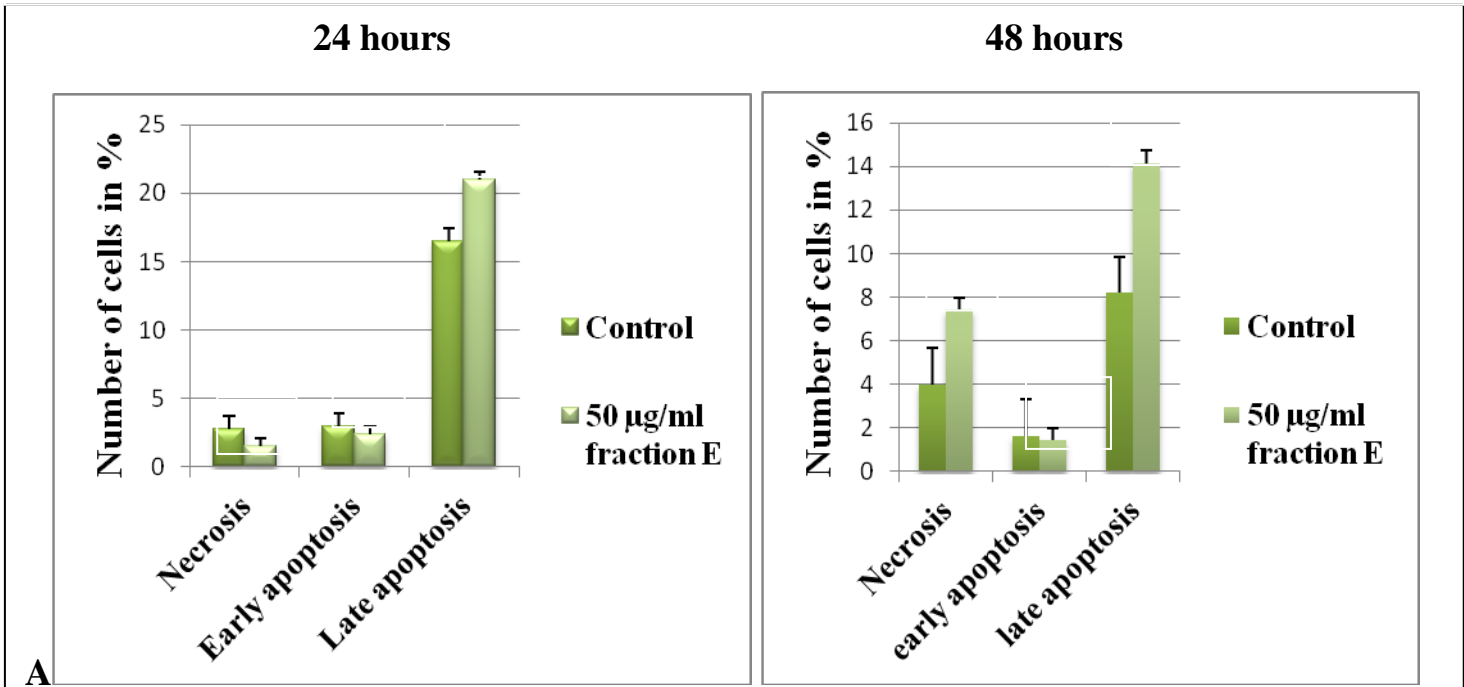


**Figure 3.28: Detection of time-dependent Apoptotic MDA468 breast cancer cells treated with purified whelk fraction E by Annexin V Staining.**

MDA468 cells were treated with purified whelk fraction E for 24 and 48 hours and then stained using Annexin V-FITC and PI provided in the Annexin V-FITC Apoptosis Detection Kit (see materials and methods). The combination of Annexin V-FITC and PI allows for the distinction between early apoptotic cells (annexin V-FITC positive), late apoptotic and/or necrotic cells (Annexin V-FITC and PI positive), necrotic (PI stained positive) and viable cells (unstained). (A) MDA468 cells treated with or without purified whelk fraction E for 24 and 48 hours. (B) Flow cytometry of MDA468 treated with or without purified whelk fraction E for 24 hours and (C) Flow cytometry of MDA468 treated with or without purified whelk fraction E for 48 hours.



**Table 4: Summary of biological effects of fraction E**

	MDA468 breast cancer cell line	MDANQ01 breast cancer cell line	3T3 normal fibroblast cell line
Proliferative assay	Inhibited cell growth	Inhibited cell growth	Supported cell growth
IC <sub>50</sub>	45.98µg/ml	41.89µg/ml	-
Cell cycle arrest	Induced cell cycle arrest at both S and G2/M phase	Induced cell cycle arrest at both S and G2/M phase	-
Apoptosis detection assay	Induced late apoptosis	Induced late apoptosis	-

## **Section 3D**

# **Characterisation and purification results for cockle GAGs**

### 3.29 Assignment of unsaturated CS disaccharides from cockle GAG extracts.

In order to ascertain the presence of CS/DS-like disaccharides in crude cockle GAG extracts, samples were degraded by chondroitinase-ABC lyase, and the unsaturated disaccharides produced were resolved by SAX-HPLC. The major disaccharides produced were non and mono-sulfated  $\Delta$  UA 1  $\rightarrow$  3GalNAc,  $\Delta$  UA 1  $\rightarrow$  3GalNAc6S and  $\Delta$  UA 1  $\rightarrow$  3GalNAc4S (Table 5). Commercial CS was analysed along side with samples for qualitative, and standardisation purposes and the digestion was monitored at 232 nm to assess when completion had occurred (Figure 3.29)

The elution profiles for crude cockle GAG extracts were compared with the reference chromatogram and they showed that the crude cockle GAG extracts contains both CS\ DS (Figure not shown.).

The first peak (I) with retention time 16 minutes is assigned to non-sulfated disaccharide ( $\Delta$ Di-0S) composed  $\Delta$ UA $\rightarrow$ 3GalNAc. The second peak (II) with retention time 19 minutes is assigned to mono-sulfated disaccharide ( $\Delta$ Di-6S) composed of  $\Delta$ UA $\rightarrow$ 3GalNAc (6S). The third peak (III) with retention time 20 minutes is assigned to mono-sulfated disaccharide ( $\Delta$ Di-4S) composed of  $\Delta$ UA $\rightarrow$ 3GalNAc (4S). The percentage compositions of each disaccharide peak from ABC lyase digested cockle GAG samples using the peak area were 60%, 20% and 20% respectively. Other unidentified peaks were also eluted along with the disaccharides which may suggest partial digestion or resistance to the enzyme's action. This result suggests that crude cockle GAG mixture contain CS/DS GAGs.

**Table 5: Disaccharides compositions of CS/DS-like glycans found in cockle GAG mixtures**

<b>Disaccharides</b>	<b>Cockle GAG mixtures disaccharide compositions in %</b>	<b>Commercial CS GAG disaccharide compositions in %</b>	<b>Retention time (Rt) in minutes</b>
$\Delta$ UA-GalNac	60	Not detected	16
$\Delta$ UA-GalNac (6S)	20	27	19
$\Delta$ UA-GalNac (4S)	20	73	20
$\Delta$ UA (2S)-GalNac	Not detected	Not detected	
$\Delta$ UA-GalNac (4S,6S)	Not detected	Not detected	
$\Delta$ UA (2S)-GalNac (6S)	Not detected	Not detected	
$\Delta$ UA <sub>2</sub> S-GalNac <sub>4</sub> S	Not detected	Not detected	

The percentage compositions of each disaccharides peak was calculated by using peak area values obtained from SAX-HPLC software.

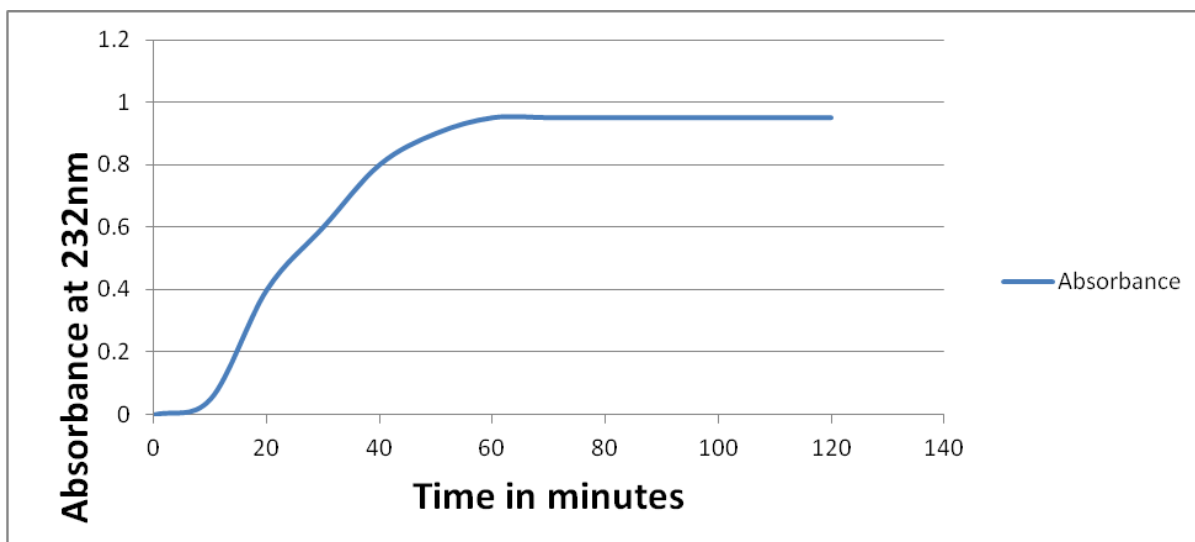


**Figure 3.29: Kinetic of chondroitinase ABC enzyme degradation of commercial CS.**

Commercial CS was dissolved in enzyme buffer and 30 $\mu$ l of the enzyme was added. Digestion was measured continuously by the change in absorbance at 232 nm on a spectrophotometer.

### 3.30 Assignment of unsaturated HS disaccharides from cockle GAG extracts

In order to examine the HS disaccharide compositions of crude cockle GAG extracts, samples were digested with heparinases 1, 11 & 111 enzymes. The resulting oligosaccharides were applied to a Pro-Pac PA-1 SAX-HPLC column (see materials and methods section for details). The number of peaks generated from crude cockle GAG extracts was compared to HS disaccharide standards obtained from complete digestion of commercial HS GAGs. The results obtained from this analysis, revealed that the invertebrate glycosaminoglycan yields mainly, the non-sulfated disaccharides  $\Delta$ UA (1 $\rightarrow$ 4) GlcNAc (I) with retention time (Rt) 16 minutes (Table 6). Both *N*-sulfated  $\Delta$ UA (1 $\rightarrow$ 4) GlcNS disaccharide and 6-*O*-sulfated  $\Delta$ UA (1 $\rightarrow$ 4) GlcNAc6S disaccharides were also detected (18 and 5% respectively).

It is noteworthy, that the two unsaturated disaccharides ( $\Delta$ UA (1 $\rightarrow$ 4) GlcNS6S and  $\Delta$ UA2S (1 $\rightarrow$ 4) GlcNS) peaks were also present in cockle HS but the percentage composition of each was less than one. Additionally, the mono-sulfated  $\Delta$ UA2S (1 $\rightarrow$ 4) GlcNAc, the rare disulfated disaccharide ( $\Delta$ UA2S (1 $\rightarrow$ 4) GlcNAc6S) and the trisulfated disaccharide ( $\Delta$ UA2S (1 $\rightarrow$ 4) GlcNS6S) were completely absent in crude cockle HS-GAG and this form the major difference between the crude and the commercial GAG mixture.

Furthermore, to confirm whether cockle GAGs contain low sulfated HS-like disaccharides, a portion of the crude extract was also digested with heparinase III enzyme and the resulting oligosaccharides resolved by SAX-HPLC revealed that the main disaccharides composition in cockle GAGs is non-sulfated  $\Delta$ UA (1 $\rightarrow$ 4) GlcNAc disaccharide. Similarly, both *N*-sulfated  $\Delta$ UA (1 $\rightarrow$ 4) GlcNS and 6-*O*-sulfated  $\Delta$ UA (1 $\rightarrow$ 4) GlcNAc6S disaccharides peaks were also detected. However, the other three disaccharides ( $\Delta$ UA (1 $\rightarrow$ 4) GlcNS,  $\Delta$ UA (1 $\rightarrow$ 4) GlcNS6S and  $\Delta$ UA2S (1 $\rightarrow$ 4) GlcNS) peaks were completely absent in cockle HS-like

GAGs, in contrast to what was observed for the commercial HS digested with heparinase III (result not shown).

These results suggest that cockle mixture contain low sulfated HS-like GAGs and the disaccharides composition analysis also suggests that this mollusc HS-like GAG contain non-sulfated  $\Delta$ UA (1 $\rightarrow$ 4) GlcNAc disaccharide as its main disaccharides.

**Table 6: HS Disaccharides compositions from heparinase digest of cockle GAG extracts**

<b>HS disaccharides</b>	<b>Cockle GAG mixtures disaccharide compositions (%)</b>	<b>Commercial HS-GAG disaccharide compositions (%)</b>
$\Delta$ UA (1 $\rightarrow$ 4) GlcNAc	75	55.00
$\Delta$ UA (1 $\rightarrow$ 4) GlcNS	18	18.00
$\Delta$ UA (1 $\rightarrow$ 4) GlcNAc6S	5.0	5.0
$\Delta$ UA2S (1 $\rightarrow$ 4) GlcNAc	Not detected	6.0
$\Delta$ UA (1 $\rightarrow$ 4) GlcNS6S	<1.0	2.0
$\Delta$ UA2S (1 $\rightarrow$ 4) GlcNS	<1.0	7.0
$\Delta$ UA2S (1 $\rightarrow$ 4) GlcNAc6S	Not detected	<1.0
$\Delta$ UA2S (1 $\rightarrow$ 4) GlcNS6S	Not detected	6.0

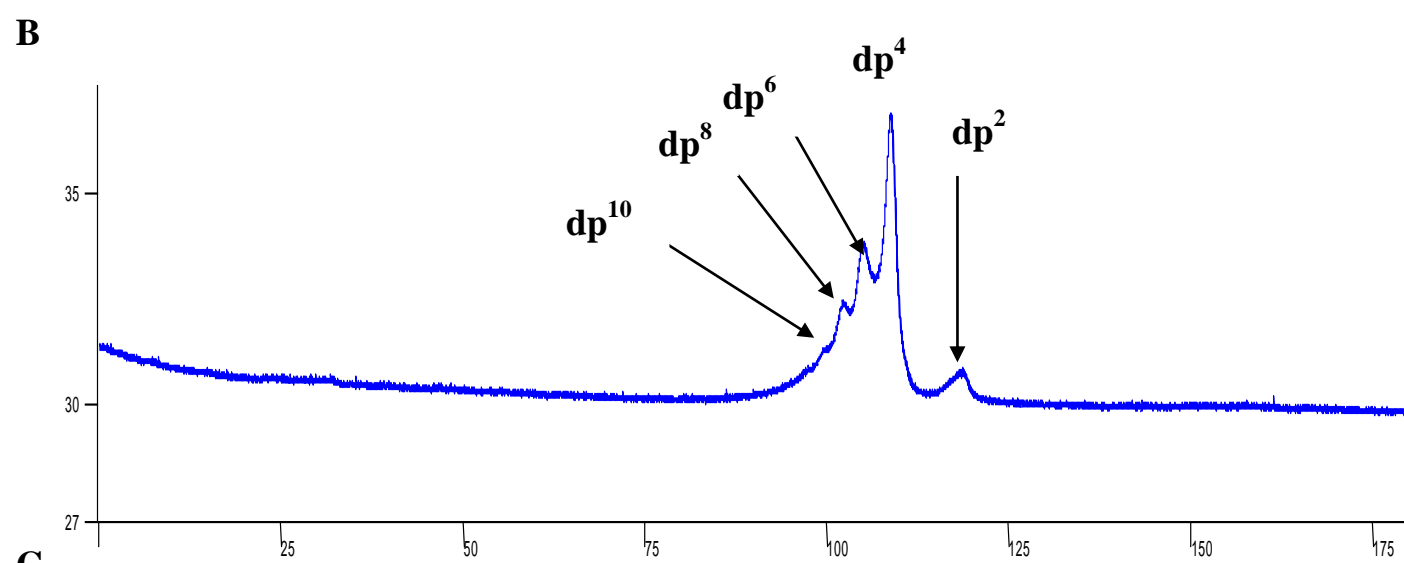
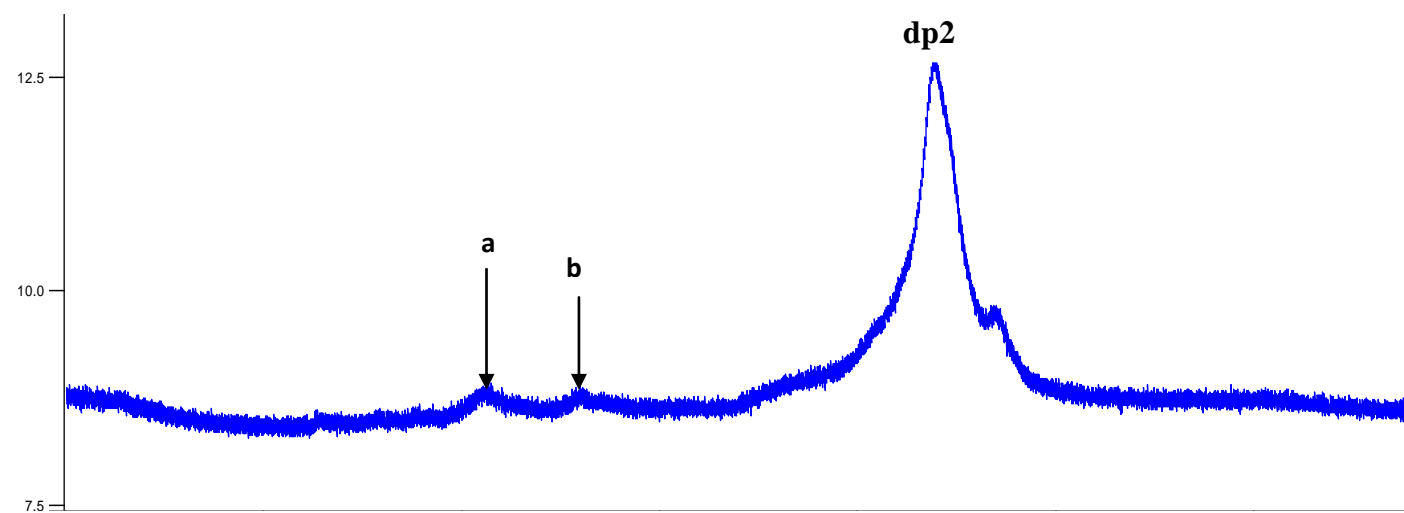
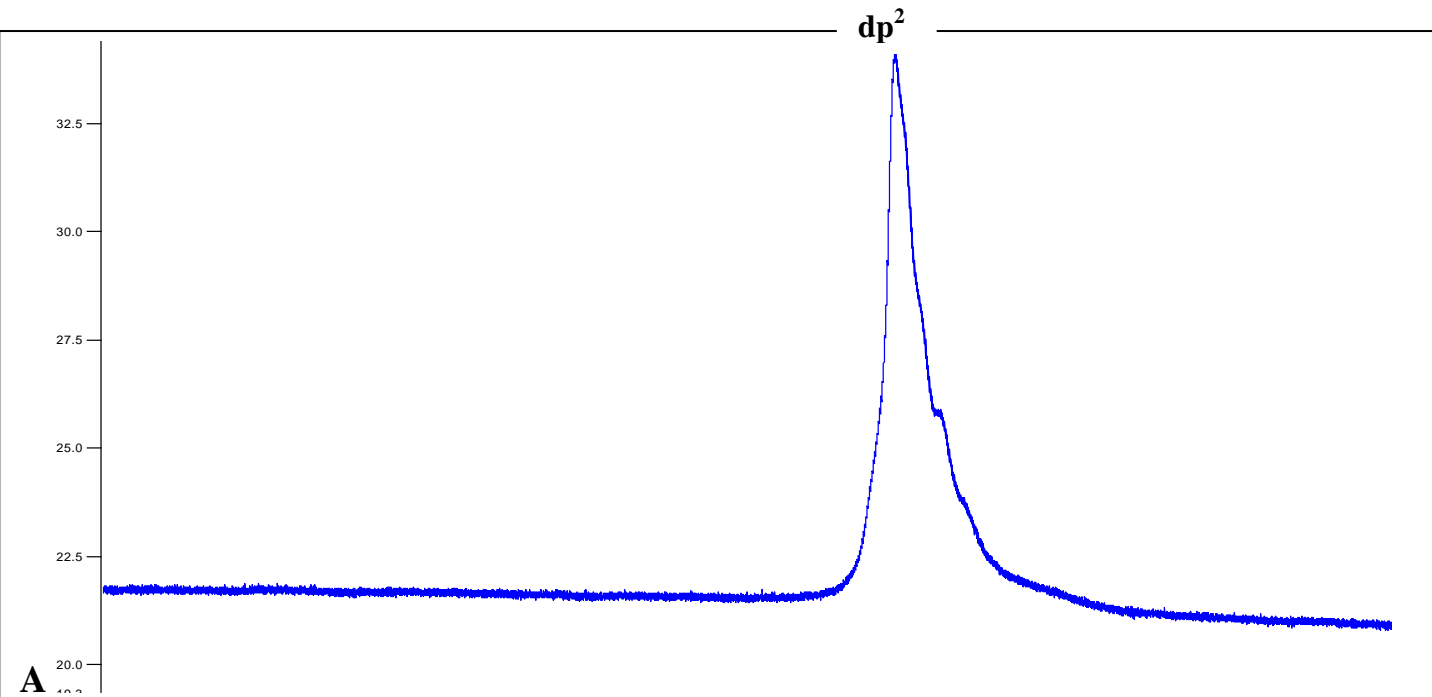
The percentage compositions of each disaccharides peak was calculated using peak area values obtained from SAX-HPLC software.



### **3.31 Gel Filtration analysis (TSK 2000PW) of heparinase degraded cockle GAG extracts**

A pilot study was conducted in order to ascertain the minimum amount of enzymes and time required to digest completely 1mg commercial HS and 1mg of crude cockle GAGs. Digestion was monitored by observing changes in the gel-filtration profile of the sample (result not shown). The digestion appeared complete after additions of 30mU of Heparinase I, II and III and incubation for a 48-hour period at 37 °C. Further addition of enzyme and incubation for a further 24 hours caused degradation of the disaccharides into smaller units (monosaccharide) (results not shown).

After 48 hours' incubation of either crude or commercial HS GAGs with Heparinase I, II and III enzymes, a 50 µl of the digested sample was applied to TSK 2000PW column and the eluted profile was monitored at 232 nm for 180 minutes. The elution profiles obtained for both commercial HS and crude cockle GAGs confirmed a complete digestion of both samples as shown in Figure 3.30 (A-B). This result confirms the SAX-HPLC finding presented in the previous section and the single broad peak obtained correspond to HS disaccharides.



Elution time in minutes

**Figure 3.30: Analytical TSK2000PW gel-filtration profiles of HS/Heparin and crude cockle GAGs after complete digestion with Heparinase I, II and III enzymes**

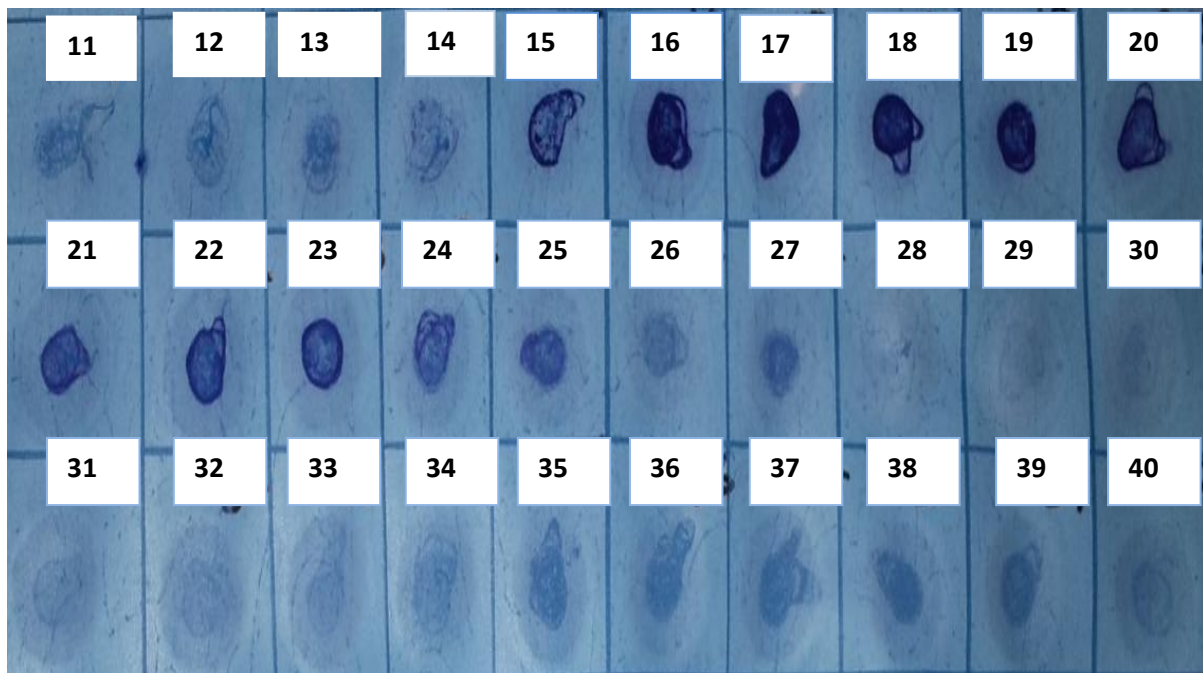
50 µg of the enzymes GAGs digest by the Heparinase I, II and III enzymes were chromatographed on a TSK2000PW analytical gel-filtration column (30 x 0.75 cm) and the elution was monitored at 232 nm for 180 minutes. (A) Elution profile for commercial HS/Heparin standard digested in Heparinase I, II, and III. (B) Elution profile for crude cockle GAGs digested in Heparinase I, II, and III. (C) Elution profile for HS/Heparin digested in Heparinase I enzyme. Abbreviations: dp<sup>10</sup>- octasaccharides: dp<sup>8</sup>- heptasaccharides: dp<sup>6</sup>- hexasaccharides: dp<sup>4</sup>- tetrasaccharides: dp<sup>2</sup>- disaccharides.

### **3.32 Superose 12 size exclusion chromatography analysis of intact cockle extracts**

#### **GAG chains**

Cockle GAG extracts were analysed for size using a superose 12 size exclusion column. GAG content of the fractions collected from this column was determined by cellulose acetate dot blotting assay. This showed that fractions 1-14 & 28-40 did not contain any GAGs (Figure 3.31), however fractions 15-27 showed distinct binding of azure A stain to the sulfated GAG components present in these fractions. The intensity of the stain is relatively proportional to the concentrations of GAGs present in each fraction i.e. the more GAGs in the fraction, the deeper the stain. Quantitative analysis of GAGs compositions in crude cockle GAG extracts was determined by densitometry analysis; the result shows two major GAGs containing peaks were eluted from the Superose 12 column. The larger molecular weight species [fractions 15- 20 (A)] were eluted first, followed by the smaller polysaccharide [fractions 21-27 (B)].

A



B

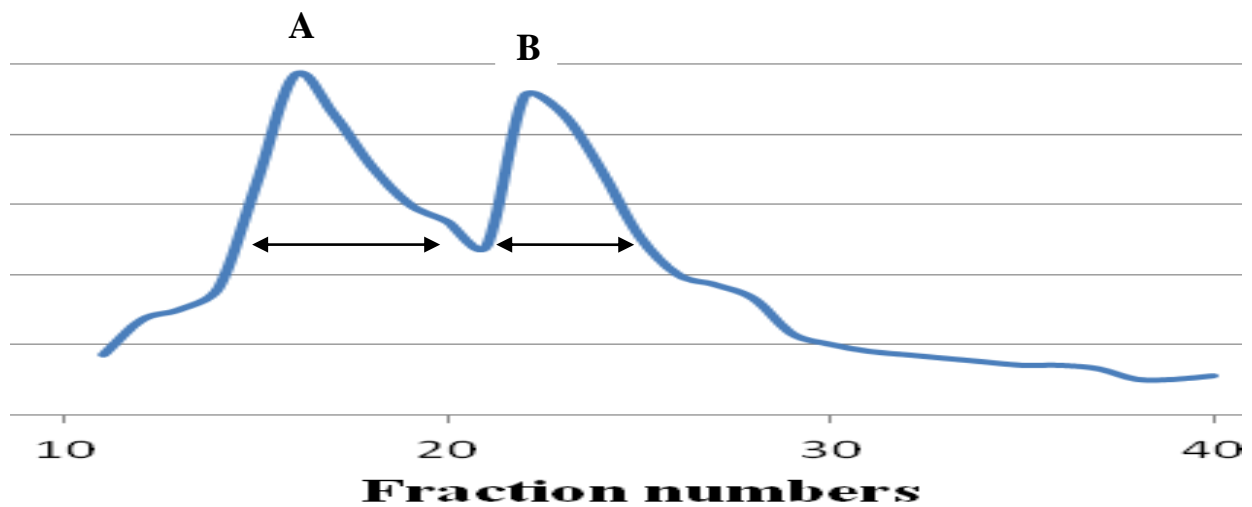


**Figure 3.31: Superose 12 size exclusion chromatography and cellulose acetate dot blotting result for crude cockle GAG mixture**

(A) Cellulose acetate dot blotting assay result for crude cockle GAG mixture (B) Densitometry and scan analysis of cellulose acetate dot blotting: each peak represents GAG with relative size based on their structural composition and ionic contents ( $\text{SO}_3^-$  and  $\text{COO}^-$ )

### **3.33 PAGE analysis of crude cockle GAG extracts and commercial GAGs after enzymatic depolymerisation.**

The crude cockle GAG extracts and commercial GAGs treated separately with heparinase (I, II, and III) and ABC lyase enzymes were analysed using PAGE. The results are presented in Figure 3.32.

All intact GAG samples show slow moving and very diffuse and unresolved bands [(Figure 3.32 (2, 3, 5 and 8)], indicating a heterogeneous mixture of GAG chains. Conversely, all the enzyme-treated samples demonstrated faster-moving bands; thus indicating shorter chain oligosaccharides due to degradation of chains by the enzymes [(Figure 3.32 (1, 4, 6 and 7)].

These results confirmed the presence of both CS/DS-like and HS-like oligosaccharides in the crude cockle GAG extracts.

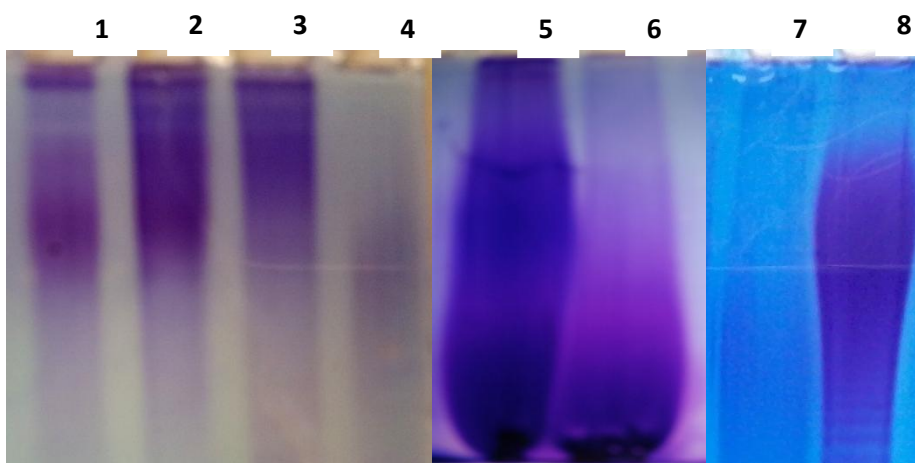


**Figure 3.32: PAGE analysis of enzymatic depolymerised GAGs.**

All the commercial GAGs and crude cockle GAG mixture were incubated with heparinase (I,II, and III) and ABC lyase enzymes separately for 48 hours and approximately 20  $\mu$ l of the degraded sample was applied to each lane. (1) Crude cockle GAG extracts digested with ABC lyase enzyme. (2) Intact crude cockle GAG extracts. (3) Intact crude cockle GAG extracts. (4) Crude cockle GAG extracts digested with Heparinase I,II, and III enzymes. (5) Intact HS commercial GAG (6) HS-GAG sample digested with Heparinase I, II, and III enzymes. (7) CS GAG digested with ABC lyase enzyme. (8) Intact CS commercial GAG.

## **Section 3E**

### **Characterisation of crude whelk**

#### **GAG mixtures**

### **3.34 Assignment of unsaturated CS disaccharides for whelk GAG extract**

Whelk GAG extracts was digested with the enzyme chondroitinase ABC lyase in order to determine the presence of CS/DS-like GAGs. The digestions were monitored spectrophotometrically at 232 nm until completion was observed (Figure 3.33A-C).



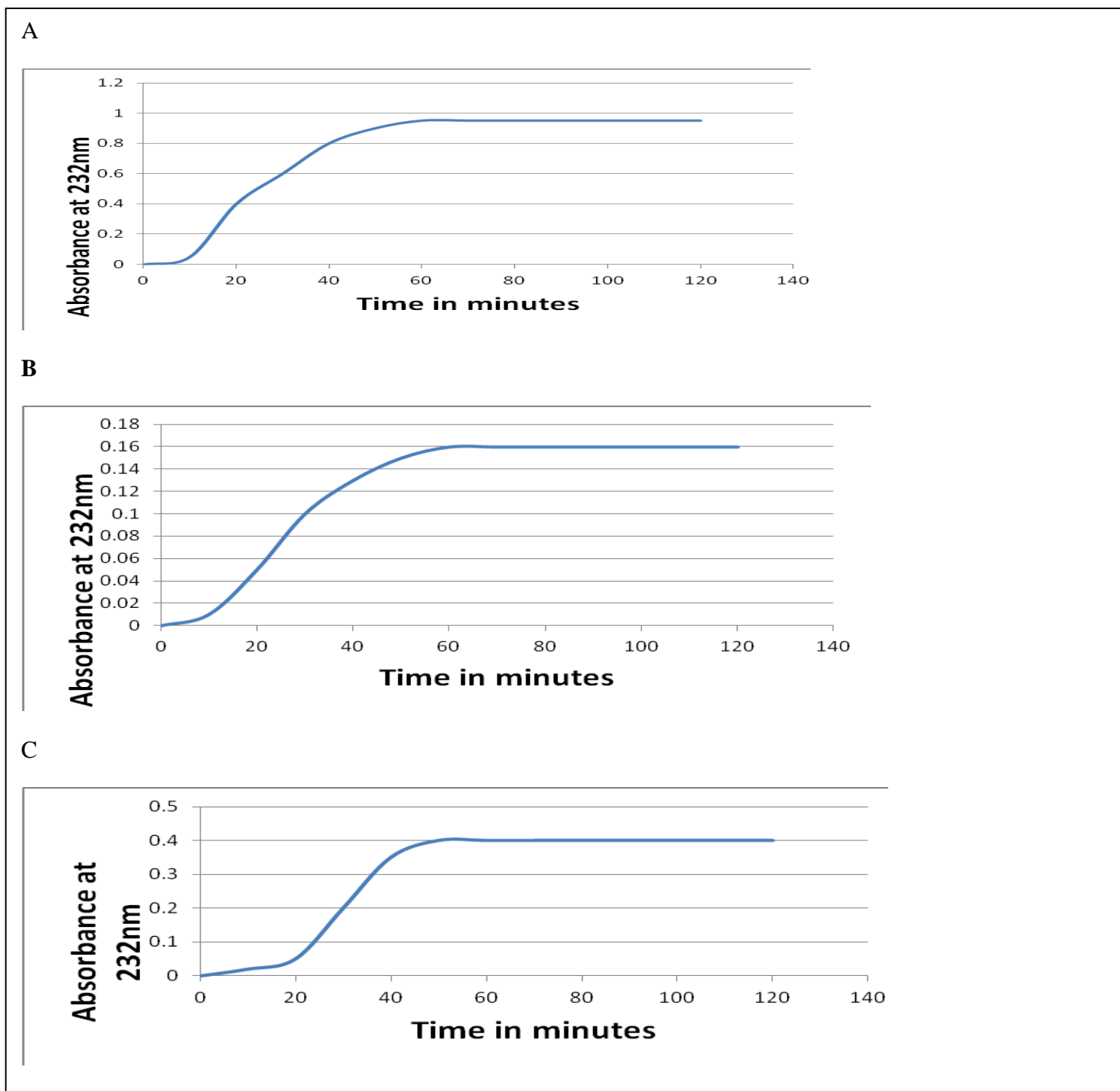


**Figure 3.33: Kinetic of chondroitinase ABC enzyme degradation of GAGs**

Commercial CS and whelk GAGs were each dissolved in enzyme buffer and 30 $\mu$ l of the enzyme was added to each dissolved sample. Digestion was measured continuously by the change in absorbance at 232 nm on a spectrophotometer. (A) Commercial CS in chondroitinase ABC enzyme (B) Crude whelk GAG in chondroitinase ABC enzyme (C) Whelk fraction C in chondroitinase ABC enzyme.

The elution profile for crude whelk GAG extracts, compared with the reference chromatogram, showed that the crude whelk GAG extracts contain both CS/DS-like disaccharides (Table 7). The percentage composition of each disaccharide peak was calculated and data recorded in table 4. The main disaccharides peaks, as resolved by SAX-HPLC, are mono-sulfated disaccharide ( $\Delta$ Di-6S) composed of  $\Delta$ UA $\rightarrow$ 3GalNAc (6S) and ( $\Delta$ Di-4S) composed of  $\Delta$ UA $\rightarrow$ 3GalNAc (4S). These two peaks compared favourably, by retention time, with the commercial CS disaccharides peaks. However, there are other broad peaks eluted along with the disaccharides, which may indicate partial digestions or resistance of the polymer to chondroitinase ABC lyase.

**Table 7: Disaccharides compositions of CS/DS-like glycans found in whelk GAG extracts**

<b>Disaccharides</b>	<b>Whelk GAG composition ( %)</b>	<b>Commercial CS composition ( %)</b>
$\Delta$ UA-GalNac	Not detected	Not detected
$\Delta$ UA-GalNac (6S)	55	73
$\Delta$ UA-GalNac (4S)	45	27
$\Delta$ UA (2S)-GalNac	Not detected	Not detected
$\Delta$ UA-GalNac (4S,6S)	Not detected	Not detected
$\Delta$ UA (2S)-GalNac (6S)	Not detected	Not detected
$\Delta$ UA2S-GalNac4S	Not detected	Not detected

The percentage compositions of each disaccharides peak was calculated using peak area values obtained from SAX-HPLC software.

### **3.35: PAGE analysis of crude whelk GAG extracts and commercial GAGs after enzymatic depolymerisation.**

The crude whelk GAG extracts and commercial GAGs were treated separately with heparinases I, II and III and with ABC lyase enzymes and analysed using PAGE. The results are presented in Figure 3.34.

All the intact GAG samples show a very diffuse bimolecular weight band [(Figure 3.34 (2, 3, 5 and 8)], indicating a long linear polymer chain with heterogenous populations. Conversely, all the enzyme treated samples showed faster moving less intensely stained bands indicating shorter chain oligosaccharides as products of enzymatic digestion, these differences can be used to determine the specific presence of GAG subfamilies based on the enzymatic specificities of the enzymes [Figure 3.34 (1,4,6 and 7)].

These results confirmed the presence of both CS/DS-like and HS-like oligosaccharides in the crude whelk GAG mixtures.

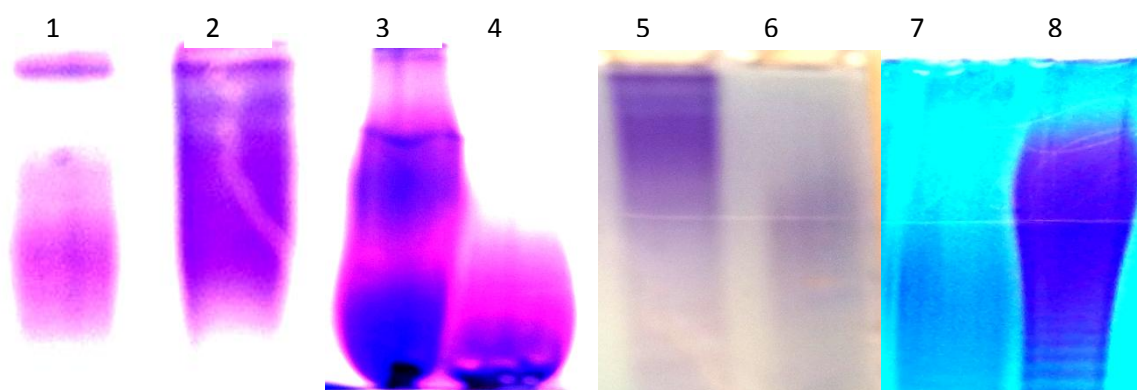


**Figure 3.34: PAGE analysis of enzymatic depolymerised GAGs.**

All the commercial GAGs and crude whelk GAG extracts were incubated with heparinase (I, II, and III) and ABC lyase enzymes separately for 48 hours and approximately 20  $\mu$ l of the degraded sample was applied to each lane. (1) Crude whelk GAG extracts digested with Heparinase I, II, and III enzymes. (2) Intact crude whelk GAG extracts. (3) Intact HS commercial GAG. (4) HS commercial GAG digested with Heparinase I, II, and III enzymes. (5) Intact whelk GAG extracts (6) Whelk GAG extracts mixture digested with ABC lyase enzyme. (7) CS commercial GAG digested with ABC lyase enzyme. (8) Intact CS commercial GAG.

### **3.36 Superose-12 size exclusion chromatography of crude whelk GAG Extracts.**

The results obtained show that crude whelk GAG extracts contain five main peaks with varying sizes, by UV monitoring and GAG binding dot blot assay. The void volume of the column ( $V_0$ ) was calculated as being at fraction 14, as shown in Figure 3.35, with fractions (15-32) contains varying concentrations of GAGs within the five peaks eluted. The qualitative analyses of the five GAG peaks were performed using densitometry of the stained dot blot. Each peak represents different populations of GAG chains eluting according to their sizes. Fractions 15-17 being the largest GAG component eluted and fractions 30-32 being the smallest.

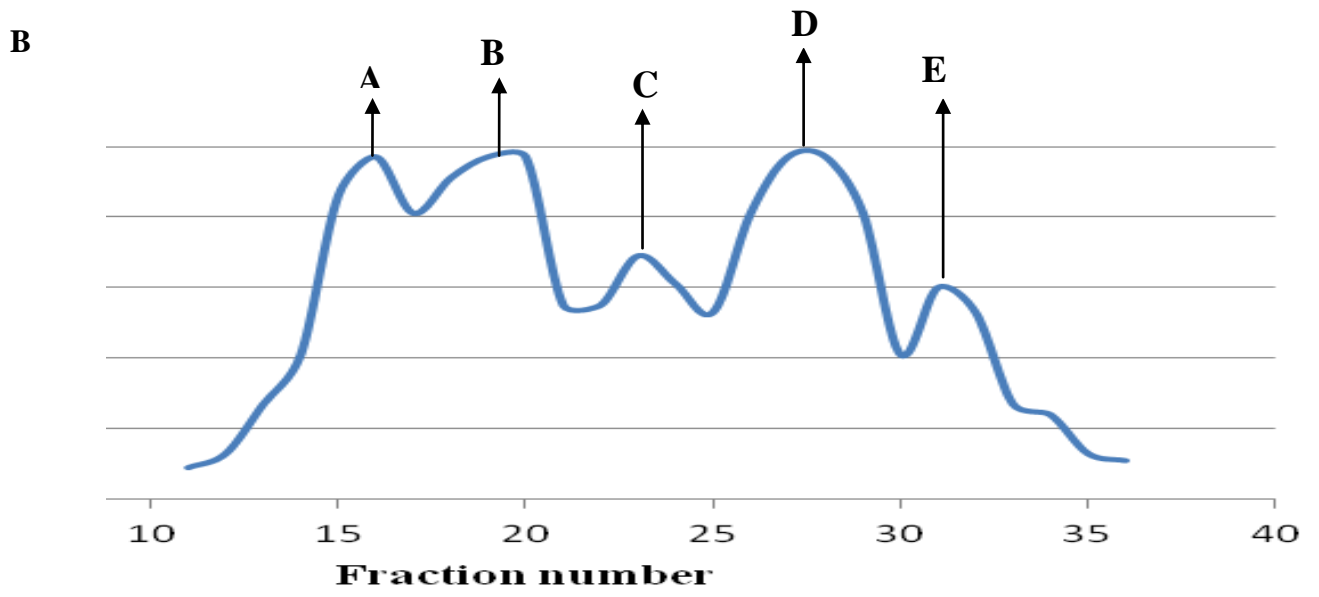
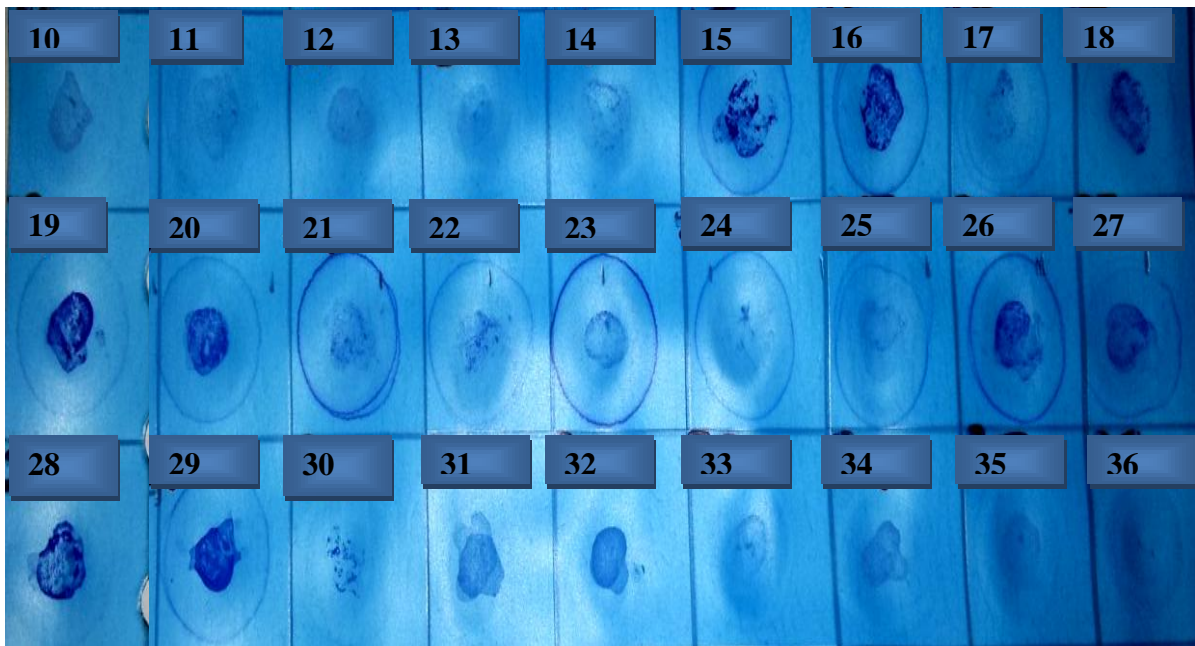


**Figure 3.35: Superose 12 size exclusion chromatography and cellulose acetate dot blotting assay of crude whelk GAG extract.**

(A) Cellulose acetate dot blotting assay result for crude whelk GAG mixture (B) Densitometry and scan analysis of cellulose acetate dot blotting.

## **SECTION 3F**

**Characterisation of purified whelk**

**GAG peaks derived by ion exchange**

**chromatography**



### 3.37 Assignment of unsaturated CS disaccharides from purified whelk GAG fractions

In order to ascertain which of the whelk GAG peaks obtained from the ion exchange column contain CS/DS-like GAGs, samples were digested with chondroitinase-ABC lyase. The resulting oligosaccharides products were analysed by SAX-HPLC. Only two fractions (B and C) from the ion exchange column (Table 8) were sensitive to depolymerisation by chondroitinase ABC lyase, the other three peaks (A, E & F) were resistant to the action of this enzyme. The depolymerised whelk GAG peaks B and C produced two major peaks which were identified as  $\Delta$  UA-GalNac6S and  $\Delta$ UA-GalNac4S. The oligosaccharides peaks were identified by comparing their elution positions with those of standard oligosaccharides obtained from commercial CS GAGs.

The SAX-HPLC separation of the unsaturated oligosaccharides produced by the action of chondroitinase-ABC on purified whelk fraction B produced three major disaccharide peaks, assigned to unsaturated non-sulfated  $\Delta$  UA-GalNac (di-0S), mono-sulfated  $\Delta$  UA-GalNac6S (Di-6S) and  $\Delta$ UA-GalNac4S (DI-4S). From the peak areas, it could be calculated that these three disaccharides contain 55%  $\Delta$  UA-GalNac, 35%  $\Delta$  UA-GalNac6S and 10%  $\Delta$ UA-GalNac4S of the total disaccharide composition (Table 8). Other unidentified peaks were also eluted with the oligosaccharides which may be an indication of contamination or incomplete digestion of the polymer.

Similarly, SAX-HPLC result of depolymerised peak C demonstrated two major disaccharides peaks with similar elution profiles to the commercial CS disaccharides (Table 5). The first peak was assigned the mono-sulfated disaccharide  $\Delta$  UA-GalNac6S ( $\Delta$ Di6S). Also from the peak areas, it could be calculated that these two disaccharides contain 22%  $\Delta$

UA-GalNac (6S) and 78 %  $\Delta$  UA-GalNac (4S). Other unidentified peaks were also eluted along with the disaccharides which may suggest contamination or resistance to chondroitinase-ABC enzyme.

Fractions A, F and the biologically active fraction E were found to be resistant to chondroitin ABC lyase treatment and did not produce any degradation peaks. Further investigation of the biologically active fraction E was obviously required in order to confirm the nature of the GAG components that it contains.

**Table 8: Disaccharides compositions of CS/DS-like GAGs present in ion-exchange purified whelk peaks B and C**

<b>Disaccharides</b>	<b>Whelk fraction B disaccharide composition ( %)</b>	<b>Whelk fraction C disaccharide composition (%)</b>	<b>Commercial CS disaccharide composition ( %)</b>
$\Delta$ UA-GalNac	55	Not detected	Not detected
$\Delta$ UA-GalNac (6S)	35	22	23
$\Delta$ UA-GalNac (4S)	10	78	77
$\Delta$ UA (2S)-GalNac	Not detected	Not detected	Not detected
$\Delta$ UA-GalNac (4S,6S)	Not detected	Not detected	Not detected

The percentage composition of each disaccharides peak was calculated using peak area values obtained from SAX-HPLC software.

### **3.38 Heparinase I-III enzymatic treatments and disaccharide analysis by SAX-HPLC of the active whelk fraction E**

To further elucidate the HS-like disaccharides in ion-exchange purified whelk GAG peak (fraction E), the pooled biologically active fraction E was digested with Heparinase I, II, and III enzymes. The resulting oligosaccharides were resolved by SAX-HPLC and showed six confirmed HS disaccharide peaks with some minor contamination from other unidentified peaks. The major disaccharides peak from the heparinase digested fraction E was assigned to *non-* sulfated HS disaccharide  $\Delta$ UA- GlcNAc, which comprised 60 % of the total disaccharide composition of fraction E (Table 9). The *N*-sulfated disaccharide  $\Delta$ UA -GlcNS was also present with a percentage composition of 29%. The 6- *O*-sulfated  $\Delta$ UA -GlcNAc6S disaccharide has a percentage composition of 2% of the total disaccharides composition. The fourth peak was assigned to the unsaturated  $\Delta$ UA-GlcNS (6S) disaccharide with a percentage composition of 7 %. The fifth peak was assigned to the rare di-sulfated  $\Delta$ UA (2S)-GlcNAc6S disaccharide with a very low composition of less than 1%. The tri-sulfated disaccharides  $\Delta$ UA (2S) (1 $\rightarrow$ 4) GlcNS (6S) was also present in this polysaccharide but the percentage composition was very low (1%). Interestingly, the 2-*O*-sulfated  $\Delta$ UA (2S)-GlcNAc and  $\Delta$ UA (2S)-GlcNS disaccharides were completely absent from this polymer and this form the major difference between this novel and the commercial HSGAGs disaccharides. However the disaccharide analysis couldn't rule out the presence of disaccharides not normally seen in HS that might account for the different activities observed with Whelk derived GAGs and commercial HS.

Fraction E was also digested with heparinases I, II, and III individually, to identify the specific enzyme or enzymes responsible for the depolymerisation of whelk fraction E. Enzymatic activities were monitored by following the increase in UV absorbance at 232 nm

with time and the resulting oligosaccharide were applied to SAX-HPLC column and resolved using a NaCl gradient. Heparinase I and II showed limited ability to degrade the fraction E GAGs. In contrast, heparinase III demonstrated significant activity against this polysaccharide (Table 10). This result suggests that whelk fraction E contains a significant proportion of low sulfated HS-like GAG chains.

**Table 9: Disaccharides compositions of HS-like GAGs found in purified whelk fraction E.**

<b>HS disaccharides</b>	<b>Whelk fraction E disaccharide composition (%)</b>	<b>Commercial HS disaccharide compositions (%)</b>
$\Delta$ UA (1 $\rightarrow$ 4) GlcNAc	60	55.00
$\Delta$ UA (1 $\rightarrow$ 4) GlcNS	29	18.00
$\Delta$ UA (1 $\rightarrow$ 4) GlcNAc6S	2	5.0
$\Delta$ UA2S (1 $\rightarrow$ 4) GlcNAc	Not detected	6.0
$\Delta$ UA (1 $\rightarrow$ 4) GlcNS6S	7	2.0
$\Delta$ UA2S (1 $\rightarrow$ 4) GlcNS	Not detected	7.0
$\Delta$ UA2S (1 $\rightarrow$ 4) GlcNAc6S	<1	<1.0
$\Delta$ UA2S (1 $\rightarrow$ 4) GlcNS6S	1	6.0

The percentage composition of each disaccharides peak was calculated using peak area values obtained from SAX-HPLC software.

**Table 10: Disaccharides compositions of HS-like GAGs found in purified whelk fraction E depolymerised by heparinase III lyase.**

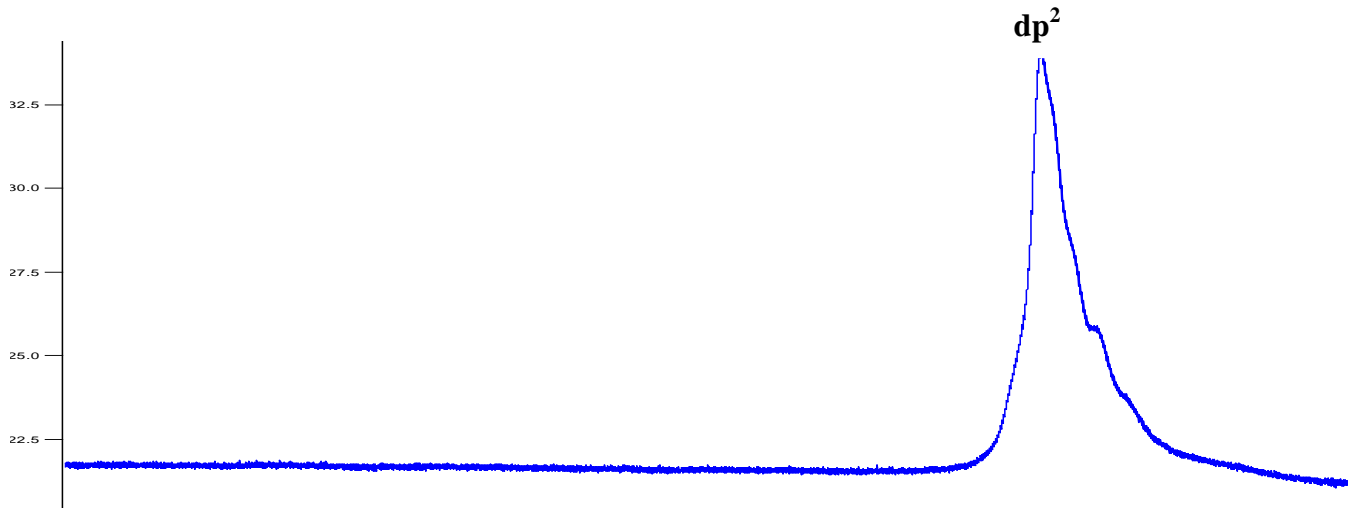
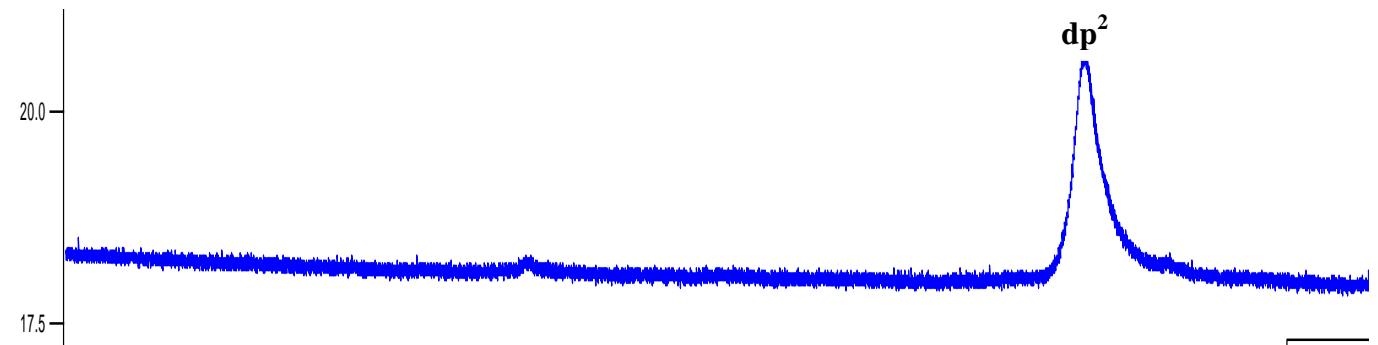
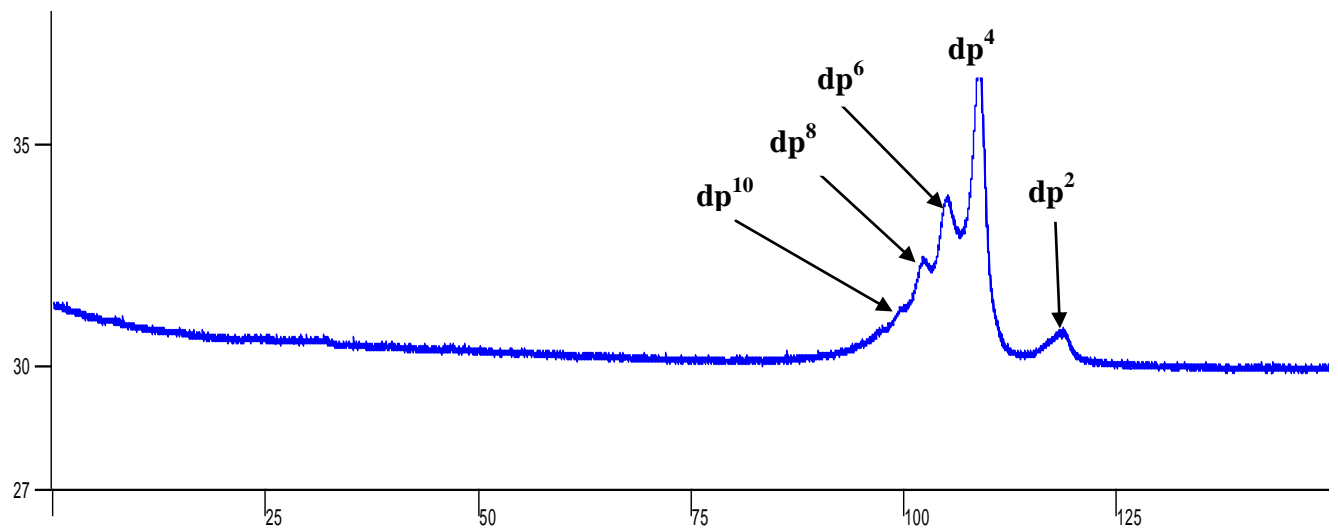
<b>HS disaccharides</b>	<b>Whelk fraction E disaccharide composition (%)</b>	<b>Commercial HS disaccharide compositions (%)</b>
$\Delta$ UA (1→4) GlcNAc	75.00	59.00
$\Delta$ UA (1→4) GlcNS	16.00	22.00
$\Delta$ UA (1→4) GlcNAc6S	1.00	4.00
$\Delta$ UA2S (1→4) GlcNAc	Not detected	7.00
$\Delta$ UA (1→4) GlcNS6S	8.00	2.00
$\Delta$ UA2S (1→4) GlcNS	Not detected	6.00
$\Delta$ UA2S (1→4) GlcNAc6S	Not detected	Not detected
$\Delta$ UA2S (1→4) GlcNS6S	Not detected	Not detected

### **3.39 HPLC Gel Filtration analysis of whelk fraction E after heparinase degradation**

The digestion of the purified whelk fraction E was monitored through changes in the gel-filtration profile of the sample (result not shown). The digestions appeared complete after additions of 30mU of Heparinase I, II and III, followed by continuous incubation for 48 hour period at 37 °C. After 48 hours' incubation of purified whelk fraction E or HS/heparin GAG with heparinase I, II and III enzymes, a 50µl of the digested sample was applied to TSK 2000PW column and the eluted profile was monitored at 232 nm for 180 minutes. The elution profiles obtained for both HS/Heparin and purified whelk fraction E confirm complete digestion of both samples as shown in Figure 3.36 (A-B). This result confirms the SAX-HPLC result described in the previous section and the single broad peak obtained corresponds to HS disaccharides (dp<sup>2</sup>).

However, heparin digested with Heparinase I enzyme for 48 hours shows a number of oligosaccharide peaks in addition to the usual disaccharide peak; an indication of incomplete degradation of the commercial GAGs. The peaks corresponding to the various oligosaccharides are also labelled appropriately in Figure 3.36 (C). Both SAX-HPLC and TSK gel-filtration results confirmed the presence of HS-like disaccharides in the purified fraction E.



**A****B****C**

**Figure 3.36: Analytical TSK2000PW gel-filtration profiles of HS/heparin and purified whelk fraction E after complete digestion with Heparinase I, II and III enzymes.**

50 µg of the enzymes GAGs digest by the Heparinase I,II and III enzymes were chromatographed on a TSK2000PW analytical gel-filtration column (30 x 0.75 cm) and the elution was monitored at 232 nm for 180 minutes. (A) Elution profile for commercial HS/Heparin standard digested in Heparinase I,II, and III. (B) Elution profile for purified whelk fraction E digested in Heparinase I, II, and III. (C) Elution profile for HS/Heparin digested in Heparinase I enzyme.

Abbreviations: dp<sup>10</sup>- octasaccharides: dp<sup>8</sup>- heptasaccharides: dp<sup>6</sup>- hexasaccharides: dp<sup>4</sup>- tetrasaccharides: dp<sup>2</sup>- disaccharides.

**3.40 PAGE analysis of purified whelk fractions and commercial GAGs after enzymatic depolymerisation.**

The purified whelk GAG extracts and commercial GAGs were digested individually and with a mixture of Heparinases I, II, and III enzymes. Similarly, these polysaccharide fractions were also digested individually with ABC chondroitinase enzyme. The resulting oligosaccharides from each enzyme digestion were analysed using PAGE (Figure 3.37).

All the intact GAG samples show a very intense and diffuse banding pattern [(Figure 3.37 (2, 3, 5 and 8))] indicating a heterogeneous mixture of polymer chains, a unique characteristic of GAGs polymers.

Conversely, all the sensitive enzyme-treated samples show less intensely staining bands and faster mobilities, suggesting breakdown into shorter chain oligosaccharides [(Figure 3.37 (1,4,6 and 7))].

This result confirmed the presence of both CS/DS and HS-like oligosaccharides in the crude and purified whelk GAG mixtures.

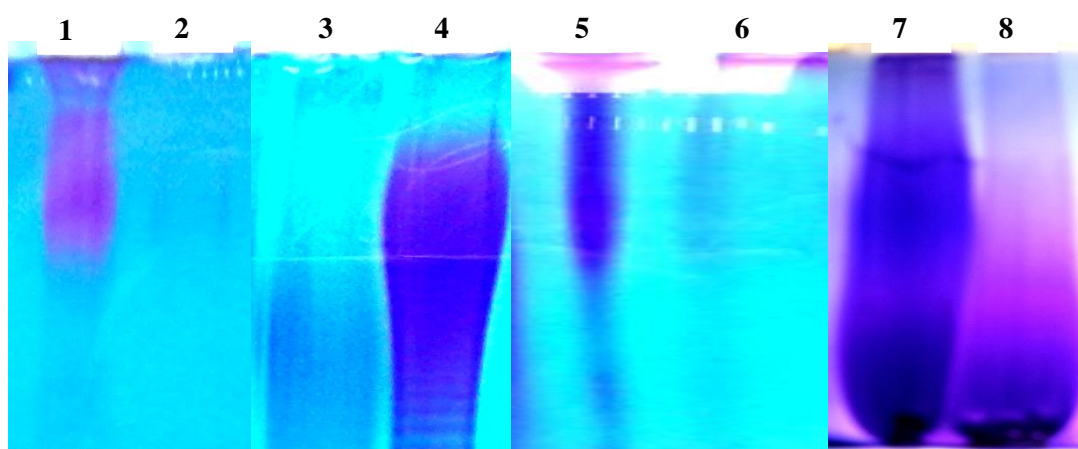


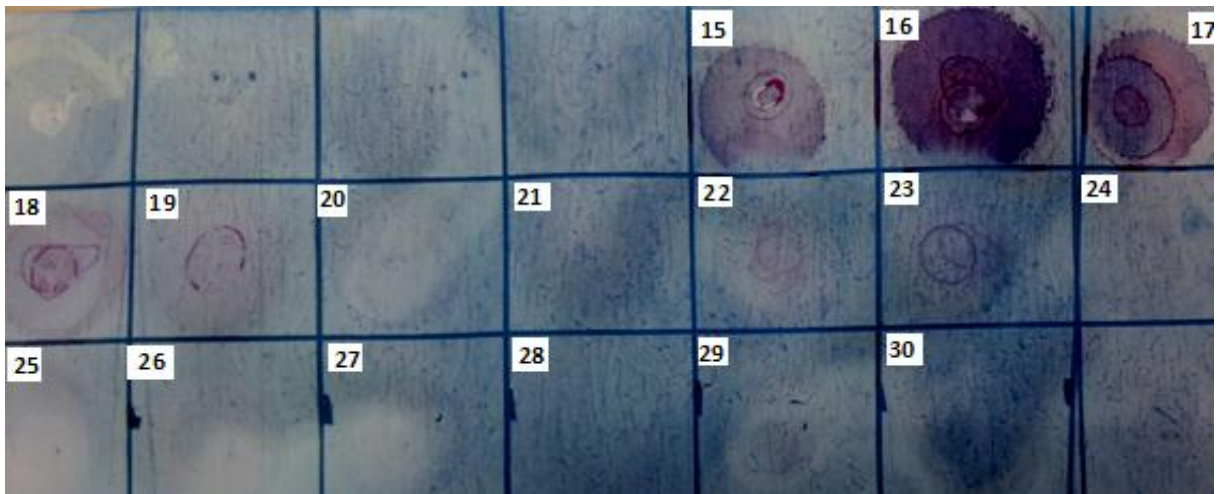
**Figure 3.37: PAGE analyses of enzymatic depolymerised whelk derived and commercial GAGs.**

All the commercial GAGs and crude purified whelk fractions were incubated with heparinase (I,II, and III) and ABC lyase enzymes separately for 48 hours.(1) Intact fraction C dissolved in enzyme buffer. (2) Purified fraction C digested with chondroitinase-ABC lyase. (3) CS commercial GAG digested with chondroitinase-ABC lyase.intact HS commercial GAG. (4) Intact CS commercial GAG dissolved in enzyme buffer (5) Intact purified whelk fraction E dissolved in enzyme buffer. (6) Purified fraction E digested with Heparinase I, II and III. (7) Intact commercial HS dissolved in enzyme buffer. (8) HS commercial GAG digested with Heparinase I,II, and III enzymes.

### **3.41 Superose-12 size exclusion chromatography of purified whelk fraction E**

The results obtained from these analyses revealed that purified whelk fraction E contain sulfated GAGs, as illustrated in Figure 3.38 since azure A binds to GAGs in this fraction. The GAG content/overall sulfate content in each fraction is proportional to the intensity of staining. Scanning densitometry analysis of the cellulose acetate dot blotting assay shows that fraction E contains one major and high molecular weight GAG component, this corresponds to the largest peak seen in the superose-12 separation of the un-fractionated crude GAG extract (Figure 3.35). It also contains a minor peak corresponding to one of the smaller GAGs eluted from initial crude whelk GAG mixture.

**A**



**B**

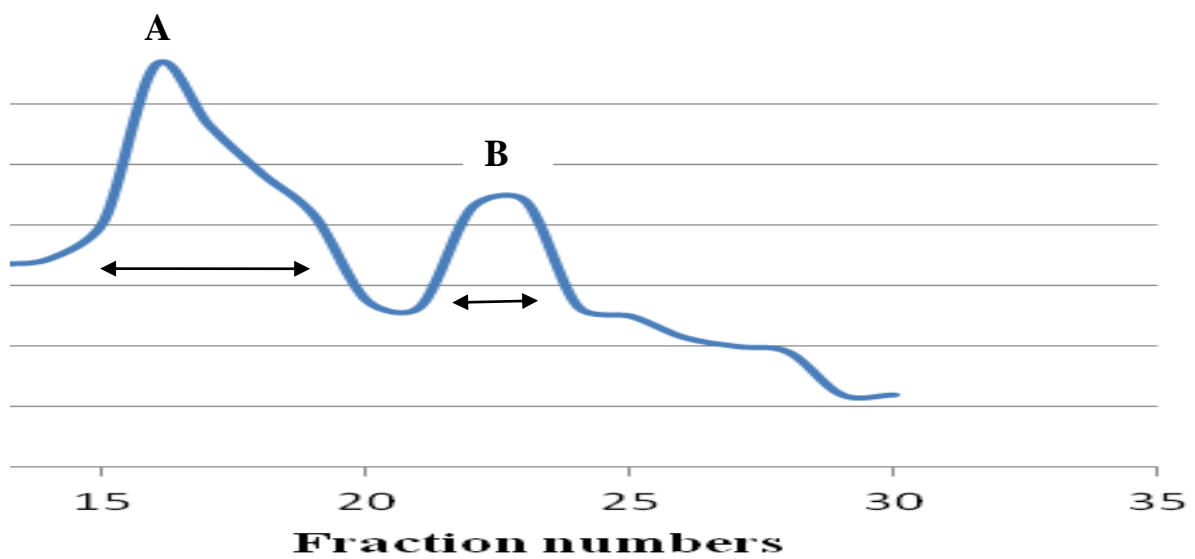


**Figure 3.38** Superose-12 size exclusion chromatography and cellulose acetate dot blotting assay for purified fraction E GAG mixtures

(A) Cellulose acetate dot blotting assay result for purified fraction E (B) Scanning densitometry analysis of cellulose acetate dot blots: each peak represents GAG with relative size based on their structural composition and ionic contents ( $\text{SO}_3$  and  $\text{COO}^-$ ).

## **Section 4**

## **Discussion**

#### 4.1 Outline of the major findings

The results of this study provide significant insight into the pharmacological properties of whelk and cockle derived GAGs in different cancer cells, including breast, cervical and leukaemia cell lines. A summary of the main findings are indicated below:

- Whelk GAGs inhibit the growth of negative estrogen receptor (ER<sup>-ve</sup>) breast cancer cell *in vitro* (MDA468 and MDANQ01)
- Whelk GAGs also inhibit the proliferation of cervical cancer cell (HeLa) *in vitro*
- They also inhibits the growth of both erythroleukaemia (K562) and lymphoblastic (MOLT-4) leukaemia cell *in vitro*
- Whelk GAGs cause cell cycle arrests in both leukaemia and breast cancer cell
- Whelk GAGs induce apoptosis in both cervical and leukaemia cell
- Whelk GAGs contain both CS/DS and HS-like GAGs
- Fraction E obtained by ion-exchange chromatography of whelk GAG extracts showed selective anti-cancer activity against breast cancer cell lines.
- Fraction E caused cell cycle arrest and initiated apoptosis in breast cancer cell lines
- Cockle derived GAGs showed selective anti-cancer activity against both erythroleukaemia and lymphoblastic leukaemia cells
- Cockle GAGs brought about cell cycle arrest on lymphoblastic leukaemia cells
- Cockle GAGs induced apoptosis on lymphoblastic leukemia cells

- Cockle GAG extracts contained both HS and CS/DS-like GAGs



## 4.2 Selective anti-cancer activity of cockle GAGs against leukemia cell lines

Previous studies have revealed the anti-cancer activities of some GAG-like compounds, for example, low molecular weight heparin, HS mimetics and some modified CS/DS compounds (Afratis et al 2012 : Babara et al 2012 : Neha et al 2010 : Mellor et al 2007). No studies have linked therapeutic activity of mollusc derived GAGs to anti-cancer activity in breast and leukemic cancer cells. GAG extracts isolated from cockle molluscs had a significant growth inhibitory effect ( $p < 0.001$ ) on erythrocytic leukemic cells (K562) and lymphoblastic leukemic cell (MOLT-4) (fig.3.3A and 3.4A). The recorded  $IC_{50}$  for the two cell lines were 16 (MOLT-4 cell line) and 50 (K562 cell line)  $\mu\text{g/ml}$  respectively. According to the standard criteria set by the National Cancer Institute (Chen et al, 1988; Geran et al, 1972), crude natural product extracts possessing an  $IC_{50}$  of less than 20  $\mu\text{g/ml}$  are considered active against appropriate cancer cell lines.

Cockle GAGs extracts revealed a recorded  $IC_{50}$  of less than 20  $\mu\text{g/ml}$  in MOLT-4 cell proliferation assay and this according to the National Cancer Institute categorise it as an active anti-leukemic cancer drug. Interestingly, this GAG mixture was non-toxic to a normal fibroblast cell line (3T3); a cell line that is frequently used as the model for the cytotoxicity testing in normal cells. Similarly, high concentration of cockle GAG extracts did not show any effect on cell proliferation of MDA468 and MDANQ01 breast cancer cells (fig.3.1A & B). In this regard, the cytotoxicity of this novel GAG was highly selective against K562 and MOLT-4 leukemic cell type and non-toxic to normal cells. It would be interesting to determine the exact biochemical nature of this selectivity and if time had allowed a LC MS/MS proteomic and pathway analysis examination would have been attempted before and after treatment with the crude GAG extracts.

### **4.3 Evidence of broader and stronger anti-cancer activity of whelk GAGs extracts**

Globally, breast cancer is currently one of the leading causes of death and the most commonly diagnosed cancer in women aged below 39 years. Among women aged 35-39 in the UK, around 1,350 cases of breast cancer are diagnosed each year (Breast cancer 1975-2010). Estrogen receptor negative (ER<sup>-ve</sup>) breast cancers are tumours with a distinct natural history, treatment response, and prognostic profile (Wang and Lin 2008). ER<sup>-ve</sup> breast cancers make up 25%–30% of all breast cancers, and their clinical course tends to be more aggressive than that of estrogen receptor positive (ER<sup>+ve</sup>) breast cancers (Wang and Lin 2008). Patients with ER<sup>-ve</sup> breast cancer generally have shorter disease-free survival and overall survival times (Wang and Lin 2008). Most patients with ER<sup>-ve</sup> tumours do not benefit from anti-hormonal therapy, and are also disadvantaged because of the resistance issues associated with many anti-cancer therapies (Wang and Lin 2008). Conventional breast cancer treatment involves surgery that may be coupled with radiation, chemotherapy and systemic adjuvant therapy (Koo et al, 2008).

The approach of modulating tumour progression with drugs that inhibit growth of tumours is one of the new concepts in adjuvant chemotherapy when used alone or in combination with classic anti-tumour drugs (Basappa et al, 2012). Currently, there is great interest in the search for new anti-cancer drugs that can improve patient responses to cancer treatment and reduce the number of deaths, while minimizing the side effects. Certain types of GAG chain have been reported to be potentially useful in cancer therapy and are predicted to have minimal side effects (Basappa et al, 2012).

Our data, which shows selective activity amongst tumour cell lines and normal tissue, would support this idea and the therapeutic use of these GAGs now seems like an even more attractive proposition.

The presence of GAGs in both vertebrates and invertebrates has been attributed to many physiological and biological roles including carcinogenesis and angiogenesis through its interaction with some growth factors and their receptors (Gomes et al, 2010). Yamada and others have reported the isolation of all groups of GAGs including sulfated and non-sulfated from many animals including molluscs (Yamada et al, 2007; Nader et al, 1983; Cassaro and Dietrich, 1977).

The whelk GAG extracts demonstrated unique anti-cancer activity against many cancer cells including Estrogen receptor (ER)-negative breast cancer *in vitro*. It is an extremely important observation for possible intervention in the hard to treat cancers. In contrast to the observed selective anti-cancer activity of cockle GAG extracts against certain cancer cells, whelk GAG extracts, was cytotoxic to all cancer cell lines tested in this work. This GAG extracts demonstrated significant ( $p < 0.001$ ) growth inhibitory effects on both MDA468 and MDANQ01 breast cancer cell with recorded  $IC_{50}$  70.96 and 25.14  $\mu\text{g/ml}$  respectively. The growth inhibitory effect of this novel GAG on the two breast cancer cell lines tested were shown to be dose-dependent and MDANQ01 was more sensitive to the GAG's treatment than MDA468.

These results suggests a possible synergy between the reductase enzyme that is present in MDANQ01 and whelk GAG mixture which may have made the cell line more susceptible to growth inhibitory effects of whelk GAG mixture. It is very likely that other gene difference play a role in the observed selectivity and only a detailed proteomic/transcriptomics and pathway analysis may resolve this. The growth inhibitory activity of whelk GAG mixture was comparable to the effect of cisplatin anti-cancer drug on the two cancer cell lines (Figure 3.9A and 3.10A).

However, the results obtained earlier for similar GAGs extracted from another shellfish (cockle GAG) did not show any inhibitory effect on the proliferation of these breast cancer cells; thereby suggesting that the inhibitory effect may be a unique fine structural feature of the GAGs derived from whelks. In addition, the non-toxic activity of all other commercial GAGs (HS/Heparin and CS/DS) tested along side whelk GAG mixtures on the two breast cancer cell lines suggest that the whelk GAG contains some unique structural features not seen in the commercial GAG samples. These structural features may be a unique pharmacological feature that makes whelk derived GAGs a potential candidate as the basis for a future anti-cancer drug.

Furthermore, whelk GAG Extracts were also cytotoxic to erythrocytic (K562) and lymphoblastic (MOLT-4) leukemic cells (Figure 3.11A&B). The cytotoxic activity of whelk GAG mixture was more pronounced on both cervical (Hela) and erythrocytic leukemic cells with recorded  $IC_{50}$  of 10.47 and 12.57  $\mu\text{g/ml}$  respectively (Figure 3.11 and 3.12). However, a higher  $IC_{50}$  of 49.11  $\mu\text{g/ml}$  was recorded for lymphoblastic leukemia cell but this GAG extract did not show any noticeable cytotoxic activity against normal fibroblast cell (3T3), an indication of selective activity against cancer cell growth. Indeed the differences in  $IC_{50}$  values for the five different cancer cell lines suggests that the whelk GAG mixtures could be selective to certain cell types and this selectivity may well be important in targeting the effects of these molecules towards tumour cells.

Additionally, in breast cancer, changes in GAG and proteoglycan expression on the cell surface and in the ECM allow tumour cells to proliferate, gain the ability to invade surrounding tissues, metastasize to distant organs and induce angiogenesis (Koo et al, 2008). Therefore, a novel exogenous GAG (like the whelk GAG extracts) with unique structural composition may modulate this effect in various ways (see later discussion), which may ultimately leads to growth inhibition observed in this study. The whelk GAG extracts may act

in several ways: by activating (agonists) or inactivating (antagonists) protein-based receptors, competing with endogenous GAGs and/or inhibiting GAG biosynthesis etc. (Ghandi and Mancera, 2010).

This result is also consistent with the findings of Linhardt and others who have identified some new classes of GAG chain-based molecules (neoglycans, low molecular weight heparin, ultra low molecular weight heparin, HS mimicking compound and heparin mimicking compound) with anticancer activity ( Linhardt 2011: Xu et al 2011:Zhou et al 2011) . Whelk GAG extracts show comparative anti-cancer activities to this class of GAG chain-based molecules with similar  $IC_{50}$ . However, native CS and unfractionated heparin did not inhibit cell death in all the cancer cells tested along with the GAG chain drugs: commercial GAGs likewise did not have any growth inhibitory effect on any of the cancer cells tested in this study (Afratis et al 2012: Linhardt and Liu 2012: Borsig et al 2011: Neha et al 2010: Pumphrey et al 2002)

#### **4.4 Selective anti-cancer activity of whelk bioactive fraction E against breast cancer cell.**

It has been reported previously that understanding the fine structure and specific biological roles of GAGs may lead to the development of novel therapeutic approaches (Afratis et al, 2012). In order to study the fine structure of the whelk GAG mixtures, the crude extract was purified by ion-exchange chromatography and the resulting fractions were tested on some cancer cell lines (Figure 3.23 and 3.24). All the fractions eluted were non-toxic to breast cancer cell except fraction E. Fraction E was found to be cytotoxic to both MDA468 and MDANQ01 with recorded  $IC_{50}$  value of 45.98 and 41.89 $\mu$ g/ml respectively. The cytotoxic effect of fraction E on both cancer cell lines was dose-dependent and similar to

the crude extracts. In contrast to the crude extract, fraction E was non-toxic to other cancer cell lines such as HeLa, K562, MOLT-4 and normal fibroblast (3T3) cell.

These results suggest that this fraction E was selective against breast cancer cells, mirroring that results seen for the original crude whelk GAG mixtures and may possess a unique structure that inhibits the growth of breast cancer cell lines tested in this study (see later discussion). The results with fraction E suggest that this fraction is the bioactive component responsible for the anti-cancer activity of whelk GAG extracts, at least those seen with the breast cancer cell lines. Further understanding the exact structural features seen in this particular fraction may open a new therapeutic approach to cancer therapy.

#### **4.5 Molecular mechanism of action of cockle GAG extracts on leukaemia cell lines**

Recently, cell cycle analysis has been used to identify a molecular target for new anti-cancer drugs (Basappa et al, 2012; Dawson et al, 2008; Marks 2007 and Tiligada et al, 2002). Cellular proliferation is mediated primarily by cell cycle which consists of four distinct sequential phases (G<sub>0</sub>/G<sub>1</sub>, S, G<sub>2</sub>, M). They are controlled by cellular signalling regulatory mechanisms involving a family of proteins that have variable level of expression according to the stage of the cell cycle (van den Heuvel 2005; Jack and Weinberg, 1996).

Perturbations in cell cycle regulation are reported as one of the most common features of the transformed cell (Weinstein, 1996), which could be associated with gain of function for uncontrolled growth due to enhanced expression of growth-factor-receptor autocrine loop (Earp et al, 1995). Several therapeutic agents including some anti-cancer drugs, such as DNA-damaging drugs, microtubule inhibitors, anti-metabolites, and topoisomerase inhibitors, take advantage of disruption in normal cell cycle regulation to target checkpoint controls and ultimately induce growth arrest or apoptosis of tumorigenic cells.

Leukemia cells are known to be very sensitive to any chemotherapeutic agents/drug that either disrupt the cell cycle or cause apoptosis (Askoy et al 2008). Some of these chemotherapeutic agents cause leukemia cell death through usual DNA disruption, while others cause cell death by programmed cell death (apoptosis); a key player in the balance between cell replication and cell death (Feng et al 2007). Many chemotherapeutic agents are effective on the cells that are in the S phase of the cell cycle (Askoy et al 2008). However, other chemotherapeutic agents such as artemisinin mainly arrests the cell cycle in the G1 phase, while paclitaxel and lycorine were shown to arrest the cell cycle in the G2/M phase and induce apoptosis by increasing the activation of caspase-8, caspase-9, or caspase-3 (Pezuto et al 1997). Similarly, an increase in the percentage of cells in the G2/M phase upon treatment with sulforaphane was observed in HT29 human colon cancer cells as well as in Jurkat T-leukemia (Singh et al 2004). Cisplatin also causes cell cycle arrest at both the G1/S and G2/M checkpoints (Roberts and Thompson, 1979).

In the present study, cockle GAG extracts caused time-dependent disruption in lymphoblastic leukaemia cell cycle regulations, resulting in G1 and G2/M-phase arrest with a concomitant marked reduction of cells at S-phase. This result is consistent with the cell cycle arrest caused by many other chemotherapeutic agents listed above which is primarily caused by the accumulation of the chemotherapeutic agent. The ultimate effects might mediate DNA strand breaks, which can cause the failure of DNA repair and subsequent arrest of the cell cycle during the G1 and G2/M-phase. This result is also similar to the actions of other chemotherapeutic agents which commonly intervene at multiple points in the cell cycle.

These drugs have been reported to have diverse mechanisms of action and exhibit specificity in terms of the stage of the cell cycle in which they have activity (Johnson and Walker, 1999). This type of checkpoint arrest (G1 and G2/M) is common to some DNA damage anti-cancer drugs like cisplatin and is one of the most established chemotherapeutic

approaches in cancer treatment (Roberts and Thompson, 1979). Zhan et al. reported the mechanisms of actions of cisplatin cell cycle arrest at G1 phase is mediated by p53, which induces an increase in p21, resulting in inhibition of cyclin/cdk2 and cyclin/cdk4 complexes and hypophosphorylation of Rb (Zhan et al, 1993). The G2/M checkpoint induced by DNA damage can occur by either p53-dependent or -independent mechanisms (Zhan et al, 1993). Both p21 and phosphorylation of cdk1 is required for entry into M and can participate in the DNA damage G2/M checkpoint.

Fan and his co-worker also reported that tumour cells in which *p53* is inactive can bypass the G1/S checkpoint and exhibit increased sensitivity to DNA-damaging agents such as cisplatin (Fan et al, 1997) as a result of failure to arrest and repair their damaged DNA. These researches indicated that chemotherapeutic agent causes cell cycle arrest at both G1 and G2/M phase of the cell cycle similar to what was observed in the present study.

Therefore the G1 and G2/M cell cycle arrest cause by cockle GAG mixture on leukemia cell may predictably has a similar mechanism of actions described by Zhan and Fan above.

Unfortunately, the cell cycle regulators (cyclins and cdk's) that control G1 and G2/M check points were not done during this project work and this may perhaps provide a better explanation for the mechanism of cell cycle arrest caused by cockle GAG extracts. This finding indicates that the cell growth inhibitory effect of cockle GAG extracts on leukaemia cells is due, in part, to its cell cycle arrest. The mechanism underlying the cell cycle arrest effect of cockle GAG mixtures remains unclear and this can easily be resolved by investigating the cell cycle regulators that control the transition of cell at G1, G1/S (CDK2, CDK4, cyclin E and D and CDKI's) and G2/M (CDK1, cyclin A and B) phase using western blotting analysis.



#### **4.6 Molecular mechanism of action of whelk GAG extracts on breast cancer cell**

The perturbation of normal cell cycle controls, which is the hallmark of cancer, provides numerous opportunities for targeting checkpoint controls to develop new therapeutic strategies for this disease. Such strategies include induction of checkpoint arrest and arrest of proliferating cells at various stages of the cell cycle, which may sensitize them to treatment with other therapeutic agents such as radiation, and targeting of therapies towards specific regulatory components of the cell cycle (Johnson and Walker 1999).

Matsui et al reported S-phase arrest caused by methotrexate and 5-fluorouracil, a known DNA-damaging agent that inhibit DNA synthesis (Matsui et al, 1996). Lowel et al also reported that tumour cells in which p53 is inactive, DNA damage induced by these drugs goes undetected, and cells progress to G2 and subsequently undergo apoptosis (Lowel et al, 1993). Heparin GAG has shown antihypertensive, anti-inflammatory, anticoagulant in different human cells including vascular smooth muscle cells (VSMC) (Leverand Page 2002). Castellot and other groups demonstrated the antiproliferative activity of heparin on VSMC, hepatoma and ovarian epithelial cell (Patel et al 2002: Fedarko et al 1989: Castllot et al 1985). It is generally accepted that heparin and heparin like GAGs including HS biological activities is linked to their structure (SAR). However, Wright and other research groups suggested the antiproliferative effect of heparin on VSMC was due to its ability to bind VSMC surface receptor, accumulation within the cell and cell cycle arrest at both G0/G1 and S phase (Reily et al 1996: Wright et al 1985). Scarffe et al, similarly reported an increase in the percentage of cells in the G2/M phase upon treatment with sulforaphane in HT29 human colon cancer cells as well as in Jurkat T-leukemia (Scarffe et al 1980).

Askoy et al in his recent in vitro work reported antiproliferative effect of heparin on lymphoblast. They demonstrated that heparin induces cell cycle arrest of lymphoblast at both

G2/M and S phase in a dose and time dependent manner. Hence, suggested that the antiproliferative effect of heparin on lymphoblast was mediated by cell cycle arrest at both G2M and S phases, and the prolonged effect of the cell cycle arrest could play a role in cell progression and proliferation (Aksoy et al 2008). These researches indicated that chemotherapeutic agents including heparin GAG elicit their antiproliferative effect partly by inducing cell cycle arrests at different stages of the cancer cell cycle. It is also shown that heparin GAG elicit its antiproliferative activity by binding to its receptor on the cell surface; accumulating within the cells and cell cycle arrests at different phases of the cell cycle.

In the present study, Whelk GAG extracts and the purified fraction E caused consistent perturbation in breast cancer cell cycle control, which ultimately resulted into cell cycle arrest at S and G2/M-phase. S-phase arrest is suggestive of cell inability to replicate, which could abrogate the progression of cell cycle to the mitotic stage, the penultimate event in the cell cycle. This GAG extracts and it's purified fraction E induces cell cycle arrest of both MDANQ01 and MDA468 breast cancer in a dose and time dependent manner (Figure 3.15-16 and 3.26&27). This result is consistent with the work of Aksoy et al on heparin GAG cell cycle arrest on lymphoblast.

Heparin is a well established GAG that is structurally similar to HS and both crude whelk and purified fraction E is a novel HS-like GAGs isolated from shellfish. The comparative effect of heparin, crude whelk and purified fraction E GAGs on cell cycle arrests may be structurally originated, however, it is difficult to conclude on this note unless a comprehensive structural elucidation of the crude and purified fraction E is done. Additionally, this result suggest that antiproliferative effects of both crude whelk and purified fraction E GAG was mediated by cell cycle arrest at both S and G2/M phase and the

accumulative effect of the cell cycle arrests could play a role in the cell cycle progression and cell proliferation.

#### **4.7 Cockle GAG mixture inhibit proliferation of MOLT-4 leukaemia cell partly by apoptosis**

Apoptosis is another familiar molecular target for new anti-cancer drugs. Apoptosis detection is of great importance in cancer research because the balance between cell proliferation and apoptosis shifts towards cell proliferation in cancer cell lines. Cancer results from the imbalance between cell proliferation and apoptosis (Wesselborg et al 1999). Therefore there is an active search for the most efficient and safe anti-cancer treatments that induce apoptosis in immortal cancer cells (Coppola et al, 2008).

Cockle GAG extracts only induced marginal early apoptotic effect on MOLT-4 leukaemia cell as shown in Figure 3.8. The apoptotic effect of cockle GAG extracts was noticeable between 24 and 48 hours post incubation. Apoptosis plays a major protective mechanism against cancer (Zhou et al 2004) and this result shows that cockle GAG extract can induce apoptosis on MOLT-4 cells. This finding is consistent with the apoptotic effects seen with chemically modified GAG chains and heparin on lymphoblast and other carcinoma as described by Erduran and other research groups (Erduran et al 2007: Erduran et al 2004: Pumphrey et al 2002: Li et al 2001: Erduran et al 1999: Manaster et al 1996). Manaster and other research groups have earlier reported the apoptotic effect of heparin on various human cells including peripheral blood neutrophils, lymphoblasts and mononuclear cells. They also suggested that heparin apoptotic effect of lymphoblasts was via an extrinsic pathway of apoptosis (Erduran et al 2007: Eduron et al 2004: Erduron et al 1999: Manaster et al 1996). Pezuto et al also reported the apoptotic effect of paclitaxel and lycorine, (known

chemotherapeutic agents) and they demonstrated that the antiapoptotic effect of these drugs were due to increase activation of caspase-3, 8 and 9 (Pezuto et al 1997). Erduran et al in their work demonstrated that low dose of heparin (20 U/mL) causes apoptosis in the lymphoblast and this low concentration also cause a high expression of Fas and a low expression of Bcl protein-2 in the lymphoblast (Erduran et al 2004). This was contrary to the in vitro work of Manaster and coworkers who reported apoptotic effect of heparin at very high concentrations (50-200 U/mL) (Manaster et al 1996). In another recent in vitro study, caspase 3 and 8 activation levels were investigated and it was shown that heparin induce apoptosis of the lymphoblasts and activation of caspase-3 and -8 (Eduvan et al., 2007)

Li et al in their work reported that heparin induce apoptosis in human nasopharyngeal carcinoma cell (CNE2) and demonstrated the apoptotic effect of heparin on this cell may be probably regulated by increased expression of c-myc and the rates of bax/ bcl-2. They suggested heparin may function as an inducer of apoptosis in carcinoma cells (Li et al 2001). These researches indicated that low-dose heparin caused significant levels of apoptosis of lymphoblasts, and apoptosis was found to increase with increased heparin levels.

It is thus suggested that the growth inhibitory effect of cockle GAG extracts on leukaemia cells is due, in large part, to cell cycle arrest and apoptosis. The apoptotic effect of cockle GAG on leukemia cell is consistent with the apoptotic effect of low concentrations of heparin on the lymphoblast and the cell cycle arrest cause by cockle GAG may provide an insight to the molecular mechanism of the apoptotic effect this novel GAGs.

#### **4.8 Crude and purified whelk GAG extracts inhibit cancer cell growth by apoptosis, analysis by annexin V staining**

Apoptosis is characterised by cell shrinkage, condensation of the nuclear chromatin, and fragmentation of the nucleus and the apoptotic bodies (Hoffbrand, 1998; Kroemer et al, 1997). The biochemical event that characterises apoptosis and appears to be related to the nuclear condensation and fragmentation is double-stranded cleavage of DNA internucleosomal sites (Koury, 1992; Arends et al, 1990).

Apoptosis is also characterised by membrane damaged, leading to a subsequent leakages of the phosphatidylserine into the outer membranes layers and Annexin V is a recombinant phosphatidylserine-binding protein that binds strongly and specifically to phosphatidylserine residues. Only the apoptotic cells are expected to stain positive for annexin V-FITC at the early stage of apoptosis while the necrotic cells stain positive for PI. However, at late apoptosis stage, the damaged cells are expected to stain positive for both PI and annexin V-FITC stains because at late apoptosis, the cells can be killed via apoptotic or necrotic pathway and distinguishing between the two processes may be difficult.

The work presented in this project has demonstrated that both crude and ion – exchange purified whelk GAG extracts can induce time-dependent apoptosis on certain cancer cell lines. Crude whelk GAG extracts induces time-dependent apoptosis on both breast cancer cells (MDA468 and MDANQ01) and cervical cell (HeLa) as shown in Figure 3.17, 3.21 and 3.22. Interestingly, the apoptotic effect of crude whelk GAG mixture was more pronounced on cervical cell with apoptotic cell population of about 50-70%. Consistently, the purified fraction E induced mild but not statistically significant ( $P>0.05$ ) late apoptosis and necrosis effect on both MDANQ01 and MDA468 cells with time-dependent increase in the number of late apoptotic cells in MDA468 cell. Concisely, DAPI Fluorescent microscopy

results also showed some cells with morphological changes that characterised late apoptosis (Figure 3.18 and 3.22). These results are consistent with the findings of Wengers and other researchers on low molecular weight GAGs and other GAGs mimetics. The work of Wengers and others showed that low molecular weight heparin elicit their anticancer activities on pancreatic cancer by apoptosis induction (Wenger et al 2009). Erduran and others have also reported apoptotic effect of heparin on different human carcinoma and lymphoblast (see section 4.7). The difference in pharmacological activities of low molecular weight GAGs and the unmodified GAGs have been attributed to their enhanced bioavailability which facilitates their uptake into the cells (Lindhardt et al 2004).

Conclusively, the apoptotic effect of whelk GAG mixture on the two mammalian cells appears to be largely associated with cell cycle arrest, DNA fragmentation, and externalization of phosphatidylserine lipids. The cell cycle arrest cause by these GAG extracts and its purified fraction E can also provide a great insight into the molecular mechanism of action of apoptotic effect of crude whelk and purified fraction E. Conversely, it is worthwhile, to investigate the activation level of the apoptotic proteins (bcl-2 and bax) as well as caspase 3, 8 and 9. This will provide more insight into the molecular mechanism of apoptotic effects of this novel GAGs.

#### **4.9 PAGE and size exclusion analysis of cockle GAG mixture**

Size exclusion assay results shows that the crude cockle extracts contain different GAG structures with varying chain sizes and ionic properties ( $\text{COO}^-$  and  $\text{SO}_3^-$ ). Although the peaks from the gel filtration analysis were not extensively studied in this present work, the densitometry analysis of the cellulose acetate dot blotting assay classified the fractions into two broad peak according to their sizes/charges. GAGs are negatively charged polymers

consist of repeating units of disaccharides containing one uronic acid or galactose and one *N*-acetylglucosamine. The variation in charge may be very large since each disaccharide is more or less sulfated. The ionic bonding between cationic dyes (Azure A) and the negatively charged GAGs are generally thought to be proportional to the number of negative charges present on the GAG chain i.e. both sulfate and carboxyl groups (stone et al, 1994). The azure A dye was only bound to the sulfated polysaccharide because of the suitable arrangement of GAG ionic sites for interactions with the dye dimer but was not found to bind with other compounds including proteins (Samir and Kost 2000). Hence, the wells stained with azure A dye in the present work suggest the presence of GAGs with varying concentrations and different sulfation levels. Electrophoresis mobility of the cockle GAG samples on PAGE was visualized with azure A staining.

Additionally, slight variations in mobilities between the crude and depolymerised samples were also observed. Difference in electrophoretic mobility of the various intact GAG chains is an indication of distinctive structures present within these polysaccharides (Vijayabaskar and Somasundaram 2012). The GAG extracts isolated in this study was compared with commercial GAGs (HS, CS/DS) (Figure 3.34&3.36) to initially determine the typical chain lengths and general level of sulfation from the mollusc derived GAG samples. Dietrich and other researchers showed that sulfated polysaccharide had different electrophoretic mobilities for different buffer system, depending on the structure of the polysaccharide (Mariana and Barbara 1999; Dietrich et al 1989). PAGE analysis results supported the evidence that crude cockle extracts did indeed contain GAGs and the GAGs-like compound isolated contained CS/DS and HS-like members of the GAG family.

However, the exact nature of the structural differences between typical commercially available porcine HS, CS, DS and the mollusc derived GAGs remains to be determined. This will be critical in determining the exact nature of the biological activity of the mollusc

derived GAGs. It is assumed that there must be subtle structural differences in these GAG chains that do not appear in the commercially available GAGs which did not show any cellular toxicity on the cancer cell lines tested in this study. The bare minimum for investigating structural differences in GAG chains is to perform a disaccharide analysis where the GAG chains are chemically or enzymatically reduced to their constituent disaccharides and then individually quantified by strong ion-exchange chromatography. This data will at best only provide limited information on structure activity relationships attributed to these GAGs. It will take many years to determine the exact nature of the GAG binding sequences involved in these observed anti-cancer activities.

#### **4.10 SAX-HPLC and gel-filtration of cockle GAG extracts**

SAX-HPLC analysis of chondroitinase ABC lyase digest confirmed the presence of three major disaccharide components in the crude cockle GAG mixture. The non-sulfated disaccharide ( $\Delta$ UA-GalAc) has the highest composition, in contrast to the commercial CS/DS in which this disaccharide was absent. The two most abundant CS/DS mono-sulfated disaccharides [ $\Delta$ UA-GalNac (6S) and  $\Delta$ UA-GalNac (4S)] were also present in the same proportion in the crude GAG mixture, whereas the commercial CS were found to contain high level of  $\Delta$ UA-GalNac (6S) and a low level of  $\Delta$ UA-GalNac (4S) disaccharides. This unique structural composition formed the major difference between the crude cockle CS and the commercial CS GAGs.

This result also suggests that this crude GAG extracts contains less sulfated CS-like GAGs: this slight structural modification may in part contribute to its growth inhibitory effect on leukaemia cells. Predictably, the anti-tumour activity of this crude GAG extracts



may in part due to the unique structural composition of its CS-like chain and the possible explanation for this bioactivity may be linked to the suggestion of Asimakopoulou and coworkers in his comprehensive review on biological Role of Chondroitin Sulfate in Cancer and Chondroitin-based Anticancer Agents. He suggested that the important roles play by this GAG molecule in cancer biology may be attributed to their involvement in various interactions with tumour cells and other effective molecules, such as growth factors and also affects several signaling pathways (Asimakopoulou et al, 2008). He also stressed the need for proper understanding of the biological role of CS in cancer, tumour angiogenesis and invasion. This suggestion has favoured the development of novel drugs which target the tumour cells and the interactions with other effective molecules of the ECM or the cell surface (Asimakopoulou et al, 2008).

Similarly, Kozlowski and other groups have reported an isolation of dermatan sulfates from *S. plicata* and *P. Nigra*. This DS was found to contain the same disaccharide core structure  $[\alpha\text{-L-IdoA}(2\text{SO}_4)\text{-}1\rightarrow 3\beta\text{-D-GalNAc}]_n$ , but sulfated at carbon 4 or 6 of the GalNAc residues, respectively (Kozlowski and Pavao, 2011; Kozlowski et al., 2011). Both ascidian dermatan sulfates regardless of the position of sulfation on the *N*-acetylgalactosamine drastically attenuate metastasis of both MC-38 colon carcinoma and B16-BL6 melanoma cells, and the infiltration of inflammatory cells in a thioglycollate peritonitis mouse model (Kozlowski and Pavao, 2011; Kozlowski et al., 2011).

Pumphrey and co-workers has also reported similar role of a novel modified CS molecule (neoglycans) on cancer cells. This molecule was found to reduce cell viability by induction of apoptosis of myeloma and cancer cells *in vitro*. Pumphrey in his work also reported that, EDAC-modified CS reduced or abolished tumour growth, when injected directly into breast tumours growing in nude mice (Asimakopoulou et al, 2008; Borsig et al, 2007; Pumphrey et al, 2002).

Several studies have reported the role of CS in promoting tumour growth and mediating events that enhance tumour invasion and metastasis effects that can be abolished by chemically modified CS, or the use of CS with altered sulfation patterns (Asimakopoulou et al, 2008; Borsig et al, 2007; Pumphrey et al, 2002). Some of these studies have proved the potential use of modified CS as a potent anti-cancer agent. Although the cockle derived CS chains appear to have an unusual disaccharide composition in comparison to commercial porcine CS, we cannot confirm absolutely that the link between these differences and the anticancer activities seen in this study.

Moreover, differences in HS structure have already been implicated in this study as being linked to the cockle GAG extracts anti-cancer activities. Structural studies of cockle GAG extracts also implicated HS in the biological activity seen on cancer cells. Quantitative and qualitative analysis of HS oligosaccharides mapping was performed by depolymerising cockle GAG extracts with a mixture of Heparinase I, II and III and then analysing the resulting unsaturated oligosaccharides by SAX-HPLC chromatography. The most important differences seen between the commercial HS GAGs and cockle extracted HS-like GAG chains is the absence of  $\Delta$ UA (2S)-GlcNAc, disulfated  $\Delta$ UA(2S)-GlcNAc(6S) and the trisulfated  $\Delta$ UA(2S)-GlcNS(6S). A very low level of  $\Delta$ UA-GlcNS (6S) and  $\Delta$ UA (2S)-GlcNS was also observed in the crude GAG mixture.

Thus, these result suggests that cockle GAG mixture contain low sulfated HS-like GAG with low 2 O sulfate group because of the absence of trisulfated  $\Delta$ UA2S (1 $\rightarrow$ 4) GlcNS6S and disulfated  $\Delta$ UA2S (1 $\rightarrow$ 4) GlcNAc6S disaccharides. PAGE analysis and TSK gel-filtration results confirmed the presence of HS-like disaccharides in the heparinase digested cockle GAG extracts.

This is an extremely unusual disaccharide compositional analysis for HS. Many studies have reported the isolation of HS-like GAGs with various disaccharides compositions

from different molluscs. Dietrich and coworkers in their work isolated highly sulfated HS-like GAGs from various molluscs, in contrast to the usual low sulfated HS-like GAGs that are usually isolated from molluscs (Volpi and Maccari 2005; Kim et al 1998; Dietrich et al 1989). Vijayabaskar and other groups had previously reported an isolation of HS-like species from molluscs (Vijayabaskar and Somasundaram, 2012; Cesaretti et al, 2004; Jordan et al, 1986 and Dietrich et al, 1985). Pejler et al also reported the isolation of HS-like GAGs containing a large amount of GlcN (3-*O*-sulfate) disaccharide from clam molluscs. This disaccharide unit is a unique marker for the antithrombin-binding region of heparin/HS disaccharide and it showed a similar antithrombin activity with unfractionated heparin (Pejler et al 1987). Chi and his co-workers in their work reported an isolation of HS with a unique structure, containing IdoA (2-*O*-sulfate)-GlcNAc as its major repeating disaccharides sequence (Acharan sulfate) from African giant snail (Chi et al 2006; Kim et al 2004). HS-like GAGs with unique disaccharide units composed of of *non*- sulfated, 2-*O*-sulfated or 3-*O*-sulfated GlcA as well as 2-*N*-sulfated and/or 6-*O*-sulfated GlcN has also been isolated from the bivalve *Nodipecten nodosus* (Gomes et al 2010). Interestingly, none of the above HS-like GAGs has been shown to have any anticancer activity.

In addition, Dreyfuss and co-workers recently reported an isolation of heparin mimetics with low 2 *O* sulfate group (similar to what was observed in this study) from shrimp. This HS structural mimetics was shown to have anti inflammatory and anti angiogenesis activities. It was clearly shown that the biological activity of this heparinoid was due to its ability to interact with angiogenic growth factors such as FGF-2. He also linked the antiangiogenic effect of this novel GAG to the presence of low content of 2-*O*-sulfate groups in the shrimp heparin like GAG which in a similar manner to the 2-*O*-desulfated-heparin, could competitively inhibit the interaction between growth factors and cell surface HS proteoglycans (Dreyfuss et al 2010). Unfortunately, Dreyfuss failed to investigate the

anticancer activity of this HS mimetics and this present study has critically investigated the anticancer activity of this unique HS-like GAG from cockle. The presence of low 2 *O* sulfate groups was also observed in the HS like GAG isolated from cockle GAG and this structural modification may explain the anticancer activity of this unique GAG.

Furthermore, there was a decrease of the specific sulfatation in position 2 of the glucuronic acid unit with a strong increase of the disaccharides bearing non-sulfated glucuronic acid and glucosamine. This decrease may also in part contribute to the inhibitory effect of cockle GAG mixture on leukaemia cells due to important role of 2-*O*-sulfated IdoA in HS-binding to FGF-2 a known survival factor for leukaemia cells grown in culture (Liuzzo and Moscatelli 1996). Walker and others had earlier reported that structurally defined oligosaccharides from HS that are rich in IdoA (2S)-containing disaccharides bind strongly to FGF-2 and that the affinity for FGF-2 increases with oligosaccharide length and IdoA (2S) content (Walker et al, 1994; Ishihara et al, 1993; Maccarana et al, 1993; Habuchi et al, 1992 and Turnbull et al, 1992).

The presence of 2-*O*-sulfated IdoA has also been reported to be required for the promotion of the growth-factor's mitogenic activity. It is also noteworthy that extracted cockle HS-like GAGs might be competed with the endogenous HS GAGs in the binding of growth factors such as FGF-2 or blocking specific interactions of the cancer growth factors (e.g.FGFs) with their receptors resulting into cell growth inhibition. It has previously been shown that GAG-based drugs elicit their pharmacological effect in several ways: by activating (agonists) or inactivating (antagonists) protein-based receptors (e.g.FGF-2), competing with endogenous GAGs and/or inhibiting GAG biosynthesis (Gandhi et al., 2010).

Intriguingly, there is evidently a role for FGF-2 in haematopoiesis and the K562 leukaemia cell line has previously been shown to express HSPG's that bind strongly to FGF-2, therefore, this may be involved in modulation of its biologic activities (Olwin and

Rapraeger, 1992 : Flaumenhaft et al, 1982). HS is also necessary for the long-term biologic activity of FGF-2, the presence of HSPGs in the K562 cell line could have significant effects on the ability of these cells to respond to FGF-2 by promoting the formation of the FGF-2/HS/TK-receptor ternary signalling complex, hence promoting cell growth (Liuzzo and Moscatelli 1996).

Structural variations between K562 HS and cockle GAG HS may impinge on the ability of FGF-2 to bind its TK cell surface receptors, thereby inhibiting cell proliferation and functions, thus, this may manifest itself partly in the anticancer activities seen with cockle GAGs on the K562 cell line.

Taken together, previous data discussed above and the results reported here strongly suggest that the novel GAGs isolated from cockle is capable of sequestering the growth factors, making them unavailable for the interaction with their receptors and thus inhibiting tumour cell proliferations. Thus, the pharmacological and biochemical properties of cockle GAG, such as anti cancer activity against leukemic cells with a very low IC<sub>50</sub> point to this compound as a compelling drug candidate for treating cancer disease.

#### **4.11 Ion- exchange fractionation of crude whelk GAG mixture**

The process of ion-exchange chromatography helped to enhance the activities of the crude whelk GAG extract by removing the unwanted salt contaminant from the GAG preparation (Saravanan et al, 2010). This partial purification of whelk GAG extracts has allowed a better understanding of the structural compositions of these whelk derived GAG chains. The ion-exchange chromatogram for crude whelk GAGs was shown in Figure 3.23. GAG chain sub-populations were eluted as a number of well defined peaks ranging from 0.9-3.0M NaCl gradient. Although, the fractions were not studied extensively in this project , in

terms of this exact structural composition, we did however identify from the chromatogram the bioactive fraction E on DEAE column. This has proven to be very informative in determining the active GAG family member in the whelk GAG extracts. It also suggested that this fraction contained high charge density, high molecular weight and or high sulfated polysaccharide chains based on its late elution position in the NaCl gradient.

This speculation was confirmed by the superose-12 size exclusion result, which clearly showed fraction E to be comprises of very high molecular weight polysaccharide chains (Figure. 3.42). Fraction E is similar in structural terms to the HS/ heparin-like fraction isolated from other molluscs (Andrade et al, 2013:Vijayabaskar and Somasundaram, 2012: Moses et al, 2002: Mariana and Barbara 1999). Although the anti-inflammatory, anticoagulant and anti-angiogenic potentials of these HS-like GAGs isolated from molluscs have been well documented, there is no information on their potential use as anti-cancer drug. However, Giulianna and others were concentrating solely on the anticoagulant activity of this fraction but failed to test the activity of this novel polysaccharide on cancer cells.

Interestingly, the result obtained in our study from the biological activity of this novel fraction showed its important role in cancer cell death and this is certainly encouraging as a platform for the future development of the whelk GAGs as an anti-cancer drug.

#### **4.12 PAGE and size exclusion analysis of both crude and ion-exchange purified whelk GAG extracts**

PAGE analysis of both crude and purified whelk extracts confirmed them to be GAG-like in nature. The electrophoresis mobility of both the crude and ion- exchange purified fractions showed that they both contained different members of the GAGs family of

polysaccharides with different structural composition. Electrophoresis mobility of the sample on PAGE was visualized with azure A staining.

There were notable differences in the electrophoretic mobility between intact samples and enzyme/chemically depolymerised GAG samples as the depolymerised samples contain smaller oligosaccharides that were capable of migrating faster than the crude sample. This gives us a rapid means of determining the presence of individual GAG family members such as HS, CS and DS in extracts taken from mollusc tissue samples. The electrophoretic mobility of the crude GAG extracts also showed difference in mobilities when compared with commercial porcine GAGs and this suggests a possible variation in both sulfate content and average chain length of GAGs derived from both sources (see next section for further details)

Difference in electrophoretic mobility of the various GAGs is certainly an indication of distinctive structures within these mollusc derived polysaccharides in comparison to the porcine derived GAGs (HS,CS and DS) which showed no anti-cancer activities with the cell lines tested in this study (Figures 3.34&3.36). Dietrich et al and Mariana and Barbara showed that a sulfated polysaccharide had different electrophoretic mobility for different buffer system, depending on the structure of the polysaccharide. Overall PAGE analysis results supported the evidence that both crude and purified whelk GAG contain GAGs and the GAGs-like compound isolated were CS/DS and HS-like GAGs.

Size exclusion assay results confirmed both crude and purified whelk fractions contain different GAGs family members with widely varying sizes and ionic properties ( $\text{COO}^-$  and  $\text{SO}_3^-$ ). Although the fractions obtained from the superose-12 gel filtration experiments were not extensively studied in the present work the densitometry analysis of cellulose acetate dot blotting assay confirmed the presence of strongly anionic

polysaccharides as a result of Azure A dye binding, which could be classified into five broad peak according to their sizes.

GAGs are negatively charged (anionic) polymers consist of repeating units of disaccharides containing one uronic acid or galactose and one *N*-acetylglycosamine. The variation in charge may be very large since each disaccharide is more or less sulfated and control of disaccharide composition is complex. The ionic bonding between charged dyes such as Azure A and the negatively charged GAGs are generally thought to be proportional to the number of negative charges present on the GAG chain, i.e., both sulfate and carboxyl groups (stone et al, 1994).

The azure A dye was only bound to the sulfated polysaccharide because of the suitable arrangement of GAG ionic sites for interactions with the dye dimer but was not found to bind with other compounds including proteins (Samir and Kost 2001). Hence, the dots stained with azure A dye in the present project work suggest the presence of GAGs with varying concentration and different sulfation level seen in the crude GAG extracts.

#### **4.13 SAX-HPLC and gel-filtration of whelk GAGs**

The qualitative and quantitative analysis of chondroitinase ABC lyase depolymerised whelk GAG mixture shows two distinct peaks when resolved by ion-exchange chromatography and their elution positions vary considerably from the commercial CS/DS GAGs oligosaccharides. The two fractions B and C derived from anion-exchange chromatographic analysis were the only two peaks from the ion exchange column that were sensitive to chondroitinase-ABC enzymes and the resulting oligosaccharides mixtures resolved by SAX-HPLC shows that fraction B contain non-sulfated  $\Delta$ UA-GalNac as its major disaccharides



peak and a low level of mono-sulfated  $\Delta$ UA-GalNac(4S). This is significantly different to the disaccharide composition analysis seen with the commercial CS/DS. The disaccharides composition of whelk fraction B is very similar to CS previously isolated from *D. melanogaster* (Toyoda et al., 2000). Many other studies have reported isolation of CS/DS with unique disaccharides compositions from invertebrates (Adamczyk et al 2010: Vilela-Silva: Pavao et al 1998: Pavao et al 1995 ), however, the disaccharide compositions of these invertebrates CS/DS are slightly different from whelk fraction B CS in terms of sulfation pattern and level.

The whelk Fraction C peak matched the elution position of commercial CS/DS when applied to the ion-exchange column which suggested a more traditional disaccharide composition for this whelk GAG sub-fraction. This prediction for the disaccharide composition of whelk fraction C was confirmed by chondroitinase ABC lyase digestion and the subsequent as resolved by SAX-HPLC showed two major disaccharides peaks eluted at the same time with similar elution pattern to the commercial CS GAGs. Furthermore, crude whelk GAG mixtures were also degraded by chondroitinase-ABC enzymes and the major disaccharides peaks shown were  $\Delta$ UA-GalNac6S and  $\Delta$ UA-GalNac4S disaccharides. The elution pattern and the retention time was also similar. It is noteworthy that crude whelk GAG mixtures and its purified fractions B and C contain low sulfated CS/DS disaccharides.

The CS disaccharides compositions of both crude and whelk fraction C is very similar to the CS isolated from Ascidians by Xu et al. This GAGs has been reported to have anti inflammatory activity, however, the author failed to investigate the anticancer activity of this unique GAGs (Xu et al 2011). Although, most CS isolated from many invertebrates are more sulfated than whelk CS and they are structurally different in terms of sulfation level and pattern, hence, no anticancer activities has been reported for any of these GAGs (Adamczyk et al 2010: Vilela-Silva: Pavao et al 1998: Pavao et al 1995). The structural differences

between other invertebrates CS and whelk CS, couple with the low sulfation composition of whelk CS may in part explain the anti cancer activity of this unique GAGs, more studies are needed to substantiate this speculation.

#### **4.14 SAX-HPLC and gel-filtration of whelk bioactive fraction E**

Qualitative analysis of HS/Heparin GAGs contained in the purified whelk fraction E was performed by depolymerisation with a mixture of heparinase's I, II and III and with the resulting unsaturated oligosaccharides analysed by SAX-HPLC. The whelk derived GAG fraction E contains six oligosaccharides peaks in contrast to the commercial HS, which contained eight standard disaccharides peaks. The major peak was assigned to non-sulfated disaccharide  $\Delta$ UA - GlcNAc. Other peaks were assigned to  $\Delta$ UA-GlcNS,  $\Delta$ UA-GlcNAc (6S),  $\Delta$ UA-GlcNS(6S),  $\Delta$ UA(2S) (1 $\rightarrow$ 4) GlcNAc(6S) and  $\Delta$ UA(2S) GlcNS(6S) disaccharides respectively. However, both  $\Delta$ UA (2S)- GlcNAc and  $\Delta$ UA(2S)GlcNS disaccharides were completely absent in this polymer and this is the major difference between the novel fraction E and the commercial GAGs.

Andrade et al in their recent work report an isolation of high sulfated HS/heparin GAG from the crab *G. Cruentata* mollusc. They demonstrated that the crab HS/heparin GAGs present intermediate structure between heparin and heparan sulfate. In addition, the crab heparin-like is rich in 2-*O*-sulfated glucuronic acid residues, possesses low levels of trisulfated disaccharides ( $\Delta$ UA (2S) GlcNS (6S) and lacks the defined pentasaccharide structure related to the antithrombin binding site (Andrade et al 2013). Brito et al in their work also isolated another HS/heparin from the shrimp. The shrimp contains mainly blocks of disulfated disaccharide units containing glucosamine *N*-sulfated/*6-O*-sulfated linked to

glucuronic acid [ $\Delta$ UA-GlcNS (6S)]. Sulfated regions consisting of glucosamine *N*-sulfated linked to iduronic acid 2-O-sulfated ( $\Delta$ UA (2S) GlcNS) are also present (Brito et al 2008). A recent work of Brito and co-workers also reported the isolation of another novel GAG with different HS/heparin like structure from shrimp head *L. vannamei*. The novel GAG from shrimp head possesses a high degree of *N*,6-sulfation and minor *N*-acetylation together with the high content of glucuronic acid and an absence of non-sulfated iduronic acid (Brito et al 2014).

These researches show that HS/heparin with unique disaccharides entity are isolated from different molluscs and the presence of high percentage of non sulfated disaccharide  $\Delta$ UA - GlcNAc (60%) suggests that this GAG is more of HS like. The presence of disulfated disaccharide  $\Delta$ UA-GlcNS(6S),  $\Delta$ UA(2S) (1 $\rightarrow$ 4) GlcNAc(6S) in whelk Fraction E is consistent with the findings of Andrade and other research groups who have isolated these disaccharides from other mollusc. However, most of the GAGs isolated from GAG molluscs described by these researchers are more sulfated than whelk fraction E GAG.

Moreover, the absence of both  $\Delta$ UA (2S)- GlcNAc and  $\Delta$ UA(2S)GlcNS disaccharides in whelk purified fraction E is extremely interesting as normally they would represent some of the major disaccharide species associated with HS derived from cells and tissues.

These major differences between whelk purified fraction E, commercial HS and other HS/heparin like GAGs from molluscs may explain the anticancer activity of this unique GAG extract. In addition, it is generally accepted that the binding of HS to FG-2 play a critical role in the biological activities of HS. This binding occurs through *N*-sulfated glucosamine and 2-*O* sulfated iduronic acid and fraction E HS GAG contains low composition of this sulfation motif. This finding and complete absence of  $\Delta$ UA (2S)- GlcNAc and  $\Delta$ UA(2S)GlcNS disaccharides in whelk fraction E oligosaccharides composition may potentiate its antiproliferative activity on MDA468 and MDANQ01 breast cancer cells. The fraction E HS

is a structural heparin/HS, and thus it could interfere with the binding and cellular modulation of many proangiogenic growth factors. It may also predictably block the specific interaction with FGF to its tyrosine kinase receptor (Fearo et al 2007), thereby impede the dimerisation of the FGFR receptor and ultimately block signalling process that leads to proliferation.

Similarly, the tri sulfated disaccharide  $\Delta$ UA2S (1 $\rightarrow$ 4) GlcNS6S composition was significantly low in the whelk fraction E HS-like GAGs (table 6). This result suggest that whelk fraction E contain low sulfated HS like due to the low composition of the trisulfated disaccharides in contrasts with data obtained for heparin, where about 80% all of disaccharides are the  $\Delta$ UA2S (1 $\rightarrow$ 4) GlcNS6S (Zhang et al 2009: Linhardt, 2009: Dietrichet al., 1998). This result is also consistent with the work of Andrade et al on shrimp GAG.

Bivalve *Anodonta anodonta* (Andrade et al 2013).

TSK gel-filtration results also confirmed the presence of HS-like disaccharides (dp<sup>2</sup>) in fraction E GAG. This result corroborates the findings of Andrade and co-workers who had previously reported the isolation of HS-like disaccharides from different molluscs (Andrade et al, 2013: Vijayabaskar and Somasundaram 2012: Brito et al 2008: Moses et al, 2000: Mariana and Barbara 1999). Brito et al also report the isolation of HS GAG with low content of 2-O-sulfate groups in the shrimp heparinoid. They suggest that the anti-angiogenic effect of this GAG may be due to the presence of this unique disaccharide composition. Possibly this compound, like the 2-O-desulfated-heparin, could competitively inhibit the interaction between growth factors and cell surface HS proteoglycans (Brito 2008). In contrast to this result, Volpi and co-workers reported the isolation of high sulfated HS/heparin like GAG from large fresh water mollusc Bivalve *Anodonta anodonta* (Volpi 2005). The heparin/HS from *Anodonta Anodonta* show a degree of sulfation similar to that of bovine mucosa heparin because of the presence of similar percentage composition of trisulfated  $\Delta$ UA2S (1 $\rightarrow$ 4) GlcNS6S. It also contains a slight modification of other oligosaccharides and a significant

amount of disaccharides bearing the sulfation group at position 3 of the N-sulfoglucosamine - 6- sulfate. Its anticoagulant activity was also similar to that of bovine.

Other researchers have also reported an isolation of low sulfated HS that composed of blocks of low sulfated GlcNAc containing disaccharides and also highly sulfated Glc2S-containing disaccharides (Yamada et al 2011) from molluscs. Chi et al also report the isolation of HS preparation with a unique structure from the giant African snail *Achatina fulica* and named acharan sulfate. The major repeating disaccharide sequence in acharan sulfate is IdoA (2-*O*-sulfate)-GlcNAc. Gomes et al in their recent work isolated a unique HS from the bivalve *Nodipecten nodosus* (Linnaeus 1758). The disaccharide units in the HS chain are composed of nonsulfated, 2-*O*-sulfated or 3-*O*-sulfated GlcA as well as 2-*N*-sulfated and/or 6-*O*-sulfated GlcN, and the anticoagulant activity of the mollusk HS was 5-fold lower than that of porcine heparin.

Interestingly, some of these HS-like GAGs isolated from other molluscs had anticoagulant activities similar to mammalian heparin GAGs (Andrade et al, 2013; Vijayabaskar and Somasundaram 2012 and Moisés et al, 2000). However, none of these studies reported anti-cancer activity associated with any of these HS-like GAGs isolated from molluscs.

The results obtained so far show that fraction E contains HS-like GAG and this may in part be associated with its biological activities seen in the present work. Many studies have shown the anti proliferative effects of heparin GAG, low molecular weight heparin, ultra low molecular weight heparin and some HS mimetics on different cells including lymphoblast, VSMC and tumour cell (Erduran et al 2007: Erduran et al 2004: Patel et al 2002: Fedarko et al 1989: Castllot et al 1985). Erduran and other research groups investigated the mechanism of antiproliferative effect of heparin. They reported the antiproliferative effect of heparin was due to apoptosis and cell cycle arrest (Aksoy et al 2008: Erduran et al 2007). Heparin is a

well established GAG with many therapeutic functions including antimetastatic and antiproliferative effects. The biological roles of this GAG is structurally related to its ability to bind growth factors including FGF-2 (Neha et al 2010). It is note worthy that the biological activities of HSGAGs are due in large part to its structural composition and thereby modulate the ability of many growth factors in their binding to their receptors. The present study demonstrated that whelk purified fraction E contain low sulfated HS-like GAG with complete absent of both  $\Delta$ UA (2S)- GlcNAc and  $\Delta$ UA(2S)GlcNS disaccharides. This unique structural composition of whelk novel GAG provide an insight into its antiproliferative activities against the breast cancer cells investigated in this study (see above discussion). The anti-cancer activity of whelk fraction E HS-like GAG is a new and unique finding in glycosaminoglycans study.

It is well known that HS binds and modulates the activities of heparin-binding growth factors and their receptors, such as FGF's which in turn control various aspects of tumour growth and angiogenesis (Dreyfuss et al, 2010). Binding of growth factors to its tyrosine kinase receptors causes dimerization and autophosphorylation/transphosphorylation of the receptors which in turn triggers activation of the cytosolic tyrosine kinase, which targets specific substrates for tyrosine phosphorylation. However, the purified whelk fraction E is structurally similar to HS GAGs and can selectively inhibit several growth factors or proteins involved in the above process and ultimately inhibit the tumour growth as observed in the present study. Early studies have shown that heparin inhibits the phosphorylation of numerous signaling pathways involved in proliferation and survival, such as mitogen activated protein kinase (MAPK), protein kinase C (PKC) and casein kinase II (CKII) (Ottlinger et al 1993; Pukac et al 1992; Castellot et al 1989 and Hathaway et al 1980).

However the exact mode of action by which the whelk fraction E kills cancerous cells, at the GAG structural level and determination of the cellular pathways involved, needs further study.

We shouldn't forget that heparinase degradation of both crude whelk and its purified fraction E GAG extracts showed abolition of the anti-cancer activities seen with both breast cancer cell lines in this study (Figures 3.13). Also complete degradation of fraction E by heparinase III lyase confirmed this purified fraction is HS-like: hence implicating HS as the contributor to the biological activities seen in this study. Further work needs to be undertaken to confirm that the anti-cancer activity seen with the whelk GAGs and the cancer cells lines is directly related to the presence of an unusual type of HS like GAG species.

#### 4.15 Overall summary

It is clear that the original aims and objectives of this study have been both met and surpassed. The study has demonstrated that both shellfish utilised contain GAG-like compounds, which were revealed experimentally to be CS/DS-like and HS-like GAGs. Anti-cancer activity of GAGs from molluscs is reported for the first time in this study. Mollusc GAGs have always been evaluated for anticoagulants and anti-inflammatory activities due to the presence of HS/Heparin-like structure in its composition. The anti-cancer activities of both molluscs studied were shown to be specific to certain cancer cells and this can also be a tool in the future development of both mollusc GAGs into anti-cancer drugs. The low and different  $IC_{50}$  recorded for the two novel GAGs on certain cancer cell lines make these polysaccharide a candidate anti-cancer drugs to be developed in the future.

It is possible for the first time to study the mechanism of anti-tumour activity of both novel GAGs using annexin V-FITC, DAPI fluorescence microscopy and flow cytometry, in contrast to the conventional antiangiogenesis inhibitor, P-selectin inhibition and L-selectin inhibition analyses that are commonly used to assess anti tumour activity of GAGs related drugs. The problem encountered with the false positive apoptosis results observed with annexin V-FITC assay was finally resolved by DAPI fluorescence microscopy and this made the apoptotic data more concise and convincing. Fractionations of whelk GAGs have enabled new insight into the heterogeneity nature of both CS/DS and HS-like GAGs in this molluscs. Enzyme depolymerisations of the two crude polysaccharides confirm the presence of different GAGs (CS/DS-like and HS-like GAGs) in their tissue. SAX-HPLC analysis of the resulting oligosaccharides from the enzyme depolymerised samples gave insight into the structural heterogeneity of different CS/DS and HS-like GAGs in the two molluscs. The structural diversity of mollusc GAGs are reportedly even greater than that of vertebrate



GAGs (Andrade et al, 2013). The compositional analysis of both CS/DS and HS-like disaccharides of the two shellfish and the commercial GAGs performed for the purposes of this study provide insight into the sulfation level of each disaccharide in the total GAG compositions. This made the structure comparison easy and the differences between the novel and commercial GAGs were clearly seen. This study reveals that the biological activities of these two polysaccharides are due largely to the presence of GAG-like compounds within their composition. The depolymerised samples did not demonstrate any anti-cancer activities in any of the cancer cells tested. Similarly, the two novel polysaccharides are revealed as non-toxic to normal fibroblast cells; this will make it a better anti-cancer drug with a less toxic effect. Finally, at this juncture, it is difficult to reach a concrete conclusion on the mechanisms of apoptosis and cell cycle arrest, signaling pathways involved in tumour growth, and more detailed structural elucidations of the two novel polysaccharides; therefore, further research is required in this specific area.

### **Limitation of this study**

This study was limited to isolation of GAGs from whelk and cockle from shell fish. Also the anticancer activities evaluated were limited to MDA468, MDANQ01, K562, MOLT-4, and HeLa cell lines. The cytotoxic effect of the two shell fish was only assessed on 3T3 normal fibroblast cell line.

Characterisation of the major components of the novel GAGs extracted from the two shell fish was only done by conventional enzymatic and chemical method of analysis; the resulting disaccharides composition were analysed by PAGE and SAX-HPLC.

## **Future Direction**

There is need for more in-depth works on all aspect of this work, most importantly;

The anticancer activities of the two novel GAGs need to be investigated on other cancer cell lines e.g MCF-7, T-47D, HL-60, MOLT-3.

The anticancer activities should also be assessed on primary tumour cell

In vivo study is also highly essential for the anticancer evaluation of these novel GAGs

The cytotoxic effects can also be investigated on more normal, non cancerous cell line e.g. MCF-12, MCF-17, HUVEC and other normal epithelial cell lines.

There is need to study the various signalling pathways involved in proliferation e.g MAPK, MEK, ERK. The effect of the novel GAGs on cell cycle regulators e.g cyclin A, B,D and E, CDKI,CDK2, CDK 4 e.t.c needs to be investigated.

Apoptosis signalling pathway e.g. caspase 3, 8 and 9, bcl-2, bax e.t.c. should also be investigated before and after treatment with the novel GAGs.

Structural and compositional analysis of the major biological components of the two novel GAGs can also be studied by MS-LC, FACE, NMR e.tc.

## References

- Adamczyk P., Zenkert C., Balasubramanian P G., Yamada S., Murakoshi S., Sugahara K., et al (2010). A non-sulfated chondroitin stabilizes membrane tubulation in cnidarians organelles. *J Biol Chem*; **285**:25613-23.
- Afratis I., Gialeli C., Nikitovic D., Tsegenidis T., Karousou E., Theocharis A D., Pava M S., Tzanakakis G N., and Karamanos N K. (2012) Glycosaminoglycans: key players in cancer cell biology and treatment. *FEBS Journal*; **279**:1177-1197
- Agarwal M L., Agarwal A., Taylor W R., Stark G. (1995). p53 controls both the G2/m and G1 cell cycle checkpoints and mediates growth arrest in human fibroblasts. *Proc. Natl. Acad. Sci. USA*; **92**: 8493–8497
- Aksoy A., Erduran E., and Gedik Y (2008). The effect of heparin on the cell cycle in human b-lymphoblasts: an in vitro study. Available from Nature Preceding <<http://hdl.handle.net/10101/npre.2008.1989.1>>
- Alkarain A., Jordan R., Slingerland J. (2004) p27 deregulation in breast cancer: Prognostic significance and implications for therapy. *J Mammary Gland Biol Neoplasia*; **9**:67–80
- Allen B L and Rapraeger A C. (2003) Spatial and temporal expression of heparin sulphate in mouse development regulates FGF and FGF receptor assembly. *J. Cell. Biol*; **163**(3) 637-648
- Allen R T., William J., Hunter III, and Agrawal D K (1997). Morphological and Biochemical Characterization and Analysis of Apoptosis. *J of Pharmacol and Toxicol Methods*; **37**: 215-228
- American Cancer Society (2008) Breast cancer facts & figures 2007-2008. Atlanta, American Cancer Society.
- Ampofo S A., Wang H M., and Linhardt R J. (1991). Disaccharide compositional analysis of heparin and heparan sulfate using capillary zone electrophoresis. *Anal. Biochem*; **199**: 249-55
- Andrade G P., Lima M A., De Souza A A Jr., Fareede J., Hoppensteadte D A, Santos E A, Chavante S F., Oliveira F W., Roch H A., Nader H B. (2013). A heparin-like compound isolated from a marine crab rich in glucuronic acid 2-O-sulfate presents low anticoagulant activity. *Carbohydrate Polymers*; **94**: 647– 654
- Arantes R M., Lourenssen S., Machado C R., Blennerhassett M G. (2000). Early damage of sympathetic neurons after co-culture with macrophages: a model of neuronal injury in vitro. *NeuroReport* ; **11**: 177–181

- Arellano M., Moreno S.(1997). Regulation of CDK/cyclin complexes during the cell cycle. *Int. J. Biochem. Cell Biol*; **29**:559–573
- Arends M J., et al. (1990) Apoptosis, the role of the endonuclease. *Am J Pathol*; **136**: 593–608
- Arnold A., Papanikolaou A. (2005). Cyclin D1 in breast cancer pathogenesis. *J Clin Oncol* ; **23**:4215–4224
- Arur S., Uche U E., Rezaul K., Fong M., Scranton V., Cowan A E., Mohler W., Han D K., (2003). Annexin I is an endogenous ligand that mediates apoptotic cell engulfment. *Dev Cell*; **4**:587–98. [PubMed:12689596]
- Ashkenazi A., Dixit V M., (1998) Death receptors: signalling and modulation. *Science* ; **281**:1305–8.[PubMed: 9721089] G2/m and G1 cell cycle checkpoints and mediates growth arrest in human fibroblasts. *Proc. Natl. Acad. Sci. USA*; **92**: 8493–97
- Asimakopoulou A P., Theocharis A D.,Tzanakakis G N and Karamanos N K. (2008). The Biological Role of Chondroitin Sulfate in Cancer and Chondroitin-based Anticancer Agents. *in vivo*; **22**: 385-390
- Atha D H., Lormeau J C., Petitou M., Rosenberg R. D.,and Choay J (1985). Contribution of monosaccharide residues in heparin binding to antithrombin III. *Biochemistry*; **24**: 6723-6729
- Aviezer D., Hecht D., Safran M., Eisinger M., David G.,Yayon A. (1994). Perlecan, basal lamina proteoglycan, promotes basic fibroblast growth factor-receptor binding, mitogenesis, and angiogenesis. *Cell*; **79**: 1005-10013.
- Basappa., Sugahara K., Kuntebommanahalli N., Thimmaiah K N., Bid H K., Houghton P J., Rangappa K S. (2012). Anti-Tumour Activity of a Novel HS-Mimetic-Vascular Endothelial Growth-Factor Binding Small Molecule. *PLoS ONE*; **7(10)**:10.137.
- Bali J P., Cousse H., Neuzil E (2001). Biochemical basis of the pharmacologic action of chondroitin sulfates on the osteoarticular system. *Semin Arthritis Rheum*; **31**: 58–68.
- Bandara L R., Girling R and LaThangue N B (1997). Apoptosis induced in mammalian cells by small peptides that functionally antagonize the Rb-regulated E2F transcription factor. *Nat Biotechnol*; **15**: 896-901
- Barry M., Bleackley R C., (2002). Cytotoxic T lymphocytes: all roads lead to death. *Nat Rev Immunol*; **2**:401–9. [PubMed: 12093006]

- Beenken A., Mohammadi M (2009). The FGF family: biology, pathophysiology and therapy. *Nat Rev Drug Discov*; **8**: 235-53
- Bellamy R W., and Horikoshi K. (1992). Heparinase produced by a microorganism belonging to the genus Bacillus. *United States Patent*; **5**:145-778
- Bellot F., Crumley G., Kaplow J M., Schlessinger J., Jaye M., Dionne C A., (1991). Ligand-induced transphosphorylation between different FGF receptors. *EMBO J*; **10**:2849
- Belting M., Borsig L., Fuster M M., et al. (2002). Tumor attenuation by combined heparan sulfate and polyamine depletion. *Proc Natl Acad Sci U S A*; **99**: 371 –376
- Berry D., Lynn D M., Sasisekharan R., Langer R (2004). Poly(beta-amino)esters promote cellular uptake of heparin and cancer cell death. *Chem Biol*; **11**: 487–498.
- Bjork I., and Lindahl U (1982). Mechanism of the anticoagulant action of heparin. *Mol.and cellular biochem*; **48**:161-182
- Blackhall F H., Merry C L., Davies E J. and Jyson G C. (2001). Heparan sulfate proteoglycans and cancer. *Br. J. Cancer*; **85**:1094–1098
- Blom W M., De Bont H J., Meijerman I., Kuppen P J., Mulder G J., Nagelkerke J F. (1999). Interleukin-2-activated natural killer cells can induce both apoptosis and necrosis in rat hepatocytes. *Hepatology* **29**: 785–792
- Bonneh-Barkay D., Shlissel M., Berman B., Shaoul E., Admon A., Vlodavsky I., Carey D J., Asundi V K., Reich-Slotky R., Ron D J. (1997). Identification of Glypican as a Dual Modulator of the Biological activity of Fibroblast Growth Factors. *Biol. Chem*; **272**: 12415-12421
- Borsig L.,Vlodavsky I., Ishai-Michaeli R., Torris G., and Vismara E (2011). Sulfated Hexasaccharides Attenuate Metastasis by Inhibition of P-selectin and Heparanase; *Neoplasia* **13**: 445–452
- Borsig L., Wang L., Cavalcante M C M., Cardilo-Reis L., Ferreira P L., Mourao P A S., Esko J D and Pavao M S G (2007). Selectin blocking activity of a fucosylated chondroitin sulphate glycosaminoglycan from sea cucumber. *J Biol Chem*. **98**: 14984-14991
- Bortner C D., Oldenburg N B., Cidlowski J A., (1995). The role of DNA fragmentation in apoptosis. *Trends Cell Biol*; **5**:21–6. [PubMed: 14731429]

- Bose P., Black S., Kadyrov M., Weissenborn U., Neulen J., Regan L., et al (2005). Heparin and aspirin attenuate placental apoptosis in vitro: implications for early pregnancy failure. *Am J Obstet Gynecol*; **192**: 23–30.
- Brauchle E., Thude S., Brucker S Y., and Layland K.S (2014). Cell death stages in single apoptotic and necrotic cells monitored by Raman microspectroscopy. *Scientific Report*; **4**: 4698
- Bratton D L., Fadok V A., Richter D A., Kailey J M., Guthrie L A., Henson P M. (1997). Appearance of phosphatidyl serine on apoptotic cells requires calcium-mediated nonspecific flip-flop and is enhanced by loss of the aminophospholipid translocase. *J Biol Chem*; **272**:26159–26165. [PubMed: 9334182]
- Breast Cancer (C50), European Age-Standardised Incidence Rates, Females, Great Britain, 1975-2010
- Brito A S., Cavalcante R S., Palhares C G F et al (2014). A non-hemorrhagic hybrid heparin/heparan sulfate with anticoagulant potential. *Carbohydrate Polymers*; **99**: 372– 378
- Brito A S., Arimateia D S., Souza L R., Lima M A., Santos V O., Medeiros V P., Ferreira P A., Silva R A., Ferreira C V., Justo G Z., Leite E L., Andrade G P., Oliveira F W., Nader H B., Chavante S F. (2008). Anti-inflammatory properties of a Heparin-like glycosaminoglycan with reduced anticoagulant activity isolated from a marine shrimp. *Bioorg Med Chem*; **16**: 9588–95.
- Brunner T., Wasem C., Torgler R., Cima I., Jakob S., Corazza N., (2003). Fas (CD95/Apo-1) ligand regulation in T cell homeostasis, cell-mediated cytotoxicity and immune pathology. *Semin Immunol*; **15**:167–176. [PubMed: 14563115]
- Bruno E., Cooper R J., Wilson E L., Gabilove J L., Hoffman R., (1993). Basic fibroblast growth factor promotes the proliferation of human megakaryocytic progenitor cells. *Blood* ;**82**:430
- Bunch R T., Eastman A. (1996). Enhancement of cisplatin-induced cytotoxicity by 7-hydroxystaurosporine (UCN-01), a new G2 checkpoint inhibitor. *Clin Cancer Res*; **2**:791–797. [PubMed]
- Burdon R H., Van Knippenberg P H. (1985). Glycoprotein and proteoglycan techniques. In: *Laboratory Techniques in Biochemistry and Molecular Biology*; Elsevier: Amsterdam, The Netherlands; **16**: 462

- Cabannes E. et al., (2009). Heparan sulphate mimetics as anti-cancer small-glyco. In: Proceedings of the 67th Harden Conference
- Cartel NJ., Post M (2005). Abrogation of apoptosis through PDGF-BB-induced sulfated glycosaminoglycans synthesis and secretion. *Am J Physiol Lung Cell Mol Physiol*; **288**: L285–L293.
- Casaro C M. and Dietrich C P. (1977). Distribution of sulfated mucopolysaccharides in invertebrates. *J. Bio.Chem*; **252** (7): 2254-2261
- Castellot J J Jr., Pukac L A., Caleb B L., Wright T C Jr., and Karnovsky M J., (1989). Heparin selectively inhibits a protein kinase C dependent mechanism of cell cycle progression in calf aortic smooth muscle cells. *J Cell Biol*; **109**: 3147-3155
- Castellot J J., Cochran D L., Karnovsky M J (1985). Effect of heparin on vascular smooth muscle cells I. Cell metabolism. *J Cell Physiol*; **124**: 21-28
- Casu B. et al., (2010). Heparin-derived heparan sulfate mimics to modulate heparan sulfate–protein interaction in inflammation and cancer. *Matrix Biol.* **29**: 442–45
- Casu B., (1985). Structure and biological activity of heparin. *Adv Carbohydrate Chem. Biochem*; **43**: 52- 134
- Cathelineau A., Daleke D L., Henson P M., Bratton D L. (2001). Loss of phospholipid asymmetry and surface exposure of phosphatidylserine is required for phagocytosis of apoptotic cells by macrophages and fibroblasts. *J Biol Chem*; **276**:1071–7. [PubMed: 10986279]
- Cesaretti M., Luppi E., Maccari M., Volpi N. (2004) Isolation and characterization of a heparin with high anticoagulant activity from the clam *Tapes philippinarum*. Evidence for the presence of a high content of antithrombin III-binding site. *Glycobiology*; **14**: 1275-1284
- Chang G 1., Spencer R H., Lee A T., Barclay M T., Rees D C. (1998). Structure of the MscL homolog from *Mycobacterium tuberculosis*: a gated mechanosensitive ion channel. *Science*; **282**(5397):2220-6.
- Chen C F., Hwang J M., Lee W., Chiang H C., Lin J C, Chen HY (1988). Search for antitumor agent for Chinese herbs I. Antitumor screening method. *Chin. Med. J. Taipei*; **41**: 177-184.

- Chen Y., Maguire T., Hileman R E., Fromm J R., Esko J D., Linhardt R J., Marks R M (1997). Dengue virus infectivity depends on envelope protein binding to target cell heparan sulphate. *Nat Med*; **3**:866-871
- Cheng J., Zhou T., Liu C., Shapiro J P., Brauer M J., Kiefer M C., Barr P J., Mountz J D., (1994). Protection from Fas mediated apoptosis by a soluble form of the Fas molecule. *Science*; **263**:1759–62. [PubMed:7510905]
- Chicheportiche Y., Bourdon P R., Xu H., Hsu Y M., Scott H., Hession C., Garcia I., Browning J L., (1997). TWEAK, a new secreted ligand in the tumour necrosis factor family that weakly induces apoptosis. *J Biol Chem*; **272**:32401–32410. [PubMed: 9405449]
- Chu C. et al., (2009). M-ONC 402, A novel non-anticoagulant heparin, inhibits P Selectin function and metastatic seeding of tumour cells in mice. In Proceedings of the 100th Annual Meeting of American Association for Cancer Research (AACR)
- CliffsNotes.com. *Cell Division*. 21 (2012) <[http://www.cliffsnotes.com/study\\_guide/topicArticleId-277792,articleId-277522.html](http://www.cliffsnotes.com/study_guide/topicArticleId-277792,articleId-277522.html)>.
- Cohen G M. (1997). Caspases: the executioners of apoptosis. *Biochem J*; **326** (Pt 1):1–16. [PubMed:9337844]
- Collins F S., Guyer M S., Chakravarti A. (1997). Variations on a Theme: Cataloging Human DNA Sequence Variation. *Science*; **278**:1580–1581
- Coltrini D., Rusnati M., Zopetti G., Oreste P., Isacchi A., Caccia P., Bergonzoni L., Presta M. (1993). Biochemical bases of the interaction of human basic fibroblast growth factor with glycosaminoglycans: New insights from trypsin digestion studies. *Eur. J. Biochem*; **214**: 51-58.
- Coltrini D., Rusnati M., Zopetti G., Oreste P., Grazioli G., Naggi A., Presta M. (1994). Different effects of mucosal, bovine lung and chemically modified Heparin on selected biological properties of basic fibroblast growth-factor. *Biochem. J*; **303** ( Pt 2): 583-90.
- Conrad H E. (1998). Heparin-Binding Proteins. San Diego: Academic Press.
- Conte P., Guarneri V., Bengala C. (2007). Evolving non endocrine therapeutic options for metastatic breast cancer: How adjuvant chemotherapy influences treatment. *Clin Breast Cancer*; **7**: 841-849.



- Coppola J M., Ross B D., Rehemtulla A., (2008). Noninvasive imaging of apoptosis and its application in cancer therapeutics. *Clin Cancer Res*; **14**: 2492–501
- Cory S., Adams J M. (2002). The Bcl2 family: regulators of the cellular life-or-death switch. *Nat Rev Cancer*; **2**:647–56. [PubMed: 12209154]
- Coster L. (1991).Structure and properties of DS proteoglycans. *Biochem. Soc. Trans*; **19**: 866-868
- Cotran R S., Kumar V., Collins T., (1999). Cellular pathology I: cell injury and cell death. In: Cortan R S., Kumar V., Collins T., editors. Robbins Pathologic Basis of Disease. 6.W.B. Saunders Co; Philadelphia, PA:. 1-29
- Couchman J R., (2010).Transmembrane signaling Proteoglycans. *Ann. Rev.cell and dev.bio*; **26**: 89-114.
- Coughlin S R., Barr P J., Cousens L S., Fretto L J., Williams L J., (1988). Acidic and basic FGFs stimulate TK activity in vivo. *J Biol Chem* **263**:988
- Cotter T G., and Curtin J F (2003). Historical perspectives. In: Essays in Biochemistry. Cotter, T.G. et al. eds. **39**:1–10
- Cowman M K., Slahetka M F., Hittner D M., Kim J., Forino M., Gadelrab G., (1984) Polyacrylamide-gel electrophoresis and alcian blue staining of sulfated glycosaminoglycan oligosaccharides. *Biochem. J*; **221**: 707–716
- Crolle G D., Este E., (1980). Glucosamine sulphate for the management of arthrosis: acontrolled clinical investigation. *Curr Med Res Opin*; **7**: 104-109
- Cross D A., Alessi D R., Cohen P., Andjelkovich M., Hemmings B A. (1995). Inhibition of glycogen synthase kinase-3 by insulin mediated by protein kinase B. *Nature*; **378(6559)**:785-9.
- Darzynkiewicz Z., Bruno S., Del Bino G., Gorczyca W., Hotz MA., Lassota P., Traganos F (1992). Features of apoptotic cells measured by flow cytometry. *Cytometry*; **13**: 795-808,
- Dawson M I., Xia Z., Jiang T., Ye M., Fontana J A., et al. (2008). Adamantyl-substituted retinoid-derived molecules that interact with the orphan nuclear receptor small heterodimer partner: effects of replacing the 1-adamantyl or hydroxyl group on inhibition of cancer cell growth, induction of cancer cell apoptosis, and inhibition of

- SRC homology 2 domain-containing protein tyrosine phosphatase-2 activity. *J Med Chem*; **51**: 5650–5662.
- DeBaun M R., Ess J. & Saunders S. (2001). Simpson–Golabi–Behmel syndrome: progress towards understanding the molecular basis for overgrowth, malformation, and cancer predisposition. *Mol. Genet. Metab*; **72**: 279–286
- Denecker G., Vercammen D., Declercq W., Vandenabeele P., (2001). Apoptotic and necrotic cell death induced by death domain receptors. *Cell Mol Life Sci*; **58**:356–70. [PubMed: 11315185]
- Desai U R. (2013). The promise of sulphated synthetic small molecules as modulators of glycosaminoglycans functions. *Future Med. Chem*; **5**: 1363-1366
- Desai U. R., Wang H M., Linhardt R J. (1993). Substrate Specificity of the Heparin Lyases from *Flavobacterium heparinum*. *Biochemistry and Biophysics*; **32**: 8140-8145
- Desai U R., Wang H., and Linhardt R. J. (1993a). Specificity studies on the Heparin lyases from *Flavobacterium heparinum*. *Biochemistry*; **32**: 8 14045
- Desai U. R., Wang H., and Linhardt R. J. (1993b). Substrate specificity of the Heparin lyases from *Flavobacterium heparinum*. *Arch. Biochem. Biophys*; **306**: 461-468.
- Devadas S., Das J., Liu C., Zhang L., Roberts A I., Pan Z., Moore P A., Das G., Shi Y., (2006). Granzyme B is critical for T-cell receptor-induced cell death of type 2 helper T cells. *Immunity*; **25**:237–47. [PubMed:16901729]
- Dickson C., Spencer-Dene B., Dillon C., and Fantl V. (2000). Tyrosine kinase signalling in breast cancer Fibroblast growth factors and their receptors. *Breast Cancer Res*; **2**:191–196
- Dietrich C P., de-Paiva J F., Moraes C T., Takahashi H K., Porcionatto M A., Nader H B. (1985). Isolation and characterisation of a Heparin with high anticoagulant activity from *Anomalocardia brasiliensis*. *Biochim. Biophys Acta*; **843**: 1-7
- Dietrich P C., Helena B N., Jose F (1989). de Paiva. Heparin in molluscs: Chemical, enzymatic degradation and <sup>13</sup>C and <sup>1</sup>H n.m.r Spectroscopical evidence for the maintenance of the structure through evolution. *Int. J. Biol. Macromol*; **11**:361-366.
- Dionex Pro-pac pa1 column for hydrophilic anionic protein separation (2012) Available online: <http://www.dionex.com/en-us/columns-accessories/biocols/cons4783.html>

- Dong Z., Saikumar P., Weinberg J M., Venkatachalam M A., (1997). Inter-nucleosomal DNA cleavage triggered by plasma membrane damage during necrotic cell death: involvement of serine but not cysteine proteases. *Am. J. Pathol*; **151**:1205–1213
- Dreyfuss J I., Regatier C V., Lima M A., Paredes-Gamero E J., Brito A S., Chavante S F., Belfort R jr., Farah M E., and Nader H B. (2010). A Heparin mimetic isolated from a marine shrimp suppresses neovascularisation. *J Throm and Haemo*; **8**:1828–1837
- Earp H S., Dawson T L., Li H and Yu H. (1995). Heterodimerization and functional interaction between EGF receptor family member: a new signaling paradigm with implications for breast cancer research. *Breast Cancer Res.Treat*; **35**: 115–132.
- Ehlers S., Benini J., Kutsch S., Endres R., Rietschel E T., Pfeffer K. (1999). Fatal granuloma necrosis without exacerbated mycobacterial growth in tumour necrosis factor receptor p55 gene-deficient mice intravenously infected with Mycobacterium avium. *Infect. Immun*; **67**: 3571–3579
- Elmore S., (2007). Apoptosis: A Review of Programmed Cell Death. *Toxicol Pathol*: **35** (4): 495–516.
- Elnemr A., Ohta T., Yachie A., Kayahara M., Kitagawa H., Ninomiya I., Fushida S., Fujimura T., Nishimura G., Shimizu K., Miwa K. (2001). Human pancreatic cancer cells express non-functional Fas receptors and counterattack lymphocytes by expressing Fas ligand; a potential mechanism for immune escape. *Int J Oncol*; **18**:33–39. [PubMed: 11115536]
- Enari M., Sakahira H., Yokoyama H., Okawa K., Iwamatsu A., Nagata S. (1998). A caspase-activated DNase that degrades DNA during apoptosis, and its inhibitor ICAD. *Nature*; **391**:43–50. [PubMed: 9422506]
- Enzyme Nomenclature, (1992). p. 425, Academic Press, San Diego, California
- Erduran E., Deger O., Albayrak D., Tekelioğlu Y., Ozdemir T (2007). In vitro investigation of the apoptotic effect of heparin on lymphoblasts by using flow cytometric DNA analysis and fluorometric caspase-3 and -8 activities. *DNA Cell Biol*; **26**; 803-808
- Erduran E., Tekelioğlu Y., Gedik Y., Bektaş I., Hacısalıhoğlu S (2004) In vitro determination of the apoptotic effect of heparin on lymphoblasts using DNA analysis and measurements of Fas and Bcl-2 proteins by flow cytometry. *Pediatr Hematol Oncol*; **21**: 383-391
- Erduran E., Tekelioğlu Y., Gedik Y., Yıldırım A (1999). Apoptotic effects of heparin on

lymphoblasts, neutrophils, and mononuclear cells: results of a preliminary in vitro study. *Am J Hematol*; **69**: 90-93

Ernst S., Langer R., Charles L. Cooney and Sasisekharan R. (1995). Enzymatic Degradation of Glycosaminoglycans. *Critical Reviews in Biochemistry and Molecular Biology*; **30(5)**:387444

Esko J D. & Lindahl U. (2001). Molecular diversity of HS. *J. Clin. Invest*; **108**: 169–173.

Eswarakumar V P., Lax I., Schlessinger J. (2005). Cellular signaling by fibroblast growth factor receptors. *Cytokine Growth-Factor Rev*; **16**: 139-49. Fadok VA., de

Fahraeus R., Lain S., Ball K L., Lane D P. (1998). Characterisation of the cyclindependent kinase inhibitory domain of the INK4 family as a model for a synthetic tumour suppressor molecule. *Oncogene*; **16**:587–96

Fåhraeus R 1., Paramio J M., Ball K L., Lain S., Lane D P. (1996). Inhibition of pRb phosphorylation and cell-cycle progression by a 20-residue peptide derived from p16CDKN2/INK4A. *Curr Biol*; **6(1)**:84-91.

Fan S., Chang J K., Smith M L., Duba D., Fornace A J, O'Connor PM (1997). Cells lacking CIP1/WAF1 genes exhibit preferential sensitivity to cisplatin and nitrogen mustard. *Oncogene* **14**:2127–2136

Fan Z., Beresford P J., Oh D Y., Zhang D., Lieberman J., (2003). Tumour suppressor NM23-H1 is a granzyme A-activated DNase during CTL- mediated apoptosis, and the nucleosome assembly protein SET is its inhibitor. *Cell*; **112**:659–672. [PubMed: 12628186]

Fedarko N S., Ishihara M., Conrad H E (1989). Control of cell division of hepatoma cells by exogenous heparan sulfate proteoglycan. *J Cell Physiol*; **139**: 287-294

Feige J-J., Baird A (1988). Glycosylation of the basic fibroblast growth-factor receptor. The contribution of carbohydrate to receptor function. *J Biol Chem*; **263**:14023

Feng Y. et al (2007). Timing of apoptosis onset depends on cell cycle progression in peripheral blood lymphocytes and lymphocytic leukemia cells. *Oncol Rep*; **17**: 1437-1444

Ferraro-Peyret C., Quemeneur L., Flacher M., Revillard J P., Genestier L., (2002). Caspase-independent phosphatidyl serine exposure during apoptosis of primary T lymphocytes. *J Immunol*; **169**:4805–4810. [PubMed: 12391190]

- Ferro V., Dredge K., Liu L., Hammond E., Bytheway I., Li C., Johnstone K., Karoli T., Davis K., Copeman E et al. (2007). PI-88 and novel heparan sulfate mimetics inhibit angiogenesis. *Semin Thromb Hemost*; **33**: 557–568.
- Ferro V. and Don R. (2003). The development of the novel angiogenesis inhibitor PI-88 as an anti-cancer drug. *Australas. Biotechnol*; **13**: 38–39
- Fiers W., Beyaert R., Declercq W., Vandenabeele P., (1998). More than one way to die: apoptosis, necrosis and reactive oxygen damage. *Oncogene*; **18**:7719–30. [PubMed: 10618712]
- Filmus, J. (2001). Glypicans in growth control and cancer. *Glycobiology*; **11**: 19R–23R.
- Fink S L and Cookson B T (2005). Eukaryotic Cells Mechanistic Description of Dead and Dying Apoptosis, Pyroptosis, and Necrosis: *Infect. Immun*; **73**(4): 1907-1916
- Flaumenhaft R., Moscatelli D., Saksela O., Rifkin D B. (1989). Role of ECM in the action of basic fibroblast growth-factor: Matrix as a source of growth-factor for long-term stimulation of plasminogen activator production and DNA synthesis. *J Cell Physiol*; **140**:75
- Folkman J., Hochberg M., (1983). Self - egulation of growth in three dimension. *J.Exp Med*; **138**: 745-753
- Fu M., Wang C., Li Z., Sakamaki T., Pestell R G. (2004). Minireview: Cyclin D1: Normal and abnormal functions. *Endocrinology*; **145**:5439–5447
- Fugedi P. (2003). The potential of the molecular diversity of Heparin and HS for drug development. *Mini Rev. Med. Chem*; **3**: 659–667
- Funderburgh J L. (2002). KS biosynthesis. *IUBMB Life* **54**:187–94
- Gabbianelli M., Sargiacomo M., Pelosi E., Testa U., Isacchi G., Peschle C (1990). “Pure” hematopoietic progenitors: Permissive action of basic fibroblast growth-factor. *Science*; **249**:1561
- Gallagher J T (2001) Heparan sulfate: growth control with a restricted sequence menu. *J Clin Invest* **108**, 357–361.
- Gallagher J T., Lyon M and Steward W P. (1986). Structure and function of HS proteoglycans. *Biochem. J*; **236**: 313–325
- Gandhi N S and Mancera R L. (2008). The Structure of Glycosaminoglycans and their

- development: therapeutically exploring the glycosaminoglycanome. *Curr. Opin. Mol. Ther.*; **8**: 521–528
- Gandhi N S., and Mancera R L. (2010). Heparin/HS-based drugs. *drug disco today*; **15**: 1058-1069
- Gardai S J., McPhillips K A., Frasch S C., Janssen W J., Starefeldt A., Murphy-Ullrich J E., Bratton D L., Oldenborg P A., Michalak M., Henson P M., (2005). Cell-surface calreticulin initiates clearance of viable or apoptotic cells through trans-activation of LRP on the phagocyte. *Cell*; **123**:321–34. [PubMed:16239148]
- Geran R I., Greenberg N H., Macdonald M M., Schumacher A M., Abbott B J (1972). Protocols for screening chemical agents and natural products against animal tumours and other biological systems. *Cancer Chemother. Rept*; **3**: 103
- Gesslbauer B., and Kungl A.J. (2006). Glycomic approaches towards drug Interactions with Proteins. *Chem Biol Drug Des*; **72**: 455–482
- Gomes A M., Stelling M P., and Pavao M S. (2013). Heparan Sulfate and Heparanase as Modulators of Breast Cancer Progression. *Bio. Med Res. Internal*; **20** (13): Article ID 852093, 11 pages.
- Gomes A M., Kozlowski E O., Pomin V H., de Barros C M., Zaganeli J L., and Pavao M S. (2010). Unique ECM HS from the bivalve *Nodipecten nodosus* (Linnaeus, 1758) safely inhibits arterial thrombosis after photochemically induced endothelial lesion. *J. Biol. Chem*; **285**: 7312–7323. [Pubmed Abstract](#)
- Goping I S., Barry M., Liston P., Sawchuk T., Constantinescu G., Michalak K M., Shostak I., Roberts D L., Hunter A M., Korneluk R., Bleackley R C. (2003). Granzyme B-induced apoptosis requires both direct caspase activation and relief of caspase inhibition. *Immunity*; **18**:355–65. [PubMed: 12648453]
- Gorbsky G J. (1997). Cell cycle checkpoints: arresting progress in Mitosis. *BioEssays*; **9**(3): 193-197
- Gospodarowicz D., Cheng J J. (1986). Heparin protects basic and acidic FGF from inactivation. *Cell Physiol*; **128**:475-84
- Greenhalgh D G., (1998). The role of apoptosis in wound healing. *Int J Biochem Cell Biol*; **30**:1019–30.[PubMed: 9785465]

- Grespi F., Soratroi C., Krumschnabel G., Sohm B., Ploner C., Geley S., Hengst L., Häcker, G and Villunger A. (2010). BH3-only protein Bmf mediates apoptosis upon inhibition of CAP-dependent protein synthesis. *Cell Death Diff*; [Epub ahead of print]
- Grimshaw J. (1997). Analysis of glycosaminoglycans and their oligosaccharide fragments by capillary electrophoresis: *Electrophoresis*; **18**: 2408-2414.
- Grootenhuis P D J., Westerduin P., Meuleman D., Petitou M., van Boeckel C A A. (1995). Rational design of synthetic Heparin analogues with tailor-made coagulation factor inhibitory activity. *Nat. Struct Mol. Biol*; **2**: 736–739
- Gu J., Kawai H., Wiederschain D., Yuan Z M, (2001). Mechanism of functional inactivation of a Li-Fraumeni syndrome p53 that has a mutation outside of the DNA-binding domain. *Cancer Res*; **61**:1741–6. [PubMed: 11245491]
- Gu K N., Linhardt R J., Laliberte M., Gu K F., Zimmermann J.(1995). Purification, characterisation and specificity of chondroitin lyases and glycuronidase from flavobacterium heparinum. *Biochem J*; **312**: 569-577
- Guo Y. and Conrad H E.(1989). The disaccharide composition of heparins and heparan sulphates. *Anal. Biochem*; **176**: 96-104.
- Guo C H., Koo C Y., Bay B H., Tan P H., Yip G W. (2007). Comparison of the effects of differentially sulphated bovine kidney and porcine intestine-derived heparan sulphate on breast carcinoma cellular behaviour. *Int J Oncol*; **31**: 1415-1423.
- Ha Y W., Jeon B T., Moon S H., Toyoda H., Toida T., Linhardt R.J., Kim Y S. (2005). Characterisation of HS from the unossified antler of cervus elaphus. *Carbohydr. Res*; **340**: 411–416.
- Habuchi H., Suzuki S., Saito T., Tamura T., Harada T., Yoshida K., and Kimata, K. (1992). Structure of a HS oligosaccharide that binds to basic fibroblast growth factor. *Biochem. J.* **285**, 805–813
- Harman D., (1992). Role of free radicals in aging and disease. *Ann N Y Acad Sci*; **673**:126–41. [PubMed:1485710]
- Hasan J., Shnyder S D., Clamp A R., McGown A T., Bicknell R., Presta M., Bibby M., Double J., Craig S., Leeming D., Stevenson K., Gallagher J T., Jayson GC (2005) Heparin octasaccharides inhibit angiogenesis *in vivo*. *Clin Cancer Res.* **11**: 8172–8179

- Hathaway G M., Lubben T H and Traugh J A., (1980). Inhibition of casein kinase II by Heparin. *J Biol Chem*; **255**: 8038-8041
- Heinegard D and Sommarin Y.(1987). Proteoglycan: an overview. *Methods Enzymology*; **144**:305-319
- Hengartner M O. (2000).The biochemistry of apoptosis. *Nature*; **407**:770–6. [PubMed: 11048727]
- Hilakivi-Clarke L.,Wang C., Kalil M., Riggins R., and Pestell G R. (2004). Nutritional modulation of the cell cycle and breast cancer.*Endocrine-Related Cancer*; **11**: 603–622.
- Hirsch T., Marchetti P., Susin S A., Dallaporta B., Zamzami N., Marzo I., Geuskens M., Kroemer G.(1997). The apoptosis-necrosis paradox. Apoptogenic proteases activated after mitochondrial permeability transition determine the mode of cell death. *Oncogene*; **15**:1573–81. [PubMed: 9380409]
- Hiyama K. and Okada S. (1975b). Crystallization and some properties of chondroitinase from *Arrhrobacter aurescens*. *J. Biol. Chem*; **250**:1824-28.
- Hofmann W K., de Vos S., Tsukasaki K., Wachsman W., Pinkus G S., Said J W., Koeffler H P. (2001). Altered apoptosis pathways in mantle cell lymphoma detected by oligonucleotide microarray. *Blood*; **98**:787–794. [PubMed: 11468180]
- Horner A A., Young E. (1982). Asymmetric distribution of sites with high affinity for antithrombin III in rat skin Heparin proteoglycans. *j.bio.chem*; **257**: 8749-8754.
- Hsu H., Xiong J., Goeddel D V., (1995). The TNF receptor 1-associated protein TRADD signals cell death and NF-kappa B activation. *Cell*; **81**:495–504. [PubMed: 7758105]
- Hu S., Snipas S J., Vincenz C., Salvesen G., Dixit V M., (1998). Caspase- 14 is a novel developmentally regulated protease. *J Biol Chem*; **273**:29648–53. [PubMed: 9792675]
- Hunter T and Pines J., (1994). Cyclins and cancer II: cyclin D and CDK inhibitors come of age. *Cell*; **79**: 573–582.
- Hurwitz H., Fehrenbacher L., Novotny W., Cartwright T., Hainsworth J., Heim W., Berlin J., Baron A., Griffing S., Holmgren E., Ferrara N., Fyfe G., Rogers B., Ross R., Kabbinavar F., (2004). Bevacizumab plus irinotecan, fluorouracil, and leucovorin for metastatic colorectal cancer. *N Engl J Med*; **350**: 2335–2342



- Hussain S., Slevin M., Ahmed N., West D., Choudhary M., Naz H., Gaffney J., (2009). Stilbene glycosides are natural product inhibitors of FGF-2-induced angiogenesis; *BMC Cell Bio*; **10**: 30-42
- Igney F H., Krammer P H. (2002). Death and anti-death: tumour resistance to apoptosis. *Nat Rev Cancer*; **2**:277–288. [PubMed: 12001989]
- Inoue Y., Nagasawa K.,(1976). Selective n-desulfation of Heparin with dimethyl sulfoxide containing water or methanol. *Carbohydr. Res*; **46**: 87–95.
- International Breast Cancer Study Group Decreased immunoreactivity for p27 protein in patients with early-stage breast carcinoma is correlated with HER-2/neu overexpression and with benefit from one course of perioperative chemotherapy in patients with negative lymphnode status: Results from International Breast Cancer Study Group Trial V. *Cancer*; **97**:1591–1600.
- Iozzo R V., San Antonio J D. (2001) HS proteoglycans: heavy hitters in the angiogenesis arena. *J Clin Invest*; **108**:349–355.
- Iozzo R V. (1985). Proteoglycans: Structure, function and role in neoplasia. *Lab.invest*; **53**: 373-396.
- Ishida K., Wierzba M K., Teruya T., Simizu S., Osada H. (2004). Novel HS mimetic compounds as anti-tumour agents. *Chem. Biol*; **11**: 367 – 77
- Ishihara M., Tyrrell D J., Stauber G B., Brown S., Cousens L S., Stack R J., (1993) Preparation of affinity-fractionated, Heparin-derived oligosaccharides and their effects on selected biological activities mediated by basic fibroblast growth-factor. *J Biol Chem*; **268**: 4675–4683
- Islam T and Linhardt R J. (2003). Chemistry, Biochemistry and Pharmaceutical potentials of Glycosaminoglycans and Related Saccharides; In; Carbohydrate-based Drug Discovery. Chi-Huey Wong (Ed.); Wiley-VCH, Weinheim; **5**: 407-433
- Itano N., Kimata K. (2002). Mammalian hyaluronan synthases. *IUBMB Life*; **54**:195–9
- Jacks T., and Weinberg R A., (1996). Cell-cycle control and its watchman. *Nature* (Lond.); **381**: 643–644
- Jackson R L., Busch S J and Bernfield M. (1991). Glycosaminoglycans: molecular properties, protein interactions, and role in physiological processes. *Physiol Review*; **2**: 481-485

- Jalkanen M., Rapraeger A., Bernfield M., (1988). Mouse mammary epithelial cells produce basement membrane and cell surface HS proteoglycans containing distinct core proteins. *J. Cell Biol*; **106**: 953–962.
- Jaye M., Schlessinger J., and Dionne C. (1992). Fibroblast growth-factor receptor tyrosine kinases: molecular analysis and signal transduction. *Biochem. Biophys Acta*; **1135**: 185-199.
- Jayson G C. et al. (1998). HS undergoes specific structural changes during the progression from human colon adenoma to carcinoma in vitro. *J. Biol. Chem*; **273**: 51–57.
- Jeney A., Timar J., Pogany G., et al. (1990). Glycosaminoglycans as novel target in anti-tumour therapy. *Tokai J Exp Clin Med*; **15**:167 – 77.
- Jimenez B., Volpert O V., Crawford S E., Febbraio M., Silverstein R L., Bouck N., (2000). Signals leading to apoptosis dependent inhibition of neovascularization by thrombospondin-1. *Nat Med*; **6**:41–48. [PubMed:10613822]
- Johnson D G and Walker C L (1999). Cyclins and cell cycle checkpoints. *Annu. Rev. Pharmacol. Toxicol*; **39**:295–312
- Jordan R E., Marcum J A. (1986). Anticoagulant active Heparin from clam (*Mercenaria mercenaria*) *Arch. Biochem. Biophys*; **248**: 690-695
- Joza N., Susin S A., Daugas E., Stanford W L., Cho S K., Li C Y., Sasaki T., Elia A J., Cheng H Y., Ravagnan L., Ferri K F., Zamzami N., Wakeham A., Hakem R., Yoshida H., Kong Y Y., Mak T W., Zuniga-Pflucker J C., Kroemer G., Penninger J M. (2001) Essential role of the mitochondrial apoptosis-inducing factor in programmed cell death. *Nature*; **410**:549–54. [PubMed: 11279485]
- Kan M., Wang F., Xu J., Crabb J W., Hou J., Mckeehan W L. (1993). An essential Heparin-binding domain in the fibroblast growth-factor receptor kinase. *Sc*; **259**: 1918-1921
- Kang S J., Wang S., Kuida K., Yuan J., (2002). Distinct downstream pathways of caspase-11 in regulating apoptosis and cytokine maturation during septic shock response. *Cell Death Differ*; **9**:1115–25. [PubMed:12232800]
- Karti SS., Ovali E., Ozgur O., Yilmaz M., Sonmez M., Ratip S., et al (2003). Induction of apoptosis and inhibition of growth of human hepatoma HepG2 cells by heparin. *Hepatogastroenterology*; **50**: 1864–1866.

- [Kaufmann R.](#), [Patt S.](#), [Kraft R.](#), [Zieger M.](#), [Henklein P.](#), [Neupert G.](#), [Nowak G.](#) (1999). PAR 1-type thrombin receptors are involved in thrombin-induced calcium signaling in human meningioma cells. *J neurooncol*; **42(2)**:131-136.
- Kerr J F., Winterford C M., Harmon B V., (1994). Apoptosis: Its significance in cancer and cancer therapy. *Cancer*; **73**:2013–2026. [PubMed: 8156506]
- Kerr J F., Wyllie A H., Currie A R., (1972). Apoptosis: a basic biological phenomenon with wide-ranging implications in tissue kinetics. *Br J Cancer*; **26**:239–257. [PubMed: 4561027]
- Kiefer M C., Baird A., Nguyen T., George N C., Mason O B., Boley L J., Valenzuela P and Barr P J.,(1991). Molecular cloning of a human basic fibroblast growth-factor receptor Cdna and expression of a biologically active extracellular domain in a baculovirus system . *Growth-Factor*; **5**:115-127.
- Kim B T., Kim W S., Kim Y S., Linhardt R J., Kim D H. (2000). Purification and characterisation of a novel heparinase from *Bacteroides stercoris* HJ-15. *J. Biochem. Tokyo*; **128**:323–328. [PubMed]
- Kim C., Goldberger O., Gallo R., and Bernfield M. (1994). Members of the sydecan family of HS proteoglycans are expressed in distinct cell- tissue and development-specific patterns. *Mol.Biol.Cell*; **5**:797-805
- Kimura J H., Lohmander V C., and Hascall J. (1984). Biochemical analysis of constitutive secretion in a semiintact cell system *J.Cell Biochem*; **26**: 261-278
- King K L., Cidlowski J A. (1998). Cell cycle regulation and apoptosis. *Annu Rev Physiol*; **60**:601–17.[PubMed: 9558478]
- King R W., Deshaies R J., Peters J M., Kirschner M W. (1996). How proteolysis drives the cell cycle. *Science*; **274**:1652–59
- Kischkel F C., Hellbardt S., Behrmann I., Germer M., Pawlita M., Krammer P H., Peter M E., (1995). Cytotoxicity-dependent APO-1 (Fas/CD95)- associated proteins form a death-inducing signaling complex (DISC) with the receptor. *Embo J*; **14**:5579–5588. [PubMed: 8521815]
- Kitagawa H., Tone Y., Tamura J., Neumann K W., Ogawa T., Oka S., Kawasaki T., Sugahara K., (1998). Molecular cloning and expression of glucuronyltransferase I involved in the biosynthesis of the glycosaminoglycan- protein linkage region of proteoglycans. *J. Biol Chem*; **273**: 6615-6618
- Kitagawa H., Kinoshita A., Sugahara K. (1995). Microanalysis of glycosaminoglycan-derived disaccharides labelled with the fluorophore 2-aminoacridone by capillary

- electrophoresis and high-performance liquid chromatography. *Anal. Biochem*; **232**: 114–121.
- Kjellen L., Petterson I., Unger E., Lindahl U. (1992). Two enzymes in one: N-deacetylation and N-sulphation in Heparin biosynthesis are catalysed by the same protein. *Adv. Exp. Med. Bio*; **313**: 107-11.
- Klagsbrun M., Baird A (1991). A dual receptor system is required for basic fibroblast growth factor activity. *Cell*; **67**:229 –231
- Koenig U., Eckhart L., Tschachler E., (2001). Evidence that caspase-13 is not a human but a bovine gene. *Biochem Biophys Res Commun*; **285**:1150–1154. [PubMed: 11478774]
- Koo C., Sen Y., Bay B and Yip G W (2008). Targeting HS Proteoglycans in Breast Cancer Treatment. *Anti-Cancer Drug Discovery*; **3**: 151-158
- Kothakota S., Azuma T., Reinhard C., Klippel A., Tang J., Chu K., McGarry T J., Kirschner M W., Kohts K., Kwiatkowski D J., Williams L T., (1997). Caspase-3-generated fragment of gelsolin: effector of morphological change in apoptosis. *Science*; **278**:294–8. [PubMed: 9323209]
- Koury M J. (1992). Programmed cell death (apoptosis) in hematopoiesis. *Exp Hematol* **20**: 391–394
- Koyama S., Koike N., Adachi S. (2001). Fas receptor counterattack against tumour-infiltrating lymphocytes in vivo as a mechanism of immune escape in gastric carcinoma. *J Cancer Res Clin Oncol*; **127**:20–6.[PubMed: 11206267]
- Kozlowski E O., and Pavao M S. (2011). Effect of sulfated glycosaminoglycans on tumor invasion and metastasis. *Front. Biosci.* 3, 1541–1551. doi: 10.2741/244  
 Pubmed Abstract | Pubmed Full Text | CrossRef Full Text
- Kozlowski E O., Pavao M S., and Borsig L. (2011). Ascidian dermatan sulfates attenuate metastasis, inflammation and thrombosis by inhibition of P-selectin. *J. Thromb. Haemost.* 9, 1807–1815. doi: 10.1111/j.1538-7836.2011.04401. Pubmed Abstract | Pubmed Full Text | CrossRef Full Text
- Kresse H., Hausses H., Schonhers E. (1993). Small proteoglycans. *Experientia*; **49**: 403-416
- Kristian P., Knut T D., (2000). Synthesis and sorting of proteoglycans. *J. of Cell Sci*; **113**: 193-205.
- Kroemer G., et al. (1997). Mitochondrial control of apoptosis. *Immunol Today* 18, 48–55.
- Kudchadkar R. et al. (2008). PI-88: a novel inhibitor of angiogenesis. *Expert Opin. Investig. Drugs*; **17**: 1769–1776

- Kurosaka K., Takahashi M., Watanabe N., Kobayashi Y., (2003). Silent cleanup of very early apoptotic cells by macrophages. *J Immunol*; **171**:4672–9. [PubMed: 14568942]
- Kusche-Gullberg M., Kjellen L. (2003). Sulfotransferases in glycosaminoglycan biosynthesis. *Curr. Opin. Struct. Biol*; **13**:605–11
- Kwan C P., Venkataraman G., Shriver Z., Raman R., Liu D., Qi Y., Varticovski L., Sasisekharan R. (2001) Probing fibroblast growth-factor dimerization and role of Heparin-like glycosaminoglycans in modulating dimerization and signaling. *J. Biol.Chem*; **276**: 23421-23429.
- LaBaer J., Garrett M D, Stevenson L F., Slingerland J M., Sandhu C., et al. (1997). New functional activities for the p21 family of CDK inhibitors. *Genes Dev*; **11**: 847–62.
- Lander A D., Selleck S B., (2000). The elusive functions of proteoglycans: *In vivo* veritas. *J Cell Biol*; **24**:227-232.
- Lansiaux A., Facompre M., Wattez N., Hildebrand M P., Bal C., Demarquay D., Lavergne O., Dennis C., Bigg H., and Bailly C. (2001). Apoptosis Induced by the Homocamptothecin Anti-cancer Drug BN80915 in HL-60 Cells. *Mol Pharmacol*; **60**:450–461
- Lapierre F., Holme K., Lam L., Tressler R J., Storm N., Wee J., Stack R J., Castellot J., Tyrrell D J.(1996). Chemical modifications of Heparin that diminish its anticoagulant but preserve its heparanase-inhibitory, angiostatic, anti-tumour and anti-metastatic properties. *Glycobiology*; **6**: 355–66.
- LeBrun L A., Linhardt R J. (2001). Degradation of HS with Heparin lyases. In: *Methods in Molecular Biology: Proteoglycan Protocols*; Iozzo, R., Ed.; Humana Press Inc.: Totowa, NJ, USA; 171.
- Lee D Y. et al., (2009). Anti-angiogenic activity of orally absorbable Heparin derivative in different types of cancer cells. *Pharm. Res*; **26**: 2667–2676
- Leist M and Jäättelä M (2001). Four deaths and a funeral: From caspases to alternative mechanisms. *Nat. Rev. Mol. Cell Biol*; **2**:589–98.
- Leist M., Single B., Castoldi A F., Kuhnle S., Nicotera P. (1997). Intracellular adenosine triphosphate (ATP) concentration: a switch in the decision between apoptosis and necrosis. *J Exp Med*; **185**:1481–1486. [PubMed: 9126928]
- Lever R., Page C P (2002). Novel drug development opportunities for heparin. *Nat Rev Drug Discov*; **2**:140-8

- Levin S., Bucci T J., Cohen S M., Fix A S., Hardisty J F., LeGrand E K., Maronpot R R., Trump B F. (1999). The nomenclature of cell death: recommendations of an ad hoc Committee of the Society of Toxicologic Pathologists. *Toxicol Pathol*; **27**:484–90. [PubMed: 10485836]
- Li H L., Ye K H., Zhang H W., Luo Y R., Ren X D, Xiong A H., et al (2001). Effect of heparin on apoptosis in human nasopharyngeal carcinoma CNE2 cells. *Cell Res*; **11**: 311–315
- Li L Y., Luo X., Wang X. (2001). Endonuclease G is an apoptotic DNase when released from mitochondria. *Nature*; **412**:95–99. [PubMed: 11452314]
- Lieberman J., Fan Z., (2003). Nuclear war: the granzyme A-bomb. *Curr Opin Immunol*; **15**:553–559. [PubMed:14499264]
- Liebmann J., Cook J A., Fisher J., Teague D. and Mitchell J B. (1994). *In vitro* studies of taxol as a radiation sensitizer in human tumour cells. *J. Natl. Cancer Inst*; **86**: 441-446.
- Lindhahl U. (2007). HS–protein interactions: a concept for drug design? *Thromb. Haemost*; **98**: 109–115
- Lindhahl U., Kusche-Gullberg M., Kjellen L. (1998). Regulated diversity of HS. *J. Biol. Chem*; **273**:24979–82
- Lindhardt R J (2004). Heparin-induced cancer cell death. *Chem and Biol*; **11**: 420-422
- Lindhardt R.J (2012). Synthetic heparin. *Curr Opin Pharmacol*; **12**(2): 217–219.
- Linhardt R J., Avci F Y., Toida T., Kim Y S., Cygler M (2006). CS Lyases: Structure, Activity, and Applications in Analysis and the Treatment of Diseases. *Advan in Pharmacol*, **53**: 187-215
- Linhardt R J., and Hileman R E. (1995). DS as a Potential Therapeutic Agent *Gen. Pharmac*; **26**: 443-451.
- Linhardt R J., Ampofo S A., Fareed J., Hoppensteadt D., Mulliken J B., and Folkman J. (1992). Isolation and characterisation of human Heparin. *Biochemistry*; **31**: 1244145.
- Linhardt R J., Wang H M., Loganathan B., Bae J H (1992a). Search for the Heparin antithrombin III binding site precursor. *J. Biol. Chem*; **267**: 2380-2387
- Linhardt R J. (1991). "Heparin: An Important Drug Enters its Seventh Decade," *Chem & Indust*; **2**: 45-50.

- Linhardt R J., Al-hakim A., et al. (1991). Structural features of DSs and their relationship to anticoagulant and antithrombotic activities. *Biochem. Pharm*; **42**: 1609-1619.
- Linhardt R J., Turnbull J E., Wang H M., Loganathan D., Gallagher J T. (1990). Examination of substrate specificity of Heparin and HS lyases. *Biochemistry*; **29**: 2611-2617
- Linhardt R J., Cohen D M., Rice K G. (1989). Nonrandom structural features in the Heparin polymer. *Biochemistr*; **28**: 2888-2894.
- Linhardt R J., Rice K G., Kim Y S., Lohse D L., Wang H M., Loganathan D. (1988). Mapping and quantification of the major oligosaccharide components of Heparin. *Biochem. J*; **254**: 781–787.
- Linhardt R J., Rice K G., Kim Y S., Lohse D L., Wang H M., and Loganathan D. (1988b). Mapping and quantification of the major oligosaccharide components of Heparin. *Biochem. J*; **254**: 781-87.
- Linhardt R J., Galfiher P M., and Cooney C L. (1986). Polysaccharide lyases. *Appl. Biochem. Biotech*; **12**: 135- 75.
- Lindahl U., Thinberg L., Backstrom G., Riesenfeld J., Nordling K. and Bjork I. (1984). Extension and structural variability of the antithrombin-binding sequence in Heparin. *J. Biol. Chem*; **259**: 12368-76.
- Linke W A., Ivemeyer M., Olivieri N., Kolmerer B., Rüegg J C. and Labeit S. (1996). Towards a molecular understanding of the elasticity of titin. *J. Mol. Biol*; **261**: 62-71.
- Liu D., Shriver Z., Venkataraman G., El Shabrawi Y., and Sasisekharan R. (2002). Tumour cell surface HS as cryptic promoters or inhibitors of tumour growth and metastasis. *Ap. Bio. Sci*; **99**: 568-573.
- Liu D., Shriver Z., Qi Y., Venkataraman G., Sasisekharan R. (2002). Dynamic regulation of tumour growth and metastasis by HS glycosaminoglycans. *Semin ThrombHemost*; **28**:67–78.
- Liuzzo J P and Moscatelli D (1996). Human Leukemia Cell Lines Bind Basic Fibroblast Growth Factor (FGF) on FGF Receptors and Heparan Sulfates: Downmodulation of FGF Receptors by Phorbol Ester. *Blood*; **87**: (1) 245-255
- Lo S L., Thike A A., Tan S Y., Lim T H., Tan I B., Choo S P., Tan P H., Bay B H., Yip G W (2011). Expression of HS in gastric carcinoma and its correlation with clinicopathological features and patient survival. *J Clin Pathol*; **64**:153-158.

- Lockshin R A., and Zakeri Z. (2001). Programmed cell death and apoptosis: origins of the theory. *Nat. Rev. Mol. Cell Biol.* **2**:545–550.
- Lockshin R A., and Williams C M. (1965). Programmed cell death. I. Cytology of degeneration in the intersegmental muscles of the pernyi silk moth. *J. Insect Physiol.* **11**:123–133.
- Locksley R M., Killeen N., Lenardo M J., (2001). The TNF and TNF receptor superfamilies: integrating mammalian biology. *Cell*; **104**:487–501. [PubMed: 11239407]
- Loganathan D., Wang H M., Mallis L M., and Linhardt R J. (1990). Structural variation in the antithrombin I11 binding site region and its occurrence in Heparin from different sources. *Biochemistry*; **29**: 4362-68.
- Lohse D L., and Linhardt R J. (1992). Purification and characterisation of Heparin lyases from *Flavobacterium heparinum*. *J. Biol. Chem*; **267**: 23347-55.
- Lowell B B., Susulic V., Hamann A., Lawitts J A., Himms-Hagen J., Boyer B B., L.P. Kozak L P., Flier J S. (1993). Development of obesity in transgenic mice after genetic ablation of brown adipose tissue. *Nature*; **366**:740–742
- Lukas J., Bartkova J & Bartek J (1996). Convergence of mitogenic signaling cascades from diverse classes of receptors at the cyclin D-cyclin-dependent kinase-pRb-controlled G1 checkpoint. *Molecular and Cellular Biology*; **16** : 6917–6925.
- Lund L R., Romer J., Thomasset N., Solberg H., Pyke C., Bissell M J., Dano K., Werb Z., (1996). Two distinct phases of apoptosis in mammary gland involution: proteinase-independent and -dependent pathways. *Development*; **122**:181–93. [PubMed: 8565829]
- Lyon M., Gallagher J T (1991). Purification and partial characterisation of the major cell-associated HS proteoglycan of rat liver. *Biochem J*; **273**: 415–422.
- Maccarana M., Casu B., and Lindahl U. (1993). Minimal sequence in Heparin/heparan sulphate required for binding of basic fibroblast growth-factor. *J. Biol. Chem*; **268**: 23898–23905
- Maimone M M., and Tollefsen D M. (1990). Structure of dermatan sulphate hexasaccharide that binds to Heparin cofactor II with high affinity. *J. Biol. Chem*; **265**: 18263-7.
- Majno G., Joris I. (1995). Apoptosis, oncosis, and necrosis: an overview of cell death, *Am. J. Pathol*; **146**: 3–15 [PubMed: 7856735]
- Malavaki C J, Theocharis A D, Lamari F N, Kanakis I, Tseggenidis T, Tzanakakis GN & Karamanos N K (2011). Heparan sulfate: biological significance, tools for biochemical analysis and structural characterization. *Biomed Chromatogr*; **25**: 11–20.



- Maloni W., Fais S and Fiorentini C. Morphological aspects of apoptosis.  
[www.cyto.purdue.edu/archive/flowcyt/research/.../malorni/malorni.htm](http://www.cyto.purdue.edu/archive/flowcyt/research/.../malorni/malorni.htm)
- Manaster J, Chezar J, Shurtz-Swirski R, Shapiro G, Tendler Y, Kristal B, et al (1996)  
 Heparin induces apoptosis in human peripheral blood neutrophils. *Br J Haematol*; **94**:  
 48–52
- Manaster J et al (1996). Heparin induces apoptosis in human peripheral blood neutrophils.  
*Br J Haematol*; **94**: 48-52
- Mandal D., Mazumder A., Das P., Kundu M., Basu J., (2005). Fas-, caspase-8-, and caspase-  
 3-dependent signaling regulates the activity of the aminophospholipid translocase and  
 phosphatidylserine externalization in human erythrocytes. *J Biol Chem*; **280**:39460–7.  
 [PubMed: 16179347]
- Marcum J A., and Rosenberg R D (1989a). The biochemistry, cell biology, and  
 patophysiology of anticoagulant active Heparin-like molecules of the vessel wall.  
 In: Heparin chemical and biological properties clinical applications. Lane D A and  
 Lindahl U., Eds., CRC Press, Boca Raton.
- Mariana S P., Barbara M. (1999). Structure and Anticoagulant Activity of Sulphated  
 fucans. *The J. of Biol. Chem*; **274**:7656-7667.
- Marks P A (2007). Discovery and development of SAHA as an anti-cancer agent. *Oncogene*;  
**26**: 1351–1356. doi: 10.1038/sj.onc.1210204
- Martinalet D., Zhu P., Lieberman J., (2005). Granzyme A induces caspase- independent  
 mitochondrial damage, a required first step for apoptosis. *Immunity*; **22**:355–70.  
 [PubMed: 15780992]
- Mascarelli F., Fuhrmann G., and Courtois Y. (1993). aFGF binding to low and high affinity  
 receptors induces both aFGF and aFGF receptors dimerization. *Growth Factors*; **8**:  
 211–233.
- Massague J. (1992). Receptor for the TGF family: *Cell*; **69**: 1067-1070.
- Matsui Y., Matsui R., Akada R., Toh-e A.(1996). Yeast src homology region 3 domain-  
 binding proteins involved in bud formation. *J Cell Biol*; **133**(4):865-78
- Matsuike A., Ishiwata T., Watanabe M., Asano G. (2001). Expression of fibroblast growth  
 factor (FGF)-10 in human colorectal adenocarcinoma cells. *J. Nippon Med. Sch*; **68**:  
 397–404

- Medeiros G F., Mendes A., Castro R A., Bau E C., Nader H B., Dietrich C P. (2000). Distribution of sulphated glycosaminoglycans in the animal kingdom: widespread occurrence of Heparin-like compounds in invertebrates. *Biochim. Biophys. Acta*; **1475**: 287-94
- Mellor P., Harvey J R., Murphy K J., Pye D., Boyle G O., Lennard T W J., Kirby J A, and Ali S (2007). Modulatory effects of Heparin and short-length oligosaccharides of Heparin on the metastasis and growth of LMD MDA-MB 231 breast cancer cells in vivo. *British Journal of Cancer*; **97**: 761 – 768
- Michelacci Y M., Horton D S P Q., and Poblacion C A. (1987). Isolation and characterisation of an induced chondroitinase-ABC from *Flavobacterium heparinum*. *Biochim. Biophys. Acta*; **923**: 29 1-301
- Michelacci Y M., and Dietrich C P. (1976). Chondroitinase C from *Flavobacterium heparinum*. *J. Biol. Chem*; **254**: 11 54-58
- Miyashita T., Krajewski S., Krajewska M., Wang H G., Lin H K., Liebermann D A., Hoffman B., Reed J C., (1994). Tumour suppressor p53 is a regulator of bcl-2 and bax gene expression in vitro and in vivo. *Oncogene*; **9**: 1799–1805. [PubMed: 8183579]
- Moffat C F., McLean M W., Long W F., and Williamson F B. (1991a). Heparinase II from *Flavobacterium heparinum* action on chemically modified heparins. *Eur. J. Biochem*; **197**: 449-59.
- Morgan D O. (1995). Principles of CDK regulation. *Nature (Lond.)*; **374**: 131–134
- Morishita R., Nakayama H., Isobe T., Matsuda T., Hashimoto Y., Okano T., Fukada Y., Mizuno K., Ohno S., Kozawa O., Kato K. and Asano T. (1995). Primary structure of a  $\gamma$  subunit of G protein,  $\gamma$  12, and its phosphorylation by protein kinase C. *J. Biol. Chem*; **270**: 29469-29475
- Moises C M., Andrade L R., Santos-Pinto P C., Straus A H., Takahashi H K., Allodi S., et al. (2002). Colocalization of Heparin and histamine in the intracellular granules of test cells from the invertebrate *Styela plicata* (Chordata-Tunicata). *J Struct Biol*; **137(3)**: 313-321
- Moise's C M. Cavalcant., Silvana Allodi., Ana-Paula V., Strausi A H., Takahashii H K., Paulo A. S. Moura and Mauro S. G. Pava (2010). Occurrence of Heparin in the Invertebrate *Styela plicata* (Tunicata) Is Restricted to Cell Layers Facing the Outside Environment. *J. Bio. Chem*; **275(46)**: 36189-36196.
- Mousa S.A. et al. (2006). Anti-metastatic effect of a non-anticoagulant low molecular-weight Heparin versus the standard low-molecular-weight Heparin,

enoxaparin. *Thromb. Haemost*; **96**: 816–821

Mundhenke C., Meyer K., Drew S. & Fried (2002). A HS proteoglycans as regulators of fibroblast growth-factor-2 receptor binding in breast carcinomas. *Am. J. Pathol*; **160**: 185–194.

Murata K., and Yokoyama Y. (1987). Characterisation of the products generated from oversulphated DS isomers with chondroitinase-B high-performance liquid chromatography. *J. Chrom*; **423**: 51-61.

Musgrove E A., Davison E A., Ormandy C J. (2004). Role of the CDK inhibitor p27 (Kip1) in mammary development and carcinogenesis: Insights from knockout mice. *J MammaryGland Biol Neoplasia*; **9**:55–66

Nader H B., Porcionatto A., et al.(1990). Purification and substrate specificity of heparitinase I and heparitinase II from *Flavobacterium heparinum*. *J. Biol.Chem*; **265**: 16807-1 3.

Nader H B., Ferreira TMPC., Paiva J F., Medeiros MGL., Jeronimo SMB., Paiva VMP., Dietrich CP. (1984). Isolation and structural studies of HSs and CSs from three species of molluscs. *J. Biol. Chem*; **259**: 1431-1435.

Nakagawa T., Zhu H., Morishima N., Li E., Xu J., Yankner B A., Yuan J., (2000). Caspase-12 mediates endoplasmic reticulum-specific apoptosis and cytotoxicity by amyloid-beta. *Nature*; **403**:98–103. [PubMed:10638761]

Nemes Z Jr., Friis R R., Aeschlimann D., Saurer S., Paulsson M., Fesus L., (1996). Expression and activation of tissue transglutaminase in apoptotic cells of involuting rodent mammary tissue. *Eur J Cell Biol*; **70**:125–33. [PubMed: 8793384]

Newman L., Xia W., Yang H Y., Sahin A., Bondy M., Lukmanji F., Hung M C., Lee M H. (2001). Correlation of p27 protein expression with HER-2/neu expression in breast cancer. *Mol Carcinog*; **30**:169–175.

Nijhawan D., Honarpour N., Wang X. (2000). Apoptosis in neural development and disease. *Annu Rev Neurosci*; **23**:73–87. [PubMed: 10845059]

Norbury C J., Hickson I D. (2001). Cellular responses to DNA damage. *Annu Rev Pharmacol Toxicol*; **41**:367–401.[PubMed: 11264462]

Nomura S., Yoshitomi H., Takano S., Shida T., Kobayashi, S., Ohtsuka, M., Kimura, F., Shimizu, H., Yoshidome, H., Kato, A., Miyazaki, M., (2008). FGF10/FGFR2 signal induces cell migration and invasion in pancreatic cancer. *Br. J. Cancer*; **99**: 305–313.

- Norrby K., (2000). 2.5 kDa and 5.0 kDa Heparin fragments specifically inhibit microvessel sprouting and network formation in VEGF165-mediated mammalian angiogenesis *Int. J. Exp. Pathol*; **81**: 191-8.
- Norrby K., Ostergaard P. (1997). Angiogenesis: New aspects relating to its initiation and control . *Int. J. Microcirc. Clin. Exp*; **17**: 314-21.
- Norrby K., Ostergaard P.(1996). Vascular endothelial growth-factor and *de novo* mammalian angiogenesis. *MicrovascInt. J. Microcirc. Clin. Exp*; **16**: 8-15.
- Olwin B B., Rapraeger A. (1992). Repression of myogenic differentiation by aFGF, bFGF, and K-FGF is dependent on cellular HS. *J Cell Biol*; **118**:631
- Opferman J T., Korsmeyer S J. (2003). Apoptosis in the development and maintenance of the immune system. *Nat Immunol*; **4**:410–415. [PubMed: 12719730]
- Ornitz D M., Xu J S., Colvin J S., McEwen D G., MacArthur C A., Coulier F., Gao G X and Goldfarb M. (1996). Receptor specificity of the fibroblast growth-factor family. *J. Biol. Chem*; **271**: 15292-15297
- Ornitz D M., and Leder P. (1992). Ligand specificity and Heparin dependence of fibroblast growth-factor receptor-1 and receptor-3. *J. Biol. Chem*; **267**:16305-16311.
- Osborne B A., (1996). Apoptosis and the maintenance of homoeostasis in the immune system. *Curr Opin Immunol*; **8**:245–54. [PubMed: 8725948]
- Ottlinger M E., Pukac L A and Karnovsky M J (1993). Heparin inhibits mitogenactivated protein kinase activation in intact rat vascular smooth muscle cells. *J Biol Chem.* **268** (26):19173-19176.
- Ozawa T., (1995). Mechanism of somatic mitochondrial DNA mutations associated with age and diseases. *Biochim Biophys Acta*; **1271**:177–89. [PubMed: 7599206]
- Pagano M. (1997). Cell cycle regulation by the ubiquitin pathway. *FASEB J*; **11**: 1067–75.
- Pangrazzi J., Gianese F. (1987). Carbohydrate Based Drug Discovery. *Haematologica*; **72**: 459-464.
- Pantoliano, M.W., Horlick, R.A., Springer, B.A., Van Dyk, D.E., Tobery, T.,Wetmore, D.R., Lear, J.D., Nahapetian, A.T., Bradley, J.D., and Sisk, W.P.(1994). Multivalent ligand–receptor binding interactions in the fibroblast growth-factor system produce a

- cooperative growth-factor and Heparin mechanism for receptor dimerization. *Biochemistry*; **33**: 10229–10248.
- Patel N J., Karuturi R., Al-Horani R A., Baranwal S., Patel J., Desai U R., and Patel BB. (2014) Synthetic, non-saccharide, Glycosaminoglycan mimetics Selectively Target Colon Cancer Stem Cells. *ACS Chem. Biol*; **9**: 1826-1833.
- Patel R C., Handy I., Patel C V (2002). Contribution of double-stranded RNA-activated protein kinase towards antiproliferative actions of heparin on vascular smooth muscle cells. *Arterioscler Thromb Vasc Biol*; **22**: 1439-1444
- Paules R S., Levedakou E N., Wilson S J., Innes C L., Rhodes N., Tlsty T D., Galloway D. A., Donehower L. A., Tainsky M. A., and Kaufmann W. K. (1995). Defective G2 checkpoint function in cells from individuals with familial cancer syndromes. *Cancer Res*; **55**: 1763-1773.
- Pavão M S., Aiello K R., Werneck C C., Silva L C., Valente A P., Mulloy B., et al (1998). Highly sulfated dermatan sulfates from Ascidians. Structure versus anticoagulant activity of these glycosaminoglycans. *J Biol Chem*; **273**: 27848-57
- Pavão M S., Mourão P A., Mulloy B., Tollefsen D M (1995) A unique dermatan sulfate-like glycosaminoglycan from ascidian. Its structure and the effect of its unusual sulfation pattern on anticoagulant activity. *J Biol Chem*; **270**: 31027-36.
- Pejler G., Danielsson A., Bjork I., Lindahl U., Nader H B., Dietrich C P. (1987). Structure and antithrombin binding properties of Heparin isolated from the clams *Anomalocardia brasiliensis* and *Tivela mactroides*. *J. Biol. Chem*; **262**: 11413-11421
- Pejler G., and David G. (1987). Basement membrane HS with high affinity for antithrombin synthesised by normal and transformed mouse mammary epithelial cells. *Biochem J*; **248**: 69-77
- Pellegrini L., Burke D F., von Delft F., Mulloy B., Blundell T L. (2000). Crystal structure of fibroblast growth-factor receptor ectodomain bound to ligand and Heparin. *Nature*; **407**: 1029-34.
- Peng J., Zhu Y., Milton J T, Price D H. (1998). Identification of multiple cyclin subunits of human P-TEFb. *Genes Dev*; **12**: 755–762.
- Perrimon N and Bernfield M., (2000). Specificities of HS proteoglycans in developmental processes. *Nature*; **404**: 725-728.
- Peter M E., Krammer P H., (1998). Mechanisms of CD95 (APO-1/Fas)- mediated apoptosis. *Curr Opin Immunol*; **10**: 545–551. [PubMed: 9794832]

- Petitou M., Herault J P., Bernat A., Driguez P A., Duchaussoy P., Lormeau J C., Herbert J M., (1999). Synthesis of thrombin-inhibiting Heparin mimetics without side effects. *Nature*; **398**:417-422
- Pezzuto J.M (1997). Plant-derived anticancer agents. *Biochem Pharm*; **53**: 121-133
- Pietenpol J A., Stewart Z A., (2002). Cell cycle checkpoint signaling: cell cycle arrest versus apoptosis. *Toxicology*; **181–182** : 475–81.
- Pinhal M A., Smith B., Olson S., Aikawa J., Kimata K., Esko J D. (2001). Enzyme interactions in HS biosynthesis: uronosyl 5-epimerase and 2-O-sulfotransferase interact in vivo. *Proc. Natl. Acad. Sci. USA*; **98**:12984–9
- Poole A. R., Webber C., Pidoux I., Choi H., Rosenberg L C., (1986). Localisation of a dermatan sulphate proteoglycans (DS-PG11) in cartilage and the presence of an immunologically related species in other tissues. *J.Histochem . Cytochem*; **34**: 619-625
- Polyak K. (2007). Breast cancer: origins and evolution. *J Clin Invest*; **117**: 3155-3163.
- Powell A K., Yates E A., Fernig D G., Turnbull J E. (2004). Interactions of Heparin/heparan sulphate with proteins: Appraisal of structural factors and experimental approaches. *Glycobiology*; **14**: 17R–30R.
- Presta M., Leali D D., Stabile H. Ronca R M. Camozzi M L. Coco E., Moroni S., Liekens and Rusnati M (2003). Heparin Derivatives as Angiogenesis Inhibitors. *Current Pharmaceutical Design*; **9(7)**: 553-66.
- Presta M.; Maier J A., Rusnati M., Ragnotti G. J. (1989). Basic fibroblast growth is released from endothelial ECM in a biologically active form. *J.Cell Physiol*; **140**:68-745
- Pukac L A., Ottlinger M E and Karnovsky M J., (1992). Heparin suppresses specific second messenger pathways for protooncogene expression in rat vascular smooth muscle cells. *J Biol Chem* **267**:3707-3711.
- Pumphrey C Y., Theus A M., Li S., Parrish R S and Sanderson R D (2002). Neoglycans, carbodiimide-modified glycosaminoglycans: a new class of anti-cancer agents that inhibit cancer cell proliferation and induce apoptosis. *Cancer Res.* **1**: 3722-3728.
- Puvirajesinghe T M., Turnbull J E (2012). Glycomics Approaches for the Bioassay and Structural Analysis of Heparin/HSs. *Metabolites*; **2**: 1060-1089.
- Rai N K., Tripathi K., Sharma D., Shukla V K., (2005). Apoptosis: a basic physiologic process in wound healing. *Int J Low Extrem Wounds*; **4**:138–44. [PubMed: 16100094]

- Ram S., Zachary S., Ganesh V., and UmaN. (2002). Roles of heparan-sulphate GAGs in cancer. *Nature*; **2**: 521-528.
- Reed J C Bcl-2 and the regulation of programmed cell death (1994). *J Cell Biol* 19; **124**: 1-6
- Reilly C F., Fritze L M S., Rosenberg R D (1986). Heparin inhibition of smooth muscle cell Proliferation: A cellular site of action. *J Cell Physiol*; **129**: 11-19
- Renehan A G., Booth C., Potten C S. (2001). What is apoptosis, and why is it important? *Bmj*; **322**:1536–8.[PubMed: 11420279]
- Renner S., Weisz J., Krajewski S., Krajewska M., Reed J C., Lichtenstein A (2000) Expression of BAX in plasma cell dyscrasias. *Clin Cancer Res*; **6**: 2371-2380
- Rice K G., and Linhardt R J. (1989). Study of structurally defined oligosaccharide substrates of Heparin and heparan monosulfate lyases. *Curb. Res*; **190**: 219-33.
- Rickert P., Seghezzi W., Shanahan F., Cho H., Lees E. (1996). Cyclin C/CDK8 is a novel CTD kinase associated with RNA polymerase II. *Oncogene*; **12**:2631–40.
- Roberts J J., Thompson A J., (1979). The mechanism of action of anti-tumour platinum compounds. *Prog. Nucleic Acid Res. Mol. Biol*; **22**:71–133
- Robertson J M., Shewach D S., Lawrence T S. (1996). Preclinical studies of chemotherapy and radiation therapy for pancreatic carcinoma. *Cancer*; **78**:674–79
- Rodén L. (1980). Structure and metabolism of connective tissue proteoglycans. In: *The Biochemistry of Glycoproteins and proteoglycan*. Edited by Lennarz WJ. New York: Plenum Press: 267-371
- Rohrmann K., Niemann R., Buddecke E. (1985). Two *N*-acetylgalactosaminyltransferase are involved in the biosynthesis of CS. *Eur J Biochem*, **148**:463-469.
- Rong J., Habuchi H., Kimata K., Lindahl U., Kusche-Gullberg M. (2001). Substrate specificity of the HS hexuronic acid 2-O-sulfotransferase. *Biochemistry*; **40**:5548–55
- Rong J., Habuchi H., Kimata K., Lindahl U and Salmivirta M. (2001) Substrate specificity of the HS hexuronic acid 2-O-Sulfotransferase. *Biochemistry*; **40**:5548-5555
- Roy R., Adamczewski J P., Seroz T., Vermeulen W., Tassan J P., et al. (1994). The M015 cell cycle kinase is associated with the TFIIH transcription-DNA repair factor. *Cell*; **79**:1093–101
- Rubio-Moscardo F., Blesa D., Mestre C., Siebert R., Balasas T., Benito A., Rosenwald A., Climent J., Martinez J I., Schilhabel M., Karran E L., Gesk S., Esteller M., deLeeuw

- R., Staudt L M., Fernandez-Luna J L., Pinkel D., Dyer M J., Martinez-Climent J A., (2005). Characterisation of 8p21.3 chromosomal deletions in B-cell lymphoma: TRAIL-R1 and TRAIL-R2 as candidate dosage-dependent tumour suppressor genes. *Blood*; **106**:3214–22. [PubMed: 16051735].
- Russell J H., Ley T J., (2002). Lymphocyte-mediated cytotoxicity. *Annu Rev Immunol*; **20**:323–70. [PubMed:11861606].
- [Rusnati M.](#), [Presta M.](#) (1996). Interaction of angiogenic basic fibroblast growth-factor with endothelial-cell HS proteoglycans. *Int. J. Clin and Lab Res*; **26** (1):15-23
- Rusnati M., Coltrini D., Caccia P., Dell'Era P., Zoppetti G., Oreste P. et al. (1994). Distinct role of 2-O-, N-, and 6-O-sulphate groups of Heparin in the formation of the ternary complex with basic fibroblast growth-factor and soluble FGF receptor-1. *Biochem Biophys Res Commun*; **203**:450–458
- Rusnati M., Urbinati C., Presta M. (1993). Internalization of basic fibroblast growth-factor (bFGF) in cultured endothelial cells: role of the low affinity Heparin-like bFGF receptors. *J Cell Physiol*; **154**(1):152–161
- Saelens X., Festjens N., Vande Walle L., van Gurp M., van Loo G., Vandenabeele P. (2004) Toxic proteins released from mitochondria in cell death. *Oncogene*; **23**:2861–2874. [PubMed: 15077149]
- Sakahira H., Enari M., Nagata S., (1998). Cleavage of CAD inhibitor in CAD activation and DNA degradation during apoptosis. *Nature*; **391**:96–9. [PubMed: 9422513]
- [Saksela O.](#), [Moscatelli D.](#), [Sommer A.](#), [Rifkin D B](#) (1988). Endothelial-cell-derived heparan sulphate binds basic fibroblast growth-factor and protects it from proteolytic degradation. *J of Cell. Bio*; **107**(2):743-51
- Salmivirta M., Lidholt K., Lindahl U. (1996). HS: a piece of information. *FASEB J*; **10**:1270-1279
- Salyers A A., Vercellotti J R., West S E H., and Wilkins T D. (1977). Fermentation of mucin and plant polysaccharides by strains of bacteroides from the human colon. *Appl. Environ. Microbiol*; **33**: 319-22.
- Samir M., Kost J. (2001). Transdermal delivery of Heparin and low molecular weight Heparin using low-frequency ultrasound. *Pharm Res*; **18**: 1151-1156



- Samuel D., Kumar T K S., Srimathi T., Hsieh H C., and Yu C (2000). Identification and characterisation of an equilibrium intermediate in the unfolding pathway of an all beta-barrel protein. *J. Biol. Chem*; 275: 34968-34975
- Sanderson R D. (2001). HS proteoglycans in invasion and metastasis. *Semin Cell Dev Biol*;12:89–98.
- Saravanan R., Vairamani S., Shanmugam A. (2010). Glycosaminoglycans from marine clam *Meretrix meretrix* (Linne) are an anticoagulant. *Prep Biochem Biotechnol*; 40 (4) 305-315
- Sasisekharan R., Raman R., and Prabhakar R. (2006). Glycomics Approach to Structure-Function Relationships of Glycosaminoglycans. *Annu. Rev. Biomed. Eng*; 8:181–231
- Sasisekharan R., Shriver Z., Venkataraman G and Narayanasami U., (2002). Roles of heparan-sulphate glycosaminoglycans in cancer. *Nature review cancer*; 2: 521-528
- Sasisekharan R and Venkataraman G. (2000). Heparin and HS: Biosynthesis, structure and function. *Current Opinion in Chemical Biology*; 4:(6):626-631
- Savill J., Fadok V. (2000). Corpse clearance defines the meaning of cell death. *Nature*; 407:784–788. [PubMed:11048729]
- Scarffe J H et al (1980). Relationship between the pretreatment proliferative activity of marrow blast cells and prognosis of acute lymphoblastic leukaemia of childhood. *Br J Cancer*; 41: 764-771
- Schimmer A D. (2004). Inhibitor of apoptosis proteins: translating basic knowledge into clinical practice. *Cancer Res*; 64:7183–7190. [PubMed: 15492230]
- Schlessinger J., Plotnikov A N., Ibrahimi O A., Eliseenkova A V., Yeh B K., Yayon A., Linhardt R J., Mohammadi M (2000). Structure of a ternary FGF-FGFR-Heparin complex reveals a dual role for Heparin in FGFR binding and dimerization *Mol. Cell*; 6 (3): 743-50.
- Schlessinger J., Ullrich A., (1992). Growth-factor signaling by receptor tyrosine kinases. *Neuron* 9:383
- Schonberger L B. (1998). New variant Creutzfeldt-Jakob disease and bovine spongiform encephalopathy. *Infect. Dis. Clin. North Am*; 12: 111-121.
- Seeberger P H., Werz D B. (2005). Automated synthesis of oligosaccharides as a basis for drug discovery. *Nat. Rev. Drug Discov*; 4:751–763

- Seeberger P H., Haase W C. (2000). Solid-phase oligosaccharide synthesis and combinatorial carbohydrate libraries. *Chem. Rev*; **100**: 4349–4394.
- Serina G et al., (2010). Antitumour activity of EP80061, a small-glyco drug in preclinical studies. In Proceedings of the AACR meeting.
- Sharif M., Osborne D J., Meadows K., Woodhouse S M., Colvin E M., Shepstone L., Dieppe P A. (1996). The relevance of chondroitine and keratin sulphate in blood markers in normal and arthritic synovial fluid. *British J. Rheumatol*; **35**: 951-957.
- Shao R G., Cao C X., Shimizu T., O’Conner P M., Kohn K W., Pommier Y. (1997). Abrogation of an S-phase checkpoint and potentiation of camptothecin cytotoxicity by 7 hydroxystaurosporine (UCN-01) in human cancer cell lines, possibly influenced by p53 function. *Cancer Res*; **57**:4029–4035.
- Shapiro G I., Edwards C D., Ewen M E., Rollins B J. (1998). p16INK4A participates in a G1 arrest checkpoint in response to DNA damage. *Mol. Cell. Biol*; **18**:378–87
- Shewach D S., Lawrence T S. (1996). Gemcitabine and radiosensitization in human tumour cells. *Invest. New Drugs*; **14**: 257– 263
- Shively J E., Conrad H E. (1976) Formation of anhydrosugars in the chemical depolymerisation of Heparin. *Biochemistry*; **15**: 3932–3942.
- Shimizu A., Masuda Y., Kitamura H., Ishizaki M., Ohashi R., Sugisaki Y., Yamanaka N. (2000). Complement-mediated killing of mesangial cells in experimental glomerulonephritis: cell death by a combination of apoptosis and necrosis, *Nephron* **86**: 152–160.
- Shively J.E., Conrad H.E (1976). Formation of anhydrosugars in the chemical depolymerisation of Heparin. *Biochemistry*; **15**: 3932–3942.
- Shukla D., Liu J., Blaiklock P., Shworak N W, Bai X., Esko J D., Cohen G H., Eisenberg R J., Rosenberg R D., Spear P G. (1999). A novel role for 3-O-sulphated HS in herpes simplex virus entry. *Cell*; **99**:13-22
- Silbert J E., Sugumaran G. (2002). Biosynthesis of chondroitin/DS. *IUBMB Life* **54**:177–86
- Simivita M., Lidhort K and Lindarl U. (1996). HS: A piece of information. *The Faseb J*; **10**: 1270-1279
- Simizu S., Ishida K., Osada H. (2004). Heparanase as a molecular target of cancer chemotherapy. *Cancer Sci*; **95**: 553 – 558.
- Singh S V., et al (2004). Sulforaphane-induced G2/M phase cell cycle arrest involves

- checkpoint kinase 2-mediated phosphorylation of cell division cycle. *J Biol Chem*; **279**: 25813-25822
- Slee E A., Adrain C., Martin S J. (2001). Executioner caspase-3, -6, and -7 perform distinct, non-redundant roles during the demolition phase of apoptosis. *J Biol Chem*; **276**:7320–7326. [PubMed: 11058599]
- Slevin M., Kumar S., and Gaffney J (2002). Angiogenic Oligosaccharides of Hyaluronan Induce Multiple Signaling Pathways Affecting Vascular Endothelial Cell Mitogenic and Wound Healing Responses. *J.of Bio. Chem*; **277** (43): 41046–41059
- Smyth M J., Godfrey D I., Trapani J A. (2001). A fresh look at tumour immune surveillance and immunotherapy. *Nat Immunol*; **2**:293–299. [PubMed: 11276199]
- Spataro V J., Litman H., Viale G., Maffini F et al. (2003). International Breast Cancer Study Group Decreased immunoreactivity for p27 protein in patients with early-stage breast carcinoma is correlated with HER-2/neu overexpression and with benefit from one course of perioperative chemotherapy in patients with negative lymph node status: Results from International Breast Cancer Study Group Trial V. *Cancer*; **97**:1591–1600.
- Spivak K T., Lemmon M A., Dikic I., Ladbury J E., Pinchasi D., Huang J., Jaye M., Crumley G., Schlessinger J., Lax I. (1994). Heparin-induced oligomerization, activation and cell proliferation. *Cell*; **79**: 1015-1024.
- Springer B A., Pantoliano M W., Barberal F A. et al (1994). Identification and concerted function of two receptor binding surfaces on basic fibroblast growth-factor required for mitogenesis. *J. Biol.chem*; **269**:26879-26884
- Steyn P L., Pot B., Segers P., Kersters K and Joubert J J. (1992). Some novel aerobic Heparin-degrading bacterial isolates System. *Appl. Microbiol*; **15**: 137-43.
- Stenstad T., Magnus J H., Husby G., Kolset S O. (1993). Purification of amyloid-associated HS proteoglycans and galactosaminoglycans free chains from human tissues. *Scand. J. Immunol*; **37**: 227–235
- Stone J E., Akhtar N., Botchway S., and Pennock C A. (1994). *Ann. Clin. Biochem*; **31**: 147–152
- Sugahara K and Kitagawa H (2000). Recent advances in the study of the biosynthesis and functions of sulphated aminoglycans: *Carbohydr and glycol*; **10**: 518-527

- Suliman A., Lam A., Datta R., Srivastava R K., (2001). Intracellular mechanisms of TRAIL: apoptosis through mitochondrial-dependent and -independent pathways. *Oncogene*; **20**:2122–2133. [PubMed:11360196]
- Susin S A., Daugas E., Ravagnan L., Samejima K., et al. (2000). Two distinct pathways leading to nuclear apoptosis. *J Exp Med*; **192**:571–80. [PubMed: 10952727]
- Sutherland R L., Musgrove E A.,(2004). Cyclins and breast cancer. *J Mammary Gland Biol Neoplasia*; **9**:95–104
- Szabo S. (1991). The mode of action of sucralfate: The  $1 \times 1 \times 1$  mechanism of action.Scand. *J. Gastroentrol.* **185 (Suppl. 26)**: 7–12.
- Taipale J., Keski-Oja J. (1997). Growth factors in the ECM. *FASEB J*; **11**:51-59.
- Tamar J., Lapis K., Duds J., Sebestyn A., Kopper L., Kovalszky I. (2002). Proteoglycans and tumour progression: Janus-faced molecules with contradictory functions in cancer. *Semin Cancer Biol*; **12**: 173–186.
- Tamm C., Kjeiiien L., and Li J (2012). Heparan Sulfate Biosynthesis Enzymes in Embryonic Stem Cell Biology. *J of Histochem and Cytochem*; **60** (12): 943–949
- Tiligada E., Miligkos V., Delitheos A. (2002). Cross-talk between cellular stress, cell cycle and anti-cancer agents: mechanistic aspects. *Curr Med Chem Anti-cancer Agents*; **2**: 553–566. doi: 10.2174/1568011023353976
- Tilly J L., Kowalski K I., Johnson A L., Hsueh A J. (1991). Involvement of apoptosis in ovarian follicular atresia and post ovulatory regression. *Endocrinology*; **129**:2799–2801. [PubMed: 1718732]
- Tischler R B., Schiff P B., Geard C R., Hall E J. (1992). Toxol: a novel radiation sensitizer. *Int. J. Radiat. Oncol. Biol. Phys*; **22**:613–17
- Toida T., Yoshida H., Toyoda H., Koshiishi I., Imanari T., Hileman R.E., Fromm J.R., Linhardt R J. (1997). Structural differences and the presence of unsubstituted amino groups in HSs from different tissues and species. *Biochem. J*; **322**: 499– 506.
- Toledo O M S., Dietrich CP, Tissue specific distribution of sulphated mucopolysaccharides in mammals (1977). *Biochem Biophys Acta*; **498**: 114-122.
- Toyoda H., Kinoshita-Toyoda A., Selleck S B (2000). Structural analysis of glycosaminoglycans in *Drosophila* and *Caenorhabditis elegans* and demonstration that *toutvelu*, a *Drosophila* gene related to EXT tumor suppressors, affects heparan sulfate in vivo. *J Biol Chem*; **275**:2269-75.

- Trapani J A., Smyth M J. (2002). Functional significance of the perforin/granzyme cell death pathway. *Nat Rev Immunol*; **2**:735–47. [PubMed: 12360212]
- Trump B F., Berezsky I K., Chang S H., Phelps P C., (1997). The pathways of cell death: oncosis, apoptosis, and necrosis. *Toxicol Pathol*; **25**:82–8. [PubMed: 9061857]
- Tsihlias J., Kapusta L., Slingerland J. (1999). The prognostic significance of altered cyclin-dependent kinase inhibitors in human cancer. *Annu Rev Med*; **50**:401–423
- Tumova S., Woods A., Couchman J R. (2000). HS proteoglycans on the cell surface: versatile coordinators of cellular functions. *Int J Biochem Cell Biol*; **32**: 269-288
- Turnbull J., Powell A. & Guimond S. (2001). HS: decoding a dynamic multifunctional cell regulator. *Trends Cell Biol*; **11**: 75–82.
- Turnbull J E., Hopwood J J., Gallagher J T. (1999). A strategy for rapid sequencing of HS and Heparin saccharides. *Proc. Nat. Acad. Sci. USA*; **96**: 2698–2703.
- Turnbull J E., Fernig D G., Ke Y., Wilkinson M C., and Gallagher J T. (1992). Identification of the basic FGF binding sequence in fibroblast heparan sulfate. *J. Biol. Chem*; **267**: 10337–10341
- Turnbull J E., Gallagher J T., (1991). Sequence analysis of HS indicates defined location of N-sulphated glucosamine and iduronate 2-sulphate residues proximal to the protein linkage region. *Biochem*; **277**: 297–303.
- Turnbull J E., (1990). Mapping and sequencing of HS. PhD thesis, University of Manchester, Manchester, UK.
- Turnbull J E., Gallagher J T., (1988). Oligosaccharide mapping of HS by polyacrylamide-gradient-gel electrophoresis and electrotransfer to nylon membrane. *Biochem. J*; **251**: 597–608
- Turner N., Grose R. (2010). Fibroblast growth-factor signaling: from development to cancer. *Nat Rev Cancer*; **10**: 116-29.
- Tyrrell D J., Ishihara M., Rao N., Horne A., Kiefer M C., Stauber G B., Lam L H., Stack R J., (1993). Structure and biological activities of a Heparin-derived hexasaccharide with high affinity for basic fibroblast growth-factor. *J Biol Chem*; **268**: 4684–4689

- Ueda K., Inoue S., Zhang Y., Kutsuna T., Inoue S., Noto K., Arai N and Noguchi M. (2009). Heparin Induces Apoptosis through Suppression of AKt in Oral Squamous Cell Carcinoma Cells. *Antican Res*; **29**: 1079-1088
- Ullrich A., Schlessinger J. (1990). Signal transduction by receptors with TK activity. *J. Cell*; **61**:203-212.
- Uyama T., Kitagawa H., Sugahara K. (2007). Biosynthesis of glycosaminoglycans and proteoglycans. In: *Comprehensive Glycoscience*; **1**: 79-99
- Van den Heuvel S (2005). Cell cycle regulation. *Wormbook*; **2**: 1-16
- Van L G., Van G M., Depuydt B., Srinivasula S M., Rodriguez I., Alnemri E S., Gevaert K., Vandekerckhove J., Declercq W., Vandenameele P. (2002). The serine protease Omi/HtrA2 is released from mitochondria during apoptosis. Omi interacts with caspase-inhibitor XIAP and induces enhanced caspase activity. *Cell Death Differ*; **9**:20–6. [PubMed: 11803371]
- Varki N M., & Varki A. (2002). Heparin inhibition of selectin mediated interactions during the hematogenous phase of carcinoma metastasis: rationale for clinical studies in humans. *Semin. Thromb. Hemost*; **28**: 53–66.
- Varley J M., Evans D G., Birch J M. (1997). Li-Fraumeni syndrome—a molecular and clinical review. *Br J Cancer*; **76**: 1–14. [PubMed: 9218725]
- Vaux D L., Cory S., Adams J M., (1988). Bcl-2 gene promotes haemopoietic cell survival and cooperates with c myc to immortalize pre-B cells. *Nature*; **335**:440–2. [PubMed: 3262202]
- Vesely J., Havlicek L., Strnad M., Blow J J., Donella-Deana A., et al. (1994). Inhibition of cyclin-dependent kinases by purine analogues. *Eur. J. Biochem*; **224**:771–86  
109a
- Vijayabaskar P., Somasundaram S T. (2012). Studies on molluscan Glycosaminoglycans (GAG) from backwater clam. *Asian pac J. Trop Biomed*; **1691**(12): 60265-2
- Vilela-Silva A C., Werneck C C., Valente A P., Vacquier V D., Mourão P A (2001). Embryos of the sea urchin *Strongylocentrotus purpuratus* synthesize a dermatan sulfate enriched in 4-*O*- and 6-*O*-disulfated galactosamine units. *Glycobiology*; **11**:433-40
- Vincent T., Molina L., Espert L., Mechti N (2003). Hyaluronan, a major non-protein glycosaminoglycans component of the extracellular matrix in human bone marrow,

- mediates dexamethasone resistance in multiple myeloma. *Br J Haematol*; **121**: 259–26920
- Vives R R., Pye D A., Salmivirta M., Hopwood J J, Lindahl U., Gallagher J T. (1999). Sequence analysis of HS and Heparin oligosaccharides. *Biochem. J.* **339**:767–773.
- Vivanco I., Sawyers C L. (2002). The phosphatidyl inositol 3-Kinase AKT pathway in human cancer. *Nat Rev Cancer*; **2**: 489–501. [PubMed: 12094235]
- Vives R R., Goodger S., Pye D A. (2001). Combined strong anion-exchange hplc and page approach for the purification of HS oligosaccharides. *Biochem. J.*; **354**: 141–147.
- Vives R., Pye D A., Salmivirta M., Hopwood J J., Lindahl U I and Gallagher J T. (1999). Sequence analysis of HS and Heparin oligosaccharides. *Biochem. J.*; **339**: 767-773
- Vlodavsky I et al., (2007). Heparanase: structure, biological functions, and inhibition by Heparin-derived mimetics of HS. *Curr. Pharm. Des*; **13**: 2057–2073
- Vohra Y., Vasani M., Venot A., Boons G J. (2008). One-pot synthesis of oligosaccharides by combining reductive openings of benzylidene acetals and glycosylations. *Org. Lett*; **10**: 3247–3250.
- Volpi N. (2006). Therapeutic applications of glycosaminoglycans. *Curr. Med. Chem*; **13**: 1799–1810
- Volpi N. (2005). Occurrence and structural characterisation of Heparin from molluscs. *ISJ*; **2**: 6-16
- Volpi N and Macari F (2005). Glycosaminoglycan Composition of the Large Freshwater Mollusc Bivalve *Anodonta anodonta*. *Biomacromolecules*; **6 (6)**: 3174–3180
- Wahl G M., Linke S P., Paulson T G., Huang L C. (1997). Maintaining genetic stability through TP53 mediated checkpoint control. *Cancer Surv*; **29**:183–219
- Wajant H. (2002). The Fas signaling pathway: more than a paradigm. *Science*; **296**:1635–1636. [PubMed:12040174]
- Walker A., Turnbull J E., and Gallagher J T. (1994). Specific heparan-sulphate saccharides mediate the activity of basic fibroblast growth-factor. *J. Biol. Chem*; **269**: 931–935
- Walker D H. (1998). Small-molecule inhibitors of cyclin-dependent kinases: molecular tools and potential therapeutics. *Curr. Top. Microbiol. Immunol*; **227**:149–65

- Wang X and Lin Y. (2008). Tumour necrosis factor and cancer, buddies or foes? *Acta Pharmacologica Sinica*; **29**: 1275–1288
- Wang X W., Harris C C., (1997). p53 tumour-suppressor gene: clues to molecular carcinogenesis. *J Cell Physiol*; **173**: 247–255. [PubMed: 9365531]
- Wang Q., Fan S., Eastman A., Worland P J., Sausville E A., O’Conner P M. (1996). UCN-01: a potent abrogator of G2 checkpoint function in cancer cells with disrupted p53. *J. Natl. Cancer Inst*; **88**: 956–65
- Wang Q., Worland P J., Clarke J L., Carlson B A., Sausville E A. (1995). Apoptosis in 7-hydroxystaurosporine-treated T lymphoblasts correlates with activation of cyclin-dependent kinases 1 and 2. *Cell Growth Differ*; **6**: 927–936
- Warny M., Keates A C., Keates S., Castagliuolo I., Zacks J K., Aboudola S., Qamar A., Pothoulakis C., LaMont J T., Kelly C P., (2000). p38 MAP kinase activation by *Clostridium difficile* toxin A mediates monocyte necrosis, IL-8 production, and enteritis. *J. Clin. Invest*; **105**: 1147–1156.
- Wastenson A. (1971). Properties of fractionated CS from ox nasal septa. *Biochem J*; **122**: 477-488.
- Weber A., Kirejczyk Z., Besch R., Potthoff S., Leverkus M. and Häcker G. (2010) Proapoptotic signalling through Toll-like receptor 3 involves TRIF-dependent activation of caspase-8 and is under the control of inhibitor of apoptosis proteins in melanoma cells. *Cell Death Diff*; **17(6)**: 942-951.
- Wei Z., Lyon M., and Gallagher J T. (2005). Distinct Substrate Specificities of Bacterial Heparinases against N-Unsubstituted Glucosamine Residues in HS. *J. of bio chem*; **280**: 16. 15742–15748
- Weiler J M., Edens R W., Lindaht R J., and Kapelanski D P. (1992). Heparin and modified Heparin inhibit complement activation in vivo. *J. Immunol*; **148**: 3210-3215
- Weinstein I B. (1996). Relevance of cyclin D1 and other molecular markers to cancer chemoprevention. *J. Cell. Biochem*; **25S**: 23–28.
- Wenger F A et al. (2009). [Chirurgisches Forum und DGAV Forum 2009](#). Impact of low-molecular-weight heparin on tumour growth and apoptosis in ductal pancreatic cancer. [Deutsche Gesellschaft für Chirurgie](#); **38**: 205-207
- Wesselborg S., Engels I H., Rossmann E., Lo M and Schulze-Osthoff K. (1999). Anti-cancer Drugs Induce Caspase-8/FLICE Activation and Apoptosis in the Absence of CD95 Receptor/Ligand Interaction. *Blood*; **93**: 3053-3063



- Wickremasinghe R.G., and Hoffbrand A.V. (1998). Biochemical and genetic control of apoptosis: relevance to normal hematopoiesis and hematological malignancies. *Blood*; **93**: 3587–3600.
- Williams M P., Streeter H B., Wusteman F S., Cryer A. (1983). HS and the binding of lipoprotein lipase to porcine thoracic aorta endothelium; *Biochim. Biophys. Acta*; **756**: 83-91.
- Wingate H., Zhang N., McGarhen M J., Bedrosian I., Harper J W., Keyomarsi K. (2005). The tumour-specific hyperactive forms of cyclin E are resistant to inhibition by p21 and p27. *J Biol Chem*; **280**: 15148–15157
- Woods C M., Zhu J., McQueney P A., Bollag D., Lazarides E. (1995). Taxol-induced mitotic block triggers rapid onset of a p53-independent apoptotic pathway. *Mol. Med*; **1**:506–26
- Wong R S Y (2011). Apoptosis in cancer: from pathogenesis to treatment. *J of Exp. & Clin Res*; **30** (87): 1-14.
- Wong C H. (2006). Carbohydrate-based drug discovery. In: analytical Techniques for the characterisation and sequencing of Glycosaminoglycans. John Wiley and sons. *Science*: 530
- Wright T C., Johnstone T V., Castellot J J., Karnovsky M J (1985). Inhibition of rat cervical epithelial cell growth by heparin and its reversal by EGF. *J Cell Physiol*; **124**:490-506
- Wyllie A H., Kerr J F., Currie A R. (1980). Cell death: the significance of apoptosis. *Int. Rev. Cytol*; **68**: 251–306.
- Xiao Z., Wenjing Z W., Yang B., Zhang Z., Guan H., and Linhardt R J. (2011). Heparinase 1 selectivity for the 3,6-di- O -sulfo-2-deoxy-2-sulfamido-  $\alpha$  -D glucopyranose (1,4) 2-O-sulfo- $\alpha$  -L-idopyranosyluronic acid (GlcNS3S6S-IdoA2S) linkages *Glycobiology*; **21**: 13 – 22
- Xiang Y Y., Ladeda V and Filmus J. (2001). Glypican-3 expression is silenced in human breast cancer. *Oncogene*; **20**: 7408–7412.
- Xiao Z., Zhao W., and Linhardt R J. (2011). Heparinase 1 selectivity for the 3,6-di-O-sulfo-2-deoxy-2-sulfamido- $\alpha$ -D-glucopyranose (1,4) 2-O-sulfo- $\alpha$ -L-idopyranosyluronic acid (GlcNS3S6S-IdoA2S) linkages. *Glycolbio*; **21**(1): 13-22
- Xiaong Y., (1996). Why are there so many CDK inhibitors. *Biochim.Biophys. Acta*; **1288**: 1–5.

- Xu C X., Jin H., Chung Y S., Shin J Y., Lee K H., Beck G R Jr et al., (2008). Chondroitin sulfate extracted from Ascidian tunic inhibit phorbol esters induced inflammatory factor VCAM-1 and COX-2 by blocking NFkappa B activation in mouse skin. *Agric Food Chem*; **56**: 9667-75
- Yamada S., Sugahara K. And Ozbek S. (2011). Evolution of glycosaminoglycans: Comparative biochemical study. *Com. & Integra Bio*; **4(2)**: 150-158
- Yamada S., Morimoto H., Fujisawa T., Sugahara K. (2007). Glycosaminoglycans in Hydra magnipapillata (Hydrozoa, Cnidaria): demonstration of chondroitin in the developing nematocyst, the sting organelle, and structural characterisation of glycosaminoglycans. *Glyco. Bio*; **17** (8): 886-894
- Yamagata T., Saito H., Habuchi O., and Suzuki S. (1968). Purification and properties of bacterial chondroitinases and chondrosulfatases. *J. Biol. Chem*; **243**: 1523-1535.
- Yanagishita M. (2001). Isolation of proteoglycans from cell cultures and tissues. In *Methods in Molecular Biology: Proteoglycan Protocols*; Iozzo, R.V., Ed.; Humana Press: Totowa, NJ, USA; **171**: 3–8.
- Yanagishita M., Midura R J., Hascall V C. (1987). Proteoglycans: Isolation and purification from tissue cultures. *Methods Enzymol*; **138**: 279–289
- Yao S L., Akhtar A J., McKenna K A., Bedi G C., Sidransky D., et al. (1996). Selective radiosensitization of p53-deficient cells by caffeine-mediated activation of p34cdc2 kinase. *Nat. Med*; **2**:1140–43
- Yates E A., Guimond S E., Turnbull J E. (2004). Highly diverse HS analogue libraries: Providing access to expanded areas of sequence space for bioactivity screening. *J. Med. Chem*; **47**: 277–280.
- Yayon A., Klagsbrun M., Esko J D., Leder P., Ornitz D M. (1991). Cell surface, Heparin-like molecules are required for binding of basic fibroblast growth-factor to its high affinity receptor. *Cell*; **64**: 841–848
- Yingbing W., Debra B S., Ikeda M., Balasubramanian N., et al. (2008). Estrogen Receptor–Negative Invasive Breast Cancer: Imaging Features of Tumours with and without Human Epidermal Growth-Factor Receptor Type 2 Overexpression, doi: 10.1148/radiol.2462070169. *Radiology*; **246**: 367-375.
- Yip G W., Koo C., Sen Y., and Bay B. (2008). Targeting HS Proteoglycans in Breast Cancer Treatment. *Recent Patents on Anti-Cancer Drug Discovery*; **3** :151-158

- Yoshida E., Arakawa S., Matsunaga T., Toriumi S., Tokuyama S., Morikawa K. and Tahara Y. (2002). Cloning, sequencing, and expression of the gene from *Bacillus circulans* that codes for a heparinase that degrades both Heparin and HS. *Biosci. Biotechnol. Biochem*; **66**: 1873-1879.
- Zeiss C J. (2003). The apoptosis-necrosis continuum: insights from genetically altered mice. *Vet Pathol*; **40**: 481–495. [PubMed: 12949404]
- Zhang Z, Xiao Z, Linhardt RJ (2009). Thin Layer Chromatography for the Separation and Analysis of Acidic Carbohydrates. *J Liq Chromatogr R T*; **32**:1711–1732
- Zhan Q., Carrier F., Fornace A J Jr. (1993). Induction of cellular p53 activity by DNA-damaging agents and growth arrest. *Mol. Cell. Biol*; **13**: 4242–4250
- Zhou H. et al., (2010). M402 – A Novel HS Proteoglycan Mimetic Targeting Tumour–Host Interactions. American Association for Cancer Research (AACR)
- Zhou H. et al. (2009). M-ONC 402-a non-anticoagulant low molecular weight Heparin inhibits tumour metastasis. In Proceedings of the 100th Annual Meeting of American Association for Cancer Research (AACR)
- Zwijsen R M L., Wientjens E., Klompmaker R., Van der Sman J., Bernards R and Michalides R J. (1997). CDK-independent activation of estrogen receptor by cyclin D1. *Cell*; **88**: 405–415.

